*Coordination Chemistry Reviews*, 69 (1986) 127–258
Elsevier Science Publishers B.V., Amsterdam – Printed in The Netherlands

# CLUSTER COMPLEXES CONTAINING OPENED TRANSITION METAL POLYHEDRA

MICHEL O. ALBERS * and DAVID J. ROBINSON

*National Chemical Research Laboratory, Council for Scientific and Industrial Research, P.O. Box 395, Pretoria 0001 (Republic of South Africa)*

NEIL J. COVILLE *

*Department of Chemistry, University of the Witwatersrand, 1 Jan Smuts Avenue, Johannesburg 2001 (Republic of South Africa)*

(Received 22 July 1985)

## CONTENTS

## ABBREVIATIONS

| | |
|---|---|
| acac | acetylacetonate |
| bipy | 2,2′-bipyridine |
| Bu | butyl |
| CHT | cyclohepta-1,3,5-triene |

---

* Authors to whom correspondence should be addressed.

0010-8545/86/$46.20

| | |
|---|---|
| COD | cycloocta-1,5-diene |
| COT | cyclooctatetraene |
| dba | dibenzylideneacetone |
| dpmp | bis(diphenylphosphinomethyl)phenylphosphine |
| dppe | 1,2-bis(diphenylphosphino)ethane |
| dppm | bis(diphenylphosphino)methane |
| Et | ethyl |
| $f_4asp$ | $Ph_2As{-}\overline{C{=}C(AsMe_2)CF_2CF_2}$ |
| $f_4fars$ | $Me_2As{-}\overline{C{=}C(AsMe_2)CF_2CF_2}$ |
| Me | methyl |
| NBD | norbornadiene |
| n-, i-, t- | normal, iso, tertiary |
| Ph | phenyl |
| phen | 1,10-phenanthroline |
| Pr | propyl |
| py | pyridine |
| R | alkyl or aryl (unless otherwise indicated) |
| THF | tetrahydrofuran |
| THT | tetrahydrothiophene |
| tmeda | *N*,*N*,*N′*,*N′*-tetramethylethylenediamine |

## A. INTRODUCTION

Transition metal complexes have played a significant role in the development of inorganic chemistry [1–8]. The last fifteen years in particular have seen major additions to the fund of knowledge concerning the coordination chemistry of metal atoms in a cluster, and how the closely interactive environment in the cluster influences the properties and the reactivity of the cluster complex [8].

Much of the interest in metal clusters has been motivated by the possible role of clusters as bridges between molecular chemistry and solid state chemistry, and the belief that this could lead to a greater understanding of surface phenomena and ultimately to the development of novel catalysts [9–12]. While the promise of many early discoveries has, however, remained largely unfulfilled in this respect, it is clear that an enormous fund of scientific knowledge has been accumulated which could lay the foundations for future, more realistic appraisals of potential applications.

One of the most important recent developments in cluster chemistry has been the recognition of the importance of the reactivity of the metal cluster core and for which the term "basic metal cluster chemistry" has been coined [13]. While this viewpoint highlights a hitherto largely neglected aspect of

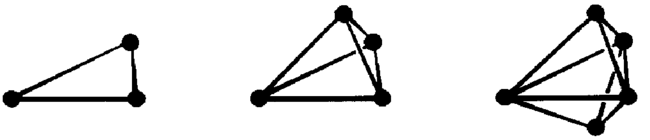

eg. [Os$_3$(CO)$_{12}$] eg. [Ir$_4$(CO)$_{12}$] eg. [Os$_5$(CO)$_{16}$]

Fig. 1.

the reactivity of metal clusters which relates to the relative stability and reactivity of metal–ligand and metal–metal bonds, it serves specifically to emphasise the importance of transformations of the metal atom framework within the context of cluster synthesis, structure and reactivity. These considerations are of crucial importance in appreciating the relationships between transition metal complexes of different metal atom nuclearity, e.g. the relationships between mono-, di- and trinuclear complexes, and the application of these relationships to an understanding of the structure and reactivity patterns of clusters. In this regard, dinuclear transition metal complexes specifically have been implicated as a possible stepping stone between the relatively well understood chemistry of mononuclear systems and the more complex chemistry of clusters [14]. (That this is not necessarily a trivial expectation though, witness the recent controversy over the substitution chemistry of the "simple" dimers [M$_2$(CO)$_{10}$](M = Mn, Re) [15–20].)

For the purposes of this review, a transition metal cluster is considered to be defined as a compound in which there are three or more transition metal atoms in a bonding interaction. Also for the purposes of this review, clusters are considered to fall into two classes. The first and the largest group contains metal clusters in which at least some of the transition metal atoms form a closed or cyclic core structure, as found in complexes such as [Os$_3$(CO)$_{12}$], [Ir$_4$(CO)$_{12}$] and [Os$_5$(CO)$_{16}$] [8] (Fig. 1). Previous reviews [1–8] have stressed the synthesis, structure and chemical reactivity of such cyclic clusters. However, to date, little emphasis has been placed on the second group of cluster complexes which have been variously described in the literature as open, linear, chain or oligomeric clusters or complexes [7,8,13,14]. In order to remove the ambiguity associated with this terminology, and consistent with that used for the first grouping of clusters, we will refer to these complexes collectively as open or acyclic cluster complexes, i.e. cluster complexes containing opened transition metal polyhedra.

eg. [Ir(CO)$_3$Cl] eg. [Pt$_4$(en)$_4$(C$_5$H$_4$NO)$_4$]$^{5+}$

Fig. 2.

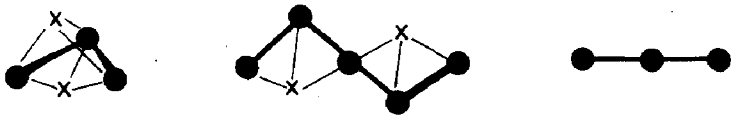

eg. $[Fe_3(CO)_9(\mu_3\text{-}S)_2]$ eg. $[AuW_2Pt_2(\eta^5\text{-}C_5H_5)_2(CO)_4(PMe_3)_4(CR)_2]PF_6$ eg. $[Os_3(CO)_{12}I_2]$

Fig. 3.

It is the objective of this review to survey the range of acyclic transition metal cluster complexes currently known with a view to indicating their relationships to cyclic clusters and also to simpler, e.g. dinuclear, metal fragments. The review will therefore not be concerned with cyclic cluster complexes, nor will it be concerned with chain complexes [21] (i.e. with solid state structures which have been shown by X-ray crystallography to contain extended arrays of repeat metal atom units e.g. $[Ir(CO)_3Cl]$ [22]) or oligomeric complexes [14,23] (i.e. aggregates of metal atom units which form, usually in solution, such as observed in the "platinum blues" and related systems [24]) (see Fig. 2) other than to indicate their possible relationships to acyclic cluster complexes.

Some examples of acyclic cluster complexes surveyed are shown in Fig. 3, viz. a linear arrangement of three metal atoms as illustrated by $[Os_3(CO)_{12}I_2]$ [25], a zig-zag arrangement of five metal atoms illustrated by $[AuW_2Pt_2(\eta^5\text{-}C_5H_5)_2(CO)_4(PMe_3)_4(\mu_3\text{-}CR)_2]$ [26], and an open triangular arrangement of metal atoms as found in $[Fe_3(CO)_9(\mu_3\text{-}S)_2]$ [27].

With regard to the use of dinuclear complexes as a stepping stone in the understanding of cluster chemistry, it is interesting to note (Fig. 3) that acyclic clusters may be viewed as being intermediate between cyclic clusters and dinuclear complexes. More specifically, linear complexes are closely related to dinuclear complexes, open triangular complexes are closely related to cyclic cluster species, while the zig-zag metal arrangement embodies elements of both the linear and open triangular complexes, and therefore may be considered to fulfill an intermediate role between these two.

Any survey concerned with complexes containing metal–metal bonds must address itself to the evidence for metal–metal bonding. In this regard, we have followed the guidelines proposed by Roberts and Geoffroy [7]. Briefly, the most reliable evidence is based upon X-ray or neutron diffraction studies, but a requirement for a metal–metal bond to exist based on spectroscopic data, the effective atom number rule and chemical reactivity also constitute valid criteria [7]. However, despite these, and other criteria, borderline cases do arise [7], and in this regard we have adopted a policy of inclusion, treating such cases on merit and highlighting these problem areas with as many recent literature citations as possible.

In the absence of bridging ligands the question of metal–metal bonding interactions is generally relatively straightforward. The presence of bridging hydrido ligands, however, poses a unique problem. In this regard we have adopted the proposals of Churchill et al. [28] and Bau et al. [29], and therefore consider that the presence of a hydride bridge between the metal atoms does signify some (albeit variable) amount of metal–metal bonding. Thus, for instance, the complex $[H_2Os_3(CO)_{10}]$ is taken to have a closed triangle of three osmium atoms [28] (and is therefore not included in this review), whereas the complex $[HRe_2Mn(CO)_{14}]$ containing a Re–H–Re–Mn bonding sequence is considered to have a significant Re–Re interaction [28,29] and is therefore included.

This survey has been arranged according to groups within the Periodic Table, the metals within each group being dealt with individually as far as possible. Further, for each metal, homo- and heteronuclear complexes have been dealt with in that order. The classification adopted for heteronuclear complexes has been in terms of a "structure controlling" atom or group of atoms, i.e. the atom or group of atoms assumed to most influence the structure of the overall cluster when compared to homonuclear analogues. In practical terms this very often amounts to being the metal atom or group of atoms bonded to the most other metal atoms, e.g. in an open triangular arrangement of metal atoms (see Fig. 3) this would be the central metal atom rather than one of the two outer metal atoms. The classification of heteronuclear complexes is elaborated upon more fully in the text. However, a comprehensive listing of all acyclic clusters including heteronuclear complexes is also given in tables in the relevant sections to facilitate cross-referencing.

Finally, it should be stressed that although an attempt has been made to provide a comprehensive survey of currently known acyclic cluster complexes, the main objective has been to delineate the different types of complexes known to date. The literature has been surveyed up to and including 1984.

## B. SURVEY ACCORDING TO METAL

### *(i) Titanium, zirconium and hafnium*

There is at present no evidence that the elements of Group IV readily form complexes containing metal–metal bonds [5–8] and relatively few clusters of titanium, zirconium or hafnium are known. As far as we are aware, there have, to date, been no reports on acyclic clusters involving these elements *.

---

* It has recently come to our attention that the complex $[(\eta^5\text{-}C_5H_5)_2Zr\{(\eta^5\text{-}C_5H_5)Ru(CO)_2\}_2]$ has been synthesized and structurally characterized (C.P. Casey, R.F. Jordan and A.L. Rheingold, Organometallics, 3 (1984) 504).

### *(ii) Vanadium, niobium and tantalum*

#### *(a) Vanadium*

Very few metal clusters containing a vanadium atom are known [5–8], and to date there have been no reports of acyclic clusters containing vanadium pertinent to this review.

#### *(b) Niobium*

Niobium, in contrast to vanadium, does form metal clusters, but generally of the type where the metal is in a high oxidation state, e.g. $[\{Nb_6Cl_{12}\}Cl_6]^{2-}$, and usually with either octahedral or triangular metal frameworks [8]. There are no acyclic clusters of niobium in which the metal could be considered to be structure controlling, and relatively few complexes, e.g. $[M(CO)_4\{(\eta^5\text{-}C_5H_5)_2Nb(CO)\}_2(\mu_2\text{-}H)_2]$ (M = Mo, W) [30] containing niobium as part of an acyclic cluster unit, have been reported. Discussion on such complexes is, however, deferred to later Sections (B.(iii)(b) and (c), B(vii)(a–c)) as the structures are best considered in terms of the central molybdenum and tungsten, and nickel, palladium and platinum atoms.

#### *(c) Tantalum*

The cluster chemistry of tantalum is closely related to that of niobium; most complexes reported to date contain the metal in a high oxidation state with octahedral or triangular metal frameworks being the rule rather than the exception [8]. Only one complex relevant to this review, $[\{(\eta^5\text{-}C_5H_5)_2Ta(CO)\}\{Mn_2(CO)_9\}(\mu_2\text{-}H)]$ [31], containing a tantalum atom as part of the metal framework has been reported (see Section B.(iv)(a) and Fig. 23).

### *(iii) Chromium, molybdenum and tungsten*

#### *(a) Chromium*

The paucity of data on chromium suggests that this metal has little propensity for forming clusters [5–8], and correspondingly there are few acyclic cluster complexes containing a chromium atom relevant to this

TABLE 1

Acyclic cluster complexes of chromium

| Formula | Complex | Fig. | Ref. [a] |
|---|---|---|---|
| $[(\eta^5\text{-}C_5H_5)_2Cr_2Fe(\mu_2\text{-}SBu^t)(CO)_3(\mu_3\text{-}S)_2]$ | **(1)** | 4 | 32* |
| $[\{(\eta^5\text{-}C_5H_5)Cr(CO)_3\}\{\overline{Pd(NMe_2C_6H_4C}H_2)\}_2(\mu_2\text{-}Cl)]$ | **(2)** | – | 33 |

[a] References marked with an asterisk refer to crystal structure determinations.

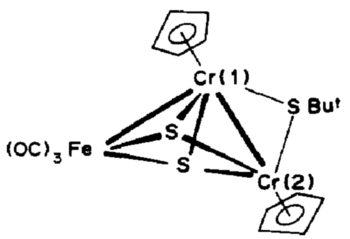

Fig. 4.

review. Two complexes have a chromium atom which may be considered to play a structure controlling role, while the remaining acyclic complexes generally have groups such as $\{(\eta^5\text{-}C_5H_5)Cr(CO)_3\}$ present as the termini in a multimetallic complex (Table 1) (see for example Sections B.(vii)(b) and (c)).

The photochemical reaction between the complex $[(\eta^5\text{-}C_5H_5)_2Cr_2(\mu_2\text{-}SBu^t)_2(\mu_2\text{-}S)]$ and iron pentacarbonyl in tetrahydrofuran yields, after purification by column chromatography, a complex of stoichiometry $[(\eta^5\text{-}C_5H_5)_2Cr_2Fe(SBu^t)(CO)_3(S)_2]$, (**1**), in 72% yield [32]. The structure of this molecule has been determined [32] (Fig. 4); the trimetal core consists of a bent Fe–Cr–Cr framework face-bridged by two sulfur atoms with the Cr–Cr edge bridged by a SBu$^t$ group (Fe–Cr(1) = 2.726, Cr(1)–Cr(2) = 2.707, Fe $\cdots$ Cr(2) = 3.110 Å; Fe–Cr(1)–Cr(2) = 71.88°). The structure of this molecule is closely related to those determined for $[Fe_3(CO)_9(\mu_3\text{-}X)_2]$ type molecules (see Section B.(v)(a) and Fig. 27) and can be viewed as a heterometallic substitution product of $[Fe_3(CO)_9(\mu_3\text{-}S)_2]$ where the unit $\{(\eta^5\text{-}C_5H_5)_2Cr_2(\mu_2\text{-}SBu^t)\}$ replaces a $\{Fe_2(CO)_6\}$ unit.

The dinuclear palladium(II) complex $[\{Pd(NMe_2C_6H_4CH_2)(\mu_2\text{-}Cl)\}_2]$ reacts with $Na[(\eta^5\text{-}C_5H_5)Cr(CO)_3]$ at room temperature to give a complex of stoichiometry $[\{(\eta^5\text{-}C_5H_5)Cr(CO)_3\}\{Pd(NMe_2C_6H_4CH_2)\}_2(\mu_2\text{-}Cl)]$, (**2**) [33]. On the basis of its spectroscopic properties it has been assigned a structure containing a bent Pd–M–Pd unit, analogous to that of $[\{(\eta^5\text{-}C_5H_5)Mo(CO)_3\}\{Pd(NMe_2CH_2C_6H_4)\}_2(\mu_2\text{-}Cl)]$ which was characterized by X-ray crystallography [33,34] (see Section B.(iii)(b), Fig. 7).

### *(b) Molybdenum*

There is only one example of a homonuclear acyclic molybdenum complex published to date. Heating the formally triple metal–metal bonded complex $[\{(\eta^5\text{-}C_5H_5)Mo(CO)_2\}_2]$ with ethyl diazoacetate in boiling toluene gives a dark green, air-stable crystalline complex of stoichiometry $[(\eta^5\text{-}C_5H_5)_3Mo_3(CO)_4(N)(O)]$, (**3**), in 5% yield [35]. The X-ray crystal structure of (**3**) has been determined [35] (Fig. 5). The most unusual feature of this molecule is the bridging nitrogen atom which is almost co-planar with the

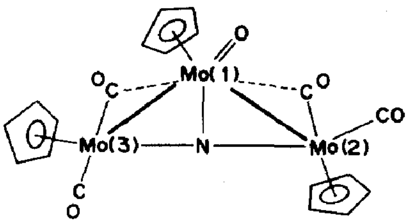

$Mo_3$ plane and has an essentially T-shaped coordination geometry (Mo(2)–N–Mo(3) = 171.8°, Mo(1)–N–Mo(3) = 93.8°, Mo(1)–N–Mo(2) = 94.4° (average values, two crystallographically independent molecules)). The averaged Mo–Mo bond lengths (Mo(1)–Mo(2) = 2.851 Å, Mo(1)–Mo(3) = 2.848 Å] are at the lower end of the range observed for Mo–Mo single bonds (generally 2.7–3.2 Å). The averaged Mo(2)–Mo(1)–Mo(3) angle is 84.5°. Another unusual feature of this molecule is the presence of molybdenum atoms in both the (formal) II and IV oxidation states. This complex is thought to be formed by a mechanism involving an intermediate that involves bridging of the Mo≡Mo unit in $[\{(\eta^5\text{-}C_5H_5)Mo(CO)_2\}_2]$ by $CH(CO_2Et)N_2$ coordinating through both the nitrogen and the ketonic oxygen atoms to molybdenum [35].

Feasey and Knox [36] have also obtained (3) by heating $[(\eta^5\text{-}C_5H_5)Mo(CO)_2(NO)]$ together with $[\{(\eta^5\text{-}C_5H_5)Mo(CO)_3\}_2]$ at 200°C. Sig-

TABLE 2

Acyclic cluster complexes of molybdenum

| Formula | Complex | Fig. | Ref. [a] |
|---|---|---|---|
| $[(\eta^5\text{-}C_5H_5)_3Mo_3(CO)_4(N)(O)]$ | **(3)** | 5 | 35*,36 |
| $[(\eta^5\text{-}C_5H_5)_3Mo_2W(CO)_4(N)(O)]$ | – | – | 36 |
| $[(\eta^5\text{-}C_5H_5)_3MoW_2(CO)_4(N)(O)]$ | **(4)** | 6 | 36 |
| $[\{(\eta^5\text{-}C_5H_5)Mo(CO)_3\}\{Pd(NMe_2CH_2C_6H_4)\}_2(\mu_2\text{-}Cl)]$ | **(5)** | 7 | 33,34* |
| $[\{(\eta^5\text{-}C_5H_5)Mo(CO)_3\}\{Pd(NMe_2C_6H_4CH_2\}_2(\mu_2\text{-}Cl)]$ | **(6)** | – | 33 |
| $[(\eta^5\text{-}C_5H_5)_2W_2Mo(CO)_4(\mu_2\text{-}CO)_2(\mu_2\text{-}CR)_2](R = C_6H_4Me\text{-}4)$ | **(7)** | 8 | 37*,38* |
| $[MoFe_2(CO)_8(\mu_2\text{-}SBu^t)_4]$ | **(8)** | 9 | 40* |
| $[Mo_3S_9]^{2-}$ | **(9)** | 10 | 41* |
| $[(PPh_3)_3Cu_2MoS_4]$ | **(10)** | 11 | 42* |
| $[(PPh_3)_3Cu_2MoOS_3]$ | **(11)** | 11 | 43* |
| $(AsPh_4)_2[(NC)_2Cu_2MoS_4]$ | **(12)** | 11 | 44*,45* |
| $[Mo(CO)_4\{(\eta^5\text{-}C_5H_5)_2Nb(CO)\}_2(\mu_2\text{-}H)_2]$ | **(13)** | 12 | 30* |

[a] References marked with an asterisk refer to crystal structure determinations.

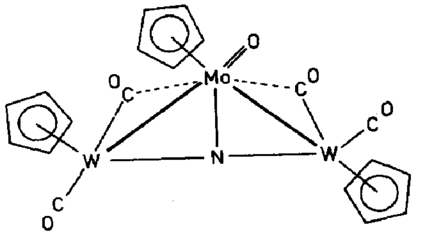

Fig. 6.

nificantly though, isotopic labelling of the nitrosyl ligand ($N^{18}O$) indicated that the oxo ligand in (**3**) is not derived from NO. The reaction was proposed to proceed via the intermediary of $[\{(\eta^5\text{-}C_5H_5)Mo(CO)_2\}_2]$ obtained by decarbonylation of $[\{(\eta^5\text{-}C_5H_5)Mo(CO)_3\}_2]$ under the conditions of the reaction [36].

Several heteronuclear acyclic clusters of molybdenum, where the molybdenum atom occupies a central, structure controlling position, have been synthesized (Table 2).

One, the complex $[(\eta^5\text{-}C_5H_5)_3MoW_2(CO)_4(N)(O)]$, (**4**), has been synthesized by heating either $[(\eta^5\text{-}C_5H_5)Mo(CO)_2(NO)]$ with $[\{(\eta^5\text{-}C_5H_5)W(CO)_3\}_2]$ or $[(\eta^5\text{-}C_5H_5)W(CO)_2(NO)]$ with $[\{(\eta^5\text{-}C_5H_5)Mo(CO)_3\}_2]$ at 300°C [36]. The analogue $[(\eta^5\text{-}C_5H_5)_3Mo_2W(CO)_4(N)(O)]$ is also obtained as a product of these reactions. The structure of (**4**) is proposed to be similar to that of (**3**) except that it contains the heterometallic W–Mo–W core (Fig. 6).

The dinuclear palladium(II) complex $[\{Pd(NMe_2CH_2C_6H_4)(\mu_2\text{-}Cl)\}_2]$ reacts readily at room temperature with $Na[(\eta^5\text{-}C_5H_5)Mo(CO)_3]$ to give a red solution from which black crystals were obtained. Microanalytical and spectroscopic data are consistent with the formulation $[\{(\eta^5\text{-}C_5H_5)Mo(CO)_3\}\{Pd(NMe_2CH_2C_6H_4)\}_2(\mu_2\text{-}Cl)]$, (**5**), which has been confirmed by X-ray crystallography [33,34]. The bent Pd–Mo–Pd framework (Pd–Mo–Pd

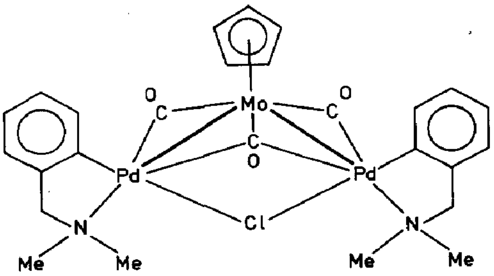

Fig. 7.

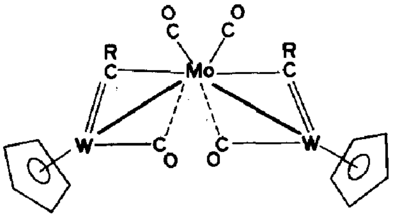

Fig. 8.

= 70.43°) has both Pd–Mo bonds (average bond length 2.810 Å) bridged by a single carbonyl group while the third carbonyl ligand triply bridges the trimetal unit; the chloro ligand bridges the open edge of the cluster [33,34] (Fig. 7). The closely related complex $[\{(\eta^5\text{-}C_5H_5)Mo(CO)_3\}\{Pd(NMe_2C_6H_4CH_2)\}_2(\mu_2\text{-}Cl)]$, (**6**), analogous to the chromium complex (**2**) has also been synthesized [33], and on the basis of its spectroscopic properties assigned a structure similar to that determined for (**5**).

The reaction of $[Mo(CO)_3(NCMe)_3]$ with $[(\eta^5\text{-}C_5H_5)W(CO)_2(\equiv CR)]$ (R $= C_6H_4Me\text{-}4$) in boiling hexane gives the purple crystalline material $[(\eta^5\text{-}C_5H_5)_2W_2Mo(CO)_4(\mu_2\text{-}CO)_2(\mu_2\text{-}CR)_2]$, (**7**), [37,38]. X-ray crystallography [37,38] has shown the molecule to possess a bent W–Mo–W framework (W–Mo–W = 148.2°) with an average Mo–W bond length of 2.938 Å. Each metal–metal bond is bridged by a $\{CC_6H_4Me\text{-}4\}$ group, and a semi-bridging carbonyl ligand (Fig. 8). The structure of (**7**) is thus closely related to that of $[(\eta^5\text{-}C_5H_5)_2W_2Pt(CO)_4(\mu_2\text{-}CR)_2]$ ($R = C_6H_4Me\text{-}4$) [39] by the isolobal mapping $\{Mo(CO)_2\} \leftarrow\!\circ\!\rightarrow \{C^{4+}\} \leftarrow\!\circ\!\rightarrow \{Pt(O)\}$. Complex (**7**) reacts with carbon monoxide to give initially the heterobimetallic complex $[(\eta^5\text{-}C_5H_5)MoW(CO)_7(\mu_2\text{-}CR)]$ and ultimately the mononuclear species $[Mo(CO)_6]$ and $[(\eta^5\text{-}C_5H_5)W(CO)_2(\equiv CR)]$. These reactions are best regarded as a stepwise displacement of $\{(\eta^5\text{-}C_5H_5)W(CO)_2(\equiv CR)\}$ units from (**7**) by carbon monoxide [37,38].

The novel molybdenum–iron thiolate complex $[MoFe_2(CO)_8(\mu_2\text{-}SBu^t)_4]$, (**8**), has recently been reported to be the major product of the reaction between $[Mo(SBu^t)_4]$ and $[Fe_2(CO)_9]$ [40]. The molecular structure of (**8**) has been determined by X-ray crystallography [40] (Fig. 9). The average Fe–Mo bond length is 2.757 Å and the Fe–Mo–Fe angle is 160.43°. Unlike many other molecules containing open structures of metal–metal bonds, this

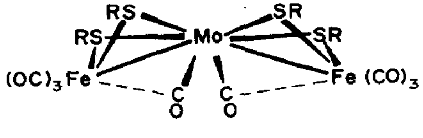

Fig. 9.

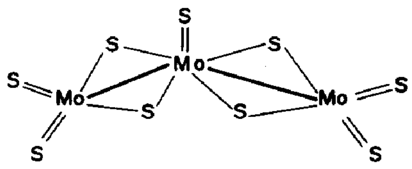

Fig. 10.

complex shows remarkable thermal stability and a variable temperature $^1H$ NMR study was performed in toluene-$d_8$ up to 110°C. At room temperature two singlets were observed for the t-butyl protons of the thiolato ligands which are observed to coalesce at approximately 70°C. The authors attribute this phenomenon to the equilibration of each pair of t-butyl substituents, but it could equally well be explained by an equilibration of the two semi-bridging carbonyl ligands by an intramolecular site exchange mechanism.

There have been several reports of molecules with all molybdenum, or central, structure controlling molybdenum atoms in which the presence of formal metal–metal bonds is less certain. In almost all examples, the molecules contain bridging sulfur ligands usually together with terminal sulfur or oxygen atoms. Brief references to a representative number of these cases are included below.

The dianion $[Mo_3S_9]^{2-}$, (**9**), has been synthesized in 77% yield by heating $(NH_4)_2MoS_4$ in *N,N*-dimethylformamide [41]. A single crystal structure determination has been carried out (see Fig. 10) but due to disorder of the central molybdenum atom and its terminal sulfido ligand the structure was refined over two sites with relative occupancies of 0.88 and 0.12. Thus two Mo–Mo–Mo bond angles were determined (155.0, 157.0°) and two sets of Mo–Mo bond lengths (2.982, 2.924 Å and 2.802, 3.082 Å) were obtained. Electronic considerations suggest the Mo $4d_{xy}$ orbital of the central metal atom lies along the Mo–Mo axis as do the $4d_{z^2}$ orbitals of the terminal molybdenum atoms. This, and the close proximity of the molybdenum atoms suggests some measure of bonding interaction between the metal atoms, although in the words of the authors [41], "lines between molybdenum atoms do not necessarily imply that metal–metal bonding is present". It should further be noted that there are a number of tungsten complexes closely related to the anion $[Mo_3S_9]^{2-}$ (see Section B.(iii)(c)) where similar bonding considerations would also apply.

The heteronuclear complexes $[(PPh_3)_3Cu_2MoS_4]$, (**10**), [42], $[(PPh_3)_3Cu_2MoS_3O]$, (**11**), [43] and $(AsPh_4)_2[(NC)_2Cu_2MoS_4]$, (**12**), [44,45], have been synthesized and structurally characterized (see Fig. 11). They generally consist of a Cu–Mo–Cu unit linked by bridging sulfido ligands. Although the Cu–Mo internuclear distances are typically in the range 2.63–2.79 Å,

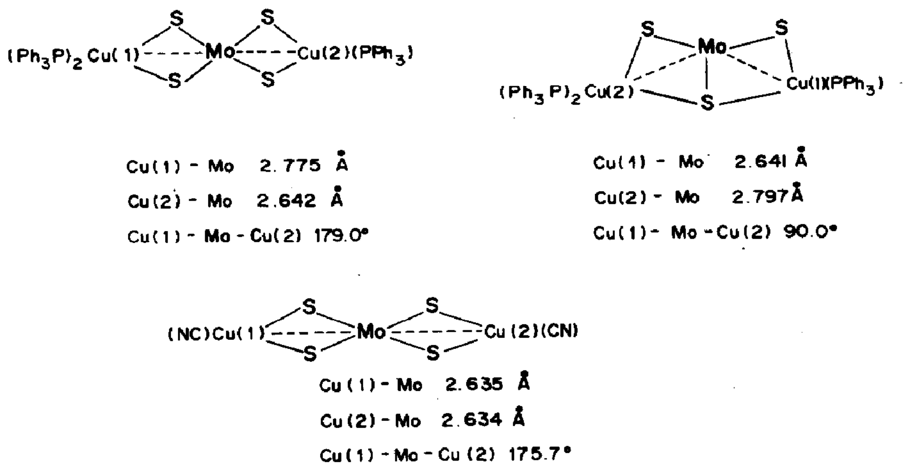

Fig. 11.

there is uncertainty about the degree of interaction between the metal atoms.

Finally, the complex $[Mo(CO)_4\{(\eta^5\text{-}C_5H_5)_2Nb(CO)\}_2(\mu_2\text{-}H)_2]$, (**13**), [30] has been synthesized from $[(\eta^5\text{-}C_5H_5)_2Nb(BH_4)]$ and $[Mo(CO)_5(THF)]$ and structurally characterized by X-ray crystallography [30] (see Fig. 12). The Mo–Nb internuclear distances of 3.579 and 3.565 Å are unusually large suggesting that direct Nb–Mo bonding may be absent. The presence, however, of hydride bridges between the molybdenum and niobium atoms suggests that indirect metal–metal bonding, namely via a Mo–H–Nb three-centre two-electron interaction, is a possibility [29]. The reasonable Mo–H (2.04, 2.06 Å) and Nb–H (1.83, 1.75 Å) distances and the non-linear Mo–H–Nb disposition (141.0, 133.1°) would serve to support this contention [29].

### *(c) Tungsten*

Acyclic cluster complexes are more numerous for tungsten than for either molybdenum or chromium (see Table 3). This is to be attributed to the great variety of organometallic complexes of tungsten containing an acyclic

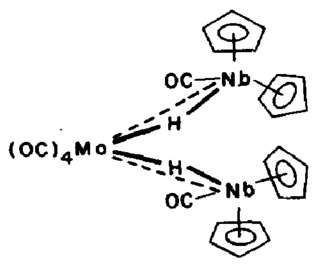

Fig. 12.

TABLE 3

Acyclic cluster complexes of tungsten

| Formula | Complex | Fig. | Ref.[a] |
|---|---|---|---|
| $[(\eta^5\text{-}C_5H_5)_2W_3(CO)_4(\mu_2\text{-}CO)_2(\mu_2\text{-}CR)_2]$ (R = $C_6H_4Me\text{-}4$) | **(14)** | – | 37,38 |
| $[(\eta^5\text{-}C_5H_5)Pt_2W(CO)_4(PR'_3)(\mu_3\text{-}CR)]$ (R = $C_6H_4Me\text{-}4$; R′ = alkyl or aryl) | **(15)** | 13 | 47* |
| $[\{(\eta^5\text{-}C_5H_5)W(CO)_2(\mu_3\text{-}CR)\}\{(\eta^5\text{-}C_5Me_5)Cu\}_2]$ (R = $C_6H_4Me\text{-}4$) | **(16)** | 14 | 48,49 |
| $[\{Pt(PMe_3)_2\}\{(\eta^5\text{-}C_5Me_5)Cu\}\{(\eta^5\text{-}C_5H_5)W(CO)_2\}(\mu_3\text{-}CR)]$ (R = $C_6H_4Me\text{-}4$) | **(17)** | 15 | 48,49* |
| $[Pt\{(\eta^5\text{-}C_5H_5)W(CO)_2\}_2\{(\eta^5\text{-}C_5Me_5)Cu\}_2(\mu_3\text{-}CR)_2]$ (R = $C_6H_4Me\text{-}4$) | **(18)** | 16 | 49 |
| $[Pt\{(\eta^5\text{-}C_5H_5)W(CO)_2\}_2\{Pt(COD)\}(\mu_2\text{-}CR)(\mu_3\text{-}CR)]$ (R = $C_6H_4Me\text{-}4$) | **(19)** | – | 26* |
| $[\{(\eta^5\text{-}C_5H_5)W(CO)_2\}_3Pt_2(\mu_2\text{-}CR)_2(\mu_3\text{-}CR)]$ (R = $C_6H_4Me\text{-}4$) | **(20)** | – | 26 |
| $[\{(\eta^5\text{-}C_5H_5)W(CO)_2\}_2Pt(\mu_2\text{-}CR)_2]$ (R = $C_6H_4Me\text{-}4$) | **(21)** | – | 26* |
| $[\{(\eta^5\text{-}C_5H_5)W(CO)_2\}_2Pt\{Pt(COD)\}_2(\mu_3\text{-}CR)_2]$ (R = $C_6H_4Me\text{-}4$) | **(22)** | – | 26 |
| $[Pt\{(\eta^5\text{-}C_5H_5)W(CO)_2\}_2\{Pt(PMe_2Ph)_2\}(\mu_2\text{-}CR)(\mu_3\text{-}CR)]$ (R = $C_6H_4Me\text{-}4$) | – | – | 26 |
| $[W_3(CO)_{10}(\mu_2\text{-}SR)_4]$ (R = alkyl or aryl) | **(23)** | 17 | 50* |
| $[(\eta^7\text{-}C_7H_7)W(\mu_2\text{-}ER')_3W(CO)(\mu_2\text{-}ER)_2W(CO)_4]$ (E = S, Se; R = alkyl or aryl) | **(24)** | 18 | 51*,52* |
| $[W_3S_9]^{2-}$ | **(25)** | 19 | 41,53* 54,55* 56,57 |
| $[W_3OS_8]^{2-}$ | **(26)** | 19 | 41,54, 56*,57, 58* |
| $[W\{Au(PMePh_2)\}_2(\mu_2\text{-}S)_4]$ | **(27)** | – | 59* |
| $[W\{Ag(PPh_3)_2\}\{Ag(PPh_3)\}\{\mu_2\text{-}S)_4]$ | **(28)** | – | 60* |
| $[W\{FeCl_2\}_2(\mu_2\text{-}S)_4]^{2-}$ | **(29)** | – | 61,62 |
| $[W(CO)_4\{(\eta^5\text{-}C_5H_5)_2Nb(CO)\}_2(\mu_2\text{-}H)_2]$ | **(30)** | – | 30 |

[a] References marked with an asterisk refer to crystal structure determinations.

framework of metal atoms that have recently been reported. Most of these complexes have been synthesized by Stone and co-workers, and the emphasis on tungsten based complexes is due to the extensive use of the carbyne complex $[(\eta^5\text{-}C_5H_5)W(CO)_2(\equiv CR)]$ (R = $C_6H_4Me\text{-}4$) as a cluster building-block [46].

The labile, tris(acetonitrile) complex $[W(CO)_3(NCMe)_3]$, reacts readily with $[(\eta^5\text{-}C_5H_5)W(CO)_2(\equiv CR)]$ (R = $C_6H_4Me\text{-}4$) to give the tri-tungsten complex $[(\eta^5\text{-}C_5H_5)_2W_3(CO)_4(\mu_2\text{-}CO)_2(\mu_2\text{-}CR)_2]$, **(14)**, [37,38] which probably has a structure similar to the heteronuclear analogue $[(\eta^5\text{-}C_5H_5)_2W_2\text{-}$

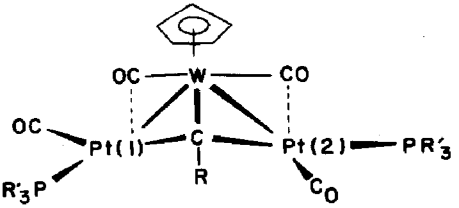

Fig. 13.

$Mo(CO)_4(\mu_2\text{-}CO)_2(\mu_2\text{-}CR)_2]$ [37,38] (see Fig. 8) and the closely related complex $[(\eta^5\text{-}C_5H_5)_2W_2Pt(CO)_4(\mu_2\text{-}CR)_2]$ ($R = C_6H_4Me\text{-}4$) [39] both of which have been characterized crystallographically (see Section B.(vii)(c)).

The trinuclear complexes $[(\eta^5\text{-}C_5H_5)Pt_2W(CO)_4(PR'_3)(\mu_3\text{-}CR)]$ (**15**; $PR'_3 = PMe_3$, $PMe_2Ph$, $PMePh_2$, $PPh_3$, $PEt_3$; $R = C_6H_4Me\text{-}4$) have been obtained by treating toluene solutions of the dinuclear compounds $[(\eta^5\text{-}C_5H_5)PtW(CO)_2(PR'_3)_2(\mu_2\text{-}CR)]$ with carbon monoxide [47]. An X-ray diffraction study has been carried out on one of these compounds ($PR'_3 = PMePh_2$) [47] (Pt(1)–W = 2.785 Å, Pt(2)–W = 2.785 Å, Pt(1) · · · Pt(2) = 2.989 Å, Pt(1)–W–Pt(2) = 64.9°). The metal atoms form a $Pt_2W$ triangle with a long Pt · · · Pt distance consistent with little or no direct metal–metal bonding (see Fig. 13). The metal triangle is capped by the $\{CC_6H_4Me\text{-}4\}$ group. The terminal phosphine and carbonyl ligands on each platinum atom are unsymmetrically *transoid* with respect to the Pt · · · Pt vector, and the two carbonyl ligands on the tungsten atom are unsymmetrically, semi-bridging to the platinum atoms [47].

The highly reactive reagent $[(\eta^5\text{-}C_5Me_5)Cu(THF)]$ has been utilized in synthesizing the heteronuclear complexes $[\{(\eta^5\text{-}C_5H_5)W(CO)_2\}\{(\eta^5\text{-}C_5Me_5)Cu\}_2(\mu_3\text{-}CR)]$, (**16**), and $[\{Pt(PMe_3)_2\}\{(\eta^5\text{-}C_5Me_5)Cu\}\{(\eta^5\text{-}C_5H_5)W(CO)_2\}(\mu_3\text{-}CR)]$, (**17**), ($R = C_6H_4Me\text{-}4$) [48,49]. Reaction of $[(\eta^5\text{-}C_5H_5)W(CO)_2(\equiv CR)]$ ($R = C_6H_4Me\text{-}4$) with excess $[(\eta^5\text{-}C_5Me_5)Cu(THF)]$ gave (**16**), characterized spectroscopically (Fig. 14). The dinuclear complex $[\{(\eta^5\text{-}C_5Me_5)Cu\}\{(\eta^5\text{-}C_5H_5)W(CO)_2\}(\mu_2\text{-}CR)]$ is proposed by the authors to be a possible intermediate in this reaction, although no evidence for its

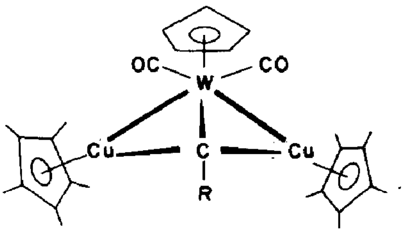

Fig. 14.

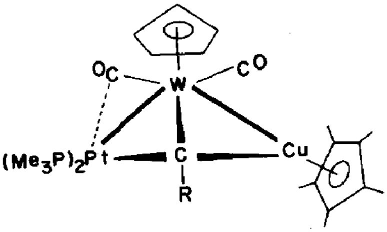

Fig. 15.

existence was obtained. The isolobal relationship between the fragments $\{(\eta^5\text{-}C_5Me_5)Cu\}$ and $\{Pt(PMe_3)_2\}$ is the basis for the synthesis of complex (**17**). Thus, treatment of $[\{Pt(PMe_3)_2\}\{(\eta^5\text{-}C_5H_5)W(CO)_2\}(\mu_2\text{-}CR)]$ with excess $[(\eta^5\text{-}C_5Me_5)Cu(THF)]$ gave $[\{Pt(PMe_3)_2\}\{(\eta^5\text{-}C_5Me_5)Cu\}\{(\eta^5\text{-}C_5H_5)W(CO)_2\}(\mu_3\text{-}CR)]$, (**17**), [49] in 62% yield. The X-ray crystal structure of (**17**) has been determined [49]. The molecule has an open Pt–W–Cu core (Pt–W–Cu = 62.2°). The Pt–W bond (2.779 Å) is bridged by a semi-bridging carbonyl ligand, while the carbyne ligand caps all three metal atoms (Fig. 15). The Cu–W bond length is 2.648 Å.

The reagent $[(\eta^5\text{-}C_5Me_5)Cu(THF)]$ has also been used to synthesize a pentanuclear complex containing a $Pt\{WCu\}_2$ core [49]. Thus, reaction of the unsaturated complex $[Pt\{(\eta^5\text{-}C_5H_5)W(CO)_2\}_2(\mu_2\text{-}CR)_2]$ with $[(\eta^5\text{-}C_5Me_5)Cu(THF)]$ yields, after work-up, red-brown microcrystals of $[Pt\{(\eta^5\text{-}C_5H_5)W(CO)_2\}_2\{(\eta^5\text{-}C_5Me_5)Cu\}_2(\mu_3\text{-}CC_6H_4Me\text{-}4)_2]$, (**18**). This complex is unstable in solution, but solid state IR and the $^{13}C$ and $^{1}H$ NMR spectra (measured at −30°C) are consistent with the proposed structure (see Fig. 16).

Stone and co-workers [26] have recently published the synthesis of further tetra- and pentanuclear acyclic clusters containing one or more tungsten atoms in the metal atom sequence, and utilizing alkylidyne carbon atoms to link the chain. These complexes are closely related to (**18**). When $[Pt(COD)_2]$ (COD = cycloocta-1,5-diene) is reacted with $[(\eta^5\text{-}C_5H_5)W(CO)_2(\equiv CR)]$ (R = $C_6H_4Me\text{-}4$) (1 : 1 molar ratio), the major product of the reaction is $[Pt\{(\eta^5\text{-}$

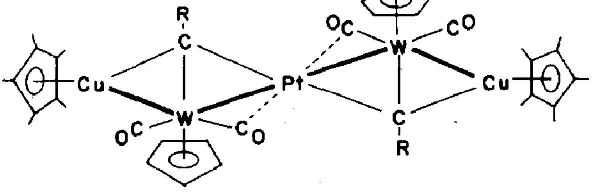

Fig. 16.

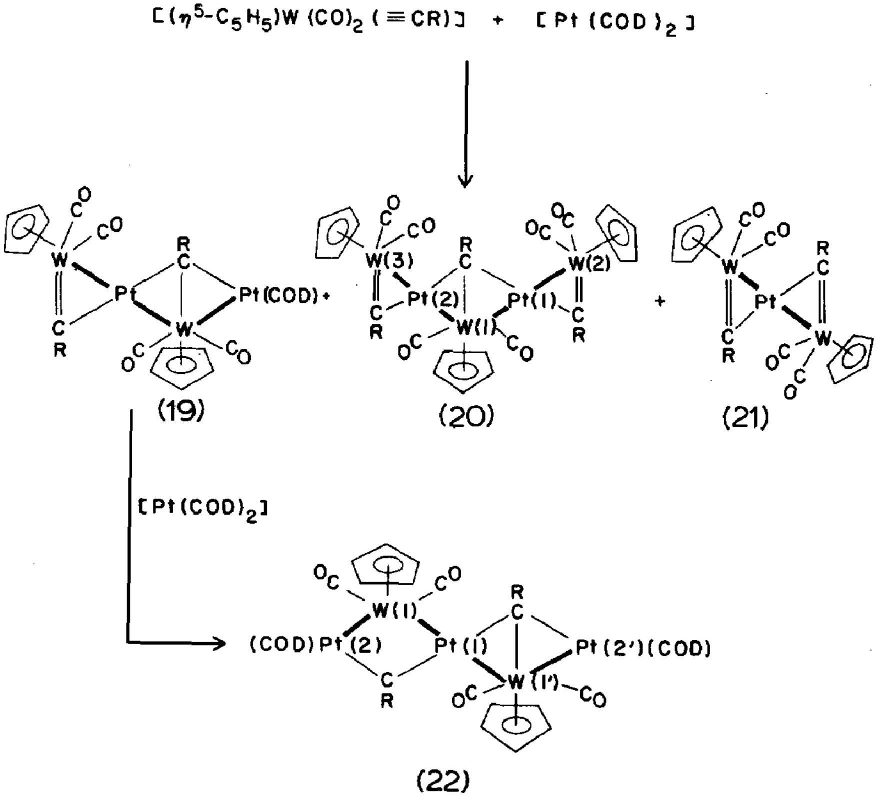

Scheme 1.

$C_5H_5)W(CO)_2\}_2\{Pt(COD)\}(\mu_2\text{-}CR)(\mu_3\text{-}CR)]$, (**19**), together with smaller amounts of the pentanuclear complex $[\{(\eta^5\text{-}C_5H_5)W(CO)_2\}_3Pt_2(\mu_2\text{-}CR)_2(\mu_3\text{-}CR)]$, (**20**), and the trinuclear complex $[\{(\eta^5\text{-}C_5H_5)W(CO)_2\}_2Pt(\mu_2\text{-}CR)_2]$, (**21**), (Scheme 1). Treatment of (**21**) with $[Pt(COD)_2]$ (1 : 1 molar ratio) also gives (**19**) which further reacts with $[Pt(COD)_2]$ to give the triplatinum-ditungsten complex $[\{(\eta^5\text{-}C_5H_5)W(CO)_2\}_2Pt\{Pt(COD)\}_2(\mu_3\text{-}CR)_2]$, (**22**). The cycloocta-1,5-diene ligand in (**19**) is readily displaced by $PMe_2Ph$ to give $[Pt\{(\eta^5\text{-}C_5H_5)W(CO)_2\}_2\{Pt(PMe_2Ph)_2\}(\mu_2\text{-}CR)(\mu_3\text{-}CR)]$, while similar displacement with $[(\eta^5\text{-}C_5H_5)W(CO)_2(\equiv CR)]$ affords (**20**).

The complexes (**20**) and (**22**) have been characterized by X-ray crystallography [26] confirming the acyclic metal core structure of these complexes (**20**: Pt(1)–W(1) = 2.773 Å, Pt(1)–W(2) = 2.718 Å, Pt(2)–W(1) = 2.723 Å, Pt(2)–W(3) = 2.713 Å, Pt(1) · · · Pt(2) = 2.949 Å, W(1)–Pt(2)–W(3) = 154.5°, W(1)–Pt(1)–W(2) = 149.0°, Pt(1)–W(1)–Pt(2) = 64.9°; **22**: Pt(1)–W(1) = 2.751 Å, Pt(2)–W(1) = 2.748 Å, Pt(1) · · · Pt(2) = 3.089 Å, Pt(1)–W(1)–Pt(2) = 68.4°, W(1)–Pt(1)–W(1′) = 176.0°). The Pt–W bonds in both complexes are semi-bridged by carbonyl ligands. In (**20**) two of the $\{CC_6H_4Me\text{-}4\}$

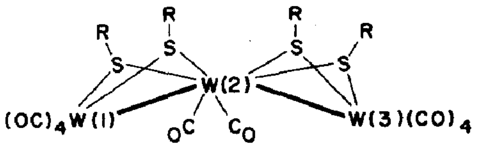

Fig. 17.

units are doubly bridging and one is triply bridging while in (**22**) both $\{CC_6H_4Me\text{-}4\}$ units are triply bridging.

A series of unusual acyclic trinuclear tungsten complexes $[W_3(CO)_{10}(\mu_2\text{-}SR)_4]$ (**23**; R = Me, Et, Pr$^i$, Ph) have been synthesized by the photochemical reaction of thiols (RSH) or disulfides (RSSR) with $[W(CO)_6]$ [50]. The dinuclear complexes $[\{W(CO)_4(\mu_2\text{-}SR)\}_2]$ are by-products of these reactions. The X-ray crystal structure of $[W_3(CO)_{10}(\mu_2\text{-}SPh)_4]$ has been determined [50], showing the tri-tungsten unit to be bent (W–W–W = 130.6°) with an average W–W bond length of 3.021 Å. The W–W bonds are each bridged by two thiolato ligands (Fig. 17).

A closely related series of complexes has been obtained from the reaction of $[(\eta^7\text{-}C_7H_7)W(CO)_2I]$ with the thiolates $Pb(SR)_2$ (R = Bu$^n$, Bu$^t$) or the selenol $C_6H_5SeH$ [51]. The tri-tungsten complexes $[(\eta^7\text{-}C_7H_7)W(\mu_2\text{-}ER)_3W(CO)(\mu_2\text{-}ER)_2W(CO)_4]$, (**24**: E = S, R = Bu$^n$, Bu$^t$; E = Se, R = Ph) were separated from the dinuclear complexes $[(\eta^7\text{-}C_7H_7)W(\mu_2\text{-}ER)_3W(CO)_3]$ by a combination of column and thin layer chromatography and characterized by elemental analysis and spectroscopic methods [51,52]. The X-ray crystal structure of $[(\eta^7\text{-}C_7H_7)W(\mu_2\text{-}SBu^n)_3W(CO)(\mu_2\text{-}SBu^n)_2W(CO)_4]$ has confirmed the formulation of these products [51,52] (Fig. 18). The bent tri-tungsten core has a W–W–W bond angle of 141.45°. The W–W bond lengths (W(1)–W(2) = 3.084 Å, W(1)–W(3) = 2.913 Å) are normal for W–W single bond lengths; the shorter bond is bridged by three n-butylthiolato ligands, and the longer one by two.

Tungsten forms an extensive series of both homo- and heteronuclear sulfido bridged complexes that are closely related to the molybdenum sulfide bridged complexes. Certain examples, usually obtained by the interaction of low oxidation state transition metal complexes with tungsten sulfur complexes, unambiguously contain metal–metal bonds (see above) but there

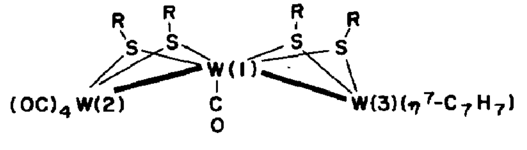

Fig. 18.

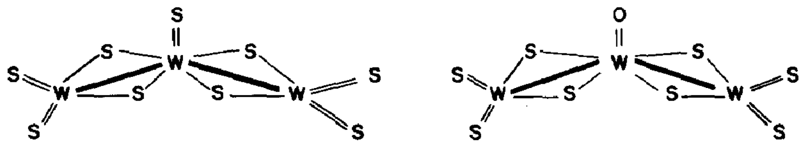

(a) (b)

Fig. 19.

are a large number of borderline cases where the extent of and indeed the existence of metal–metal interactions, is not at all clear. Several of these species will be briefly referred to below.

The dianion $[\mathrm{W_3S_9}]^{2-}$, (**25**), (Fig. 19(a)), has been obtained as the $\mathrm{Ph_4P^+}$ or $\mathrm{Ph_4As^+}$ salts from $(\mathrm{NH_4})_2\mathrm{WS_4}$ by treatment with HF followed by cation exchange, or alternatively, by heating a stirred mixture of $(\mathrm{NH_4})_2\mathrm{WS_4}$ and $\mathrm{Ph_4PCl}$ at 250°C under nitrogen [53,54]. These salts have been characterized by elemental analysis, and by IR and UV-VIS spectroscopy. The X-ray structure of $(\mathrm{PPh_4})_2[\mathrm{W_3S_9}]$ has been determined [53,55] but refinement was hampered by a severely disordered* central {W=S} unit. The dianion is proposed [54] to be stabilized by metal–metal interactions between the tungsten atoms, and analogous arguments put forward for the molybdenum analogue $[\mathrm{Mo_3S_9}]^{2-}$ [41] could be used to support this suggestion. Improved methods of synthesis of the dianion $[\mathrm{W_3S_9}]^{2-}$ [41] and a mechanism for its formation by the pyrolysis of $(\mathrm{R_4N})_2(\mathrm{WS_4})$ [57] have recently been published.

The closely related oxooctathiotritungstate anion $[\mathrm{W_3OS_8}]^{2-}$, (**26**), (Fig. 19(b)) has been obtained as a product of the acidification of an aqueous solution of $[\mathrm{WS_4}]^{2-}$ [54], probably by the reaction of $[\mathrm{W_3S_9}]^{2-}$ with air [41]. Indeed, recrystallization of salts containing the $[\mathrm{W_3S_9}]^{2-}$ dianion has been reported to give $[\mathrm{W_3OS_8}]^{2-}$ [57]. The X-ray crystal structure determination of $(\mathrm{Bu^n_4N})_2[\mathrm{W_3OS_8}]$ has been reported [56,58]. In the space group *Pc*, three asymmetric molecules per unit cell were refined. Each unit consisted of a bent W–W–W unit with an average W–W bond length of 2.97 Å. The short W–W internuclear distance would again, analogous to the $[\mathrm{W_3S_9}]^{2-}$ case, suggest some measure of bonding between the tungsten atoms.

A wide variety of heteronuclear complexes have been synthesized using the $\{\mathrm{WS_4^{2-}}\}$ group as the central, structure-controlling unit. Not surprisingly, these complexes are structurally, formally analogous to the $[\mathrm{M_3XS_8}]^{2-}$

---

* It has recently been suggested [56] that the problems of refinement relate to the crystal used in the analysis not being single.

(M = Mo, W; X = O, S) complexes, and have the general formulation $[M'(\mu_2\text{-}S)_2W(\mu_2\text{-}S)_2M'']$ (M′, M″ = transition metal containing fragment).

For example, the complexes $[W\{Au(PMePh_2)\}_2(\mu_2\text{-}S)_4]$, **(27)**, [59], $[W\{Ag(PPh_3)_2\}\{Ag(PPh_3)\}(\mu_2\text{-}S)_4]$, **(28)**, [60] and $[W\{FeCl_2\}_2(\mu_2\text{-}S)_4]^{2-}$, **(29)**, [61,62] have been reported; the X-ray crystal structures of the first two molecules have been determined, while the molybdenum analogue of the third [61,62] has also been structurally characterized.

For completeness it should also be noted that the $WS_4^{2-}$ and $WOS_3^{2-}$ anions can also act as ligands to a central metal ion giving complexes of the type $[SXW(\mu_2\text{-}S)_2M(\mu_2\text{-}S)_2WSX]^{2-}$ (X = O,S; M = Ni, Co) [63,64]. These compounds will, however, not be further considered.

Finally, the complex $[W(CO)_4\{(\eta^5\text{-}C_5H_5)_2Nb(CO)\}_2(\mu_2\text{-}H)_2]$, **(30)**, has been synthesized from $[(\eta^5\text{-}C_5H_5)_2Nb(BH_4)]$ and $[W(CO)_5(THF)]$ [30]. The structure of this molecule is proposed to be similar to that of the corresponding molybdenum complex (see Section B.(iii)(b), Fig. 12) which has been characterized by X-ray crystallography [30].

### *(iv) Manganese and rhenium*

#### *(a) Manganese*

The homonuclear manganese anion $[Mn_3(CO)_{14}]^-$, **(31)**, was first reported in 1972 as the unexpected product of the reaction between triphenylchlorosilane and $[Mn(CO)_5]^-$ [65] (see Table 4). On the basis of its IR spectrum this complex was assigned a bent $\{(CO)_5Mn\text{–}Mn(CO)_4\text{–}Mn(CO)_5\}$ framework. The same product has subsequently also been obtained by treatment of the triangular cluster $[H_3Mn_3(CO)_{12}]$ with base in alcohol solution [66]; crystallization from ethanol gave low yields of $[Mn_3(CO)_{14}]^-$ isolated as the $AsPh_4^+$ salt. The anion $[Mn_3(CO)_{14}]^-$ has also been observed, together with $[Mn(CO)_5]^-$ as the product of the electrochemical reduction of $[Mn_2(CO)_{10}]$ in *N,N*-dimethylformamide [67]. An X-ray structure determination [66] has shown the anion to possess a linear tri-manganese core (Mn–Mn (mean) = 2.895 Å) with each manganese atom

TABLE 4

Acyclic cluster complexes of manganese

| Formula | Complex | Fig. | Ref. [a] |
|---|---|---|---|
| $[Mn_3(CO)_{14}]^-$ | **(31)** | 20 | 65,66*,67 |
| $[Mn_3(CO)_{12}(N_2Me)]$ | **(32)** | 21 | 68*,69* |
| $[Mn_3(CO)_{11}(PC_6H_8)]$ | **(33)** | 22 | 70,71* |
| $[\{(\eta^5\text{-}C_5H_5)_2Ta(CO)\}\{Mn_2(CO)_9\}(\mu_2\text{-}H)]$ | **(34)** | 23 | 31* |

[a] References marked with an asterisk refer to crystal structure determinations.

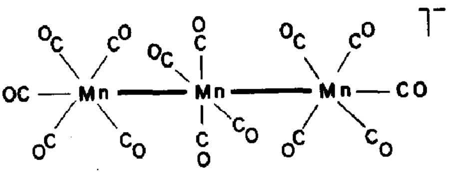

Fig. 20.

possessing pseudo-octahedral geometry and the carbonyl ligands on the central manganese atom being staggered with respect to the equatorial carbonyl ligands on the terminal manganese atoms (Fig. 20). The equatorial carbonyl ligands on the terminal manganese atoms are significantly bent inwards towards the central metal atom (C(axial)–Mn–C(equatorial) = 96.4° (mean value)). The structure of this anion is thus closely analogous to that of the isolectronic heterometallic trinuclear complex $[Mn_2Fe(CO)_{14}]$ (see Section B.(v)(a)).

The reaction between $[HMn(CO)_5]$ and diazomethane carried out at low temperature has given a complex possessing the unusual stoichiometry $[Mn_3(CO)_{12}(N_2Me)]$, (**32**), [68,69]. An X-ray crystal structure determination has revealed a bent tri-manganese skeleton (Mn–Mn–Mn = 107.4°) with manganese–manganese internuclear distances typical of single bonds (Mn(1)–Mn(2) = 2.826 Å, Mn(2)–Mn(3) = 2.807 Å). Surprisingly, the diazomethane moiety remains as an intact unit, with the two nitrogen atoms coordinating across all three manganese atoms; the terminal nitrogen atom of the ligand coordinates to two metal atoms, while the central nitrogen atom ligates only one manganese atom (Fig. 21).

Another trinuclear manganese complex containing a bent tri-manganese core, $[Mn_3(CO)_{11}(PC_6H_8)]$, (**33**), has been synthesized by the reaction of $[Mn_2(CO)_{10}]$ with 1-phenyl-3,4-dimethylphosphole [70,71]. This product was originally erroneously formulated as $[Mn_3(CO)_{12}(PC_6H_8)]$ [70], but a crystal structure determination [71] has unambiguously established its correct composition. The $Mn_3$ framework (Mn(1)–Mn(2) = 3.053 Å, Mn(1)–Mn(3) = 2.917 Å, Mn(3)–Mn(1)–Mn(2) = 99.8°) supports the phospholyl ligand system which forms bonds (via phosphorus) to Mn(3) and Mn(1), and π-bonds

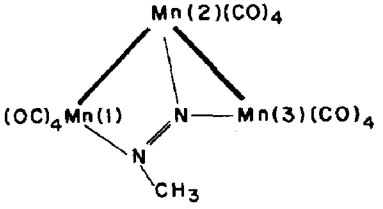

Fig. 21.

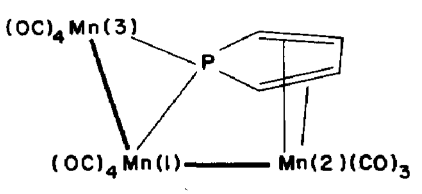

Fig. 22.

to Mn(2) (Fig. 22). This molecule may best be considered to be derived from the anion $[Mn_3(CO)_{14}]^-$ by the substitution of three carbonyl groups and phosphometallation at the central manganese atom.

The photo-induced reaction between equimolar amounts of $[(\eta^5\text{-}C_5H_5)_2TaH_3]$ and $[Mn_2(CO)_{10}]$ at 0°C gives a red solution which on prolonged cooling deposits large purple crystals [31]. An X-ray crystal structure determination [31] has revealed this product to be the complex $[\{(\eta^5\text{-}C_5H_5)_2Ta(CO)\}\{Mn_2(CO)_9\}(\mu_2\text{-}H)]$, (**34**), containing an open $Mn_2Ta$ core with a Ta–Mn(1)–Mn(2) bond angle of 108.09° (Fig. 23). The Mn(1)–Mn(2) bond length (2.938 Å) is a typical single bond value, while the hydride bridged Ta–Mn(1) bond (3.441 Å) is consistent with a Ta–H–Mn(1) three-centre, two-electron bonding interaction [29]. The red intermediate observed as the first product of this reaction has been proposed [31] to be an isomer of the purple product, possibly containing a linear trinuclear framework. Suitable crystals of this compound have, however, not been obtained and the resolution of this problem awaits further developments.

### *(b) Rhenium*

The tri-rhenium complex $[HRe_3(CO)_{14}]$, (**35**), (Table 5) was first obtained as one of the products of the acidification of $Na[Re(CO)_5]$ [72], and has subsequently also been prepared by a variety of other procedures [73–75]. The structure of this molecule was initially proposed on the basis of $^1H$ NMR and IR spectroscopic data and its chemical reactivity [76], to have a

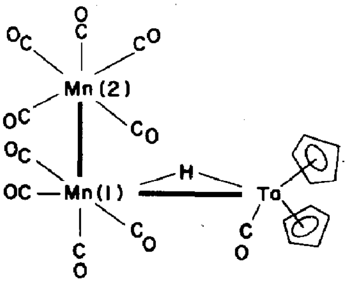

Fig. 23.

TABLE 5

Acyclic cluster complexes of rhenium

| Formula | Complex | Fig. | Ref. [a] |
|---|---|---|---|
| $[HRe_3(CO)_{14}]$ | **(35)** | – | 72–76,77* |
| $[HMnRe_2(CO)_{14}]$ | **(36)** | 24 | 72,74*,77* |
| $[HMn_2Re(CO)_{14}]$ | **(37)** | – | 72,78* |
| $[Re_3(CO)_{13}(COSiPh_3)]$ | **(38)** | 25 | 80* |
| $[(\eta^5\text{-}C_5H_5)Re_2Mo(CO)_8(\mu_3\text{-}S)\{\mu_3\text{-}SMo(\eta^5\text{-}C_5H_5)(CO)_3\}]$ | **(39)** | 26 | 81* |

[a] References marked with an asterisk refer to crystal structure determinations.

linear arrangement of rhenium atoms $\{(CO)_5Re–Re(CO)_4–Re(CO)_5\}$ with the hydrido ligand bridging two rhenium atoms [72,73]. In a synthesis analogous to that for $[HRe_3(CO)_{14}]$, the mixed metal derivatives $[HMnRe_2(CO)_{14}]$, **(36)**, and $[HMn_2Re(CO)_{14}]$, **(37)**, have also been obtained [72]. X-ray crystal structure determinations of $[HMnRe_2(CO)_{14}]$ [74,77] and $[HRe_3(CO)_{14}]$ [28,78] have resolved the question of structure for these complexes. The compound **(36)** has a non-linear arrangement of metal atoms (Re–Re–Mn = 98.1°) with a Re–Mn bond length of 2.960 Å. The rhenium–rhenium internuclear distance is 3.39 Å, a value ca. 10% longer than that expected for a normal Re–Re single bond (cf. $[Re_2(CO)_{10}]$ where Re–Re = 3.041 Å [79]), and it is inferred that the hydride ligand bridges these two atoms (Fig. 24). A three-centre, two-electron bonding interaction would best describe the Re–H–Re arrangement [28,29]. A brief mention of the X-ray structure of $[HRe_3(CO)_{14}]$ has confirmed that this molecule also has a bent trimetallic framework, and that similar bonding considerations would also apply [28,78]. The observation of bent $Re_2Mn$ and $Re_3$ frameworks for these molecules is remarkable, considering that the anionic parent $[MnRe_2(CO)_{14}]^-$ would be predicted to have a linear structure analogous to the related $[Mn_3(CO)_{14}]^-$. These complexes may, however, be considered to

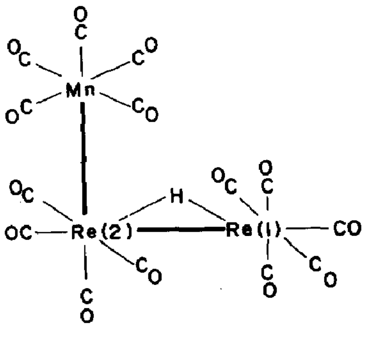

Fig. 24.

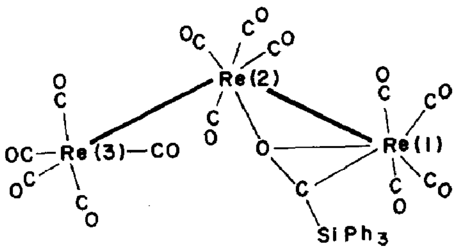

Fig. 25.

be closely related to the heteronuclear complex $[\{(\eta^5\text{-}C_5H_5)_2Ta(CO)\}\{Mn_2\text{-}(CO)_9\}(\mu_2\text{-}H)]$, **(34)**, (see Section B.(iv)(a)).

One other homonuclear complex of rhenium is pertinent to this review. The complex $[Re_3(CO)_{13}(COSiPh_3)]$, **(38)**, was obtained in low yield, and as one of several products, from the reaction of $[Re_2(CO)_{10}]$ with $LiSiPh_3$ and $CH_3FSO_3$ [80]. The structure of this complex has been determined by X-ray crystallography [80] showing the molecule to possess a non-linear tri-rhenium unit (Re(1)–Re(2) = 3.088 Å, Re(2)–Re(3) = 3.085 Å, Re(1)–Re(2)–Re(3) = 128.98°). The most striking feature of this molecule is, however, the unusual ligand system $\{Ph_3SiCO\}$ found bridging two of the rhenium atoms, as an $\eta^2$-acyl ligand to Re(1), and bonding to Re(2) through the oxygen atom only (Fig. 25).

Finally, an acyclic trinuclear $MoRe_2$ framework has been observed in the complex $[(\eta^5\text{-}C_5H_5)Re_2Mo(CO)_8(\mu_3\text{-}S)\{(\mu_3\text{-}S)Mo(\eta^5\text{-}C_5H_5)(CO)_3\}]$, **(39)**, prepared in high yield from $[\{Re(CO)_4(SSnMe_3)\}_2]$ and $[(\eta^5\text{-}C_5H_5)Mo(CO)_3Cl]$ [81] (Fig. 26). Interesting features of this molecule include the presence of both six- and seven-coordinate rhenium atoms, and the occurrence of both tri-metal and tetra-metal coordinated sulfur atoms. The metal–metal bond lengths were found to be 2.985 Å (Re–Re) and 2.909 Å (Re–Mo) with the Mo–Re–Re bond angle being 83.56° [81].

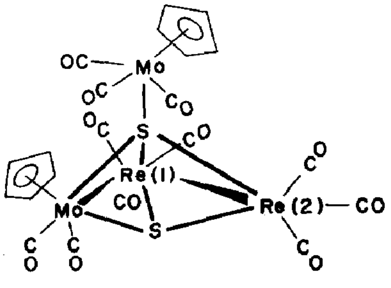

Fig. 26.

### (v) *Iron, ruthenium and osmium*

#### (a) *Iron*

The complexes of general formula $[Fe_3(CO)_{9-n}L_n(\mu_3\text{-}X)(\mu_3\text{-}Y)]$ ($n = 0$–$3$; L = CO, group V donor ligand etc.; X, Y = S, Se, Te etc.) in which the tri-iron framework defines an open triangle capped by two triply bridging ligand systems, form the largest class of acyclic iron cluster complexes, and in fact the largest class of acyclic clusters in general (see Table 6). The ubiquity of the $\{Fe_3(\mu_3\text{-}X)(\mu_3\text{-}Y)\}$ framework is emphasised by the remarkable variation in the capping ligand groups X and Y, and by the narrow ranges that cover important structural parameters such as the Fe–Fe, Fe–X and Fe–Y bond lengths and the Fe–Fe–Fe bond angles.

The parent complexes of this structural class, $[Fe_3(CO)_9(\mu_3\text{-}X)_2]$ (X = S, Se, Te) were first reported by Hieber and Gruber in 1958 [82], although earlier (incorrect) formulations almost certainly referred to these complexes [83]. In their 1958 publication, Hieber and Gruber reacted the anion $[Fe(CO)_4]^{2-}$ with sulfurous, selenous and tellurous acids and isolated products with the stoichiometry $[Fe_3(CO)_9X_2]$ (**40–42**; X = S, Se, Te respectively). The exact identity and properties of these complexes, and in particular those of $[Fe_3(CO)_9S_2]$, were called into question by King in 1963 [84]. In this publication the structure of $[Fe_3(CO)_9S_2]$ (and by implication that of the other members of the series) was proposed to consist of an open triangle of iron atoms, face bridged by the two S atoms with each iron atom further ligated by three terminal carbonyl groups (Fig. 27).

The spectral and physical discrepancies between Hieber's and King's compounds were later resolved by Harlin and Knox [83] and also by Wei and Dahl [85]. The X-ray crystal structures of (**40**)–(**42**) have been determined [85–87] (complex (**40**) was a 1 : 1 mixture with $[Fe_2(CO)_6(\mu_2\text{-}S)_2]$) confirming King's proposals [84] for the structure of these complexes (Fig. 27). The average Fe–Fe (bonding) and Fe···Fe (non-bonded) distances increase in the order S < Se < Te ((**40**) 2.60 and 3.37 Å, (**41**) 2.65 and 3.51 Å, (**42**) 2.741 and 3.771 Å). Also, as might be expected, the average Fe–X bond

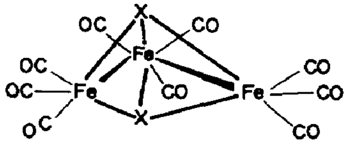

(X = S, Se, Te)

Fig. 27.

TABLE 6

Acyclic cluster complexes of iron

| Formula | Complex | Fig. | Ref. [a] |
|---|---|---|---|
| $[Fe_3(CO)_9(\mu_3\text{-}S)_2]$ | **(40)** | 27 | 82–84,85*,<br>88–94,96,<br>97,115,120 |
| $[Fe_3(CO)_9(\mu_3\text{-}Se)_2]$ | **(41)** | – | 82,83,86*,<br>96,97 |
| $[Fe_3(CO)_9(\mu_3\text{-}Te)_2]$ | **(42)** | – | 82,83,87*,<br>95–97 |
| $[Fe_3(CO)_9(\mu_3\text{-}S)(\mu_3\text{-}Se)]$ | **(43)** | – | 97,99 |
| $[Fe_3(CO)_9(\mu_3\text{-}S)(\mu_3\text{-}Te)]$ | **(44)** | – | 97,99 |
| $[Fe_3(CO)_9(\mu_3\text{-}Se)(\mu_3\text{-}Te)]$ | **(45)** | – | 97,99 |
| $[Fe_3(CO)_9(\mu_3\text{-}ER)_2]$ (E = P, As, Sb; R = alkyl or aryl) | **(46)** | 29 | 90,100,<br>101*,102,<br>103,104 |
| $[Fe_3(CO)_{9-n}L_n(\mu_3\text{-}PPh)_2]$ ($n$ = 1–3; L = group V donor ligand) | – | – | 100,104* |
| $[Fe_3(CO)_9(\mu_3\text{-}AsPh)_2]$ | **(47)** | – | 105*,106* |
| $[Fe_3(CO)_9(\mu_3\text{-}N\text{–}N{=}CPh_2)_2]$ | **(48)** | 30 | 107*,108* |
| $[Fe_3(CO)_9(NCH_3)_2]$ | **(49)** | 31 | 109,110* |
| $[Fe_3(CO)_9(\mu_3\text{-}S)(\mu_3\text{-}SO)]$ | **(50)** | 32 | 112*,113–115 |
| $[Fe_3(CO)_9(\mu_3\text{-}S)(\mu_3\text{-}ER)]$ (E = P, As; R = alkyl or aryl) | **(51)**,**(52)** | 33 | 90,114*,<br>116–118 |
| $[Fe_3(CO)_9(\mu_3\text{-}ER)\{\mu_3\text{-}SM(CO)_5\}]$ (E = P, As; R = alkyl or aryl; M = Cr, W) | **(53)** | 34 | 118* |
| $[Fe_2Mn(CO)_9(\mu_3\text{-}S)\{\mu_3\text{-}SMn(CO)_5\}]$ | **(54)** | 35 | 119* |
| $[Fe_3(CO)_9(\mu_3\text{-}S)(\mu_3\text{-}NC_6H_4Me\text{-}4)]$ | **(55)** | 36 | 92,93* |
| $[Fe_3(CO)_9(\mu_3\text{-}S)\{\mu_3\text{-}\overline{CS(CH)_2S}\}]$ | **(56)** | 37 | 120 * |
| $[Fe_3(CO)_9(\mu_3\text{-}CMe)(\mu_3\text{-}OMe)]$ | **(57)** | 38 | 121,122* |
| $[Fe_3(CO)_9(\mu_2\text{-}X)(\mu_3\text{-}SR)]$ (X = Cl, $PR'_2$, $AsR'_2$, $SbR'_2$, SR$'$, SeR$'$; R, R$'$ = alkyl or aryl) | **(58)**–**(61)** | 39 | 123*,124* |
| $[Fe_3(CO)_9(SBu^t)_2]$ | **(62)** | 40 | 88,89 |
| $[Fe_3(CO)_{9-n}L_n(\mu_3\text{-}X)(\mu_3\text{-}Y)]$ ($n$ = 1–3; X, Y = S, Se, Te; L = group V donor ligand) | – | – | 96–99,125 |
| $[Fe_3(CO)_8(C_3Ph_2)(\mu_3\text{-}S)_2]$ | **(63)** | 44 | 127* |
| $[Fe_3(CO)_8(C_3H_2S_2)(\mu_3\text{-}S)_2]$ | **(64)** | 45 | 128* |
| $[(f_4fars)Fe_3(CO)_9]$ ($f_4fars$ = $Me_2AsC{=}\overline{C(AsMe_2)CF_2C}F_2$) | **(65)** | 47 | 129,130*,<br>131* |
| $[\{As_2(CH_3)_2CH_2\}Fe_3(CO)_9]$ | **(66)** | 48 | 129 |
| $[(f_4asp)Fe_3(CO)_9]$ ($f_4asp$ = $Ph_2PC{=}\overline{C(AsMe_2)CF_2C}F_2$) | **(67)** | 49 | 132* |
| $[Fe_3(CO)_8(PhC_2Ph)_2]$ | **(68)** | 50 | 133* |
| $[Fe_3(CO)_7\{Ph_2PC_4(CF_3)_2\}PPh_2]$ | **(69)** | – | 134,135*,<br>136* |

TABLE 6 (continued)

| Formula | Complex | Fig. | Ref. [a] |
|---|---|---|---|
| $[\mathrm{Fe_3(CO)_7(\mu_2\text{-}SRS)}]$ ($\mathrm{R = (CH_2)_n}$; $n = 2, 3$) | **(70)** | 51 | 137* |
| $[\mathrm{Fe_3(CO)_8(\mu_3\text{-}\eta^6\text{-}C_6H_4CH_2NC_6H_5\text{-}2)}]$ | **(71)** | 52 | 138* |
| $[\mathrm{Fe_3\{\mu_3\text{-}\eta^6\text{-}C_6H_4CH_2N(N{=}CHC_6H_5)\text{-}2\}(CO)_8}]$ | **(72)** | 54 | 139 |
| $[\mathrm{Fe\{Fe(CO)_5\}_2](SbF_6)_2}$ | – | – | 140 |
| $[\mathrm{Fe(CO)_4(AuPPh_3)_2}]$ | **(73)** | – | 142* |
| $[\mathrm{Fe(CO)_4\{(triars)M\}_2}]$ (triars $=$ 1,1,1-$\mathrm{(Me_2AsCH_2)_3\text{-}CCH_3}$, $\mathrm{(Me_2AsC_6H_4\text{-}2)_2AsCH_3}$; M = Cu, Ag) | **(74)**,**(75)** | – | 143 |
| $[\mathrm{\{Fe(CO)_4\}\{AuPh_2PC_6H_4\cdot C_6H_4PPh_2Au\}}]$ | **(76)** | 55 | 144 |
| $[\mathrm{\{Fe(CO)_4\}\{Pt(py)_2Cl\}_2}]$ | **(77)** | – | 145 |
| $[\mathrm{MM'Fe(CO)_{14}}]$ (M, M′ = Mn, Re) | **(78)**–**(80)** | 56 | 146–149,150*, 151*, 152–154 |
| $[\mathrm{(\eta^5\text{-}C_5H_5)MFe_2(CO)_6(\mu_3\text{-}Te)_2}]$ (M = Co, Rh) | **(81)** | – | 155,156 |
| $[\mathrm{(\eta^5\text{-}C_5H_5)RhFe_2(CO)_5(PPh_3)(\mu_3\text{-}Te)_2}]$ | – | – | 155 |
| $[\mathrm{(\eta^5\text{-}C_5H_5)MnFe_2(CO)_8L(\mu_3\text{-}PR)}]$ (L = CO, group V donor ligand; R = alkyl or aryl) | **(82)**–**(84)** | 57 | 157*,158–160, 161*,162* |
| $[\mathrm{Fe_2Co(CO)_9(\mu_2\text{-}PRH)(\mu_3\text{-}PR)}]$ (R = alkyl or aryl) | **(85)** | 59 | 103* |
| $[\mathrm{FeRu_2(CO)_8L_2(\mu_2\text{-}Cl)}]$ (L = group V donor ligand) | **(87)** | 60 | 163*,164*,165 |
| $[\mathrm{FeRu_2(CO)_8L_2(\mu_2\text{-}OH)}]$ (L = group V donor ligand) | **(88)** | 61 | 165* |
| $[\mathrm{FeRu_2(CO)_8(dppe)(\mu_2\text{-}Cl)_2}]$ | **(89)** | – | 166 |
| $[\mathrm{Fe_3(CO)_4(NO)_3(\mu_2\text{-}PMe_2)_3}]$ | **(90)** | 62 | 167*,168* |
| $[\mathrm{Fe_2Co(CO)_5(NO)_2(\mu_2\text{-}PMe_2)_3}]$ | **(91)** | 62 | 167*,168* |
| $[\mathrm{\{\overline{Pd(NMe_2CH_2C}_6H_4)\}_2\{Fe(CO)_3(NO)\}(\mu_2\text{-}Cl)}]$ | **(92)** | 63 | 33,34 |

[a] References marked with an asterisk refer to crystal structure determinations.

lengths and Fe–Fe–Fe angles increase in the same order ((**40**) 2.23 Å and 81.0°, (**41**) 2.35 Å and 82.9°, (**42**) 2.532 Å and 86.9°).

A range of synthetic methods for obtaining the complexes $[\mathrm{Fe_3(CO)_9(\mu_3\text{-}X)_2}]$ (X = S, Te) have been published. For instance, $[\mathrm{Fe_3(CO)_9(\mu_3\text{-}S)_2}]$ has been isolated from the reaction of $[\mathrm{Fe_3(CO)_{12}}]$ with $\mathrm{Bu^tSH}$ [88,89] or $\mathrm{RP(S)Cl_2}$ ($\mathrm{R = Ph, C_6H_4Me\text{-}4}$) and metallic magnesium in THF [90], from the reaction of $[\mathrm{Fe_2(CO)_9}]$ with thiobenzophenones [91] or $\mathrm{Bu^tN{=}S{=}NBu^t}$ [92,93], and from the reaction of $[\mathrm{Fe(CO)_5}]$ with bis(fluorocarbonyl)disulfane [94]. While no new routes have apparently been reported for the seleno analogue, the complex $[\mathrm{Fe_3(CO)_9(\mu_3\text{-}Te)_2}]$ has been synthesized by the treatment of $[\mathrm{Fe(CO)_4I_2}]$ with $\mathrm{Na_2Te}$ [87]. Lesch and Rauchfuss [95] have recently reported a more detailed investigation of the Hieber synthesis of $[\mathrm{Fe_3(CO)_9(\mu_3\text{-}Te)_2}]$. Using the synthetic method reported by Hieber and Gruber [82], treatment of a basic solution of $[\mathrm{Fe(CO)_5}]$ with $\mathrm{K_2TeO_3}$ gave a mixture containing primarily $[\mathrm{Fe_3(CO)_9(\mu_3\text{-}Te)_2}]$. Separation of the reaction products by non-aqueous gel permeation chromatography gave $[\mathrm{Fe_3(CO)_9(\mu_3\text{-}Te)_2}]$, (**42**), and $[\mathrm{Fe_2(CO)_6(\mu_2\text{-}Te_2)}]$. Reaction of the latter dinuclear complex with $[\mathrm{Fe(CO)_5}]$ and $\mathrm{Me_3NO}$ gave (**42**) and a complex of stoichiom-

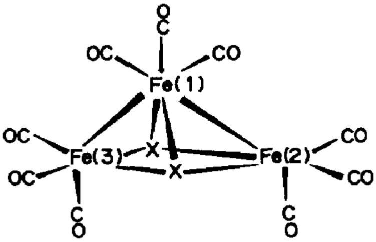

Fig. 28.

etry $[Fe_3(CO)_{10}(Te)_2]$, which was shown by loss of a carbonyl ligand to be an intermediate in the Hieber synthesis of $[Fe_3(CO)_9(\mu_3\text{-}Te)_2]$ [95].

Carbonyl ligand mobility in the complexes $[Fe_3(CO)_9(\mu_3\text{-}X)_2]$ (X = S, Se, Te) has been investigated kinetically by means of both isotopic exchange studies [96] and by $^{13}C$ NMR spectroscopy [97]. Exchange reactions with labelled CO [96] provided clear evidence of a first-order rate of exchange for the complexes $[Fe_3(CO)_9(\mu_3\text{-}X)_2]$ (X = S, Se), whereas for $[Fe_3(CO)_9(\mu_3\text{-}Te)_2]$, an associative component was also detected, viz.

$$[Fe_3(CO)_9(\mu_3\text{-}Te)_2] + CO \rightleftharpoons [Fe_3(CO)_{10}(Te)_2]$$

These results have been corroborated by the investigation of the reactions with other donor ligands, e.g. phosphines [98] (see below). Variable temperature $^{13}C$ NMR studies [97] of $[Fe_3(CO)_9(\mu_3\text{-}X)_2]$ (X = S, Se, Te, NMe) have shown that there are two distinguishable pathways for carbonyl exchange in these molecules. In the first, the carbonyls of the apical iron atom Fe(1) become equivalent, and in the second, those of the basal iron atoms (Fe(2) and Fe(3)) are also equilibrated (Fig. 28).

The mixed ligand complexes $[Fe_3(CO)_9(\mu_3\text{-}X)(\mu_3\text{-}Y)]$ (X, Y = S, Se, Te) have been synthesized by a modification of the Hieber syntheses of $[Fe_3(CO)_9(\mu_3\text{-}X)_2]$. Iron pentacarbonyl was reacted at 0°C in alkaline methanol solution with an equimolar mixture of sodium sulfite and selenite, sodium sulfite and tellurite, and sodium selenite and tellurite [99]. The structures of the complexes $[Fe_3(CO)_9(\mu_3\text{-}S)(\mu_3\text{-}Se)]$, (**43**), $[Fe_3(CO)_9(\mu_3\text{-}S)(\mu_3\text{-}Te)]$, (**44**), and $[Fe_3(CO)_9(\mu_3\text{-}Se)(\mu_3\text{-}Te)]$, (**45**), are presumed to be analogous to those of the parent derivatives. The mechanisms of CO exchange [99], and dynamic properties and solution structures of these complexes have also been reported [97].

The first example of a complex $[Fe_3(CO)_9(\mu_3\text{-}ER)_2]$ (E = P, As, Sb; R = alkyl, aryl) was reported by Treichel et al. [100]. Iron pentacarbonyl and phenylphosphine ($PhPH_2$) were reacted in decalin for 16 h at high temperature. Chromatography followed by crystallization gave red crystals (43% yield) of $[Fe_3(CO)_9(\mu_3\text{-}PPh)_2]$, (**46**), characterized on the basis of elemental

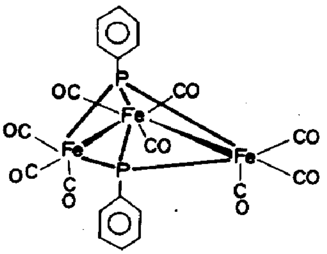

Fig. 29.

analysis and spectroscopic properties [100]. The substituted derivatives $[Fe_3(CO)_{9-n}\{P(OMe)_3\}_n(\mu_3\text{-}PPh)_2]$ ($n = 1$–$3$) were obtained by the reaction of the parent carbonyl complex with $P(OMe)_3$ in boiling xylene [100]. The preparation of $[Fe_3(CO)_9(\mu_3\text{-}PPh)_2]$ by the reaction of $[Fe_3(CO)_{12}]$ with $PPhH_2$ has been reported by Evans and co-workers [101], who have also determined the X-ray crystal structure of this complex [101]. The $Fe_3$ backbone consists of an open triangle of iron atoms (Fe–Fe–Fe = 81.4°, Fe–Fe = 2.717 Å (mean values for two independent molecules)) essentially symmetrically capped by the two $\{\mu_3\text{-}PPh\}$ groups (Fe–P(mean) = 2.218 Å) (Fig. 29). Reaction of the dinuclear complex $[Fe_2(CO)_6(\mu_2\text{-}PHPh)_2]$ with $[Fe_3(CO)_{12}]$ has also given $[Fe_3(CO)_9(\mu_3\text{-}PPh)_2]$ [102,103]; similar reactions of $[Fe_2(CO)_6(\mu_2\text{-}PHR)_2]$ (R = Me, Bu$^t$, $C_6H_4Me$-4) with $[Fe_3(CO)_{12}]$ have given the analogous trinuclear complexes $[Fe_3(CO)_9(\mu_3\text{-}PR)_2]$ [102,103]. The complex $[Fe_3(CO)_9(\mu_3\text{-}PPh)_2]$ has also been isolated in low yield (< 1%) from the reaction of $[Fe_3(CO)_{12}]$ with $PhP(S)Cl_2$ in the presence of metallic magnesium [90].

An extensive series of substituted derivatives of $[Fe_3(CO)_9(\mu_3\text{-}PPh)_2]$ has recently been reported [104]. The thermal and photochemical activation of $[Fe_3(CO)_9(\mu_3\text{-}PPh)_2]$ in acetonitrile or propionitrile has provided the reactive species $[Fe_3(CO)_8(NCR)(\mu_3\text{-}PPh)_2]$ and $[Fe_3(CO)_7(NCR)_2(\mu_3\text{-}PPh)_2]$. The X-ray crystal structure of $[Fe_3(CO)_7(NCMe)_2(\mu_3\text{-}PPh)_2]$ has been determined [104]. The molecule contains a bent tri-iron framework (Fe(1)–Fe(2) = 2.772 Å, Fe(2)–Fe(3) = 2.683 Å, Fe(1) · · · Fe(3) = 3.552 Å, Fe(1)–Fe(2)–Fe(3) = 81.24° (mean values for two crystallographically independent molecules)). An interesting feature of this molecule is the unexpected observation that both nitrile ligands are coordinated on the same (basal) iron atom. The complexes $[Fe_3(CO)_8(NCR)(\mu_3\text{-}PPh)_2]$ and $[Fe_3(CO)_7(NCR)_2(\mu_3\text{-}PPh)_2]$ react readily with a range of donor ligands to give the complexes $[Fe_3(CO)_8(L)(\mu_3\text{-}PPh)_2]$ (L = $PPh_3$, $AsPh_3$, $PF_3$, $P(OMe)_3$) and $[Fe_3(CO)_7(L)_2(\mu_3\text{-}PPh)_2]$ (L = $P(OMe)_3$). A variable temperature $^{13}C$ NMR study of the complex $[Fe_3(CO)_9(\mu_3\text{-}PPh)_2]$ [104] has shown that the carbonyl ligands scramble rapidly on the apical iron atom even at

203 K, whereas the scrambling process on the basal iron atoms is frozen out at this temperature. The difference in the activation energies for scrambling at the different iron sites was explained by the authors in terms of the "nominal seven-coordinate character" of the apical iron site (as compared to the six-coordinate basal sites). Similar variable temperature NMR studies have been performed on several substituted derivatives [104] confirming these observations. It is interesting to note though, that even at elevated temperatures exchange between apical and basal sites was not discernable by NMR spectroscopy.

The corresponding phenylarsenido complex $[Fe_3(CO)_9(\mu_3\text{-AsPh})_2]$, (**47**), was first obtained as an unexpected product of the reaction between $[Fe_2(CO)_9]$ and $[(\eta^5\text{-}C_5H_5)Mn(CO)_2(AsPhCl_2)]$ [105], and then also by the controlled reaction between $Na_2[Fe(CO)_4]$ and $AsPhCl_2$ (yield 4%) [106].The X-ray crystal structure of this molecule has been reported [105,106]. The three iron atoms form an open triangle (Fe–Fe = 2.752, 2.796 Å, Fe · · · Fe = 3.705 Å, Fe–Fe–Fe = 83.82°) face bridged by two $\{\mu_3\text{-AsPh}\}$ groups (Fe–As (mean) = 2.331 Å) [106], and is thus entirely analogous to $[Fe_3(CO)_9(\mu_3\text{-PPh})_2]$ [101] and other $[Fe_3(CO)_9(\mu_3\text{-X})_2]$derivatives.

The first examples of complexes of the type $[Fe_3(CO)_9(\mu_3\text{-X})_2]$ containing nitrogen donors as capping ligands were reported almost simultaneously by Mills and co-workers [107,108], and by Dekker and Knox [109]. The former workers reacted diaryldiazomethanes either with $[Fe(CO)_5]$ under photochemical conditions, or with $[Fe_3(CO)_{12}]$ under thermal conditions [107,108], obtaining two products, one orange and one black. The orange product was characterized as a dinuclear species [108], while the black product has been characterized crystallographically [107] as the complex $[Fe_3(CO)_9(\mu_3\text{-N–N=CPh}_2)_2]$, (**48**). The structure shows the familiar $\{Fe_3(CO)_9\}$ open triangular framework (Fe–Fe (mean) = 2.445 Å, Fe · · · Fe = 3.06 Å, Fe–Fe–Fe = 77.47°) symmetrically capped by two unchanged diphenyldiazomethane molecules (Fe–N (mean) = 1.95 Å) (Fig. 30).

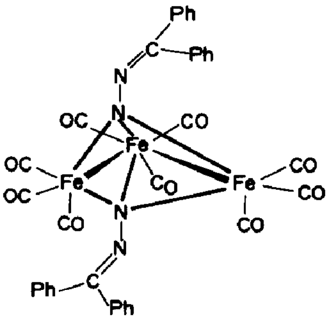

Fig. 30.

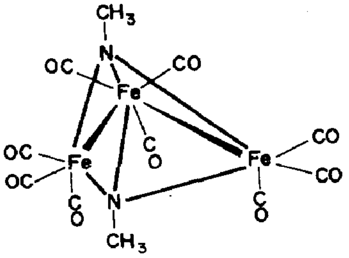

Fig. 31.

Dekker and Knox [109] have investigated the inorganic products of the iron carbonyl catalyzed decomposition of azides. Nitrenes are assumed to be the immediate decomposition product of azides, and indeed these were found as ligands in the iron carbonyl products of the reaction [109]. For instance, methyl azide reacts with $[Fe_2(CO)_9]$ to give an extensive range of products, including one of stoichiometry $[Fe_3(CO)_9(NMe)_2]$, (**49**). The same product was also obtained in good yield from the reaction of $[Fe_2(CO)_9]$ with nitromethane [109]. The X-ray crystal structure of this molecule has been determined [110]. The three iron atoms form an open triangle (Fe–Fe (mean) = 2.462 Å, Fe $\cdots$ Fe = 3.044 Å, Fe–Fe–Fe = 76.4°), essentially symmetrically capped by the triply bridging NMe groups (Fig. 31). Surprisingly, few new complexes of this kind have been reported, and little interest has apparently been shown in their undoubtedly extensive chemistry [111].

In addition to the complexes $[Fe_3(CO)_9(\mu_3\text{-}X)(\mu_3\text{-}Y)]$ (X, Y = S, Se, Te; **43**–**45**) containing different capping groups, a range of other acyclic clusters of iron have been reported. For example, the controlled oxidation of $[Fe(CO)_4]^{2-}$ with $H_2O_2$ and $Na_2SO_3$ has given the unusual hetero-capped complex $[Fe_3(CO)_9(\mu_3\text{-}S)(\mu_3\text{-}SO)]$, (**50**), in 10% yield as dark brown, air-stable crystals [112]. The X-ray crystal structure of (**50**) has been determined [112], and the molecule found to contain the familiar bent arrangement of three iron atoms, in this case, however, capped by a S atom and an SO group (Fe(1)–Fe(2) = 2.623 Å, Fe(2)–Fe(3) = 2.647 Å) (Fig. 32). The triply bridging SO ligand group is significantly closer to Fe(1) and Fe(3) than to Fe(2), while for the capping sulfido ligand the opposite effect is observed. A

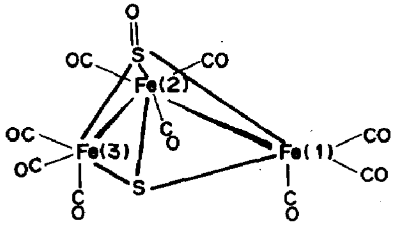

Fig. 32.

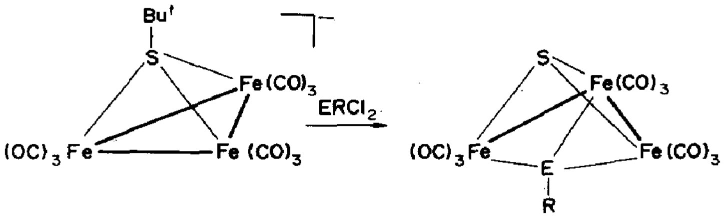

Scheme 2.

further interesting feature of this structure is that the S···S internuclear distance is only 2.72 Å, significantly shorter than the sum of the van der Waals radii of sulfur (3.70 Å), suggesting some measure of S–S interaction, similar to that observed in $[Fe_2(CO)_6(\mu_2\text{-}X)_2]$ type complexes [113]. The complex (**50**) has subsequently also been synthesized by the reaction of the cluster anion $[Fe_3(CO)_9(\mu_3\text{-}SBu^t)]^-$ with $SOCl_2$ [114] and by the oxidation of one of the sulfide capping ligands in $[Fe_3(CO)_9(\mu_3\text{-}S)_2]$ with *m*-chloroperbenzoic acid [115].

Complexes of the type $[Fe_3(CO)_9(\mu_3\text{-}S)(\mu_3\text{-}ER)]$ (E = P, As; R = alkyl, aryl) form the largest class of compounds containing the $\{Fe_3(CO)_9\}$ framework and two different capping ligand systems. Rational syntheses of the acyclic clusters $[Fe_3(CO)_9(\mu_3\text{-}S)(\mu_3\text{-}ER)]$ have been reported by Huttner and co-workers [114]. The clusters anion $[Fe_3(CO)_9(\mu_3\text{-}SBu^t)]^-$ reacts readily with $ERCl_2$, eliminating $Bu^tCl$ and $Cl^-$, to give the complexes $[Fe_3(CO)_9(\mu_3\text{-}S)(\mu_3\text{-}ER)]$ (**51**, E = P, R = Me, Bu$^t$, $C_6H_{11}$, Ph, $C_6H_4Br$-4, $C_6H_4OMe$-4, $NEt_2$; **52**, E = As, R = Bu$^t$, Ph, $C_6H_{11}$) in good yield [114] (Scheme 2). In a similar manner, reaction of $[Fe_3(CO)_9(\mu_3\text{-}PR)]^{2-}$ (obtained by the double deprotonation of $[Fe_3(CO)_9(\mu_2\text{-}H)_2(\mu_3\text{-}PR)]$) with $SCl_2$ has given the same products. The X-ray crystal structures of $[Fe_3(CO)_9(\mu_3\text{-}S)(\mu_3\text{-}EPh)]$ (E = P, As) have been determined [114]. In all respects these structures are essentially identical.

Seyferth and Withers [90] have also published a synthesis of $[Fe_3(CO)_9(\mu_3\text{-}S)(\mu_3\text{-}PR)]$ (**51**; R = Bu$^t$, Ph, $C_6H_4Me$-4). Reaction of $[Fe_3(CO)_{12}]$ with $RP(S)Cl_2$ in the presence of metallic magnesium in THF has given a mixture of the complexes $[Fe_3(CO)_9(\mu_3\text{-}S)(\mu_3\text{-}PR)]$, $[Fe_3(CO)_9(\mu_3\text{-}S)_2]$ and $[Fe_3(CO)_9(\mu_3\text{-}PR)_2]$, all in low yield. In the absence of magnesium, improved yields of $[Fe_3(CO)_9(\mu_3\text{-}S)(\mu_3\text{-}PR)]$ were obtained. A further synthetic route to $[Fe_3(CO)_9(\mu_3\text{-}S)(\mu_3\text{-}PR)]$ complexes involves treatment of $RP(S)Cl_2$ with $Na_2[Fe(CO)_4]$ in ether [116,117]. The complexes $[Fe_3(CO)_9(\mu_3\text{-}S)(\mu_3\text{-}PR)]$ (**51**; R = Me, Ph, $C_6H_4OMe$-4) were prepared in low (6–10%) yield, and two of them (R = Ph, $C_6H_4OMe$-4) structurally characterized [117]; the X-ray structure of the former had, however, already been reported [114]. In all regards the structure of $[Fe_3(CO)_9(\mu_3\text{-}S)(\mu_3\text{-}PC_6H_4OMe\text{-}4)]$ is, however, equivalent to that of the other derivatives

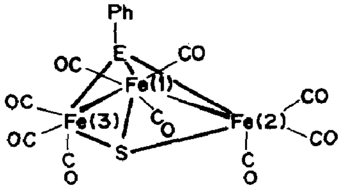

| | E = P | E = As |
|---|---|---|
| Fe(2)-Fe(1)-Fe(3)(°) | 82.8 | 83.2 |
| Fe(2)-Fe(1) (Å) | 2.664 | 2.679 |
| Fe(1)-Fe(3) (Å) | 2.646 | 2.667 |
| Fe(2)........Fe(3)(Å) | 3.511 | 3.555 |

Fig. 33.

(Fe–Fe (mean) = 2.660 Å, Fe $\cdots$ Fe = 3.499 Å, Fe–Fe–Fe = 82.23°) (see Fig. 33).

The complexes $[Fe_3(CO)_9(\mu_3\text{-}S)(\mu_3\text{-}ER)]$ (E = P, As; R = alkyl, aryl) react with $[M(CO)_5(THF)]$ (M = Cr, W) under mild conditions to give the adducts $[Fe_3(CO)_9\{\mu_3\text{-}SM(CO)_5\}(\mu_3\text{-}ER)]$ in good yield [118]. The X-ray crystal structures of $[Fe_3(CO)_9\{\mu_3\text{-}SM(CO)_5\}(\mu_3\text{-}PBu^t)]$ (**53**; M = Cr, W) have been determined [118], and as might have been expected, have proved to be entirely analogous to that of $[Fe_3(CO)_9(\mu_3\text{-}S)(\mu_3\text{-}PPh)]$, except for adduct formation via the triply bridging sulfur atom (Fig. 34).

A bimetallic complex of similar overall structure has also been reported [119]. The photoinduced reaction of $[Fe_2(CO)_6(\mu_2\text{-}S)_2]$ with $[Mn_2(CO)_{10}]$ in THF solution has given a complex of stoichiometry $[Fe_2Mn_2(CO)_{14}S_2]$ [119]. On the basis of X-ray crystallography, Mössbauer and mass spectral data, the structure $[Fe_2Mn(CO)_9\{\mu_3\text{-}SMn(CO)_5\}(\mu_3\text{-}S)]$, (**54**), has been established [119] (Fig. 35). The molecule contains an $Fe_2Mn$ core with one Fe–Fe bond (2.580 Å) and one Fe–Mn bond (2.714 Å); the Fe–Fe–Mn bond angle is 82.90°.

The complex $[Fe_3(CO)_9(\mu_3\text{-}S)(\mu_3\text{-}NC_6H_4Me\text{-}4)]$, (**55**), was isolated from the reaction of $[Fe_2(CO)_9]$ with R–N=S=N–R (R = $C_6H_4Me$-4) [92,93]. The X-ray crystal structure of the complex has been determined [93]; it is analogous to that of $[Fe_3(CO)_9(\mu_3\text{-}S)_2]$ and $[Fe_3(CO)_9(\mu_3\text{-}NR)_2]$ and contains an open triangle of iron atoms (Fe–Fe = 2.51 Å, Fe–Fe–Fe = 78.5° (average values for two independent molecules)) triply bridged by a nitrene (RN) moiety and a sulfur atom (Fig. 36).

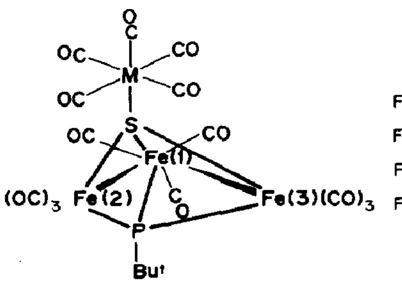

| | M = Cr | M = W |
|---|---|---|
| Fe(2)-Fe(1)-Fe(3)(°) | 81.8 | 81.7 |
| Fe(2)-Fe(1) (Å) | 2.696 | 2.654 |
| Fe(1)-Fe(3)(Å) | 2.652 | 2.677 |
| Fe(2)........Fe(3)(Å) | 3.501 | 3.488 |

Fig. 34.

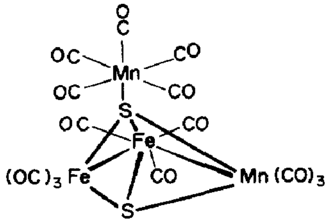

Fig. 35.

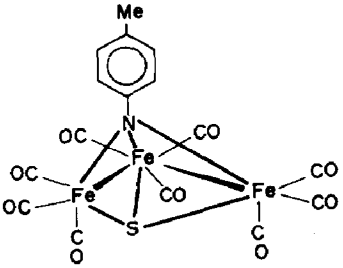

Fig. 36.

Iron pentacarbonyl has been found to react with ethylenetrithiocarbonate under photochemical conditions in a number of ways which lead to $[Fe_3(CO)_9(\mu_3\text{-}S)_2]$, and the major product $[Fe_3(CO)_9(\mu_3\text{-}S)\{\mu_3\text{-}CS(CH_2)_2\text{-}S\}]$, (**56**), [120]. Complex (**56**) has been completely characterized by X-ray crystallography [120] which has revealed a novel dithiocarbene ligand capping an open triangle of iron atoms by forming a methylene bridge between two iron atoms and linking up with the third iron atom via a sulfur atom (Fig. 37). The feature which most clearly manifests the diatomic nature of the $\mu_3$-bridge is the widening of the Fe(2)–Fe(1)–Fe(3) angle to a relatively large 91.4°. Noteworthy too is the inequivalence of the bond lengths between the iron atoms (Fe(1)–Fe(2) = 2.681 Å, Fe(1)–Fe(3) = 2.572 Å).

Finally, an unusual example of an $[Fe_3(CO)_9(\mu_3\text{-}X)(\mu_3\text{-}Y)]$ type complex has been reported by Wilkinson and co-workers [121,122]. The ($\mu_3$-

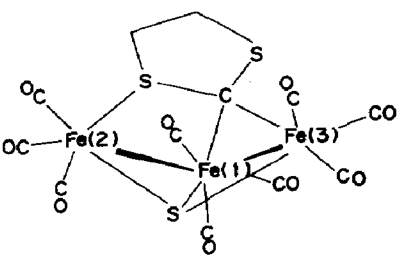

Fig. 37.

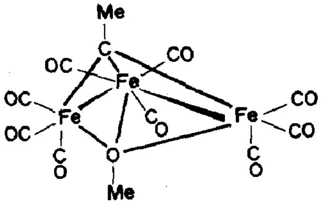

Fig. 38.

acetyl)nonacarbonylferrate (1 − ) ion, $[Fe_3(CO)_9(\mu_3\text{-}MeCO)]^-$, reacts with methyl fluorosulfate at room temperature (reaction time 7 days) to give $[Fe_3(CO)_9(\mu_3\text{-}CMe)(\mu_3\text{-}OMe)]$, (**57**), isolated as dark red crystals. The X-ray structure has been determined [122]. The complex has an open tri-iron structure (50 electrons, $\mu_3$-OMe classed as a five-electron ligand) with Fe–Fe (bonded) interactions of 2.459 and 2.472 Å, and an Fe · · · Fe (non-bonded) interaction of 3.059 Å (Fig. 38).

Closely related to the complexes of general formula $[Fe_3(CO)_9(\mu_3\text{-}X)(\mu_3\text{-}Y)]$ is a class of compounds only recently synthesized, $[Fe_3(CO)_9(\mu_2\text{-}X)(\mu_3\text{-}SR)]$ [123,124]. The cluster anion $[Fe_3(CO)_9(\mu_3\text{-}SBu^t)]^-$ reacts with halogens ($X_2$) and halogenating agents (e.g. *N*-halosuccinimides) to give the neutral, $\mu_2$-halo bridged complexes $[Fe_3(CO)_9(\mu_2\text{-}X)(\mu_3\text{-}SBu^t)]$ (**58**; X = Cl, Br, I) in good yield (Scheme 3). The X-ray crystal structure of $[Fe_3(CO)_9(\mu_2\text{-}Cl)(\mu_3\text{-}SBu^t)]$ has been determined [123]. The tri-iron core of the molecule forms an open triangle of iron atoms (Fe–Fe (mean) = 2.681 Å, Fe · · · Fe = 3.338 Å, Fe–Fe–Fe = 77.0°) with a symmetrical (Fe–Cl (mean) = 2.341 Å) edge-bridging chloro ligand, and a face-bridging $SBu^t$ group. It is interesting to note that the bridging halogeno ligand can be removed from (**58**) by reaction with nucleophiles [123] ($Bu^tO^-$ for X = Cl; $I^-$ or $H^-$ for X = I) leading back to the closed cluster anion $[Fe_3(CO)_9(\mu_3\text{-}SBu^t)]^-$. Reaction of the cyclic cluster $[Fe_3(CO)_9(\mu_3\text{-}SR)]^-$ (R = $Bu^t$, $C_6H_{11}$) with the monohalides XCl (X = $PR'_2$, $AsR'_2$ $SbR'_2$, SR′, SeR′; R′ = alkyl, aryl) gives an extensive range of neutral complexes $[Fe_3(CO)_9(\mu_2\text{-}X)(\mu_3\text{-}SR)]$ [124] (Fig. 39) analogous to the $\mu_2$-halogeno complexes discussed above. The X-ray crystal structures of $[Fe_3(CO)_9(\mu_2\text{-}X)(\mu_3\text{-}SR)]$ (**59**, X = $AsMe_2$, R = $Bu^t$; **60**, X = SPh, R = $C_6H_{11}$; **61**, X = SePh, R = $C_6H_{11}$) have been determined [124]. As expected,

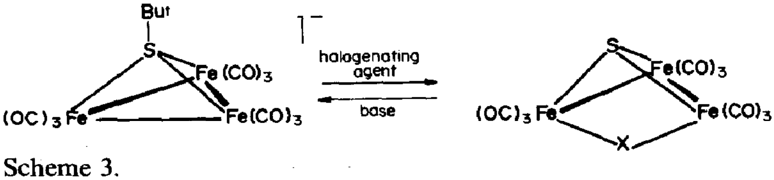

Scheme 3.

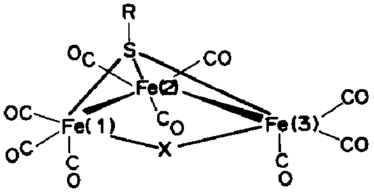

Fig. 39.

all three molecules have very similar structural characteristics. The three iron atoms in each complex are in the form of an open triangle (Fe(1)–Fe(2)–Fe(3) = 81.59° (**59**), 79.1° (**60**), 80.5° (**61**)); the Fe–Fe bond lengths are very similar both within each molecule, and also between molecules (Fe(1)–Fe(3) = 2.713 Å (**59**), 2.692 Å (**60**), 2.703 Å (**61**); Fe(2)–Fe(3) = 2.699 Å (**59**), 2.675 Å (**60**), 2.677 Å (**61**); Fe(1) · · · Fe(3) = 3.526 Å (**59**), 3.419 Å (**60**), 3.475 Å (**61**)). In all three molecules the $\mu_2$-bridging ligand symmetrically spans the open edge of the triangle (Fe–As (mean) = 2.377 Å; Fe–S (mean) = 2.331 Å; Fe–Se (mean) = 2.443 Å) while the $\mu_3$-SR group is symmetrically bonded to Fe(1) and Fe(2) (Fe–S (mean) = 2.242 Å (**59**), 2.227 Å (**60**), 2.221 Å (**61**)), but is consistently closer to Fe(3) (Fe(3)–S = 2.145 Å (**59**), 2.142 Å (**60**), 2.141 Å (**61**)). There are analogous structural similarities within the molecule (**58**; X = Cl) [123].

Related to these complexes is a product of stoichiometry $[Fe_3(CO)_9(S\text{-}Bu^t)_2]$, (**62**), isolated from the reaction of Bu$^t$SH and $[Fe_3(CO)_{12}]$ in boiling benzene solution [88,89]. On the basis of IR and NMR spectroscopic data and mass spectrometric analysis, the authors propose the structure shown in Fig. 40.

A wide range of ligand substituted derivatives of $[Fe_3(CO)_9(\mu_3\text{-X})(\mu_3\text{-Y})]$ have been synthesized (see Table 6) of which the mono- and disubstituted complexes $[Fe_3(CO)_8L(\mu_3\text{-X})(\mu_3\text{-Y})]$ and $[Fe_3(CO)_7L_2(\mu_3\text{-X})(\mu_3\text{-Y})]$ form the two largest classes. Relatively few trisubstituted complexes $[Fe_3(CO)_6L_3(\mu_3\text{-X})(\mu_3\text{-Y})]$ have been prepared.

The simple substitution products $[Fe_3(CO)_8L(\mu_3\text{-X})(\mu_3\text{-Y})]$ [98] (see Table 6) have generally been obtained by the thermal substitution of a carbonyl

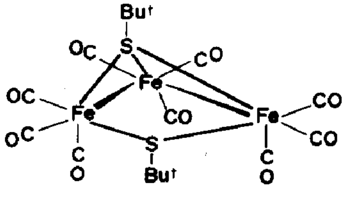

Fig. 40.

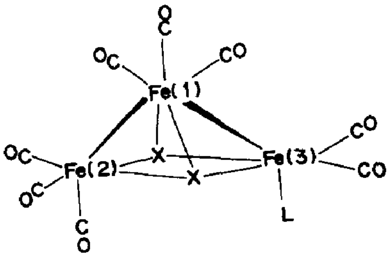

Fig. 41.

ligand in the parent complex by a suitable donor ligand, e.g. trialkyl or triaryl phosphine or arsine. The substitution reactions produce product mixtures, and chromatography or crystallization has generally to be employed to purify the required product.

A variable temperature $^{13}C$ NMR study [97] has established that the likely site of substitution by nucleophiles is in the axial position at a basal iron atom (Fe(2) or Fe(3)), although previously substitution had been suggested to occur at an apical iron atom (Fig. 41) [125].

Kinetic studies of the carbonyl exchange and ligand substitution processes in $[Fe_3(CO)_9(\mu_3\text{-}X)_2]$ complexes have been reported [96]. For the complex $[Fe_3(CO)_9(\mu_3\text{-}S)_2]$ a purely dissociative mechanism for the substitution of a carbonyl ligand by L (L = $PBu^n_3$, $P(OPh)_3$, $AsPh_3$) was found

$$[Fe_3(CO)_9(\mu_3\text{-}X)_2] + L \rightarrow [Fe_3(CO)_8L(\mu_3\text{-}X)_2] + CO$$

Similar results were obtained for the complex $[Fe_3(CO)_9(\mu_3\text{-}Se)_2]$ (except for L = $P(OPh)_3$ where a two-term rate law was observed). In contrast, however, substitution of $[Fe_3(CO)_9(\mu_3\text{-}Te)_2]$ was found to conform to an $S_N2$ process. In accordance with this, reaction of $[Fe_3(CO)_9(\mu_3\text{-}Te)_2]$ with donor ligands has been found to give the unusual adducts $[Fe_3(CO)_9L(Te)_2]$ as the first products of the reaction. These adducts may then dissociate either the nucleophile to regenerate the starting material, or a carbonyl group to give the substitution product, depending upon the nature of the substituting ligand L. The nature of the intermediate adduct $[Fe_3(CO)_9L(Te)_2]$ could not be deduced unequivocally but the authors favoured attack at a tellurium atom rather than at iron [96]. In this regard, a variable temperature $^{13}C$ NMR study of the adduct $[Fe_3(CO)_9(PBu^n_3)(Te)_2]$ has also been reported [97]; the authors considered the structural alternatives (a)–(c) shown in Fig. 42 but favoured (c) [97]. An elegant study by Lesch and Rauchfuss has, however, shown that contrary to these suggestions, the nucleophile is to be found coordinated at an iron centre and not at a tellurium atom [126]. An X-ray structure determination of the $PPh_3$ adduct $[Fe_3(CO)_9(PPh_3)(\mu_3\text{-}Te)_2]$ [126], has shown that the molecule con-

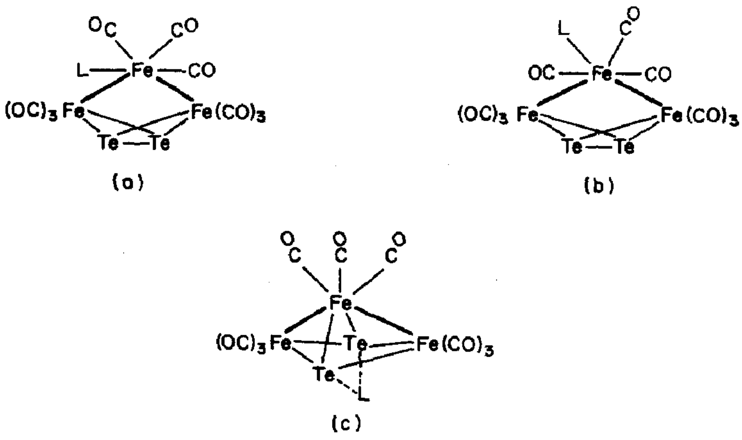

Fig. 42.

sists of an isosceles triangle of iron atoms capped by tellurium atoms. The basal iron atoms only are linked by an iron–iron bond while the apical $\{Fe(CO)_3(PPh_3)\}$ group has an octahedral geometry with two coordination sites occupied by bonds to the capping tellurium atoms (Fig. 43).

A kinetic investigation of ligand substitution in the mixed ligand complexes $[Fe_3(CO)_9(\mu_3\text{-}X)(\mu_3\text{-}Y)]$ (X, Y = S, Se, Te) has also been reported [99]. The substitution reactions were found to conform to a two-term rate law, rate $= k_1[\text{complex}] + k_2[\text{complex}][\text{ligand}]$, in which the relative values of $k_1$ and $k_2$ depend on the nature of X, Y and L. Complexes containing tellurium atoms, in parallel with the complex $[Fe_3(CO)_9(\mu_3\text{-}Te)_2]$, showed a tendency towards an associative step when compared to sulfur, with selenium having an intermediate influence between these two extremes.

The formally monosubstituted product $[Fe_3(CO)_8(C_3Ph_2)(\mu_3\text{-}S)_2]$, (**63**), has been obtained from the reaction of diphenylcyclopropenethione with $[Fe_2(CO)_9]$ in tetrahydrofuran over several days [127]. Complex (**63**) was separated from the other products of the reaction and characterized by X-ray crystallography (Fig. 44) [127]. In a similar fashion, reaction of $[Fe_2(CO)_9]$ with 1,3-dithiole-2-thione has given a complex of stoichiometry

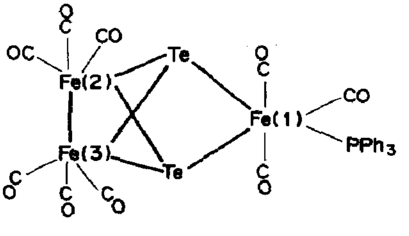

Fig. 43.

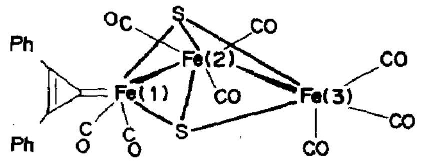

Fig. 44.

$[Fe_3(CO)_8(C_3H_2S_2)(S)_2]$, (**64**), in 43% yield [128]. X-ray crystallography [128] has been used to confirm the presence of the carbenic ligand $\{C_3H_2S_2\}$ and to establish a structure not unlike that reported for (**63**) (Fig. 45). Replacement of one carbonyl ligand in $[Fe_3(CO)_9(\mu_3\text{-}S)_2]$ by the carbene ligands in (**63**) and (**64**) results in significant perturbations in the Fe–Fe and Fe–S bond lengths. For instance Fe(1)–Fe(2) is lengthened ((**63**), 2.607 Å; (**64**), 2.620 Å) relative to $[Fe_3(CO)_9(\mu_3\text{-}S)_2]$ (2.598 Å), and Fe(2)–Fe(3) is shortened ((**63**), 2.535 Å; (**64**), 2.577 Å) relative to the parent complex (2.590 Å). These variations are in agreement with the electronic character of carbene ligands, which are stronger σ-donors and weaker π-acceptors than the carbonyl ligand. It has been suggested [128] that the mechanism of formation of (**64**) involves desulfurization of the thione by $[Fe_2(CO)_9]$ giving $[Fe_3(CO)_9(\mu_3\text{-}S)_2]$ which reacts with the intermediate carbene giving (**64**). Similar considerations would also apply to the reaction leading to (**63**).

In a manner similar to the monosubstituted products, a range of disubstituted complexes $[Fe_3(CO)_7L_2(\mu_3\text{-}X)(\mu_3\text{-}Y)]$ have been synthesized [98] (see Table 6). One crystal structure determination has been carried out, that of $[Fe_3(CO)_7(NCMe)_2(\mu_3\text{-}PPh)_2]$ [104] (see above). Also variable temperature $^{13}C$ NMR studies have been reported which throw light on the possible solution structures of these species [97]. Monosubstitution is proposed to occur at a basal iron atom with the nucleophile entering into an axial position (see above). In the case of the disubstituted product $[Fe_3(CO)_7L_2(\mu_3\text{-}X)_2]$, two positional isomers are obtained (Fig. 46 (a) and (b)). In the most abundant isomer, (a), (determined for $L = PBu^n_3$, $X = Se$), the second molecule of phosphine replaces a carbonyl ligand in an equatorial position at the $\{Fe(3)(CO)_3\}$ unit, whereas in the least abundant isomer, (b), the second substitution occurs at the $\{Fe(1)(CO)_3\}$ unit. On

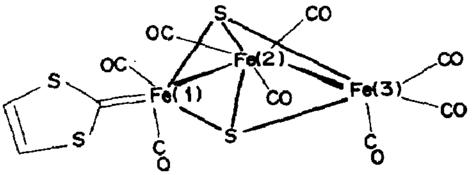

Fig. 45.

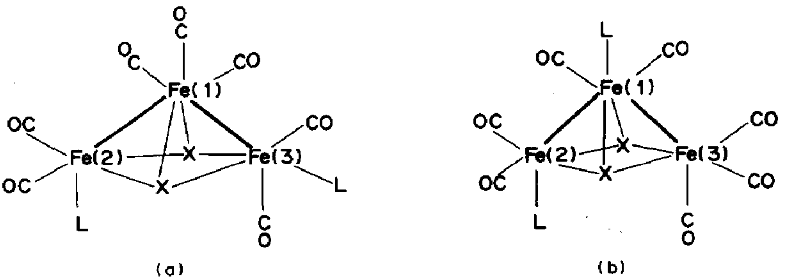

Fig. 46.

raising the temperature, a concerted exchange process in the most abundant isomer (a), (L = $P(OPh)_3$) has also been identified (Scheme 4).

The trisubstituted complexes $[Fe_3(CO)_6L_3(\mu_3\text{-}S)_2]$ (L = pyridine, piperidine) have been synthesized by the direct thermal reaction between $[Fe_3(CO)_9(\mu_3\text{-}S)_2]$ and the amine in a suitable solvent mixture [125]. Trisubstitution with less basic ligands such as triphenylphosphine could not be achieved under similar conditions, while the use of carbonyl substitution catalysts or the decarbonylating agent trimethylamine-*N*-oxide has, to date, not been reported. As far as we are aware, no crystal structure determinations on the complexes $[Fe_3(CO)_6L_3(\mu_3\text{-}X)_2]$ have been reported.

The ditertiary arsine $Me_2As\text{–}C{=}C(AsMe_2)CF_2CF_2$ ($f_4$fars) can act as both a bidentate and a tridentate ligand (the double bond acting as the third electron donor ligand in the latter case). Reaction of $f_4$fars with $[Fe_3(CO)_{12}]$ gives the substitution product $[(f_4fars)Fe_3(CO)_{10}]$ [129] containing the closed triangle of metal atoms still intact. However, further heating in cyclohexane for 1 h gives a second product, of stoichiometry $[(f_4fars)Fe_3(CO)_9]$, **(65)**, while extended heating (6 h) gives a product of stoichiometry $[\{As_2(CH_3)_2CH_2\}Fe_3(CO)_9]$, **(66)**, [129]. The complex **(65)** has been characterized by X-ray crystallography [130,131] revealing both a ligand and metal cluster framework rearrangement. The molecule consists formally of an open triangle of iron atoms (Fe(1)–Fe(2) = 2.917 Å, Fe(2)–Fe(3) = 2.667 Å, Fe(1)–Fe(2)–Fe(3) = 88.4°); the novel arrangement of the ligand is shown in Fig. 47. The structure of **(66)** has not been established crystallographically, but it is proposed, on the basis of spectroscopic data, to be as shown in Fig. 48 [129].

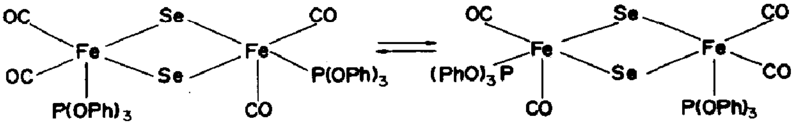

Scheme 4.

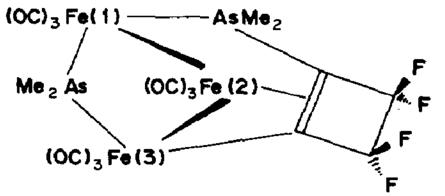

Fig. 47.

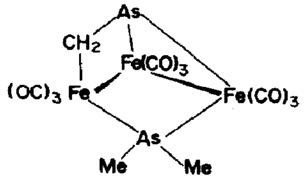

Fig. 48.

In a similar manner, reaction of $[Fe_3(CO)_{12}]$ with $Ph_2P{-}C{=}C(AsMe_2)CF_2CF_2$ ($f_4asp$) gives the substitution product $[(f_4asp)Fe_3(CO)_{10}]$, which on subsequent heating converts to $[(f_4asp)Fe_3(CO)_9]$, (**67**), a product also characterized by X-ray crystallography [132]. This molecule has a structure analogous to (**65**) (Fe(1)–Fe(2) = 2.676 Å, Fe(2)–Fe(3) = 2.866 Å, Fe(1)–Fe(2)–Fe(3) = 92.4° (mean values for two crystallographically independent molecules)) (Fig. 49).

The reaction of $[Fe_3(CO)_{12}]$ with diphenylacetylene in methanol yields a violet material of stoichiometry $[Fe_3(CO)_8(PhC_2Ph)_2]$ which in boiling benzene or petroleum ether undergoes rearrangement to a more stable black isomer (**68**). The X-ray structures of both complexes have been determined [133], the former consisting of a closed triangle of iron atoms and corresponds to disubstitution of $[Fe_3(CO)_{12}]$ by diphenylacetylene. On the other hand, however, (**68**) is best regarded as containing a ferracyclopentadiene moiety, the $Fe_3$ framework consisting of an open triangular array with mean

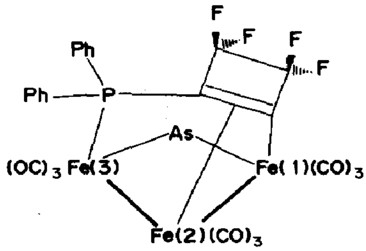

Fig. 49.

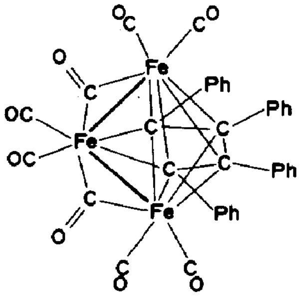

Fig. 50.

Fe–Fe bonding distances of 2.432 Å, and an Fe–Fe–Fe angle subtended at the central iron atom of 87.6° (Fig. 50) [133].

The complex [$Fe_3(CO)_8\{Ph_2PC_4(CF_3)_2\}PPh_2$], one of the products obtained from the reaction of [$Fe_3(CO)_{12}$] with $Ph_2PC{\equiv}CCF_3$ [134] converts under thermal conditions to a complex of stoichiometry [$Fe_3(CO)_7\{Ph_2PC_4(CF_3)_2\}PPh_2$], (**69**), (Scheme 5) [135,136]. The solid state structure of (**69**) has been determined by X-ray crystallography [135,136] and the molecule has been found to possess an open triangle of iron atoms (Fe(1)–Fe(2) = 2.662 Å, Fe(2)–Fe(3) = 2.531 Å, Fe(1)–Fe(2)–Fe(3) = 124.2°) supporting a formally dimerized phosphinoacetylene in the form of a *trans*-butadiene moiety, and a bridging diphenylphosphide group.

The reaction of 1,2- and 1,3-dithiols, HSRSH, with [$Fe_3(CO)_{12}$] gives low yields of a red material of stoichiometry [$Fe_3(CO)_7(SRS)_2$], (**70**, R = $C_2H_4$, $C_3H_6$) together with the major product, the dinuclear complex [$Fe_2(CO)_6(SRS)$] [137]. An open triangular framework of iron atoms would be expected for (**70**), and this has been confirmed by X-ray crystallography for the complex [$Fe_3(CO)_7(\mu_2\text{-}SCH_2CH_2S)_2$] (Fig. 51). The mean Fe–Fe distance is 2.551 Å, with an Fe(2)–Fe(1)–Fe(3) angle of 151.8° [137].

*N*-(Benzylidene)aniline (Ph–CH=N–Ph) reacts with [$Fe_3(CO)_{12}$] to give together with the dinuclear complex (Fig. 52(a)), the closely related trinuclear species (**71**) [138] shown in Fig. 52(b). The X-ray crystal structure of (**71**) has been determined [138] (Fe(1)–Fe(2) = 2.452 Å, Fe(2)–Fe(3) = 2.822

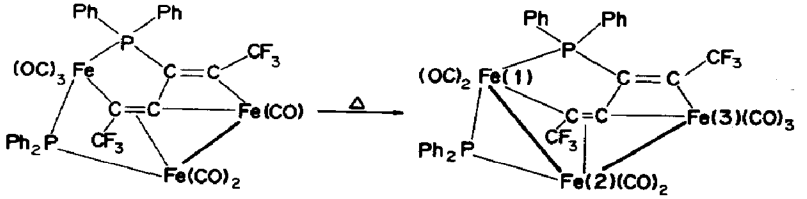

Scheme 5.

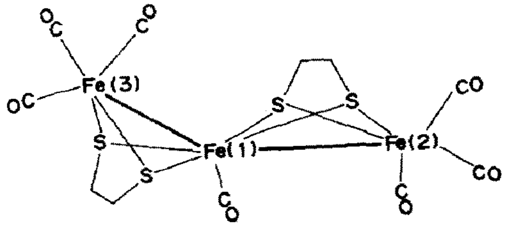

Fig. 51.

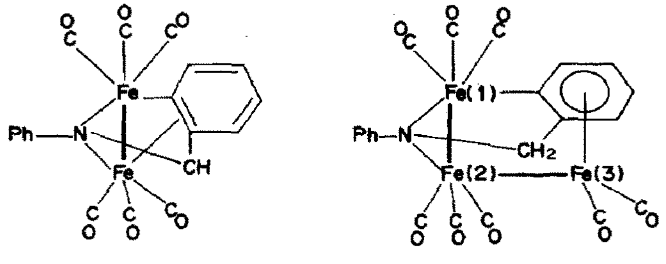

(a) (b)

Fig. 52.

Å, Fe(1)···Fe(3) = 3.967 Å, Fe(1)–Fe(2)–Fe(3) = 97.32°). The most unusual feature of this molecule is the bridging aromatic moiety, and in this regard the authors also postulate a second bonding form involving a carbene interaction to Fe(1) and a $\eta^5$-hexadienyl interaction between the ring and Fe(3) (see Fig. 53).

The reaction of benzalazine with $[Fe_3(CO)_{12}]$ has given the complex $[Fe_3(CO)_8\{\mu_2\text{-}\eta^6\text{-}C_6H_4CH_2N(N{=}CHC_6H_5)\text{-}2\}]$, (**72**) [139], characterized by mass spectrometry, IR and $^1H$ and $^{13}C$ NMR as having a structure closely related to (**71**) (see Fig. 54).

Finally, an unusual oligomeric complex of iron has been proposed for the product obtained from the interaction of iron pentacarbonyl with the strong acid salt $Fe(SbF_6)_2$ [140]. The product of stoichiometry $[Fe\{Fe(CO)_5\}_2](SbF_6)_2$, is proposed, on the basis of IR and Mössbauer data, to contain two

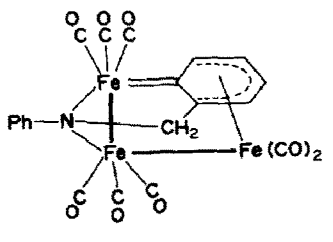

Fig. 53.

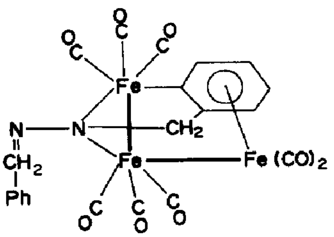

Fig. 54.

intact {Fe(CO)$_5$} units acting as weak electron donor ligands to the metal cation, with the iron atoms as the only point of attachment. It is interesting to note in this regard that a range of complexes have recently been synthesized containing 18-electron complexes acting as electron donors to coordinatively unsaturated complexes, e.g. $[(PMe_3)(CO)_4Os \rightarrow W(CO)_5]$ [141].

The first examples of complexes of iron containing other metals as part of the structural framework were reported by Nyholm and co-workers in 1964 [142]. The $[Fe(CO)_4]^{2-}$ anion was reacted with $[PPh_3AuCl]$ to give a complex of stoichiometry $[Fe(CO)_4(AuPPh_3)_2]$, (**73**), which on the basis of the similarity of its IR spectrum to that of *cis*-$[Fe(CO)_4I_2]$ was assigned a *cis* configuration of {AuPPh$_3$} groups. In a similar manner the complexes $[Fe(CO)_4\{M(triars)\}_2]$ (triars = 1,1,1-tris(dimethylarsinomethyl)ethane, bis (*o*-dimethylarsinophenyl)methyl arsine; **74**, M = Cu; **75**, M = Ag) have also been synthesized [143] and again assigned a *cis*, di-equatorial disposition of {M(triars)} groups. Further in this regard, Chiswell and Venanzi reacted $[H_2Fe(CO)_4]$ with the novel complex shown in Fig. 55 and obtained a product of stoichiometry $[\{Fe(CO)_4\}\{AuPh_2PC_6H_4 \cdot C_6H_4PPh_2Au\}]$, (**76**), where the bidentate gold ligand can only occupy two *cis* coordination sites [144]. The infrared carbonyl stretching frequencies of this complex and $[\{Fe(CO)_4\}(AuPPh_3)_2]$ [142] are similar, confirming the *cis* arrangement of the gold atoms in this latter complex. In contrast, however, treatment of $[Fe(CO)_4]^{2-}$ with two equivalents of *trans*-$[Pt(py)_2Cl_2]$ in methanol gives the complex $[\{Fe(CO)_4\}\{Pt(py)_2Cl\}_2]$, (**77**), as an orange crystalline solid [145]. On the basis of IR spectroscopy the two {Pt(py)$_2$Cl} groups are assigned a *trans* configuration, the metal framework thus consisting of a linear Pt–Fe–Pt unit.

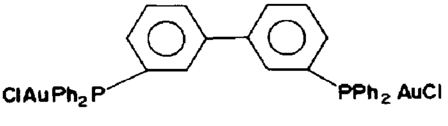

Fig. 55.

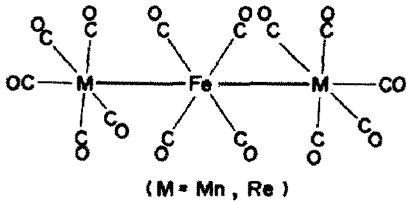

Fig. 56.

The linear trimetallic complexes $[M_2Fe(CO)_{14}]$, (**78**, M = Mn; **79**, M = Re) [146,147] and $[MnReFe(CO)_{14}]$, (**80**) [148], have been obtained by photochemical irradiation of iron pentacarbonyl with $[Mn_2(CO)_{10}]$, $[Re_2(CO)_{10}]$

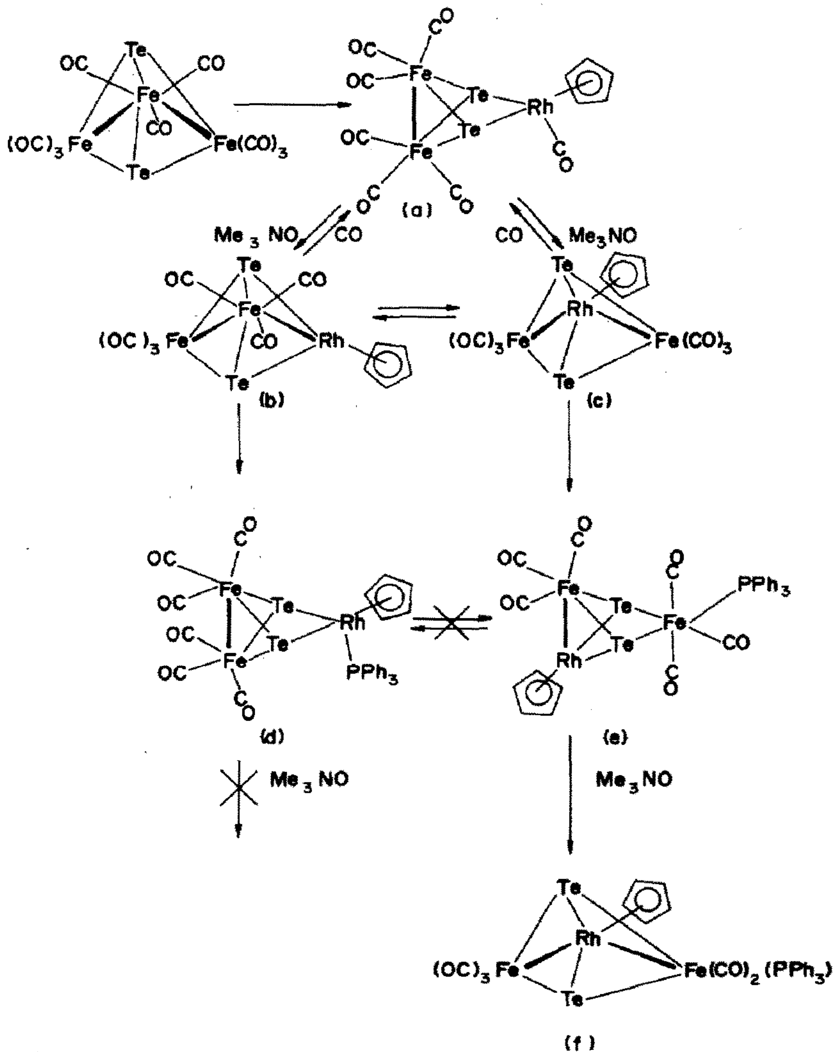

Scheme 6.

and $[MnRe(CO)_{10}]$ respectively. Also, the treatment of $[Fe(CO)_4I_2]$ with excess $Na[M(CO)_5]$ (M = Mn, Re) has recently been used to prepare complexes (**78**) and (**79**) [149]. The X-ray crystal structures of both $[Mn_2Fe(CO)_{14}]$ [150] and $[Re_2Fe(CO)_{14}]$ [151] have been determined. In both cases a linear M–Fe–M framework has been observed (Fig. 56) (Mn–Fe = 2.80, 2.83 Å, Re–Fe = 2.8758, 2.8493 Å (two molecules per asymmetric unit)]. The environment of each Mn or Re atom is nearly octahedral, although the equatorial groups lean appreciably in towards the centre of the molecule, e.g. Fe–Mn–C(eq) = 86.6°. The conformation of both molecules about the Fe–M bond axis is staggered. The far-infrared spectra [152] and the electronic structures and spectra [153,154] of these molecules have been reported.

The cluster $[Fe_3(CO)_9(\mu_3\text{-}Te)_2]$ reacts with $[(\eta^5\text{-}C_5H_5)Rh(CO)_2]$ (Scheme 6) to give a good yield of the complex $[(\eta^5\text{-}C_5H_5)RhFe_2(CO)_7(\mu_3\text{-}Te)_2]$ (a), [155]. This compound undergoes $Me_3NO$ induced decarbonylation to give two isomers of $[(\eta^5\text{-}C_5H_5)RhFe_2(CO)_6(\mu_3\text{-}Te)_2]$, (**81**), (b) and (c). Reaction of both isomers with CO gave (a) in pure form, whereas reaction with $PPh_3$ gave two isomers of $[(\eta^5\text{-}C_5H_5)RhFe_2(CO)_6(PPh_3)(\mu_3\text{-}Te)_2]$ (d) and (e) which differ in the metal atom arrangement and which do not interconvert. A remarkable aspect of the complexes (b) and (c) is the ease with which metal–metal bonds are cleaved by the nucleophiles CO and $PPh_3$. Upon treatment of (d) and (e) with $Me_3NO$, only (e) underwent decarbonylation to give the *nido* cluster $[(\eta^5\text{-}C_5H_5)RhFe_2Te_2(CO)_5(PPh_3)]$ (f) [155].

As just described for $[(\eta^5\text{-}C_5H_5)Rh(CO)_2]$, $[(\eta^5\text{-}C_5H_5)Co(CO)_2]$ reacts with $[Fe_3(CO)_9(\mu_3\text{-}Te)_2]$ to give the product $[(\eta^5\text{-}C_5H_5)CoFe_2(CO)_7(\mu_3\text{-}Te)_2]$ (Scheme 7) via a similar transmetallation process [156]. Decarbonyla-

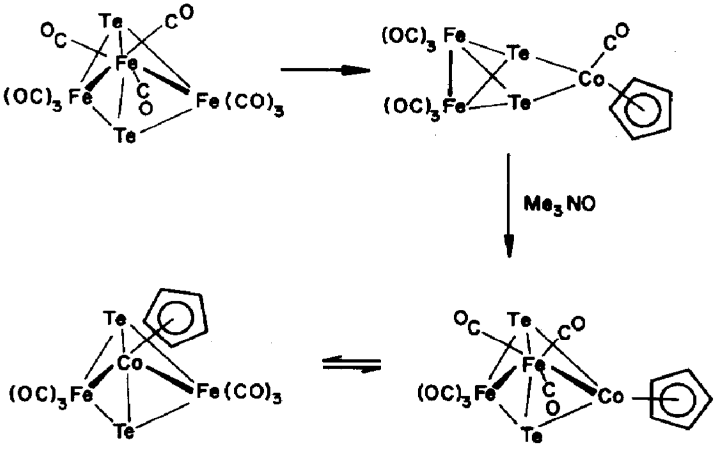

Scheme 7.

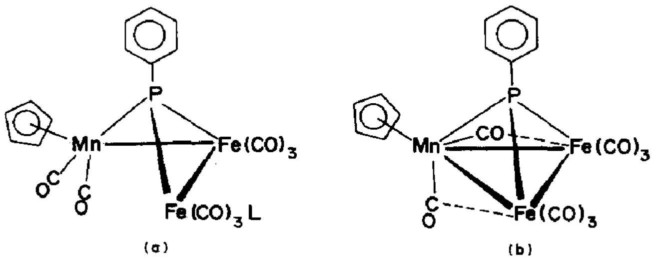

Fig. 57.

tion of $[(\eta^5\text{-}C_5H_5)CoFe_2(CO)_7(\mu_3\text{-}Te)_2]$ with trimethylamine-*N*-oxide gives two isomers of $[(\eta^5\text{-}C_5H_5)CoFe_2(CO)_6(\mu_3\text{-}Te)_2]$, isoelectronic with $[Fe_3(CO)_9(\mu_3\text{-}Te)_2]$ and containing a similar acyclic $\{M_3(\mu_3\text{-}Te)_2\}$ type framework.

An extensive series of heteronuclear, manganese–iron complexes $[(\eta^5\text{-}C_5H_5)MnFe_2(CO)_8L(\mu_3\text{-}PR)]$ (L = CO, $ER_3$, R = alkyl or aryl) (see Table 6) have recently been reported by Huttner and co-workers [157–161]. Reaction of $[(\eta^5\text{-}C_5H_5)Mn(CO)_2(PPh_2Cl)]$ with $[Fe_2(CO)_9]$ [157] gave a green material of stoichiometry $[(\eta^5\text{-}C_5H_5)MnFe_2(CO)_9(PPh)]$, (**82**), and a red material $[(\eta^5\text{-}C_5H_5)MnFe_2(CO)_8(\mu_3\text{-}PPh)]$ (Fig. 57, (a) and (b) respectively). The X-ray crystal structure of (**82**) has been determined [157] and has shown the molecule to consist of an open Mn–Fe–Fe triangle, face bridged by the PPh group. The Fe–Fe bond length was found to be 2.74 Å and the Mn–Fe bond length to be 2.94 Å. The angle of the Mn–Fe–Fe framework subtended at the central iron atom was found to be 88.2° [157]. The crystal structures of the closely related complexes $[(\eta^5\text{-}C_5H_5)MnFe_2(CO)_8(PPh_3)(\mu_3\text{-}PPh)]$, (**83**), and $[(\eta^5\text{-}C_5H_5)MnFe_2(CO)_8(SbPh_3)(\mu_3\text{-}PPh)]$, (**84**), have also been reported, [160,162] and not surprisingly found to be very similar to that of (**82**), (**83**, Fe–Fe = 2.801 Å, Mn–Fe = 2.908 Å, Mn–Fe–Fe = 87.4°; **84**, Fe–Fe = 2.786 Å, Mn–Fe = 2.928 Å, Mn–Fe–Fe = 87.3°]. Huttner and co-workers have also explored the relationship between the complexes (a) and (b) (Fig. 57) and shown them to be intimately related [158,159,161]. Reaction of (b) with donor ligands (L = CO, $ER_3$) results in opening of an Mn–Fe bond giving (a) in good yield. These reactions may also be reversed under thermal or photochemical conditions with reformation of the metal–metal bond, or taken further with additional amounts of nucleophile to give cleavage of the remaining Mn–Fe bond and products of the type $[(\eta^5\text{-}C_5H_5)MnFe_2(CO)_8(L)(L')(\mu_3\text{-}PR)]$ containing only a single metal–metal bond (see Fig. 58).

The dinuclear complexes $[Fe_2(CO)_6(PR_2H)_2]$ react with $[Co_2(CO)_8]$ to form the complexes $[Fe_2Co(CO)_9(\mu_2\text{-}PRH)(\mu_3\text{-}PR)]$ (**85**; R = Me, Ph) and $[Fe_2Co_2(CO)_{11}(\mu_4\text{-}PR)_2]$ (**86**; R = Me, Ph) [103] separable by column chro-

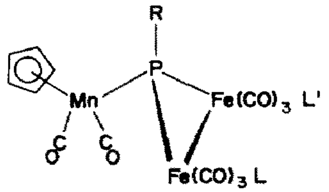

Fig. 58.

matography. The X-ray crystal structure of (**85**; R = Ph) has been determined (Fe–Co (mean) = 2.719 Å, Fe···Fe = 3.470 Å, Fe–Co–Fe = 79.3°) (Fig. 59). The complexes (**85**) have been found not to be intermediates in the formation of the tetranuclear species.

The reaction of $[RuCl_2(PR_3)(arene)]$ complexes with $Fe_2(CO)_9$ in benzene or dichloromethane at room temperature (24 h) gives a mixture of trinuclear complexes separable by silica gel chromatography [163,164]. Together with the clusters $[Ru_3(CO)_{10}(PR_3)_2]$, $[FeRu_2(CO)_{10}(PR_3)_2]$ and $[Fe_2Ru(CO)_{11}(PR_3)]$, the acyclic heterotrimetallic complex $[FeRu_2(CO)_8(PR_3)_2(\mu_2\text{-}Cl)_2]$, (**87**), was obtained as the major product. The X-ray crystal structure of $[FeRu_2(CO)_8\{PPh_2(C{\equiv}CBu^t)\}_2(\mu_2\text{-}Cl)_2]$ has been determined [163,164], and the molecule shown to consist of a bent Ru–Fe–Ru backbone with the two chloro bridges spanning the open edge of the triangle. The mean Fe–Ru distance is 2.809 Å, Ru···Ru = 3.185 Å and the Ru–Fe–Ru angle is 69.07° (Fig. 60). Reaction of the trinuclear complexes $[FeRu_2(CO)_8L_2(\mu_2\text{-}Cl)_2]$ (L = $PPh_3$, $PMe_3$, $AsPh_3$) with aqueous $NaCO_3$ leads to the substitution of the chloro bridges giving the novel hydroxo bridged complexes $[FeRu_2(CO)_8L_2(\mu_2\text{-}OH)_2]$, (**88**), [165] (Fig. 61). The X-ray structure of the complex $[FeRu_2(CO)_8(PPh_3)_2(\mu_2\text{-}OH)_2]$ shows a similar Ru–Fe–Ru core to $[FeRu_2(CO)_8\{PPh_2(C{\equiv}CBu^t)\}_2(\mu_2\text{-}Cl)_2]$ (Ru–Fe (mean) = 2.806 Å, Ru···Ru = 3.032 Å, Ru–Fe–Ru = 65.41 Å). Treatment of $[FeRu_2(CO)_8(PPh_3)_2(\mu_2\text{-}Cl)_2]$ with $NaCO_3$ in i-propanol gives the same bis(hydroxo) bridged complex as obtained in aqueous solution, together, however, with the mixed hydrido, hydroxo bridged complex $[FeRu_2(CO)_8$

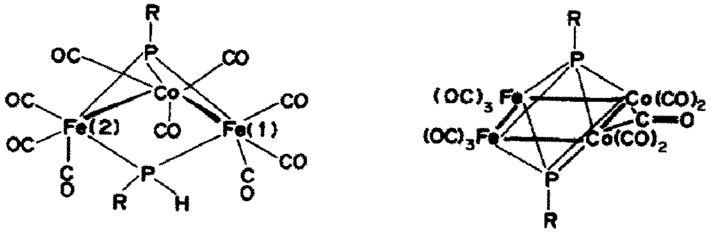

Fig. 59.

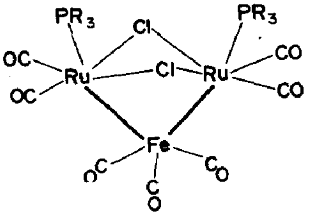

Fig. 60.

$(PPh_3)_2(\mu_2\text{-}H)(\mu_2\text{-}OH)]$ [165]. The reactions of the binuclear complex $[\{RuCl_2(p\text{-cymene})\}_2(dppe)]$ with $[Fe_2(CO)_9]$ have given the complexes $[Ru_3(CO)_8(dppe)(\mu_2\text{-}Cl)_2]$ and $[FeRu_2(CO)_8(dppe)(\mu_2\text{-}Cl)_2]$, (**89**), [166]. The structure of the latter complex (**89**) is proposed to be analogous to that of $[FeRu_2(CO)_8\{PPh_2(C{\equiv}CBu^t)\}_2(\mu_2\text{-}Cl)_2]$ [163,164]. The complex $[FeRu_2(CO)_8(dppe)(\mu_2\text{-}Cl)_2]$ was found to disproportionate under mild thermal conditions to give $[Ru_3(CO)_8(dppe)(\mu_2\text{-}Cl)_2]$ as the ruthenium containing product.

Recently, Keller and Vahrenkamp [167,168], in attempting to synthesize phosphido bridged mixed metal dimers by the reaction of $[Fe(CO)(NO)_2(PMe_2H)]$ with $[(\eta^3\text{-}C_3H_5)Co(CO)_3]$, obtained the complexes shown in Fig. 62 together with several mononuclear products. The X-ray crystal structures of both trinuclear species have been determined, and found to be almost identical (**90**, Fe–Fe = 2.668 Å, Fe–Co = 2.659 Å, Fe–Fe–Co = 160.1°; **91**, Fe(1)–Fe(2) = 2.658 Å, Fe(2)–Fe(3) = 2.711 Å, Fe(1)–Fe(2)–Fe(3) = 161.1°).

The reaction of $[\{(PdNMe_2CH_2C_6H_4)(\mu_2\text{-}Cl)\}_2]$ with metal carbonyl anions has been found to lead to a range of open triangular complexes containing the Pd–M–Pd core [33,34] (see Sections B.(iii)(a) and (b)). Reaction with $K[Fe(CO)_3(NO)]$ gives red crystals of a complex with the stoichiometry $[\{PdNMe_2CH_2C_6H_4\}_2\{Fe(CO)_3(NO)\}(\mu_2\text{-}Cl)]$, (**92**), (yield 95%). Although (**92**) has not been characterized by X-ray crystallography, and is relatively unstable even at −20°C, there is good evidence for the formulation [33,34], and the proposed structure shown in Fig. 63.

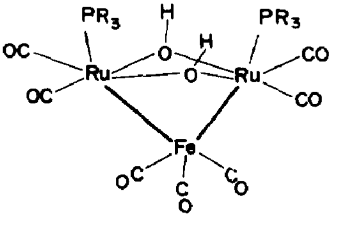

Fig. 61.

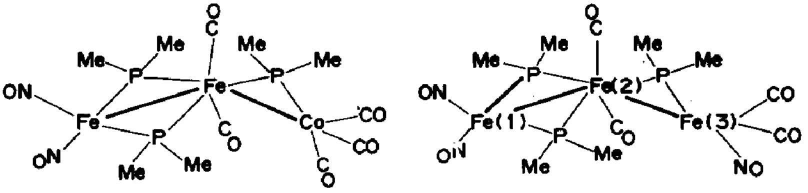

Fig. 62.

### (b) Ruthenium

Of the three elements in the iron triad, ruthenium forms the smallest group of complexes relevant to this review (see Table 7). As there are numerous structural similarities between both iron and osmium complexes it would appear that ruthenium has, to date, simply not attracted the same interest as either iron or osmium. For example, although numerous derivatives of the complexes $[Fe_3(CO)_9(\mu_3\text{-}X)_2]$ are known, only the parent complexes $[Ru_3(CO)_9(\mu_3\text{-}S)_2]$, **(93)**, and $[Ru_3(CO)_9(\mu_3\text{-}Se)_2]$, **(94)**, have been synthesized for ruthenium [169]. These products have been obtained by the direct reaction of $[Ru_3(CO)_{12}]$ with sulfur and selenium, and are presumed to have similar structures to the iron analogues (Fig. 64) (see Section B.(v)(a)).

The structurally related acyclic tri-ruthenium complexes $[Ru_3(CO)_{10}(\mu_2\text{-}X)_2]$ (**95**–**97**; X = Br, I, NO respectively) have been synthesized by the reaction of $[Ru_3(CO)_{12}]$ with LiBr or NaI assisted by decarbonylation with trimethylamine-*N*-oxide/ [170], and by the direct reaction of $[Ru_3(CO)_{12}]$ with nitric oxide [171,172] respectively. The structure of $[Ru_3(CO)_{10}(\mu_2\text{-}I)_2]$ has been determined by X-ray diffraction methods [170] (Fig. 65). The three ruthenium atoms define an open triangle (Ru(2)–Ru(1)–Ru(3) = 70.36°) with Ru–Ru bond lengths of 2.858 Å (Ru(1)–Ru(2)) and 2.870 Å (Ru(1)–Ru(3)). The Ru(2) · · · Ru(3) internuclear distance is 3.301 Å and corresponds to little or no net bonding interaction.

The nitrosyl bridged complex $[Ru_3(CO)_{10}(\mu_2\text{-}NO)_2]$ has also been the subject of an X-ray structure determination [172]. A similar open triangle of ruthenium atoms was found (Ru–Ru (mean) = 2.866 Å, Ru · · · Ru = 3.150 Å, Ru–Ru–Ru = 66.69°) with the two nitrosyl ligands bridging the open

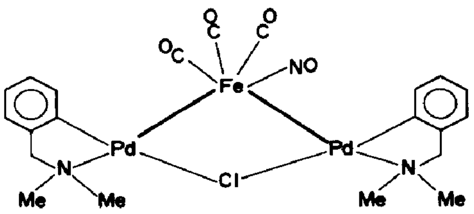

Fig. 63.

TABLE 7

Acyclic cluster complexes of ruthenium

| Formula | Complex | Fig. | Ref. [a] |
|---|---|---|---|
| $[Ru_3(CO)_9(\mu_3\text{-}S)_2]$ | **(93)** | 64 | 169 |
| $[Ru_3(CO)_9(\mu_3\text{-}Se)_2]$ | **(94)** | 64 | 169 |
| $[Ru_3(CO)_{10}(\mu_2\text{-}Br)_2]$ | **(95)** | – | 170 |
| $[Ru_3(CO)_{10}(\mu_2\text{-}I)_2]$ | **(96)** | 65 | 170* |
| $[Ru_3(CO)_{10}(\mu_2\text{-}NO)_2]$ | **(97)** | 66 | 171,172* |
| $[Ru_3(CO)_{10}(\mu_2\text{-}NCO)(\mu_2\text{-}NC_6H_{10})]$ | **(98)** | 67 | 173* |
| $[Ru_3(CO)_{10}(\mu_2\text{-}X)(\mu_3\text{-}O{=}CR)]$ (X = halide; R = alkyl group) | – | 68 | 174 |
| $[Ru_3(CO)_9(\mu_2\text{-}Cl)(\mu_3\text{-}\eta^1,\eta^2,\eta^2\text{-}C{=}CPh)]$ | **(99)** | 69 | 175* |
| $[Ru_3(CO)_9(\mu_2\text{-}H)(\mu_2\text{-}PPh_2)(\mu_3\text{-}\eta^2\text{-}PhC{\equiv}CPh)]$ | **(100)** | 70 | 179* |
| $[Ru_3(CO)_8(C_{16}H_{22})]$ | **(101)** | 71 | 182* |
| $[Ru_3(CO)_8(HC_2Bu^t)_3]$ | **(102)** | 72 | 183* |
| $[RuFe_2(CO)_8(PhC_2Ph)_2]$ | **(103)** | – | 184 |
| $[Ru_3(CO)_8(SnCl_3)(\mu_2\text{-}H)_2(\mu_2\text{-}Cl)(\mu_3\text{-}S)]$ | **(104)** | 73 | 185* |
| $[Ru_3(CO)_7(dppm)(\mu_3\text{-}PPh)(\mu_2\text{-}CHPPh_2)]$ | **(105)** | 74 | 186* |
| $[Ru_3(CO)_8(C_9H_6NO)_2]$ | **(106)** | 75 | 187* |
| $[(Me_3P)_4Ru(\mu_2\text{-}CH_2)_2Ru(\mu_2\text{-}CH_2)_2Ru(PMe_3)_4](BF_4)_2$ | **(107)** | 76 | 188* |
| $[Ru(CO)_4\{(\eta^5\text{-}C_5H_5)Ru(CO)_2\}_2]$ | **(108)** | 77 | 189* |
| $[Ru(CO)_4\{Mn(CO)_5\}_2]$ | **(109)** | – | 190 |
| $[(\eta^5\text{-}C_5H_5)_2Ru_4(CO)_6(\mu_3\text{-}C_5H_4)_2]$ | **(110)** | – | 191 |
| $[(\eta^5\text{-}C_5H_5)_2Ru_4(CO)_5\{P(OMe)_3\}(\mu_3\text{-}C_5H_4)_2]$ | **(111)** | 78 | 191* |
| $[Ru_4(CO)_{13}(\mu_3\text{-}EPh)_2]$ (E = P, As) | **(112)**,**(113)** | 79 | 192* |

[a] References marked with an asterisk refer to crystal structure determinations.

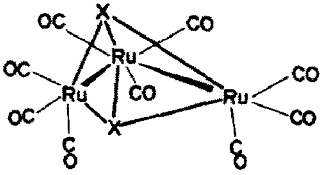

Fig. 64.

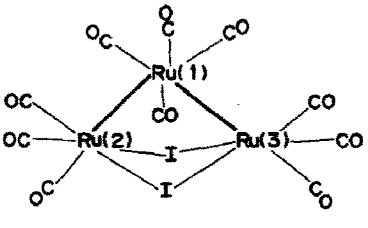

Fig. 65.

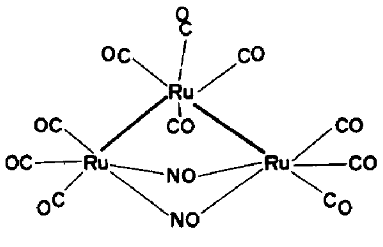

Fig. 66.

edge (Fig. 66). Spectroscopic data for the complexes $[Ru_3(CO)_{10}(\mu_2\text{-}X)_2]$ (X = Br, I, NO) suggest that the solution and solid state structures are the same [170–172]. It should be pointed out that these complexes are structurally, closely related to the complexes $[Ru_3(CO)_{10}(\mu_2\text{-}H)(\mu_2\text{-}X)]$ (X = Cl, Br, I) and $[Ru_3(CO)_9(\mu_2\text{-}H)(\mu_3\text{-}I)]$ each containing a three-centre, two-electron M–H–M interaction [170].

The complex $[Ru_3(CO)_{10}(\mu_2\text{-}NCO)(\mu_2\text{-}NC_6H_{10})]$, (**98**), has been prepared by reacting $[Ru_3(CO)_{12}]$ with pentamethylene diazirene in toluene at 90°C [173]. The structure of this complex has been established by X-ray crystallography [173]. The tri-ruthenium backbone forms an open triangle of ruthenium atoms (Ru–Ru (mean) = 2.841 Å, Ru · · · Ru = 3.038 Å, Ru–Ru–Ru = 64.6°) with the open edge bridged by a linear isocyanate group and by the $\{C_6H_{10}{=}N\}$ moiety (Fig. 67).

Reaction of the edge bridged complexes $[Ru_3(CO)_{10}(\mu_2\text{-}H)(\mu_2\text{-}X)]$ (X = Cl, Br, I) with ethylene and carbon monoxide has been found to give the haloacyl complexes $[Ru_3(CO)_{10}(\mu_2\text{-}X)(\mu_2\text{-}O{=}CC_2H_5)]$ in good yield [174]. Reaction of $[Ru_3(CO)_{10}(\mu_2\text{-}H)(\mu_2\text{-}Br)]$ with propene and carbon monoxide has given the propionyl halide complex $[Ru_3(CO)_{10}(\mu_2\text{-}Br)(\mu_2\text{-}O{=}CR)]$ (R = n- or i-$C_3H_7$, ratio 10 : 1). These products have been characterized by a combination of $^1H$ and $^{13}C$ NMR spectroscopy and elemental analysis (Fig. 68) [174].

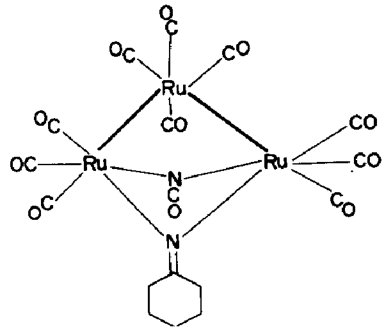

Fig. 67.

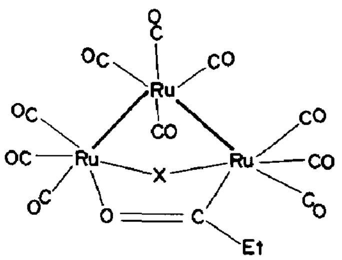

Fig. 68.

The reaction of $[Ru_3(CO)_{12}]$ with $PhC{\equiv}CX$ ($X = Cl$, Br) results in C–X bond cleavage and has been found to give the complex $[Ru_3(CO)_9(\mu_2\text{-}X)(\mu_3\text{-}\eta^1,\eta^2,\eta^2\text{-}C{\equiv}CPh)]$, (**99**), probably the first example of simple oxidative addition of a halocarbon at a tri-metallic centre [175]. The X-ray structure determination of (**99**) ($X = Cl$) has shown the molecule to possess an open triangle of ruthenium atoms with an Ru–Ru–Ru angle of 71.3° (Fig. 69). The Ru–Ru bond lengths are 2.815 and 2.805 Å. The chloro ligand bridges the open side of the triangle; the Ru · · · Ru internuclear distance of this edge is 3.277 Å and is in accord with a zero Ru–Ru bond order. It should be noted that the $\{Ru_3(CO)_9(C_2R)\}$ structural unit is well known, being present in a diversity of cyclic cluster complexes $[Ru_3(CO)_9(\mu_2\text{-}X)(\mu_3\text{-}\eta^1,\eta^2,\eta^2\text{-}C_2R)]$ ($X = H$, $PR_2$, HgBr, $AuPPh_3$) [176–178].

The tri-ruthenium cluster complex $[Ru_3(CO)_9(\mu_2\text{-}H)(\mu_2\text{-}PPh_2)]$ reacts with diphenylacetylene (via 4-electron addition with Ru–Ru bond cleavage and no loss of carbon monoxide) to give the complex $[Ru_3(CO)_9(\mu_2\text{-}H)(\mu_2\text{-}PPh_2)(\mu_3\text{-}\eta^2\text{-}PhC{\equiv}CPh)]$, (**100**), [179]. The X-ray structure of this complex has been determined [179] (Fig. 70). The phosphido ligand bridges the open edge of the $Ru_3$ triangle (Ru(1)–Ru(2) = 2.813 Å, Ru(1)–Ru(3) = 2.908 Å, Ru(2) · · · Ru(3) = 3.838 Å, Ru(2)–Ru(1)–Ru(3) = 84.2°). The hydride ligand was located along the Ru(1)–Ru(3) vector (Ru(1)–H = 1.54 Å, Ru(3)–H = 1.89 Å), the longer of the two Ru–Ru bonds [180,181].

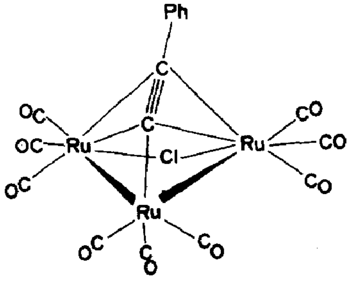

Fig. 69.

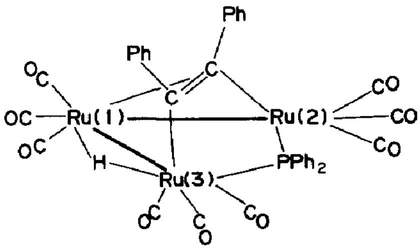

Fig. 70.

The reaction of ruthenium cluster species with acetylenes follows similar patterns to the corresponding reactions of iron clusters, namely via oligomerization of the acetylenic moiety together with metal–metal bond cleavage in the cluster. These open structures are then stabilized by the transformed organic moiety (see Section B.(v)(a)). An example is the reaction of $[HRu_3(CO)_9(C{\equiv}CBu^t)]$ with excess i-propenylacetylene in hydrocarbon solvents. Several products are obtained from this reaction of which one, of stoichiometry $[Ru_3(CO)_8(C_{16}H_{22})]$, (**101**), has been isolated by preparative TLC and characterized by X-ray analysis [182]. The bent Ru(1)–Ru(2)–Ru(3) chain (bond angle 118.1°) has two metal–metal bonds of different magnitude (Ru(1)–Ru(2) = 2.731 Å, Ru(2)–Ru(3) = 2.838 Å). The $C_{16}H_{22}$ organic fragment apparently produced by isopropenylacetylene condensation with the t-butylacetylide ligand, interacts with the metal atoms through a chain of seven carbon atoms (Fig. 71).

Reaction of $[Ru_3(CO)_{12}]$ or $[HRu_3(CO)_9(C{\equiv}CBu^t)]$ with excess $Bu^tC{\equiv}CH$, or of $[(\eta^5\text{-}C_5H_5)_2Ni_2(HC_2Bu^t)]$ with $[Ru_3(CO)_{12}]$ gives a product of stoichiometry $[Ru_3(CO)_8(HC_2Bu^t)_3]$, (**102**), [183]. This complex has been completely characterized by X-ray diffraction [183]. The three ruthenium atoms form an open triangle (Ru(1)–Ru(2) = 2.669 Å, Ru(2)–Ru(3) = 2.661 Å, Ru(1) · · · Ru(3) = 3.73 Å, Ru(1)–Ru(2)–Ru(3) = 88.8°). Of particular

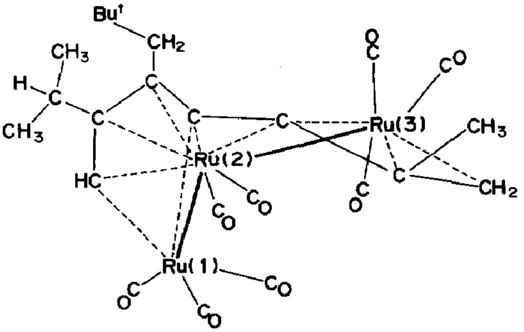

Fig. 71.

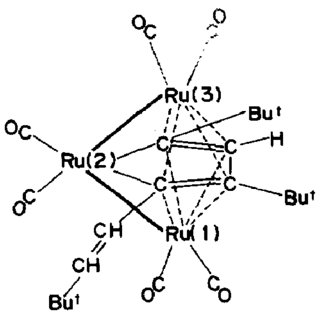

Fig. 72.

interest though is the organic fragment formed from the trimerization of $Bu^tC{\equiv}CH$. This fragment froms two σ-bonds to the central ruthenium atom giving rise to a metallocyclopentadiene ring; the terminal metal atoms lie on each side of this ring with bonding interactions between these metal atoms and the unsaturation of the ring (Fig. 72). A closely related heterometallic complex $[RuFe_2(CO)_8(PhC_2Ph)_2]$, (**103**), has been obtained from the reaction of the cyclic cluster complex $[RuFe_2(CO)_9(PhC_2Ph)]$ with phenylacetylene [184]. A structure analogous to the iron complex $[Fe_3(CO)_8(PhC_2Ph)_2]$ [133] (see Section B.(v)(a), Fig. 50) has been proposed, except with a ruthenium atom replacing the central iron atom.

The oxidative cleavage of metal–metal bonds in cyclic cluster species as a synthetic route to acyclic cluster complexes is well illustrated by the reaction of $SnCl_4$ with $[Ru_3(CO)_9(\mu_2\text{-}H)_2(\mu_3\text{-}S)]$ [185]. Reaction occurs at room temperature within 45 min yielding, after product workup, a yellow crystalline material of stoichiometry $[Ru_3(CO)_8(SnCl_4)(H)_2(S)]$, (**104**), in excellent yield. This complex has been structurally characterized [185] and found to consist of an open triangle of ruthenium atoms (Ru(1)–Ru(2) = 2.959, 2.942 Å, Ru(2)–Ru(3) = 2.931, 2.924 Å, Ru(1) · · · Ru(3) = 3.458, 3.481 Å, Ru(1)–Ru(2)–Ru(3) = 71.91, 72.80° (two crystallographically independent molecules)). Each metal–metal bond is bridged by one hydrido ligand, while a sulfido ligand bridges all three metal atoms. The bridging chlorine atom and the trichlorostannate ligands essentially replace one carbonyl ligand and one metal–metal bond (see Fig. 73).

Another example of oxidative addition to a cyclic tri-ruthenium cluster has recently been reported. Reaction of dppm with $[Ru_3(CO)_{12}]$ under mild conditions leads to the substituted species $[Ru_3(CO)_8(dppm)_2]$ [186]. Under more vigorous thermal conditions this product has been found to undergo a facile transformation via intramolecular oxidative cleavage of a coordinated dppm ligand giving the complex $[Ru_3(CO)_7(dppm)(\mu_3\text{-}PPh)(\mu_3\text{-}CHPPh_2)]$, (**105**), [186]. This product has been completely characterized by X-ray crystallography [186]. The bent tri-ruthenium framework (Ru(1)–Ru(2) =

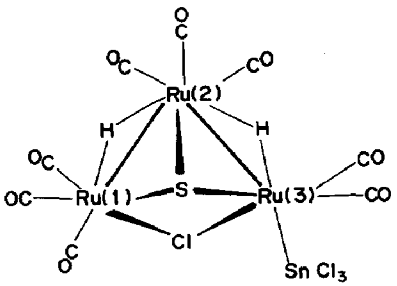

Fig. 73.

2.843 Å, Ru(2)–Ru(3) = 2.884 Å, Ru(1) · · · Ru(3) = 4.081 Å, Ru(1)–Ru(2)–Ru(3) = 90.91°) has one ruthenium–ruthenium bond still bridged by dppm. It is further supported by two face bridging organic moieties, a phenylphosphinidene unit, and the {$CHPPh_2$} fragment which functions as a tridentate ligand through the bridging carbon atom and the phosphorus atom (Fig. 74).

Reaction of [$Ru_3(CO)_{12}$] with 8-quininol in tetrahydrofuran has given, in good yield, a complex of stoichiometry [$Ru_3(CO)_8(C_9H_6NO)_2$], (**106**), shown by X-ray crystallography to contain an open triangle of ruthenium atoms (Ru(1)–Ru(3) = 2.774 Å, Ru(2)–Ru(3) = 2.773 Å, Ru(1) · · · Ru(2) = 3.039 Å, Ru(1)–Ru(3)–Ru(2) = 66.4°) [187]. The two quinolinolate ligands bridge the open ruthenium–ruthenium edge (Fig. 75). A series of closely related complexes containing other hydroxy hydrocarbylpyridine ligands have also been synthesized and characterized spectroscopically [187].

Two essentially linear tri-ruthenium complexes have been reported to date. The most remarkable is the di-cationic complex [$(Me_3P)_4Ru(\mu_2\text{-}CH_2)_2Ru(\mu_2\text{-}CH_2)_2Ru(PMe_3)_4](BF_4)_2$, (**107**), [188] isolated from the reaction of aqueous $HBF_4$ with a red oil obtained during the synthesis of [$Ru_2(\mu_2\text{-}CH_2)_3(PMe_3)_6$]. The di-cation consists of an almost linear arrangement of three ruthenium atoms (Ru–Ru = 2.637 Å, Ru–Ru–Ru = 179.3°). Each pair of ruthenium atoms is bridged by two methylene units; the central metal atom is formally coordinated only by the four bridging $CH_2$ units and

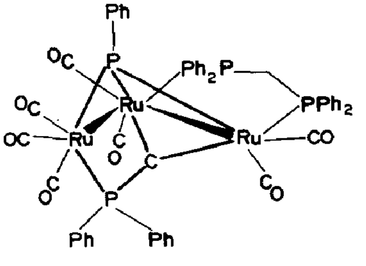

Fig. 74.

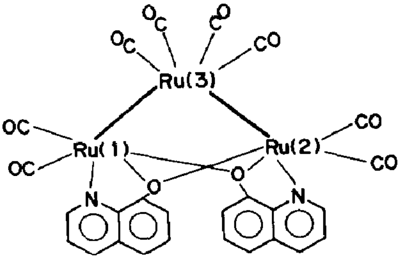

Fig. 75.

has a tetrahedral geometry. The two outer ruthenium atoms are octahedrally coordinated with bonds to two methylene units and to four trimethylphosphine ligands (Fig. 76). The authors propose bonding interactions between the ruthenium atoms, which assuming the molecule to consist of a Ru(III)–Ru(IV)–Ru(III) unit, gives a ruthenium–ruthenium bond order of 1.5 [188]. The second linear tri-ruthenium complex $[Ru(CO)_4\{(\eta^5\text{-}C_5H_5)Ru(CO)_2\}_2]$, (**108**), has been obtained as a by-product in the synthesis of $[\{(\eta^5\text{-}C_5H_5)Ru(CO)_2\}_2]$ from $[Ru_3(CO)_{12}]$ and cyclopentadiene [189]. The same product has also been isolated, albeit in low yield, from the reaction of $[(\eta^5\text{-}C_5H_5)Ru(CO)_2I]$ with $[Ru(CO)_4]^{2-}$ [189]. Crystallographic analysis [189] has determined that the tri-ruthenium unit is linear with a ruthenium–ruthenium bond length of 2.889 Å. All the carbonyl ligands adopt an eclipsed conformation, and the cyclopentadienyl rings have a *trans* disposition with respect to each other (Fig. 77). Closely related to these complexes is the linear, heterometallic complex $[Ru(CO)_4\{Mn(CO)_5\}_2]$, (**109**), obtained by pyrolysis of $[Ru_3(CO)_{12}]$ and $[Mn_2(CO)_{10}]$ in an evacuated sealed tube (205°C, 50 h) [190]. The complex has been characterized by physical measurements and by mass spectrometry. It is presumed to possess a linear Mn–Ru–Mn framework analogous to that observed in $[Fe(CO)_4\{Mn(CO)_5\}_2]$ [150].

Only three acyclic complexes of ruthenium with nuclearity > 3 have been reported to date. Recently, ultraviolet irradiation of the dimer $[\{(\eta^5\text{-}C_5H_5)Ru(CO)_2\}_2]$ in toluene for 3 days has been reported to give a mixture of products including the novel tetranuclear complex $[(\eta^5\text{-}C_5H_5)_2Ru_4(CO)_6$

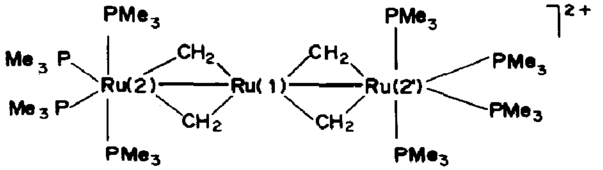

Fig. 76.

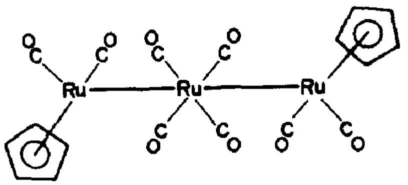

Fig. 77.

$(\mu_3\text{-}C_5H_4)_2]$, **(110)**, [191]. Although suitable crystallographic crystals of this material could not be obtained, the substituted derivative $[(\eta^5\text{-}C_5H_5)_2Ru_4\text{-}(CO)_5\{P(OMe)_3\}(\mu_3\text{-}C_5H_4)_2]$, **(111)**, (obtained from the photochemically initiated reaction between the parent complex and $P(OMe)_3$) has been structurally characterized by X-ray crystallography [191]. The molecule consists of a Z-shaped $Ru_4$ backbone (Fig. 78) (Ru(1)–Ru(2)–Ru(3) = 101.7°, Ru(2)–Ru(3)–Ru(4) = 99.6°). The central Ru(2)–Ru(3) bond length (2.887 Å) was found to be significantly longer than the outer ones (Ru(1)–Ru(2) = 2.755 Å, Ru(3)–Ru(4) = 2.767 Å) and thus the molecule may best considered to be an oligomer, made up of two, linked, $Ru_2$ units. An unusual feature of this molecule is that two $\{C_5H_4\}$ units each bridge three ruthenium atoms, $\eta^5$- to one and $\eta^1$- to each of the other two.

The complexes $[Ru_4(CO)_{10}(\mu_2\text{-}CO)(\mu_4\text{-}EPh)_2]$ (E = P, As) readily and reversibly, add carbon monoxide to give the acyclic clusters $[Ru_4(CO)_{13}(\mu_3\text{-}EPh)_2]$ [192]. Crystal structure determinations [192] on these compounds show that the molecules contain a puckered $Ru_4$ unit (**112**, E = P, Ru(1)–Ru(4) = 2.903 Å, Ru(2)–Ru(3) = 2.885 Å, Ru(3)–Ru(4) = 2.926 Å; **113**, E = As, Ru(1)–Ru(4) = 2.928 Å, Ru(2)–Ru(3) = 2.927 Å, Ru(3)–Ru(4) = 2.969 Å), $\mu_3$-capped by the {E-Ph} units (see Fig. 79). Structurally these molecules are thus related to $[Ru_3(CO)_9(\mu_3\text{-}ER)_2]$ (E = P, As) type complexes, and can be considered to be formally derived from them by insertion of a $\{Ru(CO)_4\}$ moiety into one of the six Ru–P or Ru–As bonds [192].

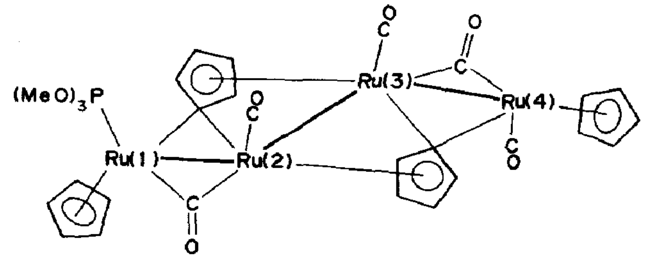

Fig. 78.

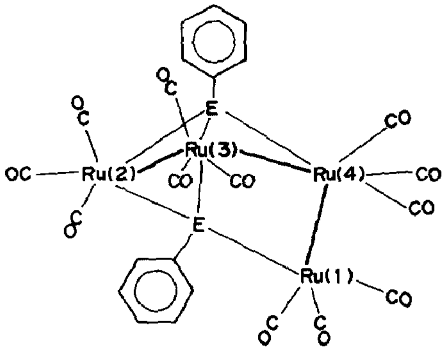

Fig. 79.

*(c) Osmium*

Iron complexes containing the $\{M_3(CO)_9\}$ open triangular unit capped by two triply bridging ligand systems, form an extensive series of compounds (see section B.(v)(a)). Surprisingly, relatively few ruthenium or osmium compounds of this type have been synthesized, and for osmium these are essentially restricted to the parent derivatives, e.g. $[Os_3(CO)_9(\mu_3\text{-}S)_2]$ (see Table 8). Lewis and co-workers were the first to report the synthesis of the complexes $[Os_3(CO)_9(\mu_3\text{-}X)_2]$ (X = S, Se, Te) [169]. Treatment of $[Os_3(CO)_{12}]$ with elemental sulfur, selenium or tellurium in boiling n-octane for 15 h generally gave a mixture of three products identified by analytical and spectroscopic data as $[Os_3(CO)_9H_2X]$, $[Os_3(CO)_9X_2]$ and $[Os_4(CO)_{12}H_2X_2]$ [169]. Improved yields of these products could be obtained by carrying out the reactions under a pressure of $CO/H_2$ (35 atm., 1 : 1), while under CO pressure alone, reduced yields of the hydrido complexes were obtained. The complex $[Os_3(CO)_9(\mu_2\text{-}H)_2(\mu_3\text{-}X)]$ contains a closed triangle of osmium atoms, while the complexes $[Os_4(CO)_{12}(\mu_2\text{-}H)_2(\mu_3\text{-}X)_2]$ have been structurally characterized [169] (X = Se) as containing a chain of four osmium atoms (see below). The X-ray crystal structures of $[Os_3(CO)_9(\mu_3\text{-}S)_2]$, (**114**), and $[Os_3(CO)_9(\mu_3\text{-}Se)_2]$, (**115**), have been determined (Fig. 80) [193,194]. The molecules are analogous to the iron derivatives, and contain an open triangle of three osmium atoms triply bridged by two sulfur or selenium atoms. The average Os–Os (bonding) and Os $\cdots$ Os (non bonded) distances increase in the order S < Se (**114**, 2.813

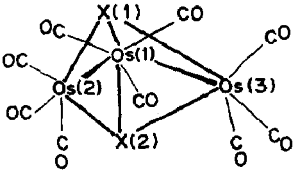

Fig. 80.

and 3.662 Å; **115**, 2.842 and 3.791 Å). In both molecules the Os–X distances to the central metal atom Os(1) (**114**, Os(1)–S(1) = 2.454 Å, Os(1)–S(2) = 2.434 Å; **115**, Os(1)–Se(1) = 2.551 Å, Os(1)–Se(2) = 2.539 Å) are larger than those to the terminal metal atoms Os(2) and Os(3) (**114**, Os(2)–S(1) = 2.415 Å, Os(2)–S(2) = 2.392 Å, Os(3)–S(1) = 2.402 Å, Os(3)–S(2) = 2.390 Å; **115**, Os(2)–Se(1) = 2.513 Å, Os(2)–Se(2) = 2.497 Å, Os(3)–Se(1) = 2.509 Å, Os(3)–Se(2) = 2.493 Å).

A range of substituted derivatives of the complex $[Os_3(CO)_9(\mu_3\text{-}S)_2]$ have been reported. Reaction with $PMe_2Ph$ or $PPh_2H$ at room temperature has given $[Os_3(CO)_8L(\mu_3\text{-}S)_2]$ (**116**, L = $PMe_2Ph$ [193], $PPh_2H$ [195]) in good yield. Reaction of $[Os_3(CO)_{12}]$ with $CS_2$ in hexane at 130°C under 10 atm. pressure of CO/Ar (1 : 1) has given $[Os_3(CO)_8(CS)(\mu_3\text{-}S)_2]$, (**117**), [196]. The complex $[Os_3(CO)_8(CS)(\mu_3\text{-}S)_2]$ has also been synthesized by the irradiation of $[HOs_3(CO)_{10}(\mu_3\text{-}SPh)]$ in the presence of $CS_2$ [197]. The X-ray crystal structures of $[Os_3(CO)_8L(\mu_3\text{-}S)_2]$ (L = $PMe_2Ph$, (**116**); CS, (**117**)) have been determined [193,196] (see Fig. 81). Both molecules have the expected open triangular framework of three osmium atoms, capped by two triply bridging sulfur atoms (**116**, Os(1)–Os(2) = 2.770 Å, Os(1)–Os(3) = 2.856 Å, Os(2) · · · Os(3) = 3.713 Å, Os(1)–S(1) = 2.452 Å, Os(1)–S(2) = 2.446 Å, Os(2)–S(1) = 2.426 Å, Os(2)–S(2) = 2.405 Å, Os(3)–S(1) = 2.413 Å, Os(3)–S(2) = 2.389 Å, Os(2)–Os(1)–Os(3) = 82.57°; **117**, Os(1)–Os(2) = 2.830 Å, Os(2)–Os(3) = 2.780 Å, Os(1) · · · Os(3) = 3.642 Å, Os(2)–S(1) = 2.440 Å, Os(2)–S(2) = 2.408 Å, Os(1)–S(1) = 2.380 Å, Os(1)–S(2) = 2.365 Å, Os(3)–S(1) = 2.400 Å, Os(3)–S(2) = 2.381 Å, Os(1)–Os(2)–Os(3) = 81.0°). The bridging sulfur atoms are, as in the parent complex $[Os_3(CO)_9(\mu_3\text{-}S)_2]$, unsymmetrically bridging the three osmium atoms. In both complexes the substituent ligand is coordinated at a basal osmium atom.

While many acyclic cluster complexes of osmium have their analogues in iron and ruthenium chemistry, the linear tri-osmium complexes of general formula $[Os_3(CO)_{12}X_2]$ (X = halide, H, alkyl, etc.) have, to date, no iron or ruthenium analogues.

The first examples of these complexes, $[Os_3(CO)_{12}X_2]$ (**118**, X = Cl, Br, I), were obtained by reaction of the trinuclear cluster $[Os_3(CO)_{12}]$ with the

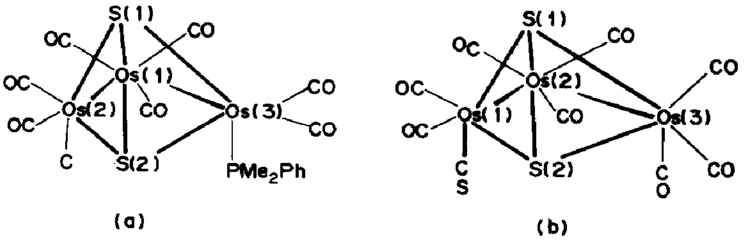

(a) (b)

Fig. 81.

TABLE 8

Acyclic cluster complexes of osmium

| Formula | Complex | Fig. | Ref. [a] |
|---|---|---|---|
| $[Os_3(CO)_9(\mu_3\text{-}S)_2]$ | **(114)** | 80 | 169,193★ |
| $[Os_3(CO)_9(\mu_3\text{-}Se)_2]$ | **(115)** | 80 | 169,194★ |
| $[Os_3(CO)_9(\mu_3\text{-}Te)_2]$ | – | – | 169 |
| $[Os_3(CO)_8L(\mu_3\text{-}S)_2]$ ($L = PMe_2Ph, PPh_2H$) | **(116)** | 81 | 193,194★,195 |
| $[Os_3(CO)_8(CS)(\mu_3\text{-}S)_2]$ | **(117)** | 81 | 196★ |
| $[Os_3(CO)_{12}X_2]$ ($X = Cl, Br, I$) | **(118)** | 82 | 198,199,202★,<br>203,223 |
| $[Os_3(CO)_{10}(PEt_3)_2Cl_2]$ | **(119)** | – | 204 |
| $[Os_3(CO)_{12}(AuPPh_3)Cl]$ | **(120)** | – | 205 |
| $[Os_3(CO)_{12}(SnCl_3)Cl]$ | **(121)** | – | 206 |
| $[Os_3(CO)_{12}(SiXCl_2)_2]$ ($X = Me, Cl$) | **(122)** | 83 | 207★ |
| $[Os_3(CO)_{12}H_2]$ | **(123)** | – | 208–210, |
| $[Os_3(CO)_{12}R_2]$ ($R$ = alkyl) | – | – | 211,212,213★,214 |
| $[Os_3(CO)_{10}(\mu_2\text{-}OMe)_2]$ | **(124)** | 84 | 199,201,215,216★ |
| $[Os_3(CO)_{10}(\mu_2\text{-}X)_2]$ ($X = Cl, Br, I$) | **(125)** | – | 204,217 |
| $[Os_3(CO)_8(PPh_3)_2(\mu_2\text{-}Cl)_2]$ | **(126)** | – | 204,217 |
| $[Os_3(CO)_{10}(\mu_2\text{-}NO)_2]$ | **(127)** | – | 218,219 |
| $[Os_3(CO)_9L(\mu_2\text{-}NO)_2]$ ($L$ = py, $P(OMe)_3$, $PPh_3$, $NMe_3$) | **(128)** | – | 218,219,220★,221★ |
| $[Os_3(CO)_{10}(\mu_2\text{-}ER)_2]$ ($E = S, Se$; $R$ = alkyl or aryl) | **(129)** | 85,86 | 222 |
| $[Os_3(CO)_{10}(\mu_2\text{-}O{=}CMe)(\mu_2\text{-}O{=}CEt)]$ | **(130)** | – | 223 |
| $[Os_3(CO)_{10}(\mu_2\text{-}X)(\mu_2\text{-}O{=}CR)]$ ($X = Cl, Br, I$; $R$ = alkyl) | – | – | 223,224 |
| $[Os_3(CO)_{10}(\mu_2\text{-}OH)(\mu_2\text{-}O{=}CMe)]$ | – | – | 224 |
| $[Os_3(CO)_{10}(CH_3OCON{=}NCO_2CH_3)]$ | **(131)** | 87 | 225,226★ |
| $[Os_3(CO)_{11}(CH_3OCON{=}NCO_2CH_3)]$ | **(132)** | – | 225,226 |
| $[Os_3(CO)_{12}(CH_3OCON{=}NCO_2CH_3)]$ | **(133)** | – | 226★ |
| $[Os_3(CO)_{10}(CON_3Ph)L]$ ($L = MeCN, C_5H_5N$) | **(134)** | 88 | 227★,228★ |
| $[Os_3(CO)_9\{\mu_3\text{-}C(CNBu^t)CPh\}(\mu_2\text{-}PPh_2)]$ | **(135)** | 89 | 229 |
| $[Os_3(CO)_9(C\{C(NHR)(NHBu^t)\}CPh)(\mu_2\text{-}PPh_2)]$ ($R$ = alkyl) | **(136)** | 90 | 229★ |
| $[Os_3(CO)_9(\mu_3\text{-}S)(\mu_3\text{-}NSiMe_3)]$ | – | 91 | 230★ |
| $[Os_3(CO)_9(\mu_3\text{-}PR)(\mu_3\text{-}C_6H_4)]$ ($R$ = alkyl or aryl) | **(137)** | 92 | 231★ |
| $[Os_3(CO)_9(\mu_3\text{-}C_6H_4)(\mu_2\text{-}AsMe_2)]$ | **(138)** | 93 | 232★ |
| $[HOs_3(CO)_9(\mu_3\text{-}C_6H_4)(\mu_2\text{-}SR)]$ ($R$ = alkyl) | **(139)** | 94 | 233★ |
| $[Os_3(CO)_8(PMe_2Ph)(\mu_3\text{-}S)(\mu_3\text{-}\eta^2\text{-}SCH_2)]$ | **(140)** | – | 234★,236★ |
| $[Os_3(CO)_7(PMe_2Ph)\{P(OMe)_3\}(\mu_3\text{-}S)(\mu_3\text{-}\eta^2\text{-}SCH_2)]$ | **(141)** | 95 | 237★ |
| $[HOs_3(CO)_7(PMe_2Ph)(\mu_3\text{-}S)(\mu_3\text{-}\eta^2\text{-}SCH_2)(SnMe_3)]$ | **(142)** | 96 | 239★ |
| $[H_2Os_3(CO)_7(PMe_2Ph)(\mu_3\text{-}S)(\mu_3\text{-}\eta^2\text{-}SCH_2)]$ | **(143)** | 97 | 239★ |
| $[HOs_3(CO)_9(\mu_3\text{-}S)(\mu_2\text{-}HC{=}NR)]$ ($R$ = alkyl or aryl) | **(144)** | 98 | 240,241,<br>254–256 |
| $[HOs_3(CO)_9(\mu_3\text{-}S)(\mu_2\text{-}\overline{C{=}NCH_2CH_2S})]$ | **(145)** | – | 242 |
| $[Os_3(CO)_8(\mu_2\text{-}H)_2(\mu_3\text{-}S)_2]$ | **(146)** | 99 | 197,243★ |
| $[Os_3(CO)_7(CS)(\mu_2\text{-}H)_2(\mu_3\text{-}S)_2]$ | – | 100 | 244★ |
| $[HOs_3(CO)_9(\mu_2\text{-}H)(\mu_2\text{-}OH)(\mu_3\text{-}C{=}C{=}CPh_2)]$ | **(147)** | – | 245★ |

TABLE 8 (continued)

| Formula | Complex | Fig. | Ref. [a] |
|---|---|---|---|
| $[Os_3(CO)_{11}\{C(CH_2)_2\}]$ | **(148)** | 101 | 246* |
| $[HOs_3(CO)_{10}(PEt_3)(CF_3CCHCF_3)]$ | **(149)** | 102 | 247*,248 |
| $[Os_4(CO)_{13}(\mu_3\text{-}S)_2]$ | **(150)** | 104 | 250* |
| $[Os_3W(CO)_{12}(PMe_2Ph)_2(\mu_2\text{-}S)_2]$ | **(151)** | 106 | 252* |
| $[Os_4(CO)_{12}(\mu_2\text{-}H)_2(\mu_3\text{-}X)_2]$ (X = S, Se) | **(152)** | 107 | 169*,253 |
| $[H_2Os_6(CO)_{17}(\mu_4\text{-}S)(\mu_2\text{-}HC{=}NR)]$ (R = Ph, $C_6H_4F$-4) | **(153)** | – | 254*,256* |
| $[H_4Os_6(CO)_{15}(\mu_4\text{-}S)(\mu_3\text{-}S)(\mu_3\text{-}S)(\mu_2\text{-}HC{=}NPh)_2]$ | **(154)** | – | 255* |
| $[H_6Os_6(CO)_{14}(\mu_4\text{-}S)(\mu_3\text{-}S)(\mu_2\text{-}HC{=}NPh)_2]$ | **(155)** | – | 255* |
| $[Os_6(CO)_{14}(\mu_4\text{-}S)(\mu_3\text{-}S)(\mu_2\text{-}PPh_2)_2]$ | **(156)** | – | 195* |
| $[Os(CO)_4(AuPPh_3)_2]$ | **(157)** | – | 257 |
| $[Os(CO)_4\{M(CO)_5\}_2]$ (M = Mn, Re) | – | 108 | 190 |
| $[OsPt_2(CO)_5(PPh_3)_2(\mu_3\text{-}MeC_2Me)]$ | **(158)** | 109 | 258* |
| $[OsPt_2(CO)_6(PPh_3)(\mu_3\text{-}MeC_2Me)]$ | – | – | 258 |

[a] References marked with an asterisk refer to crystal structure determinations.

halogens in benzene [198,199]. These results contrast with the corresponding reactions of the iron and ruthenium carbonyls $[M_3(CO)_{12}]$ (M = Fe, Ru), the products of which include the mononuclear complexes of the type $[M(CO)_4X_2]$ and in the case of ruthenium, the complex $[Ru_3(CO)_{12}X_6]$ [200]. This difference in behaviour most probably reflects the increase in stability of the metal–metal bond towards oxidation on descending the triad or is due to a kinetic effect in which case a complex $[Ru_3(CO)_{12}X_n]$ could be visualized as an intermediate en route to $[Ru(CO)_4X_2]$ [198].

On the basis of the effective atomic number rule a linear arrangement of metal atoms was proposed for the complexes $[Os_3(CO)_{12}X_2]$ (X = Cl, Br, I) while the IR spectra [199,201] were interpreted as being consistent with $D_{4h}$ symmetry i.e. the halogen atoms being axial (*trans*) to the metal–metal bonds. Molecular ions $[Os_3(CO)_{12}X_2]^+$, together with ions of the type $[Os_3(CO)_{12-n}X_2]^+$ ($n = 1$–$12$), $[Os_2(CO)_{8-n}X_2]^+$ ($n = 1$–$8$) and $[Os(CO)_{4-n}X_2]^+$ ($n = 1$–$4$) were observed in the mass spectra of these complexes. This pattern contrasts sharply with that observed for the cyclic tri-osmium cluster systems, and strongly supports the linear formulation [199].

The question of the structure of these complexes has been unequivocally resolved for $[Os_3(CO)_{12}I_2]$ [202]. The molecule comprises a linear unit of three osmium atoms with the iodine atoms occupying equatorial sites *trans* to one another on the terminal osmium atoms (see Fig. 82). Each osmium atom has an octahedral configuration, with the equatorial ligands on the

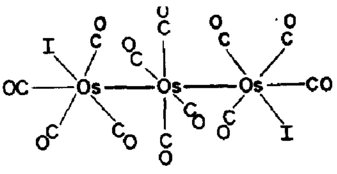

Fig. 82.

terminal osmium atoms staggered with respect to the four carbonyl groups on the central osmium atom. The Os–Os bond length is 2.935 Å.

The kinetics of the reaction of $[Os_3(CO)_{12}]$ with halogens have been investigated [203]. The reaction with chlorine was found to be consistent with the mechanism

$$[Os_3(CO)_{12}] + Cl_2 \rightleftharpoons [Os_3(CO)_{12} \cdot Cl_2] \rightarrow [Os_3(CO)_{12}Cl_2]$$

where the intermediate $[Os_3(CO)_{12} \cdot Cl_2]$ could be either a charge-transfer, or a Lewis acid–base complex formed between $[Os_3(CO)_{12}]$ and chlorine. In the case of bromine, direct evidence for a similar intermediate was not obtained, while the reaction with iodine was complicated and was not studied in great detail [203].

The substituted derivative $[Os_3(CO)_{10}(PEt_3)_2Cl_2]$, **(119)**, has been obtained by the reaction of the disubstituted cluster complex $[Os_3(CO)_{10}(PEt_3)_2]$ with chlorine in carbon tetrachloride [204]. The structure of this product is not known, although it might be anticipated that due to the steric bulk of the phosphine ligand, a diaxial disposition of the phosphine ligands would prevail.

Closely related complexes containing the linear tri-osmium skeleton have been synthesized by the oxidative addition of gold, tin and silicon halides to $[Os_3(CO)_{12}]$. Reaction of $[(PPh_3)AuCl]$ with $[Os_3(CO)_{12}]$ has given the complex $[Os_3(CO)_{12}(AuPPh_3)(Cl)]$, **(120)**, proposed to contain an unusual Os–Os–Os–Au core [205]. The complex is monomeric in chloroform and its IR spectrum is consistent with the linear arrangement of metal atoms. The corresponding bromide $[Os_3(CO)_{12}(AuPPh_3)(Br)]$ has been prepared in a similar manner although reactions of $[Os_3(CO)_{12}]$ with $[(PPh_3)AuI]$, $[(AsPh_3)AuCl]$, $[(PPh_3)_3CuCl]$ and $[(PPh_3)_3AgBr]$ were not successful [205]. Tin tetrachloride also reacts with $[Os_3(CO)_{12}]$ giving a product of stoichiometry $[Os_3(CO)_{12} \cdot SnCl_4]$, **(121)**, and which presumably also contains a similar linear tri-osmium core [206].

The complexes $[Os_3(CO)_{12}(SiXCl_2)_2]$ (**122**, X = Me, Cl) have been obtained by the reaction of $[Os_3(CO)_{12}]$ with the appropriate silane $SiXCl_2H$ at 140°C under carbon monoxide pressure (80 atm.) [207]. The X-ray crystal structure of $[Os_3(CO)_{12}(SiCl_3)_2]$ has been determined [207]. The molecule has a linear $Si–Os_3–Si$ core (Os–Os = 2.912 Å, Os–Si = 2.377 Å). The

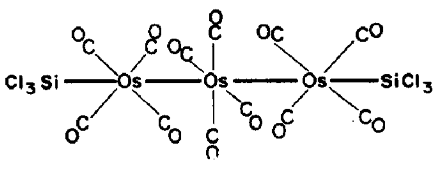

Fig. 83.

carbonyl groups on the terminal osmium atoms are staggered with respect to those on the central osmium atom (see Fig. 83). A notable feature of this molecule is that the silyl groups are disposed *trans* to the Os–Os bonds in contrast to the *cis* disposition of the iodide ligands in $[Os_3(CO)_{12}I_2]$ [202]. This can be rationalized in terms of unfavourable steric interactions between the chlorine atoms of the $SiCl_3$ ligand and the carbonyl ligands on the central osmium atom, if the silyl moieties were placed *cis* to the Os–Os bond. This suggests that other related molecules, e.g. $[Os_3(CO)_{12}(AuPPh_3)$-$Cl]$, $[Os_3(CO)_{12}(SnCl_3)(Cl)]$, might contain a linear metal or metal–metalloid chain, but that the single halogeno ligand might still adopt a *cis* configuration relative to the linear core.

Molecules containing the linear $\{Os_3(CO)_{12}\}$ core structure have also been synthesized with hydride and alkyl substituents. The complex $[Os_3(CO)_{12}H_2]$, (**123**), was first reported by Moss and Graham [208] in 1970. It was synthesized by the high pressure carbonylation of osmium tetroxide in the presence of hydrogen and in good yields by the reduction of $[Os_3(CO)_{12}Br_2]$ with the reducing system zinc dust/acetic acid/methanol [208]. Low product yields were obtained using $NaBH_4$ as the reducing agent [208]. By a modification of this procedure, $[Os_3(CO)_{12}D_2]$ could also be synthesized. On the basis of their spectroscopic properties [208,209] and chemical reactivity [210] (e.g. reaction with $CX_4$ ($X = Cl$, Br) gives the complexes $[Os_3(CO)_{12}X_2]$) the most probable structure for these complexes is similar to that of $[Os_3(CO)_{12}I_2]$, i.e. a linear arrangement of osmium atoms with terminal hydrides occupying equatorial positions on the end osmium atoms [209].

Complexes of composition $[Os_3(CO)_{12}R_2]$ have been obtained as decomposition products of $[Os(CO)_4(H)R]$ [211,212]. Their stoichiometry has been established by mass spectrometry, and on the basis of their spectroscopic properties (which are similar to those of $[Os_3(CO)_{12}H_2]$), a linear tri-osmium structure, equatorially disubstituted with alkyl groups was proposed [211]. This has been confirmed by a single crystal X-ray analysis of $[Os_3(CO)_{12}$ $(CH_3)_2]$ [213]. A related product of the decomposition of $[Os(CO)_4(H)(Et)]$ is one tentatively assigned the stoichiometry $[Os_3(CO)_{12}(H)(Et)]$ [212] which presumably has a structure closely related to those of $[Os_3(CO)_{12}H_2]$ and $[Os_3(CO)_{12}(CH_3)_2]$.

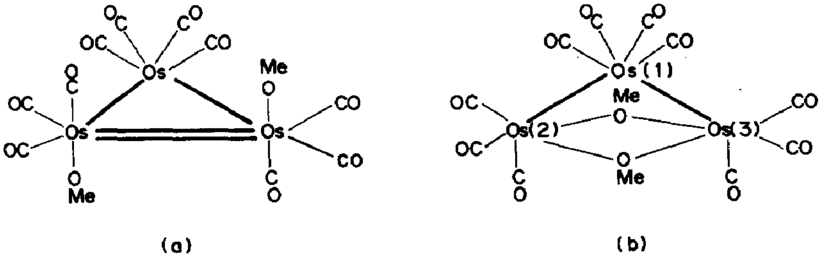

Fig. 84.

The complex $[Os_3(CO)_{12}(CH_3)_2]$ decomposes rapidly at 90°C to give $[Os_3(CO)_{12}]$ and methane [214]. The reaction probably proceeds via homolytic Os–C bond cleavage to give methyl radicals that subsequently abstract a hydrogen atom from the solvent giving methane. Reaction with excess HBr in $CCl_4$ gives $[Os_3(CO)_{12}Br_2]$, while reaction with one equivalent of HBr gives the mixed ligand complex $[Os_3(CO)_{12}(CH_3)(Br)]$, the latter presumably similar in structure to the former. In contrast, reaction with iodine leads to metal–metal bond cleavage, giving *cis*-$[Os(CO)_4(CH_3)I]$ and $[Os_2(CO)_8(CH_3)(I)]$ as the products.

Carbonylation of osmium tetroxide in methanol has given a range of triosmium complexes including the unusual product $[Os_3(CO)_{10}(\mu_2\text{-OMe})_2]$, (**124**), [215]. On the basis of the Effective Atomic Number (EAN) rule, two structures, shown in Fig. 84, were proposed for this molecule [199,201,215]. The X-ray crystal structure determination [216] has shown the molecule to have the structure (b), namely an open triangle of osmium atoms, with the open edge bridged by the two methoxy ligands (Os(1)–Os(3) = 2.823 Å, Os(1)–Os(2) = 2.815 Å, Os(3) · · · Os(2) = 3.078 Å; Os(3)–Os(1)–Os(2) = 66.17°). The relatively short "non-bonded" Os(3) · · · Os(2) distance does, however, suggest that metal–metal interaction cannot be ruled out completely; it is interesting to note in this regard that a study of the vibrational spectra of this molecule [201] revealed three intense Raman lines attributable to $\nu$(Os–Os), although only two bands attributable to metal–metal vibrations were observed in the far-infrared spectrum.

Prolonged heating of the linear $Os_3$ complexes $[Os_3(CO)_{12}X_2]$ (X = Cl, Br, I) in benzene results in loss of two molar equivalents of carbon monoxide and formation of the products $[Os_3(CO)_{10}(\mu_2\text{-}X)_2]$ (**125**, X = Cl, Br, I) in good yield [204, 217]. These complexes are believed to have the same structure as the complex $[Os_3(CO)_{10}(\mu_2\text{-OMe})_2]$, namely an open triangle of osmium atoms, with the open edge bridged by two halogeno ligands [204]. Carbonylation of $[Os_3(CO)_{10}(\mu_2\text{-}X)_2]$ (140 atm.) regenerates the linear complexes, although, somewhat surprisingly, reaction with $PPh_3$ (X = Cl) does not result in bridge-splitting but rather substitution, giving the

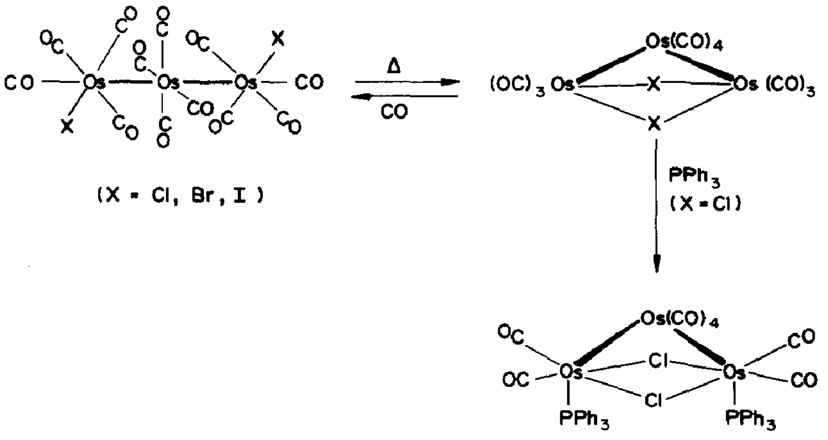

Scheme 8.

complex $[Os_3(CO)_8(PPh_3)_2(\mu_2\text{-}Cl)_2]$, **(126)** (see Scheme 8). Presumably substitution occurs at the two bridge-head osmium atoms.

Osmium, like ruthenium, forms trinuclear complexes containing an open triangle of atoms where the open edge is bridged by two, three-electron donor nitrosyl ligands (see Fig. 66). Tri-osmium dodecacarbonyl reacts directly with nitrous oxide in n-octane at 126°C to give mainly the trinuclear cyclic cluster species $[Os_3(CO)_9(NO)_2]$, together with small amounts of the acyclic cluster complex $[Os_3(CO)_{10}(\mu_2\text{-}NO)_2]$, **(127)**, [218,219]. The former contains a closed triangle of osmium atoms, with terminal, three-electron donor nitrosyl ligands, while **(127)** has an acyclic structure, with the open edge bridged by the two nitrosyl ligands. Despite these differences, both complexes are closely related chemically [218,219]; this is particularly clear when the reactions of $[Os_3(CO)_9(NO)_2]$ with donor ligands are considered [218,219]. $[Os_3(CO)_9(NO)_2]$ reacts with carbon monoxide at 80°C to form **(127)**, and also reacts directly with pyridine to form the complex $[Os_3(CO)_9(py)(\mu_2\text{-}NO)_2]$, **(128)**, the latter containing an open, bridged triangle of osmium atoms similar to **(127)**. Further, $[Os_3(CO)_9(NO)_2]$ reacts readily with $P(OMe)_3$ or $PPh_3$ to give the complexes $[Os_3(CO)_8L(NO)_2]$ ($L = P(OMe)_3$, $PPh_3$), the latter complexes reacting readily with carbon monoxide in boiling heptane to give complexes of the type $[Os_3(CO)_9L(\mu_2\text{-}NO)_2]$.

The X-ray crystal structure of two complexes $[Os_3(CO)_9L(\mu_2\text{-}NO)_2]$ ($L = NMe_3$ [220], $P(OMe)_3$ [221]) have been determined. (The complex $[Os_3(CO)_9(NMe_3)(\mu_2\text{-}NO)_2]$ has been synthesized by the reaction of $[Os_3(CO)_{10}(\mu_2\text{-}NO)_2]$ with $Me_3NO$ [192].) Both molecules have the same open, edge-bridged $\{Os_3(\mu_2\text{-}NO)_2\}$ unit (Os(1)–Os(3) = 2.885 Å, Os(2)–Os(3) = 2.875 Å, Os(1) $\cdots$ Os(2) = 3.197 Å, Os(1)–Os(3)–Os(2) =

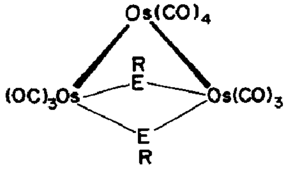

Fig. 85.

67.4° and Os(1)–Os(2) = 2.888 Å, Os(3)–Os(2) = 2.894 Å, Os(3) · · · Os(1) = 3.217 Å, Os(1)–Os(2)–Os(3) = 67.6° respectively). In both cases the ligands $NMe_3$ and $P(OMe)_3$ occupy a coordination site on the bridge-head osmium atom; as expected, the metal–metal bond *trans* to the donor ligand is slightly longer than the other osmium–osmium bond.

The cluster $[Os_3(CO)_{11}(NCMe)]$ reacts with the compounds RE–ER (E = S, R = Me, Ph, $CH_2Ph$; E = Se, R = Ph) to give the complexes $[Os_3(CO)_{10}(\mu_2\text{-}ER)_2]$, (**129**), in ca. 50% yield [222]. The IR spectra of these complexes are closely related to those of $[Os_3(CO)_{10}(\mu_2\text{-}X)_2]$ (X = Cl, Br, I) [204], indicating a similar molecular geometry, i.e. a triangular of three osmium atoms with the long (non-bonded) edge spanned by two $\{\mu_2\text{-}ER\}$ bridging groups (Fig. 85). The authors propose that the molecule $R_2E_2$ initially displaces the labile acetonitrile ligand, which, followed by an intramolecular oxidative addition of the RE–ER moiety to an Os–Os bond with CO loss gives the final product. Three isomers could be envisaged for these products; these are shown below (Fig. 86(a)–(c)). Only one of the three isomers is produced for each product, although $[Os_3(CO)_{10}(\mu_2\text{-}SMe)_2]$ does undergo irreversible thermal isomerization to give, finally, an isomer isostructural with $[Os_3(CO)_{10}(\mu_2\text{-}OMe)_2]$ [216]. The compound $[Os_3(CO)_{10}(\mu_2\text{-}SCH_2Ph)_2]$ on heating produced small amounts of $[Os_3(CO)_9(\mu_3\text{-}S)_2]$, while $[Os_3(CO)_{10}(\mu_2\text{-}SPh)_2]$ gave a small amount of $[Os_3(CO)_9(\mu_2\text{-}SPh)(\mu_3\text{-}SPh)]$, believed to have a similar structure to the related iron complex $[Fe_3(CO)_9(SBu^t)_2]$ [88,89]. The compound $[Os_3(CO)_{10}(\mu_2\text{-}SePh)_2]$ under-

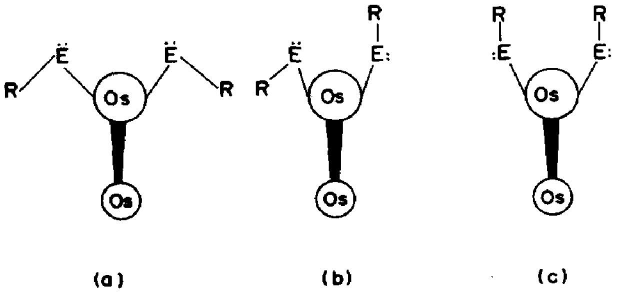

(a) (b) (c)

Fig. 86.

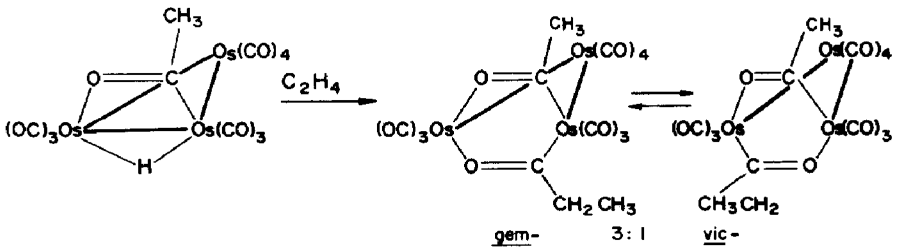

Scheme 9.

goes thermal decomposition in hot n-octane to give low yields of $[Os_3(CO)_9(\mu_3\text{-Se})_2]$ and a second isomeric form of $[Os_3(CO)_{10}(\mu_2\text{-SePh})_2]$ with an IR spectrum related to that of $[Os_3(CO)_9(\mu_2\text{-OMe})_2]$.

The complexes *vic*- and *gem*-$[Os_3(CO)_{10}(\mu_2\text{-O=CMe})(\mu_2\text{-O=CEt})]$, (**130**), have been synthesized by the action of ethylene (136 atm., 140°C, 48 h) on $[Os_3(CO)_{10}(\mu_2\text{-H})(\mu_2\text{-O=CMe})]$ (Scheme 9) [223]. A similar reaction in ruthenium chemistry takes place under milder reaction conditions (3 atm., 25°C), and does not lead to a trimetallic bis(acyl) complex, but via extrusion of "$Ru(CO)_4$" (recovered as $[Ru_3(CO)_{12}]$) gives the dinuclear complex *gem*-$[Ru_2(CO)_6(\mu_2\text{-O=CMe})(\mu_2\text{-O=CEt})]$ [174].

The complexes $[Os_3(CO)_{10}(\mu_2\text{-O=CR})_2]$ (R = Me, Ph) have been synthesized in a two step sequence from $[Os_3(CO)_{12}]$ (Scheme 10). Treatment of $[Os_3(CO)_{12}]$ with two equivalents of methyl- or phenyllithium (0°C, THF) gives instantaneously the dianions $[Os_3(CO)_{10}\{C(O)R\}_2]^{2-}$. Oxidation with either $Me_3OSbCl_6$ or $CuBr_2$ (2 equivalents, THF, −10°C) gives pure *vic*-$[Os_3(CO)_{10}(\mu_2\text{-O=CR})_2]$. In $CHCl_3$ solution, *vic*-$[Os_3(CO)_{10}(\mu_2\text{-O=CMe})_2]$ isomerizes within 1 h at 25°C to a solution containing 2.4 : 1

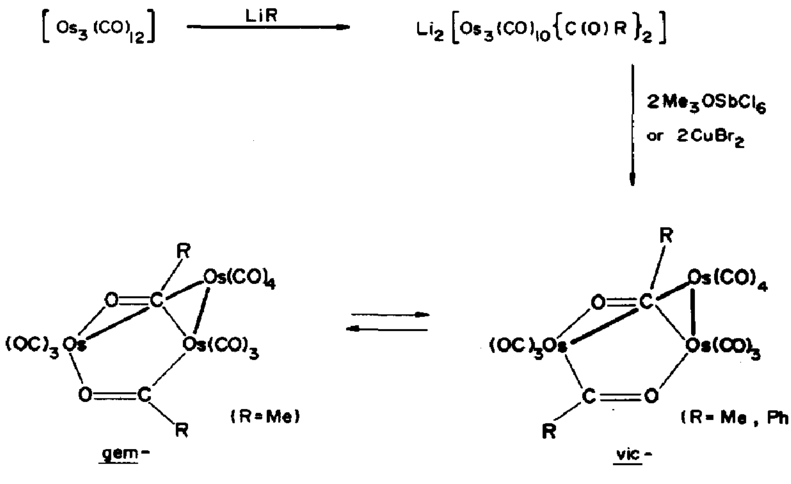

Scheme 10.

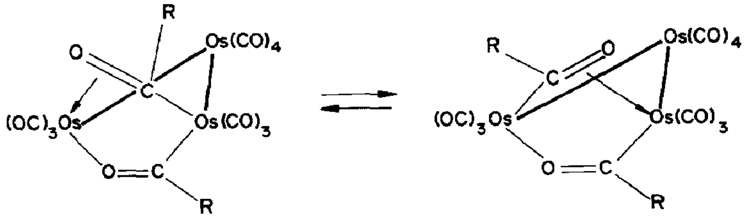

Scheme 11.

*gem* : *vic*; pure *gem*-[$Os_3(CO)_{10}(\mu_2$-O=CMe$)_2$] can be selectively crystallized out of this mixture by slow evaporation of the solvent [223]. These results are notable for they provide the first example of acyl group migration. The most likely mechanism for this process involves bridging $\sigma$-, $\pi$-bonded acyl intermediates (Scheme 11) [223].

It is interesting to note that the column chromatographic purification of *vic*-[$Os_3(CO)_{10}(\mu_2$-O=CR$)_2$] (R = Me, Ph) [223], synthesized using $Me_3OSbCl_6$ as oxidant, also yielded small quantities (~ 2%) of [$Os_3(CO)_{10}(\mu_2$-Cl$)_2$] and [$Os_3(CO)_{10}(\mu_2$-Cl$)(\mu_2$-O=CR)], both compounds containing the acyclic, di-bridged $Os_3$ triangle.

Similarly, attempts to purify the bis(acyl) complex [$Os_3(CO)_9\{C(O)R\}(\mu_2$-O=CMe)] (obtained by alkylation of [$Os_3(CO)_{10}(\mu_2$-O=CCH$_3$)]$^-$ with $ROSO_2CF_3$; R = $CH_3$, $CD_3$) resulted in disproportionation to [$Os_3(CO)_9\{C(OR)R\}(\mu_2$-O=CMe$)(\mu_2$-H)] and [$Os_3(CO)_{10}(\mu_2$-OH$)(\mu_2$-O=CMe)] [224]. Due to the presence of chloride ion in the mixture, the complex [$Os_3(CO)_{10}(\mu_2$-Cl$)(\mu_2$-O=CMe)] was also isolated (Scheme 12). The halogen impurity isolated for the case R = $CD_3$ was [$Os_3(CO)_{10}(\mu_2$-I$)(\mu_2$-O=CCD$_3$)]. The bromo complex [$Os_3(CO)_{10}(\mu_2$-Br$)(\mu_2$-O=CMe)] has been isolated as a minor product present after the alkylation of [$Os_3(CO)_9(\mu_2$-H$)(\mu_2$-O=CMe$)\{C(O)R\}$] [224].

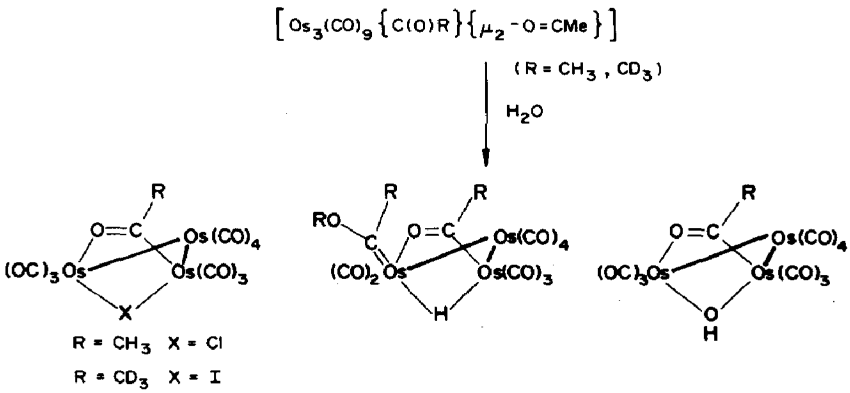

Scheme 12.

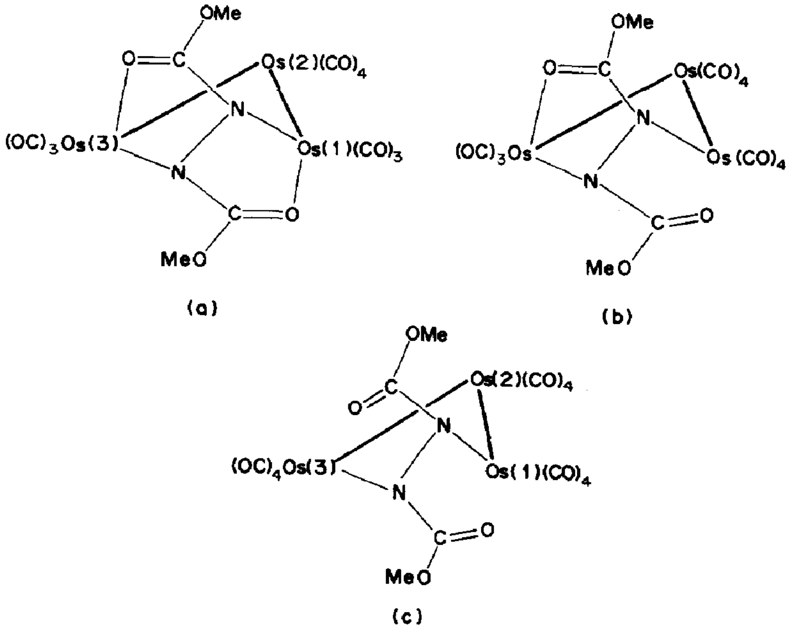

Fig. 87.

$[Os_3(CO)_{11}(NCMe)]$ or $[Os_3(CO)_{10}(NCMe)_2]$ react with excess dimethylazodicarboxylate to yield the complex $[Os_3(CO)_{10}(CH_3O_2CN{=}NCO_2CH_3)]$, (**131**), [225,226] (Fig. 87(a)). In the case of $[Os_3(CO)_{11}(NCMe)]$, a precursor of (**131**), $[Os_3(CO)_{11}(CH_3O_2CN{=}NCO_2CH_3)]$, (**132**), (Fig. 87(b)), is isolated when the reaction is carried out under mild conditions [226]. Complex (**131**) reacts quantitatively with carbon monoxide (102 atm.) to give $[Os_3(CO)_{12}(CH_3O_2CN{=}NCO_2CH_3)]$, (**133**), [226] (Fig. 87(c)). The X-ray crystal structures of (**131**) and (**133**) have been determined [226]. Complex (**131**) has an open triangle of three osmium atoms (Os(1)–Os(2) = 2.9638 Å, Os(2)–Os(3) = 2.9704 Å, Os(1) · · · Os(3) = 4.1615 Å, Os(1)–Os(2)–Os(3) = 89.06°) with the azo ligand spanning one edge. The ligand forms two five-membered chelate rings and acts as a six-electron donor. In this regard it should be viewed as being strictly analogous to the complexes $[Os_3(CO)_{10}(\mu_2\text{-}X)_2]$ already discussed. Complex (**133**) is essentially related to (**131**) by having two carbonyl ligands occupying the coordination sites previously filled by the coordinated methoxycarbonyls. The molecule has a similar open triangle of three osmium atoms (Os(1)–Os(2) = 2.9672 Å, Os(2)–Os(3) = 3.0078 Å, Os(1) · · · Os(3) = 4.1979 Å, Os(1)–Os(2)–Os(3) = 89.27°). It is best viewed as being derived from $[Os_3(CO)_{12}]$ by the replacement of one Os–Os bond by a bridging two electron donor hyrdazide ligand. It is interesting to note that, formally, (**133**) is related to the complexes $[Os_3(CO)_{12}X_2]$ which possess linear tri-osmium skeletons, but that because of the constraints

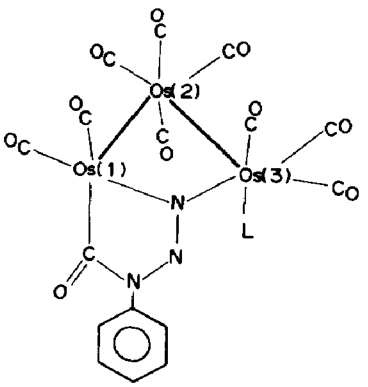

Fig. 88.

imposed by the chelating hydrazide ligand, the triangular disposition of the osmium atoms is maintained. The structure of (**132**), deduced by IR and NMR spectroscopy, is intermediate between those of (**131**) and (**133**), and is derived from (**131**) by replacement of one coordinated methoxycarbonyl by a CO ligand. Complex (**133**) could not be synthesized directly from $[Os_3(CO)_{12}]$ and dimethylazodicarboxylate. Heating of (**133**) in benzene (70°C, 5 h) gave (**132**) in quantitative yield, as did treatment of (**133**) with $Me_3NO$. Complex (**131**) was not found to be a product of these decarbonylation reactions [226].

The clusters $[Os_3(CO)_{11}(NCMe)]$ and $[Os_3(CO)_{11}(NC_5H_5)]$ have been treated with phenyl azide to give the complexes $[Os_3(CO)_{10}(CON_3Ph)(L)]$ (**134**, L = MeCN, $C_5H_5N$) [227,228] both of which have been characterized by a combination of spectroscopic techniques and X-ray crystallography [227,228]. In both complexes the tri-osmium unit defines an open triangle (**134**, L = MeCN, Os(1)–Os(2) = 2.943 Å, Os(2)–Os(3) = 2.937 Å, Os(1) · · · Os(3) = 3.612 Å, Os(1)–Os(2)–Os(3) = 75.8°; **134**, L = $C_5H_5N$, Os(1)–Os(2) = 2.936 Å, Os(2)–Os(3) = 2.929 Å, Os(1) · · · Os(3) = 3.615 Å, Os(1)–Os(2)–Os(3) = 76.1°) with the azide ligand bridging the open edge (see Fig. 88). The acetonitrile and pyridine ligands occupy an axial coordination site on Os(3). The mechanism of formation of the complexes (**134**) is proposed to occur via ligand (acetonitrile or pyridine) dissociation from $[Os_3(CO)_{11}L]$ giving the reactive intermediate $[Os_3(CO)_{11}]$ which then reacts with phenyl azide followed by recombination with the ligand [228].

t-Butyl isonitrile has been found to undergo regiospecific addition to the $\alpha$-carbon atom of the cluster bound $\mu_3$-$\eta^1,\eta^2$-acetylide in $[Os_3(CO)_9(\mu_3\text{-}\eta^1,\eta^2\text{-}C{\equiv}CPh)(\mu_2\text{-}PPh_2)]$ generating $[Os_3(CO)_9\{\mu_3\text{-}C(CNBu^t)CPh\}(\mu_2\text{-}PPh_2)]$, (**135**). Complex (**135**) is aminated by $RNH_2$ (R = Me, Et, $Bu^n$) to give $[Os_3(CO)_9(C\{C(NHR)(NHBu^t)\}CPh)(\mu_2\text{-}PPh_2)]$, (**136**), [229]. The structure of (**135**) is proposed to be that shown in Fig. 89 on the basis of an

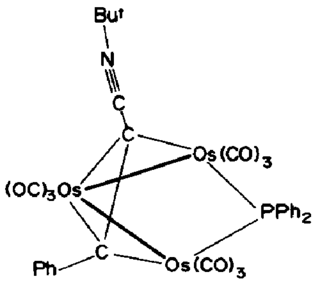

Fig. 89.

X-ray structure determination carried out on the related complex $[HRu_3(CO)_9\{C(CNBu^t)CPh\}]$ [229]. On the other hand, complex (**136**) has been the subject of an X-ray crystallographic study (Fig. 90); the molecule contains an open triangle of osmium atoms (Os(1)–Os(2) = 2.831 Å, Os(2)–Os(3) = 2.844 Å, Os(1) · · · Os(3) = 3.850 Å, Os(1)–Os(2)–Os(3) = 105.0°). In both (**135**) and (**136**) the high field $^{31}P$ NMR chemical shift for the bridging phosphido ligand suggests little or no osmium–osmium interaction between these particular osmium atoms [229].

The thermal reaction of $[Os_3(CO)_{12}]$ with $S(NSiMe_3)$ yields the complex $[Os_3(CO)_9(\mu_3\text{-}S)(\mu_3\text{-}NSiMe_3)]$ [230]. In the solid state, the osmium atom framework defines an open isosceles triangle which is bridged by both an inorganic sulfur ligand and a trimethylsilyl nitrene ligand (Fig. 91) [230]. The osmium–osmium bonding distances are 2.774 and 2.777 Å compared with 3.498 Å for the open edge. A variable temperature $^{13}C$ NMR study of the structure of this molecule in solution has shown the presence, at elevated temperatures, of two different structures. The authors have interpreted this observation in terms of a reversible opening and closing of the tri-osmium triangle in solution; the bridging sulfur and nitrene ligands are envisaged as playing a key role in accommodating these changes [230].

Thermolysis of $[Os_3(CO)_{11}(PPh_2R)]$ (R = Me, Et, Ph) in boiling n-nonane for 1 h gives as the products, complexes of the stoichiometry $[Os_3(CO)_9(PR)(C_6H_4)]$, (**137**), (yield 70–80%) [231]. The X-ray crystal struc-

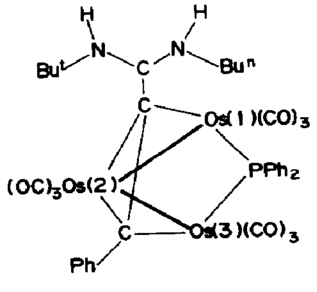

Fig. 90.

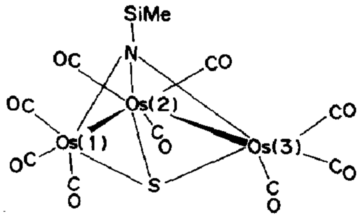

Fig. 91.

ture of (**137**, R = Et) has been determined [231]. The molecule has an open triangle of three osmium atoms, one side face-bridged by the {PEt} ligand system, and the other by a benzyne ligand $\{C_6H_4\}$ (Os(1)–Os(2) = 2.789 Å, Os(2)–Os(3) = 2.929 Å, Os(1) · · · Os(3) = 4.008 Å, Os(1)–Os(2)–Os(3) = 89.0°) (Fig. 92). The authors consider that the formulation shown in Fig. 92 is not necessarily the best description of the bonding of the benzyne ligand, but that a contribution from a form with a measure of carbenoid bonding to Os(3) is also relevant [231]. The spectroscopic properties of the complexes $[Os_3(CO)_9(\mu_3\text{-}C_6H_4)(\mu_3\text{-}PR)]$ (R = Me, Ph) indicate them to be structurally, entirely analogous to $[Os_3(CO)_9(\mu_3\text{-}C_6H_4)(\mu_3\text{-}PEt)]$ [231].

The complex $[HOs_3(CO)_9(\mu_3\text{-}C_6H_4)(\mu_2\text{-}AsMe_2)]$, (**138**), is one of the products of the reaction between $[Os_3(CO)_{12}]$ and $AsMe_2Ph$ [232]. The structure of (**138**) has been determined by X-ray crystallography [232] (see Fig. 93). The molecule has an open triangular framework of osmium atoms (Os(1)–Os(2) = 2.946 Å, Os(1)–Os(3) = 2.839 Å, Os(2) · · · Os(3) = 3.929 Å, Os(2)–Os(1)–Os(3) = 85.5°). The $\{AsMe_2\}$ unit bridges the open edge of this triangle, while the $\{C_6H_4\}$ unit (acting as a four electron donor ligand) is coordinated via σ bonds to Os(2) and Os(3), and a π bond to Os(1). The longer Os–Os bond (Os(1)–Os(2)) is presumed to be bridged by the hydrido ligand although it was not located crystallographically. The related complex $[HOs_3(CO)_9(\mu_3\text{-}C_6H_3Pr^i)(\mu_2\text{-}AsMe_2)]$ has also been synthesized, and on the basis of its spectroscopic properties is expected to have a structure entirely analogous to (**138**).

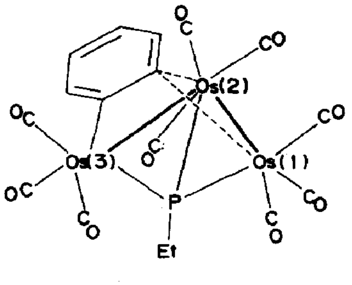

Fig. 92.

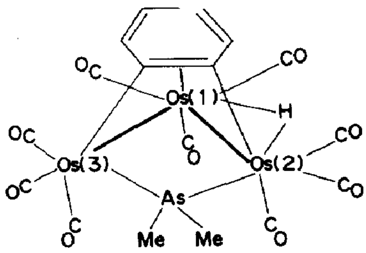

Fig. 93.

The reaction of the alkylphenylsulfides RSPh (R = Me, $Pr^i$) with $[Os_3(CO)_{12}]$ in boiling n-nonane has given low yields (< 5%) of $[HOs_3(CO)_9(\mu_3\text{-}C_6H_4)(\mu_2\text{-}SR)]$, (**139**), [233], complexes entirely analogous to the $\mu_2$-dimethylarsino complexes $[HOs_3(CO)_9(\mu_3\text{-}C_6H_3R)(\mu_2\text{-}AsMe_2)]$ (R = H, $Pr^i$) reported by Deeming et al. [232]. The sulfido complexes have been characterized by IR and NMR spectroscopy, and by an X-ray analysis of (**139**, R = Me) [233]. The open triangle of three osmium atoms (Os(1)–Os(2) = 2.833 Å, Os(2)–Os(3) = 2.939 Å, Os(1) · · · Os(3) = 3.791 Å, Os(1)–Os(2)–Os(3) = 82.09°) is bridged by the $\mu_2$-methanethiolate group and the triply bridging benzyne ligand (Fig. 94).

The complex $[Os_3(CO)_8(PMe_2Ph)(\mu_3\text{-}S)(\mu_3\text{-}\eta^2\text{-}SCH_2)]$, (**140**), has recently been obtained as the decarbonylation product of both the dithioformato complex $[HOs_3(CO)_9(PMe_2Ph)(\mu_2\text{-}SCH)]$ and the thioformaldehyde complex $[Os_3(CO)_9(PMe_2Ph)(\mu_3\text{-}S)(\mu_2\text{-}SCH_2)]$ (Scheme 13) [234–236]. Complex (**140**) has been characterized by X-ray crystallography [234–236], showing the molecule to contain an open triangle of three osmium atoms (Os(1)–Os(2) = 2.849 Å, Os(1)–Os(3) = 2.838 Å, Os(2) · · · Os(3) = 4.061 Å, Os(2)–Os(1)–Os(3) = 91.11°), a triply bridging sulfido ligand, and a triply bridging thioformaldehyde group. Reaction of (**140**) with trimethylphosphite yields the substitution product $[Os_3(CO)_7(PMe_2Ph)\{P(OMe)_3\}(\mu_3\text{-}S)(\mu_3\text{-}\eta^2\text{-}SCH_2)]$, (**141**), characterized by a combination of spectroscopic methods

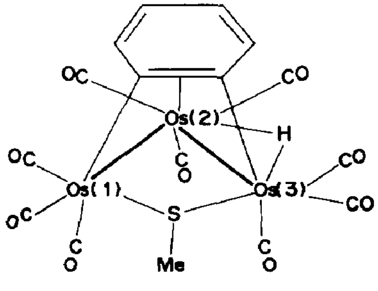

Fig. 94.

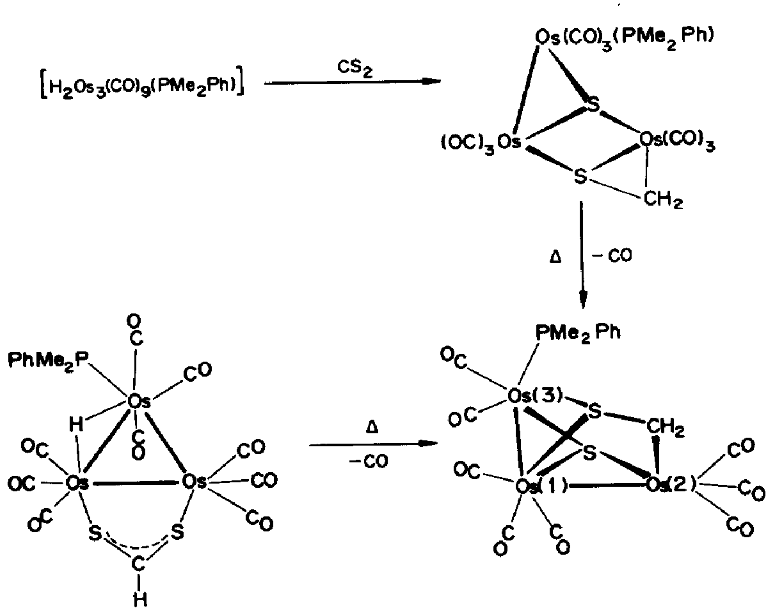

Scheme 13.

and by X-ray crystallography [237]. Surprisingly, it was found that the trimethylphosphite ligand is coordinated at the phosphine substituted osmium atom (Os(1)–Os(2) = 2.894 Å, Os(1)–Os(3) = 2.837 Å, Os(2) · · · Os(3) = 4.079 Å, Os(2)–Os(1)–Os(3) = 90.73°) (see Fig. 95). In contrast, reaction of (**140**) with HCl in dichloromethane results in metal–metal bond cleavage giving the complex [$HOs_3(CO)_8(PMe_2Ph)(\mu_3\text{-}S)(\mu_3\text{-}\eta^2\text{-}SCH_2)Cl$] which contains only a single osmium–osmium bond [237,238].

Reaction of (**140**) with $Me_3SnH$ in boiling heptane has given a mixture of products, from which two, identified as [$HOs_3(CO)_7(PMe_2Ph)(\mu_3\text{-}S)(\mu_3\text{-}\eta^2\text{-}SCH_2)SnMe_3$], (**142**), and ($H_2Os_3(CO)_7(PMe_2Ph)(\mu_3\text{-}S)(\mu_3\text{-}\eta^2\text{-}SCH_2)$], (**143**), have been separated [239]. Both (**142**) and (**143**) have been characterized by X-ray crystallography [239]. The open triangle of osmium atoms in (**142**) (Os(1)–Os(2) = 2.957 Å, Os(1)–Os(3) = 2.942 Å, Os(2) · · · Os(3) = 4.063 Å, Os(2)–Os(1)–Os(3) = 87.06°) is triply bridged by a sulfido

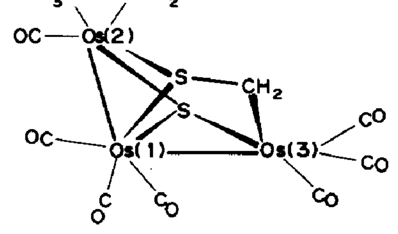

Fig. 95.

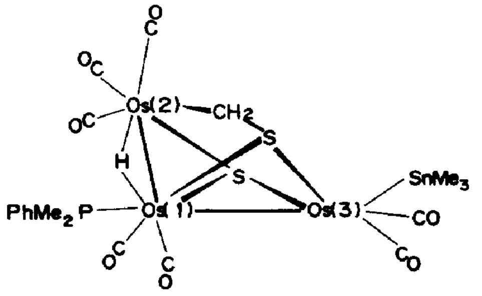

Fig. 96.

ligand, and by a triply bridging $\eta^2$-thioformaldehyde ligand in which the sulfur atom bridges the Os(1)–Os(3) bond and the carbon atom is coordinated solely to Os(2). The hydrido ligand (not located crystallographically) is inferred to be bridging the Os(1)–Os(2) bond, while the trimethylstanno ligand is coordinated solely to Os(3) (Fig. 96). Complex (**143**) (Fig. 97) is structurally very similar to both (**140**) and (**142**) (Os(1)–Os(2) = 2.903 Å, Os(1)–Os(3) = 2.818 Å, Os(2) · · · Os(3) = 4.115 Å, Os(2)–Os(1)–Os(3) = 92.00°). As for (**142**), the hydride ligands were not observed crystallographically, but are presumed to be bridging the metal–metal bonds [239].

A sequence of products has been isolated and structurally characterized from the reactions of $[H_2Os_3(CO)_{10}]$ with the organoisothiocyanates RN=C=S (R = Ph, Me, $C_6H_4F$-4, $C_6H_4Me$-4) including the complexes $[HOs_3(CO)_9(\mu_3\text{-}S)(\mu_2\text{-}HC{=}NR)]$, (**144**), which contain an open triangle of osmium atoms (Fig. 98) [240,241]. The complex $[HOs_3(CO)_9(\mu_3\text{-}S)(\mu_2\text{-}HC{=}NC_6H_4F\text{-}4)]$ has been completely characterized by X-ray crystallography [240,241]. The three osmium atoms are triply bridged by a sulfur atom, and a formimidoyl ligand bridges the open edge of the triangle (Os(1)–Os(2) = 2.836 Å, Os(2)–Os(3) = 2.988 Å, Os(1) · · · Os(3) = 3.779 Å, Os(1)–Os(2)–Os(3) = 88.88°). The hydrido ligand was not located, but is presumed to bridge the longer Os–Os bond [241].

Closely related to the complexes $[HOs_3(CO)_9(\mu_3\text{-}S)(\mu_2\text{-}HC{=}NR)]$ (R = Ph, Me, $C_6H_4Me$-4, $C_6H_4F$-4) is the complex $[HOs_3(CO)_9(\mu_3\text{-}S)(\mu_2\text{-}$

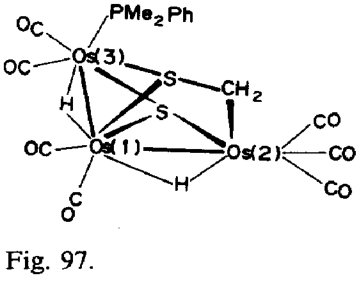

Fig. 97.

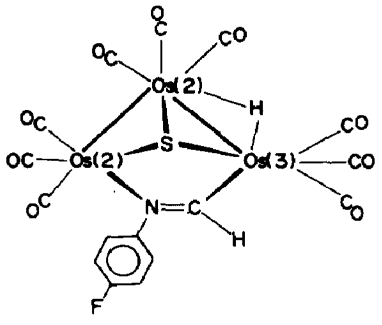

Fig. 98.

$C{=}NCH_2CH_2S)]$, (**145**), obtained by thermolysis of the cluster complex $[HOs_3(CO)_9(\mu_2\text{-}S\text{-}C{=}NCH_2CH_2S)]$ in acetone [242]. Complex (**145**) exists in two isomeric forms which interconvert rapidly on the NMR timescale (Scheme 14).

Irradiation of $[HOs_3(CO)_{10}(\mu_2\text{-}SPh)]$ under an atmosphere of $H_2S$ gives, via loss of both benzene and a single carbonyl ligand, the complex $[Os_3(CO)_8(\mu_2\text{-}H)_2(\mu_3\text{-}S)_2]$, (**146**), [197]. Complex (**146**) has also been obtained by the reaction of dihydrogen (1 atm., 110°C) with the complex $[\{Os_3(CO)_8(\mu_3\text{-}S)_2\}_2]$ [243], a product of the ultraviolet irradiation of $[Os_3(CO)_9(\mu_3\text{-}S)_2]$ (see below). The X-ray crystal structure of (**146**) has been determined [243]. The molecule contains an open triangle of three osmium atoms (Os–Os (mean) = 2.802 Å, Os · · · Os = 3.707 Å, Os–Os–Os = 82.84°) and two triply bridging sulfur atoms. The hydrido ligands bridge the two metal–metal bonds (Fig. 99). The complex (**146**) can thus be viewed as being formally derived from $[Os_3(CO)_9(\mu_3\text{-}S)_2]$ by replacement of one carbonyl ligand (on the apical osmium atom) by two edge-bridging hydrido ligands, or derived from $[Os_3(CO)_9(\mu_2\text{-}H)_2(\mu_3\text{-}S)]$ by carbonyl displacement and metal–metal bond cleavage with a further capping sulfur atom filling the available coordination sites.

Refluxing of $[Os_3(CO)_8(NCMe)(\mu_2\text{-}H)_2(\mu_3\text{-}S)]$ with $CS_2$ in cyclohexane leads, after purification by thin layer chromatography, to the isolation of a

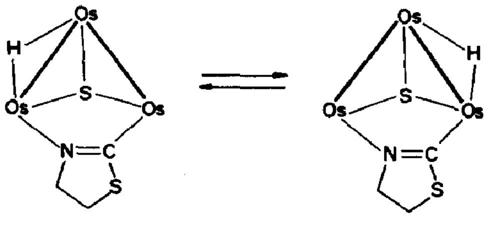

Scheme 14.

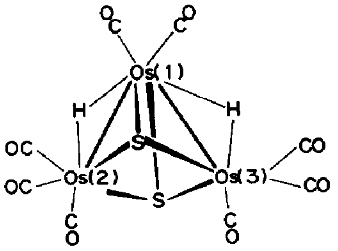

Fig. 99.

product with the stoichiometry $[Os_3(CO)_7(CS)(\mu_2\text{-}H)_2(\mu_3\text{-}S)_2]$ [244]. The three osmium atoms define an open triangle (Os(1)–Os(2) = 2.813 Å, Os(1)–Os(3) = 2.808 Å, Os(2) $\cdots$ Os(3) = 3.70 Å, Os(2)–Os(1)–Os(3) = 82.8°) capped by the two sulfur ligands (Fig. 100). The thiocarbonyl ligand is coordinated tó a basal osmium atom. In all respects then, this complex is formally a substitution product of the complex $[Os_3(CO)_8(\mu_2\text{-}H)_2(\mu_3\text{-}S)_2]$ (see above).

The complex $[HOs_3(CO)_9(\mu_3\text{-}C{\equiv}CCPh_2OH)]$, has been prepared by the reaction of $[Os_3(CO)_{12}]$ with $HOPh_2CC{\equiv}CCPh_2OH$ [245]. When treated with trifluoroacetic acid in chloroform, isomerization occurs with migration of the hydroxyl group from carbon to the metal framework of the complex (Scheme 15) giving $[Os_3(CO)_9(\mu_2\text{-}H)(\mu_2\text{-}OH)(\mu_3\text{-}C{=}C{=}CPh_2)]$, (**147**), [245]. This compound has been characterized by X-ray crystallography [245] (Os(1)–Os(2) = 2.905 Å, Os(2)–Os(3) = 2.861 Å, Os(1)–Os(3) = 3.374 Å, Os(3)–Os(2)–Os(1) = 71.6°). The hydroxo ligand bridges the open edge of the triangle while the hydrido ligand was deduced to bridge the longer Os–Os bond. The unusual 3,3-diphenylallene-1,1-diyl ligand is σ-bonded to Os(2) and Os(3), and π-bonded to Os(1).

The reaction of $[Os_3(CO)_{11}(NCMe)]$ with allene has given the product $[Os_3(CO)_{11}\{C(CH_2)_2\}]$, (**148**), characterized by X-ray crystallography [246]. The "allyl" group $\{C(CH_2)_2\}$ acts as a four-electron donor (π-bonding to Os(3) and σ-bonding to Os(1)) to the $Os_3$ framework (Fig. 101)

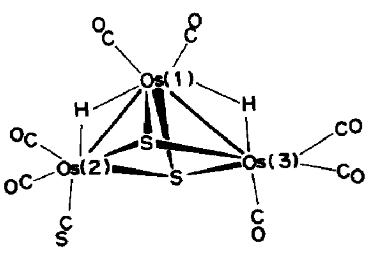

Fig. 100.

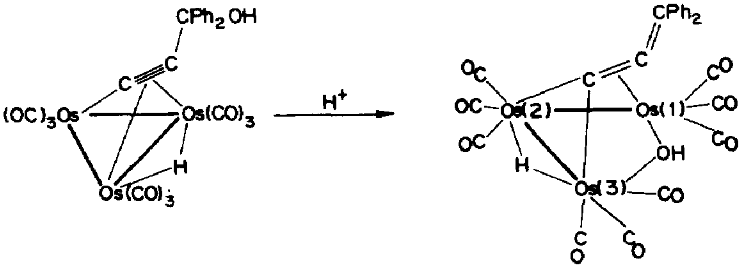

Scheme 15.

(Os(1)–Os(2) = 2.917, 2.925 Å; Os(1)–Os(3) = 2.947, 2.935 Å; Os(2) · · · Os(3) (average) = 3.860 Å; Os(2)–Os(1)–Os(3) = 81.7, 83.0°).

A suspension of $[HOs_3(CO)_{10}(CF_3CCHCF_3)]$ in hexane reacts with an equimolar quantity of triethylphosphine to give a number of products, of which the major component (ca. 30% yield) is a complex with the stoichiometry $[HOs_3(CO)_{10}(PEt_3)(CF_3CCHCF_3)]$, (**149**), [247,248]. The X-ray structure of this molecule has been determined [247], showing it to possess an unusual, bent tri-osmium backbone (Os(1)–Os(2) = 2.907 Å, Os(2)–Os(3) = 2.848 Å, Os(1)–Os(2)–Os(3) = 162.3°) supporting the vinylic $\{CF_3CCHCF_3\}$ ligand ($\eta^1$-bonded to Os(3) and $\eta^2$-bonded to Os(2)) (see Fig. 102). The reaction of $[HOs_3(CO)_{10}(CF_3CCHCF_3)]$ with $PEt_3$ to give a product arising from metal–metal bond cleavage is very unusual when compared to other reactions of trinuclear osmium complexes with two-electron donor ligands which have previously been observed. This unusual reaction may perhaps be rationalized by the suggestion that the metal–metal bonds in $[HOs_3(CO)_9(CF_3CCHCF_3)]$ are best viewed as dative metal–metal bonds which could be expected to cleave readily with donor ligands [248].

The cluster complex $[Os_4(CO)_{12}(\mu_3\text{-}S)_2]$ consists of a butterfly arrangement of four osmium atoms with sulfido ligands bridging the two open triangular faces (see Fig. 103) [249]. The internuclear distances in the cluster core suggest the existence of five metal–metal bonds, but two of these are

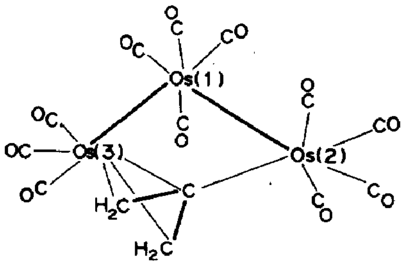

Fig. 101.

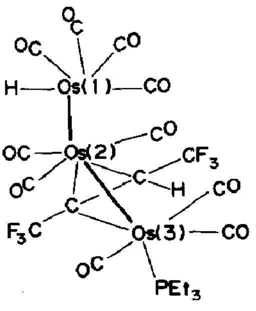

Fig. 102.

relatively long when compared to the other three which are consistent with Os–Os single bonds. In this regard, electron counting assigns 64 electrons to the core, whereas an "electron precise" tetranuclear cluster with five metal–metal bonds would require a total of only 62 electrons. Thus the complex would be expected to react readily, with metal–metal bond cleavage, to generate an electron precise 66-electron acyclic cluster [249]. This has indeed been found to be the case. Thus reaction of $[Os_4(CO)_{12}(\mu_3\text{-}S)_2]$ with carbon monoxide readily gives $[Os_4(CO)_{13}(\mu_3\text{-}S)_2]$, (**150**), characterized by mass spectrometry and structurally investigated by X-ray crystallography [250]. The complex contains a planar arrangement of four osmium atoms linked by three metal–metal bonds (Os(1)–Os(2) = 2.910 Å, Os(2)–Os(3) = 2.897 Å, Os(3)–Os(4) = 2.800 Å, Os(1) · · · Os(4) = 3.659 Å; Os(1)–Os(2)–Os(3) = 70.70°, Os(2)–Os(3)–Os(4) = 127.01°). Two triply bridging sulfido ligands bridge three of the metal atoms, but on opposite sides of the $Os_4$ plane (Fig. 104).

Closely related to the complex $[Os_4(CO)_{12}(\mu_3\text{-}S)_2]$ is the heterometallic complex $[Os_3W(CO)_{12}(PMe_2Ph)(\mu_3\text{-}S)_2]$ (see Fig. 105), obtained in 27% yield from the photochemical reaction between $[Os_3(CO)_9(\mu_3\text{-}S)_2]$ and $[W(CO)_5(PMe_2Ph)]$ [251,252]. Formally, electron counting again assigns 64 electrons to the cluster core, two too many for an electron precise tetranuclear cluster with five metal–metal bonds. Thus it is not unexpected that

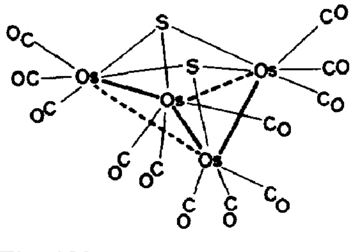

Fig. 103.

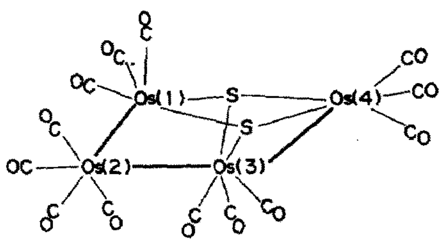

Fig. 104.

$[Os_3W(CO)_{12}(PMe_2Ph)(\mu_3\text{-}S)_2]$ reacts readily with the two-electron donor ligand $PMe_2Ph$ to give $[Os_3W(CO)_{12}(PMe_2Ph)_2(\mu_3\text{-}S)_2]$, (**151**), an electron precise 66-electron acyclic cluster. The molecular structure of (**151**) has been determined by X-ray crystallography [252], showing this molecule to be closely related to (**150**) (see Fig. 106) (Os(1)–Os(2) = 2.895 Å, Os(2)–Os(3) = 2.887 Å, Os(3)–W = 3.044 Å, Os(1) · · · W = 3.612 Å; Os(1)–Os(2)–Os(3) = 70.90°, Os(2)–Os(3)–W = 123.20°) [251,252].

One of the products of the reaction between $[Os_3(CO)_{12}]$ and elemental sulfur or selenium (see above) is the tetranuclear osmium complex $[Os_4(CO)_{12}(\mu_2\text{-}H)_2(\mu_3\text{-}X)_2]$ (**152**, X = S, Se) [169]. The X-ray crystal structure of $[Os_4(CO)_{12}(\mu_2\text{-}H)_2(\mu_3\text{-}Se)_2]$ has been determined [169]. The four osmium atoms and two selenium atoms form a distorted trigonal prism with a puckered chain of osmium atoms (Fig. 107) (Os(1)–Os(2) = 2.884 Å, Os(1)–Os(4) = 2.965 Å, Os(2)–Os(3) = 2.966 Å, Os(2)–Os(1)–Os(4) = 86.1°, Os(1)–Os(2)–Os(3) = 85.7°). Each selenium atom caps a triangular arrangement of osmium atoms while the two hydrido ligands probably edge-bridge the two long Os–Os bonds (Os(1)–Os(4), Os(2)–Os(3)). The complex $[Os_4(CO)_{12}(\mu_2\text{-}H)_2(\mu_3\text{-}S)_2]$, also synthesized by the reaction of $[Os_4(CO)_{12}(\mu_3\text{-}S)]$ with $H_2S$ (98°C, 4 h), is presumed to have an analogous structure [253].

Recently, Adams et al. have shown that sulfur and phosphorus containing clusters of osmium can be induced to condense to form higher nuclearity complexes [195,254–256]. The molecules $[HOs_3(CO)_9(\mu_3\text{-}S)(\mu_2\text{-}HC{=}NR)]$

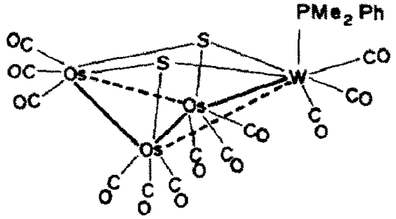

Fig. 105.

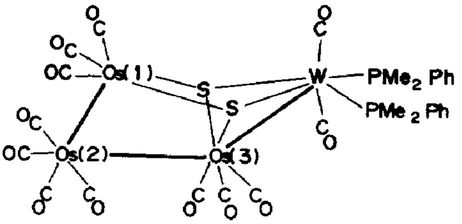

Fig. 106.

(**144**, R = Ph, $C_6H_4F$-4) lose carbon monoxide when heated in octane and condense to form, amongst other products, the higher nuclearity carbonyl complex $[H_2Os_6(CO)_{17}(\mu_4\text{-}S)(\mu_3\text{-}S)(\mu_2\text{-}HC{=}NR)_2]$ (**153**, R = Ph, $C_6H_4F$-4) (Scheme 16) [254,256]. The complex (**153**, R = $C_6H_4F$-4) has been completely characterized by X-ray crystallography [254, 256]. The molecule contains two open triangles of three osmium atoms each linked by a tetracoordinate, bridging sulfur atom (Os(1)–Os(2) = 2.914 Å, Os(1)–Os(3) = 2.918 Å, Os(4)–Os(5) = 2.951 Å, Os(4)–Os(6) = 2.803 Å; Os(2)–Os(1)–Os(3) = 75.28°, Os(5)–Os(4)–Os(6) = 80.93°). A $\eta^2$-formimidoyl ligand bridges the open edge of each triangle of osmium atoms. The hydrido ligands are probably located bridging Os(4)–Os(5) and Os(4)–Os(6). The formation of (**153**) from (**144**) is probably initiated via a dissociative loss of CO from (**144**). The empty coordination site may then be filled by the donation of a lone pair of electrons of the triply bridging sulfur atom from a second molecule of (**144**). An intercluster carbonyl shift could follow the cleavage of an osmium–sulfur bond in the added cluster, completing the formation of (**153**) [254, 256].

Thermal decarbonylation of $[HOs_3(CO)_9(\mu_3\text{-}S)(\mu_2\text{-}HC{=}CR)]$ (**144**, R = Ph) under an atmosphere of dihydrogen has given products different to those isolated when heated under an inert atmosphere (Scheme 17) [255]. The principle product (formed in 47% yield) is $[H_4Os_6(CO)_{15}(\mu_4\text{-}S)(\mu_3\text{-}S)(\mu_2\text{-}HC{=}NPh)_2]$, (**154**), characterized by a combination of spectroscopic

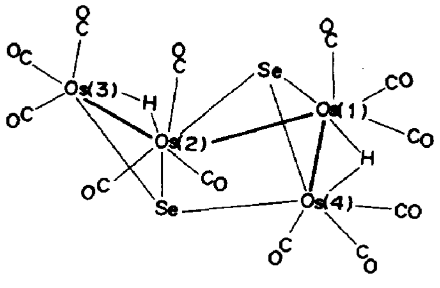

Fig. 107.

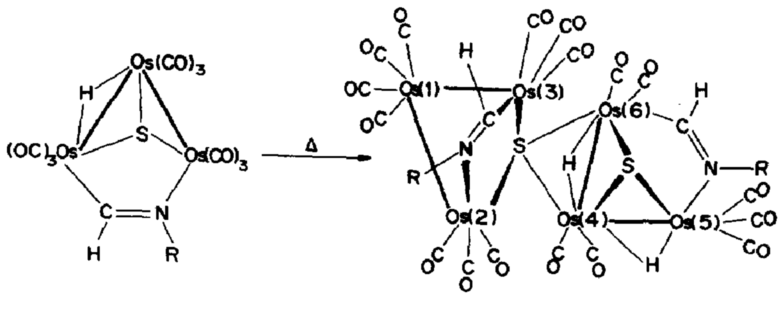

Scheme 16.

techniques and X-ray crystallography [255]. The molecule is best viewed as a combination of two open triangular complexes of (**144**), Os(1)–Os(2)–Os(3) and Os(5)–Os(4)–Os(6), joined by the Os(1)–S(1) and Os(2)–Os(6) bonds. There are five metal–metal bonds (Os(1)–Os(2) = 3.011 Å, Os(2)–Os(3) = 2.957 Å, Os(2)–Os(6) = 3.166 Å, Os(4)–Os(5) = 2.837 Å, Os(4)–Os(6) = 3.019 Å), four of which are significantly longer than the Os–Os separation found in $[Os_3(CO)_{12}]$ and are thus presumed to be bridged by the hydrido ligands. The minor product of the decarbonylation (Scheme 17), isolated in 12% yield, has been identified as $[H_6Os_6(CO)_{14}(\mu_4\text{-}S)(\mu_3\text{-}S)(\mu_2\text{-}HC{=}NPh)_2]$, (**155**), by X-ray crystallography [255]. The molecule is structurally closely related to (**154**) and is also best described as a combination of two open

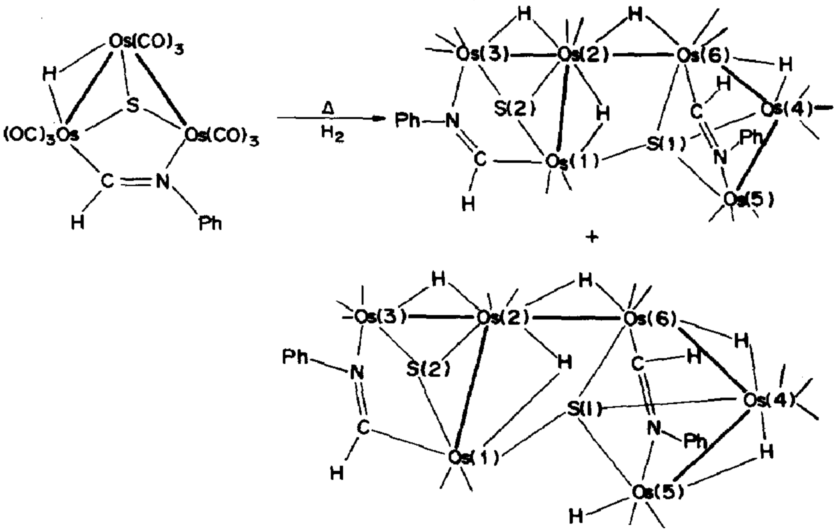

(carbonyl ligands omitted for clarity)

Scheme 17.

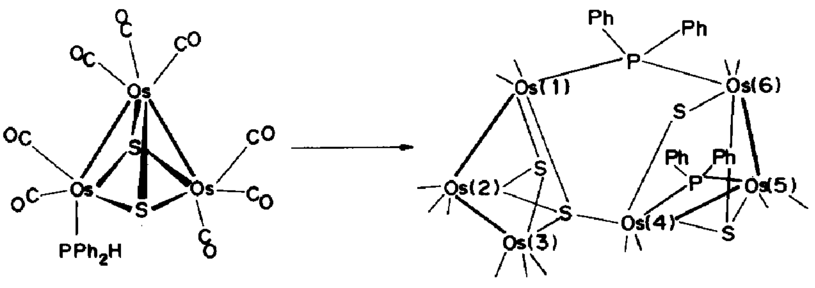

(carbonyl ligands omitted for clarity)

Scheme 18.

trinuclear complexes linked by a metal–sulfur donor bond Os(1)–S(1) and a metal–metal bond Os(2)–Os(6). The $^1H$ NMR spectrum of (**155**) shows six hydride resonances, five of which are possibly bridging ligands while the sixth is probably terminally coordinated. In support of this, the five metal–metal bonds in (**155**) (Os(1)–Os(2) = 2.996 Å, Os(2)–Os(3) = 2.969 Å, Os(2)–Os(6) = 3.159 Å, Os(4)–Os(5) = 3.033 Å, Os(4)–Os(6) = 3.039 Å) are all significantly longer than the Os–Os separation in $[Os_3(CO)_{12}]$, and are thus probably each bridged by a hydrido ligand. Further, the coordination of Os(5) in (**155**) is different from that of Os(5) in (**154**) by the absence of one carbonyl ligand. It is presumed that the terminal hydrido ligand occupies this site.

Thermal degradation of the complex $[Os_3(CO)_8(PPh_2H)(\mu_3\text{-}S)_2]$, (**116**), [195] at 125°C in octane under a nitrogen atmosphere leads to decarbonylation and formation of the complex $[Os_6(CO)_{14}(\mu_4\text{-}S)(\mu_3\text{-}S)(\mu_2\text{-}PPh_2)_2]$, (**156**), in 11% yield (Scheme 18) [195]. This product has been characterized by X-ray crystallography [195]. The molecule consists of two open tri-osmium units linked by a bridging dipenylphosphido ligand and a quadruply bridging sulfido ligand. Each $Os_3$ unit is structurally similar to the parent molecule $[Os_3(CO)_9(\mu_3\text{-}S)_2]$ although the metal–metal bonds are significantly inequivalent (Os(1)–Os(2) = 2.907 Å, Os(2)–Os(3) = 2.773 Å, Os(4)–Os(5) = 2.960 Å, Os(5)–Os(6) = 3.020 Å) suggesting therefore that they are more closely related to the substituted complexes $[Os_3(CO)_8L(\mu_3\text{-}S)_2]$ (L = $PMe_2Ph$, CS) [193,196].

Surprisingly, there are relatively few mixed metal acyclic clusters containing an osmium atom in a structure controlling role. Reduction of $[Os_3(CO)_{12}]$ with sodium in liquid ammonia followed by reaction with $[Ph_3PAuCl]$ gives the complex $[Os(CO)_4\{AuPPh_3\}_2]$, (**157**), in good yield [257]. The geometry of the $\{AuPPh_3\}$ groups about the osmium atom is, on the basis of IR spectroscopy, consistent with a *cis*-disposition, analogous to the corresponding iron complexes (see Section B.(v)(a)).

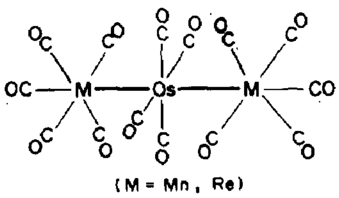

Fig. 108.

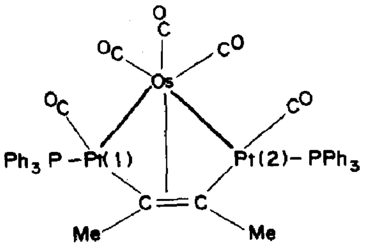

Fig. 109.

Thermolysis of $[M_2(CO)_{10}]$ (M = Mn, Re) with $[Os_3(CO)_{12}]$ (200–250°C, 50 h) has given the linear mixed metal complexes $[Os(CO)_4\{M(CO)_5\}_2]$ [190]. The structure is presumed to be similar to that of $[Fe(CO)_4\{Mn(CO)_5\}_2]$ [150], i.e. as shown in Fig. 108.

Reaction of the acyclic cluster complex $[Os_3Pt(CO)_{10}(\mu_2\text{-}H)_2(PPh_3)]$ with but-2-yne gives a mixture of products of which $[OsPt_2(CO)_5(PPh_3)_2(\mu_3\text{-}MeC_2Me)]$, (**158**), has been characterized and its structure established by X-ray diffraction [258] (Fig. 109). The metal atoms form an open triangle (Pt(1)–Os = 2.664 Å, Pt(2)–Os = 2.669 Å, Pt(1) · · · Pt(2) = 3.033 Å, Pt(1)–Os–Pt(2) = 69.33°) with little or no direct bonding interaction between Pt(1) and Pt(2). The three metal atom unit is face-bridged by the but-2-yne molecule. Another product of this reaction, $[OsPt_2(CO)_6(PPh_3)(\mu_3\text{-}MeC_2Me)]$, is proposed to have a structure very similar to that of (**158**) except with a carbonyl group replacing a $PPh_3$ ligand [258].

### *(vi) Cobalt, rhodium and iridium*

#### *(a) Cobalt*

Of the acyclic homonuclear cobalt cluster complexes reported to date examples of both linear tri-cobalt, and open triangular structures are known (see Table 9). Complexes of the formula $[Co_3Yb_2(\eta^5\text{-}C_5Me_5)_4(\eta^5\text{-}C_5H_4R)_2(CO)_4]$ (**159**, R = H, Me, $SiMe_3$) contain an almost linear Co–Co–Co core with the $\{(\eta^5\text{-}C_5Me_5)_2Yb\}$ groups attached via Co–C–O–Yb bridges (Fig. 110) [259]. These complexes are obtained in high yield (60–65%) from $[(\eta^5\text{-}C_5Me_5)_2Yb(OEt_2)]$ and $[(\eta^5\text{-}C_5H_4R)Co(CO)_2]$. Blue/purple crystals of

TABLE 9

Acyclic cluster complexes of cobalt

| Formula | Complex | Fig. | Ref. [a] |
|---|---|---|---|
| $[Co_3Yb_2(\eta^5\text{-}C_5Me_5)_4(\eta^5\text{-}C_5H_4R)_2(CO)_4]$ (R = H, Me, $SiMe_3$) | **(159)** | 110 | 259* |
| $[(\eta^5\text{-}C_5H_5)_3Co_3(\mu_3\text{-}\eta^1\text{-}CBu^n)_2(\mu_2\text{-}SMe)]^+$ | **(160)** | – | 260* |
| $[Co(CO)_4\{Pd(NMe_2CH_2C_6H_4)\}_2(\mu_2\text{-}Cl)]$ | **(161)** | 111 | 33*,34* |

[a] References marked with an asterisk refer to crystal structure determinations.

all three compounds were obtained from toluene solution, and a crystal structure determination on one of them (R = $SiMe_3$) gave an average Co–Co bond length of 2.363(1) Å and a Co–Co–Co angle of 176.5° [259].

An open triangular tri-cobalt complex, $[(\eta^5\text{-}C_5H_5)_3Co_3(\mu_3\text{-}\eta^1\text{-}CBu^n)_2(\mu_2\text{-}SMe)]^+$, **(160)**, was obtained in high yield from the reaction of the cyclic cluster $[(\eta^5\text{-}C_5H_5)_3Co_3(\mu_3\text{-}\eta^1\text{-}CBu^n)_2]$ and dimethyl(methylthio)sulfonium tetrafluoroborate (Scheme 19) [260]. A crystal structure determination established an average Co–Co bond length of 2.388 Å and a non-bonded Co · · · Co distance of 2.738 Å; the Co–Co–Co bond angle was found to be 70° [260].

The majority of acyclic heterometallic complexes containing cobalt involve $\{Co(CO)_4\}$ or $\{Co(CO)_3L\}$ groups metal–metal bonded to a central metal atom such as platinum or palladium (see Section B.(vii)(b) and (c)). Few such complexes have a cobalt atom as the central (structure controlling) atom. One example, the complex $[Co(CO)_4\{Pd(NMe_2CH_2C_6H_4)\}_2(\mu_2\text{-}Cl)]$, **(161)**, has been obtained by the reaction of $[\{Pd(NMe_2CH_2C_6H_4)(\mu_2\text{-}Cl)\}_2]$

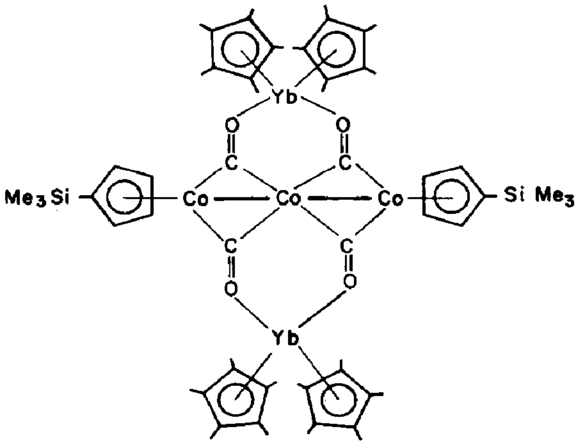

Fig. 110.

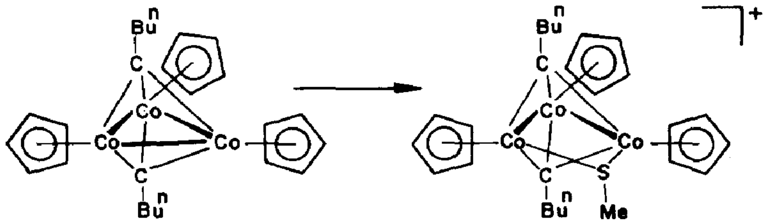

Scheme 19.

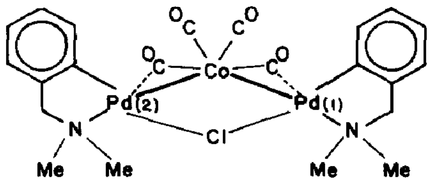

Fig. 111.

with $[Co(CO)_4]^-$ [33,34]. The X-ray crystal structure of (**161**) has been determined (Fig. 111) [33,34]. The Pd–Co–Pd framework forms an open triangle (Pd(1)–Co = 2.594 Å, Pd(2)–Co = 2.595 Å, Pd(1) · · · Pd(2) = 3.442 Å, Pd(1)–Co–Pd(2) = 83.13°) bridged by a single chloro ligand. The Co–Pd bonds support semi-bridging carbonyl ligands. Two complexes analogous to (**161**) containing the 2-dimethylamino toluene and 8-methylquinoline ligands chelating the palladium atoms have also been synthesized. On the basis of their spectroscopic properties, a similar structure to (**161**) is proposed [33].

### *(b) Rhodium*

Rhodium has a propensity for catenation which is almost unique in the Periodic Table. This is evidenced, for instance, by the formation of oligomeric species in solutions of cationic rhodium(I) isocyanide complexes [261–265]. Thus, the oligomers $[Rh(CNR)_4]_n^{n+}$ ($R = Pr^i$, $Bu^t$, Cy, vinyl, Ph; $n = 2$–$4$) have been characterized from characteristic transitions in the electronic absorption spectra. They were interpreted in terms of interactions between the occupied $a_{1g}$ ($d_{z^2}$) and unoccupied $a_{2u}$ ($p_z$, $\pi^*$(CNR)) monomer orbitals [262,263]. This work has been extended by Gray and co-workers [262] by the use of oligomeric rhodium(I) complexes containing bridging diisocyanide ligands, e.g. $[Rh_2(L_2)_4]X_2$ ($L_2 = CN(CH_2)_3NC$, $X = Cl$, $BPh_4$). A study of the effects of concentration on the electronic spectra of methanol solutions of such species have suggested the existence of the oligomers $[Rh_2(L_2)_4]_n^{2n+}$ ($n = 2$–$4$) [264]. Oxidation reactions are an important manifestation of the reactivity of cationic rhodium(I) isocyanide species [261,264–267], and a range of oligomeric rhodium isocyanide com-

TABLE 10

Acyclic cluster complexes of rhodium

| Formula | Complex | Fig. | Ref. [a] |
|---|---|---|---|
| $[Rh(CNR)_4]^{n+}$ (R = alkyl or aryl; $n = 3, 4$) | – | – | 261–265 |
| $[Rh_2(L_2)_4]_n^{2+}$ ($L_2 = CN(CH_2)_3NC$; $n = 2$–4) | **(162)** | 112 | 261,264–267, 268* |
| $[Rh_3(CNCH_2C_6H_5)_{12}I_2]X_3$ (X = I, Br) | **(163)** | 113 | 269* |
| $[Rh_3(\mu_3\text{-dpmp})_2(CO)_3X_2]$ (X = Cl, Br) | **(164)** | 114,116 | 270*,271 |
| $[Rh_3(\mu_3\text{-dpmp})_2(\mu_3\text{-I})(\mu_2\text{-CO})(CO)_2]^+$ | – | – | 271 |
| $[Rh_3(\mu_3\text{-dpmp})_2(\mu_2\text{-I})(\mu_3\text{-I})(\mu_2\text{-CO})(CO)_2]^+$ | – | 115 | 271* |
| $[Rh_3(\mu_3\text{-dpmp})_2(CO)I_4]^+$ | – | 117 | 272* |
| $[Rh_4\{\mu_3\text{-2,6-}(PPh_2)_2C_5H_3N\}_2(\mu_2\text{-CO})$ $(\mu_2\text{-Cl})_2(CO)_2Cl_2]$ | **(165)** | 118 | 273* |
| $[Rh_2(L_2)_4Mn_2(CO)_{10}](PF_6)_2$ | **(166)** | 119 | 274* |
| $[\{RhFe(\mu_2\text{-PPh}_2)_2(\mu_2\text{-CO})(CO)_3\}_2]$ | **(167)** | 120 | 277*,278* |
| $[Rh\{(\eta^5\text{-}C_5H_4Me)Fe(CO)_2(\mu_2\text{-PPh}_2)\}_2]$ | **(168)** | 121 | 279*,280*, 281,282 |
| $[Rh\{(\eta^5\text{-}C_5H_5)Fe(CO)_2(\mu_2\text{-PR}_2)\}_2]^+$ (R = $C_6H_4Me$-4) | **(169)** | – | 283,284 |
| $[Rh\{(\eta^5\text{-}C_5H_5)Fe(CO)_2(SR)\}_2]^+$ (R = Et, $Bu^t$) | **(170)** | – | 279,281, 282 |

---

[a] References marked with an asterisk refer to crystal structure determinations.

plexes has been identified on the basis of electronic spectroscopy including tetra-, hexa-, octa- and decanuclear complexes. Of particular note is the tetranuclear rhodium cation $[Rh_4(L_2)_8Cl]^{5+}$, (**162**; $L_2 = CN(CH_2)_3NC$) recently obtained by the addition of $CoCl_2 \cdot 6H_2O$ to a 12 M HCl solution of $[Rh_2(L_2)_4](BF_4)_2$, and characterized by X-ray crystallography [268] (see Table 10). The tetranuclear complex is made up of two binuclear $\{Rh_2(L_2)_4\}^{3+}$ units linked by an Rh–Rh bond (see Fig. 112). The chloride ion bridges the $\{Rh_4(\text{bridge})_8\}^{6+}$ units to form a rigorously linear, infinite chain of repeat $\{Rh_4Cl\}$ units. The Rh–Rh bond length in the dinuclear units (Rh(1)–Rh(2) = 2.932 Å, Rh(3)–Rh(4) = 2.923 Å) is considerably longer than the central Rh–Rh bond length (Rh(2)–Rh(3)) of 2.775 Å. Within each dinuclear unit the ligand systems are approximately eclipsed, although the two dinuclear units in each tetrameric unit are staggered with respect to each other.

Further, a most remarkable homometallic tri-rhodium complex $[Rh_3(CNCH_2C_6H_5)_{12}I_2]X_3$ (**163**, X = I, Br) [269] has been obtained by three-centre oxidative addition of iodine to $[Rh(CNCH_2C_6H_5)_4]X$ (1 : 3 molar ratio) in dichloromethane. Similar products, e.g. $[Rh_3(CNBu^n)_{12}I_2]I_3$ have been obtained by air oxidation of methanol solutions of $[Rh(CNR)_4]I$ in the presence of excess iodide. The structure of $[Rh_3(CNCH_2C_6H_5)_{12}I_2]Br_3$

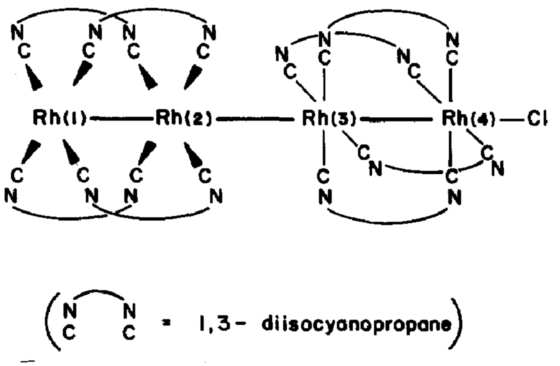

Fig. 112.

has been determined by X-ray crystallography [269]. The molecule contains an almost linear I–Rh–Rh–Rh–I unit (Rh–Rh–Rh = 180°, Rh–Rh–I = 175.5°) with a mean Rh–Rh bond length of 2.796 Å. The coordination about each rhodium atom is pseudo-octahedral with the four isocyanide ligands each at the corners of a square; these squares are staggered 38° from one rhodium atom to the next (see Fig. 113). The solution behaviour of these cations is complex and is dominated by dissociation into smaller fragments

$$[\mathrm{Rh_3(CNR)_{12}X_2}]^{3+} \rightleftharpoons [\mathrm{Rh_2(CNR)_8X_2}]^{2+} + [\mathrm{Rh(CNR)_4}]^{+}$$

$$[\mathrm{Rh_2(CNR)_8X_2}]^{2+} \rightleftharpoons [\mathrm{Rh(CNR)_4X_2}]^{+} + [\mathrm{Rh(CNR)_4}]^{+}$$

Remarkably, these changes due to dissociation are reversible, and evaporation of dissociated solutions prepared from $[\mathrm{Rh_3(CNR)_{12}I_2}]\mathrm{I_3}$ yields the starting complex [269].

The tendency for rhodium to form metal–metal interactions is also indicated by the range of homo- and heterometallic acyclic clusters which have been synthesized and characterized (Table 10). Numerous linear and bent trimetallic complexes (where the central rhodium atom is best considered to be structure controlling) and also linear and bent tetrametallic complexes (where dirhodium units are structure controlling) are known, paralleling the formation of the oligomeric rhodium isocyanide cations.

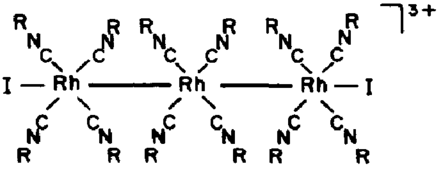

Fig. 113.

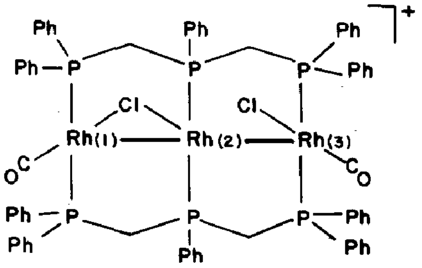

Fig. 114.

Thus, perhaps for no other metal can the relationships between monomers, dimers, acyclic clusters and oligomers be seen as clearly as for rhodium.

The novel tridentate phosphine ligand bis(diphenylphosphinomethyl) phenylphosphine (dpmp) has been used to synthesize a series of trinuclear rhodium cations of general formula $[Rh_3(\mu\text{-dpmp})_2(CO)_nX_m]^+$, (**164**), (see Table 10). Reaction of dpmp with $[\{Rh(CO)_2Cl\}_2]$ in dichloromethane-methanol yields a rose coloured solution from which the cation $[Rh_3(\mu_3\text{-dpmp})_2(\mu_2\text{-Cl})(CO)_3Cl]^+$ was isolated in 40% yield with a variety of counter-anions [270]. The X-ray crystal structure [270] of this compound (chloride salt) shows the trimetal framework to consist of a slightly bent metal array (Rh(1) · · · Rh(2) · · · Rh(3) = 157.4°), bridged by two triphosphine ligands (see Fig. 114). The Rh–Rh internuclear distances (Rh(1) · · · Rh(2) = 3.164 Å, Rh(2) · · · Rh(3) = 3.180 Å) are longer than that expected for Rh–Rh single bonds (2.7–2.9 Å), but that significant bonding interactions do occur is demonstrated by the position of the proximity shifted absorption band which occurs at 560 nm [270].

A variety of complexes related to (**164**) have been synthesized by the same authors from the chloride salt by metathesis with sodium halide in dichloromethane-methanol [271]. An X-ray structure determination [271] on $[Rh_3(\mu_3\text{-dpmp})_2(\mu_2\text{-I})(\mu_3\text{-I})(\mu_2\text{-CO})(CO)_2]BPh_4$, however, showed a significantly different structure (Fig. 115). The basic $Rh_3(dpmp)_2$ unit remains

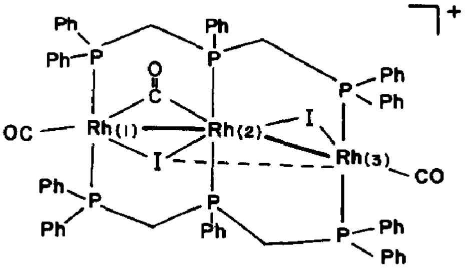

Fig. 115.

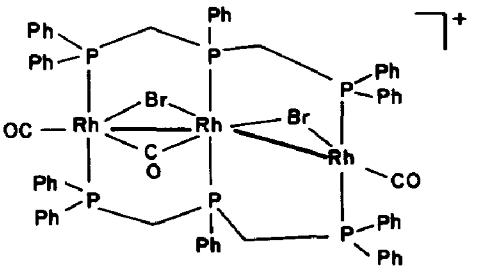

Fig. 116.

intact but is bent (Rh(1)–Rh(2) · · · Rh(3) = 127.6°) to accommodate bridging iodo and carbonyl ligands. The Rh–Rh separations are also considerably shortened relative to the chloro derivative (Rh(1)–Rh(2) = 2.760 Å, Rh(2) · · · Rh(3) = 3.03 Å). Metathesis of $[Rh_3(\mu_3\text{-dpmp})_2(\mu_2\text{-Cl})(CO)_3Cl]BPh_4$ with NaBr [271] yields brown $[Rh_3(\mu_3\text{-dpmp})_2Br_2(CO)_3]BPh_4$ which on the basis of its IR and $^{31}P\ \{^1H\}$ NMR spectra is assigned the structure shown in Fig. 116.

The complex $[Rh_3(\mu_3\text{-dpmp})_2(\mu_2\text{-I})(\mu_3\text{-I})(\mu_2\text{-CO})(CO)_2]BPh_4$ has been shown to undergo a variety of transformations including carbonylation, decarbonylation and oxidative addition [272]. These reactions and the stoichiometry of the reaction products are summarized in Scheme 20. These reactions apparently involve the opening and closing of sites of reactivity such as metal–metal bonds and metal–halide bridges. The X-ray characterization of only one of these products, $[Rh_3(\mu_3\text{-dpmp})_2(CO)I_4]BPh_4$, has thus far been reported [272]. The molecule contains a bent $Rh_3$ core (Rh(1)–Rh(2)–Rh(3) = 113.19°) with the Rh–Rh internuclear separations (Rh(1)–Rh(2) = 2.839 Å, Rh(2)–Rh(3) = 2.920 Å) consistent for single Rh–Rh bonds (see Fig. 117).

A tetra-rhodium complex has been reported by Balch and co-workers [273]. The complex $[Rh_4\{\mu_3\text{-}2,6\text{-}(PPh_2)C_5H_3N\}_2(\mu_2\text{-CO})(\mu_2\text{-Cl})_2(CO)_2Cl_2]$,

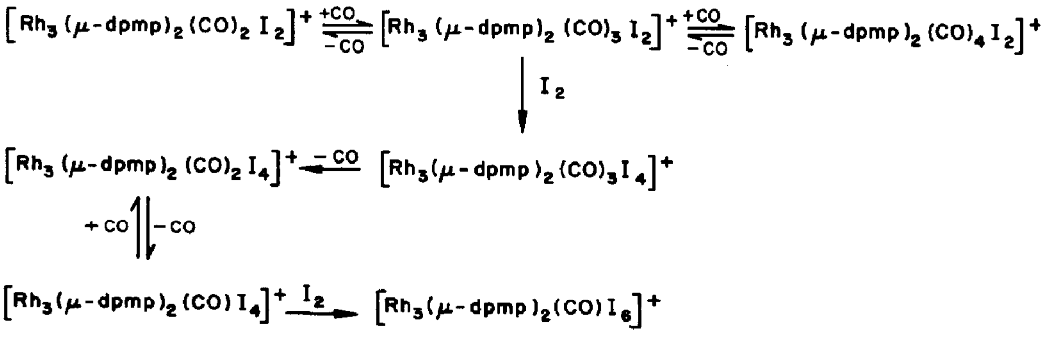

Scheme 20.

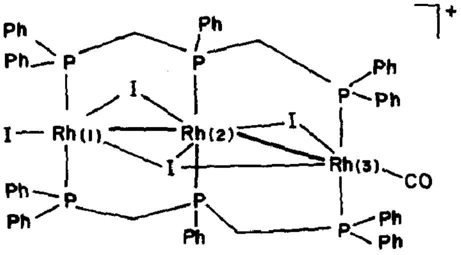

Fig. 117.

(**165**), was obtained from [$\{Rh(CO)_2Cl\}_2$] and 2,6-bis(diphenylphosphino) pyridine [$2,6-(PPh_2)_2C_5H_3N$] in 75% yield. An X-ray structure determination [273] has shown that each phosphine ligand bridges three rhodium atoms (Fig. 118). The central dinuclear portion of the molecule is closely related to that of the dinuclear complex [$Rh_2\{\mu_2-2,6-(PPh_2)_2C_5H_3N\}_2(\mu_2-CO)Cl_2$]. Thus, the Rh(2)–Rh(2′) distance in the tetra-rhodium complex, 2.594 Å, is similar to that in the dimer (2.612 Å) and although the Rh(1)–Rh(2) separation is significantly longer (2.921 Å), a metal–metal interaction is still postulated [273].

Two mixed metal tetranuclear complexes have been reported. Both contain a di-rhodium core supported by bridging ligands. The complex [$Rh_2(L_2)_4Mn_2(CO)_{10}$]$(PF_6)_2$, (**166**), has been obtained by the sunlight initiated reaction between [$Rh_2(L_2)_4$]$(PF_6)_2$ ($L_2$ = 2,5-dimethyl-2,5-diisocyanohexane) and [$Mn_2(CO)_{10}$] in acetone [274]. An X-ray structure determination [274] has shown the molecule to possess an approximately linear Mn–Rh–Rh–Mn core (Fig. 119) (mean Mn–Rh–Rh angle of 178.2°) with Rh(1)–Rh(2), Mn(1)–Rh(1) and Mn(2)–Rh(2) distances of 2.922, 2.905 and 2.883 Å respectively. The two $\{Rh(CN)_4\}$ units are twisted away from an eclipsed conformation with respect to each other by a 25° angle. This is

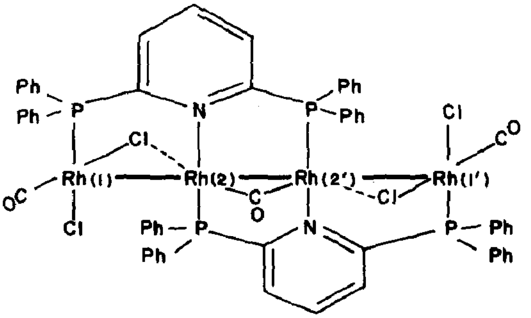

Fig. 118.

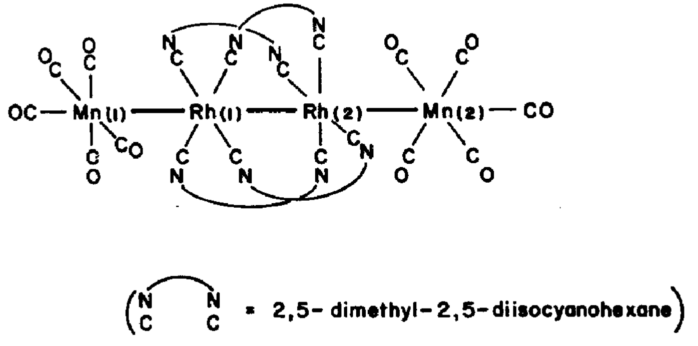

Fig. 119.

similar to the conformation observed in the dinuclear complex $[Rh_2(2,5\text{-dimethyl-}2,5\text{-diisocyanohexane})_4](PF_6)_2 \cdot CH_3CN$, in which the $\{Rh(CN)_4\}$ units are twisted away from an eclipsed conformation by an angle of 31° [275,276]. The mechanism of formation of (**166**) is proposed to proceed via the intermediacy of $\{Mn(CO)_5\}$ radicals which are then efficiently scavenged by the $[Rh_2(\text{bridge})_4]^{2+}$ ions in solution [274].

The iron–rhodium tetranuclear complex $[\{RhFe(\mu_2\text{-}PPh_2)_2(\mu_2\text{-}CO)(CO)_3\}_2]$, (**167**), has been synthesized from $[Fe(CO)_4PPh_2H]$ and $[\{Rh(\eta^3\text{-}C_3H_5)_2Cl\}_2]$ in a CO saturated ethanol solution at room temperature [277,278]. An X-ray structure determination [277,278] has shown the molecule to contain a Fe–Rh–Rh–Fe chain with the two iron atoms in a *trans* disposition with respect to the central Rh–Rh bond (Fe–Rh–Rh′ = 154.3°) (Fig. 120). The mean Rh–Rh′ and Rh–Fe bond lengths are 2.723 and 2.623 Å respectively. NMR evidence has also been obtained for the existence of an isomer of this complex, where the two iron atoms are proposed to be in a *cis* disposition about the Rh–Rh bond [277,278].

Several heteronuclear tri-metallic complexes containing the Fe–Rh–Fe core have been synthesized (see Table 10). The reaction of $[\{Rh(C_8H_{12})Cl\}_2]$, $[\{Rh(CO)_2Cl\}_2]$ or $RhCl_3 \cdot 3H_2O$ in methanol, or $[Rh(C_8H_{12})(THF)_2]^+$ in tetrahydrofuran, with an excess of $[(\eta^5\text{-}C_5H_4Me)Fe(CO)_2(PPh_2)]$ in the presence of large counter-anions, gave a product characterized as $[Rh\{(\eta^5\text{-}$

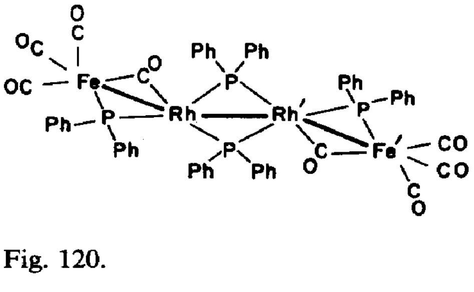

Fig. 120.

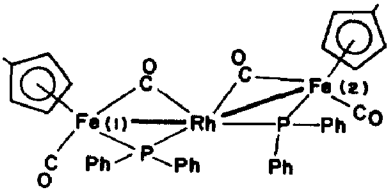

Fig. 121.

$C_5H_4Me)Fe(CO)_2(\mu_2\text{-}PPh_2)\}_2]X$ (**168**; X = $BPh_4$, $PF_6$, $SbF_6$) [279]. The X-ray crystal structure of (**168**) (X = $PF_6$) has been determined [279,280], and has shown the molecule to possess an open triangular arrangement of metal atoms (Rh–Fe(1) = 2.674 Å, Rh–Fe(2) = 2.659 Å, Fe(1)–Rh–Fe(2) = 145.03°) (Fig. 121).

The structure of the cation (**168**) is retained in non-coordinating solvents, but in solvents such as acetone and tetrahydrofuran, IR data are consistent with solvent coordination leading to derivatives containing terminal carbonyls only and no metal–metal interactions (see Scheme 21). These solvolysis reactions are reversible. The controlled reaction of (**168**) with either chloride ion or donor ligands L (L = $P(OMe)_3$, $PPh_3$) in a non-coordinating solvent gives the metal–metal bonded trimers which still contain a bridged structure, as shown in Scheme 21 [279,281,282]. Carbonylation of (**168**) in chloroform results in breakdown of the bridged structure; heating of the tricarbonyl adduct regenerates (**168**) (Scheme 21) [282]. A range of other

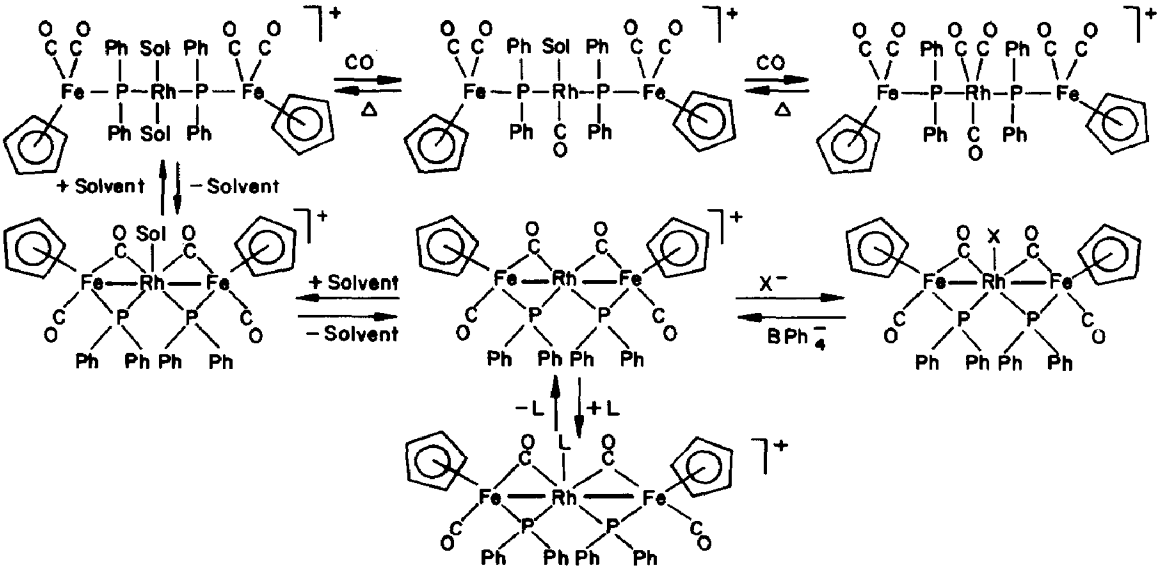

Scheme 21.

TABLE 11

Acyclic cluster complexes of iridium

| Formula | Complex | Fig. | Ref. [a] |
|---|---|---|---|
| $[Ir\{(\eta^5\text{-}C_5H_4R)Fe(CO)_2(\mu_2\text{-}PR'_2)\}_2]^+$ (R = H, Me; R' = $C_6H_5$, $C_6H_4Me$-4) | **(171)** | 122 | 279,282,283 |
| $[Ir\{(\eta^5\text{-}C_5H_4R)Ru(CO)_2(\mu_2\text{-}PR'_2)\}_2]^+$ (R = H, Me; R' = $C_6H_5$, $C_6H_4Me$-4) | **(172)** | 122 | 279,282,283 |
| $[\{(\eta^5\text{-}C_5H_4R)M(CO)_2(\mu_2\text{-}PR'_2)\}_2Ir(CO)Cl]$ (M = Fe, Ru; R = H, Me; R' = $C_6H_5$, $C_6H_4Me$-4) | – | – | 282,283 |

[a] References marked with an asterisk refer to crystal structure determinations.

complexes related to (**168**) have also been synthesized, including $[Rh\{(\eta^5\text{-}C_5H_5)Fe(CO)_2(\mu_2\text{-}PR_2)\}_2]^+$ (**169**; R = $C_6H_4Me$-4) [283,284] and $[Rh\{(\eta^5\text{-}C_5H_5)Fe(CO)_2(SR)\}_2]^+$, (**170**; R = Et, $Bu^t$) [279,281,282] (the latter complex is formed by reaction of $[(\eta^5\text{-}C_5H_5)Fe(CO)_2(SR)]$ with $[Rh(C_8H_{12})(\text{ethanol})_x]^+$).

### *(c) Iridium*

Few acyclic cluster complexes of iridium have been reported (Table 11), and these all form a group of cations of general formula $[Ir\{(\eta^5\text{-}C_5H_4R)M(CO)_2(\mu_2\text{-}PR'_2)\}_2]^+$ (**171**, M = Fe; **172**, M = Ru; R = H, Me; R' = $C_6H_5$, $C_6H_4Me$-4) [279,282,283] closely related to the analogous rhodium complexes (see above). The iridium cations are synthesized in moderate yields by treatment of the intermediate $[\{(\eta^5\text{-}C_5H_4R)M(CO)_2(\mu_2\text{-}PR'_2)\}_2Ir(CO)Cl]$ (obtained from the reaction of $[(\eta^5\text{-}C_5H_4R)M(CO)_2(PR'_2H)]BF_4$ with $[Ir(CO)_2(p\text{-toluidine})Cl]$) with $AgBF_4$ in THF [283]. The complexes $[Ir\{(\eta^5\text{-}C_5H_4R)Fe(CO)_2(\mu_2\text{-}PR'_2)\}_2]$ have also been prepared from the reaction of $[(\eta^5\text{-}C_5H_4R)Fe(CO)_2(PPh_2)]$ with $[Ir(C_8H_{12})(\text{solvent})_x]^+$ [279,282]. An infrared study suggests that these complexes have a structure similar to the rhodium analogues, namely a bent trimetal framework M–Ir–M (M = Fe, Ru) with both metal–metal bonds bridged by one carbonyl ligand and either a dialkyl or diaryl phosphido ligand (see Fig. 122) [282].

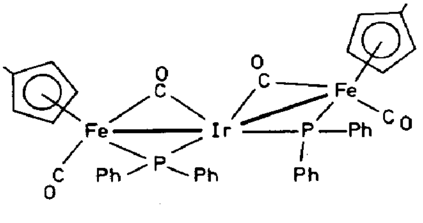

Fig. 122.

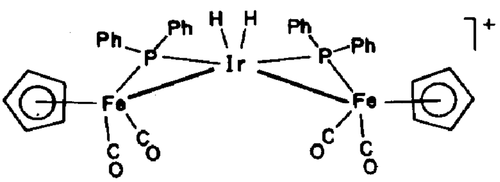

Fig. 123.

The complexes $[Ir\{(\eta^5-C_5H_5)M(CO)_2(\mu_2-PPh_2)\}_2]^+$ have been found to react readily with small molecules, including CO and $H_2$ [282,283]. In the case of dihydrogen, reaction is essentially complete in minutes at one atmosphere $H_2$ and gives the adduct with the proposed structure shown in Fig. 123. This reaction is reversible, although side reactions do prevent quantitative recovery of the starting material.

Reaction with carbon monoxide leads to a complex of stoichiometry $[Ir(CO)_3\{(\eta^5-C_5H_5)Fe(CO)_2(\mu_2-PPh_2)\}_2]^+$ proposed to be analogous to the known $[IrL_2(CO)_3]^+$ cations, and hence containing no metal–metal bonds as observed for the corresponding rhodium complexes [279,280]. Carbon monoxide also reacts readily with the dihydrogen adduct to give the complex $[\{IrH_2(CO)_2\}\{(\eta^5-C_5H_5)Fe(CO)_2(\mu_2-PPh_2)\}_2]$. Both these reactions are irreversible.

### *(vii) Nickel, palladium and platinum*

#### *(a) Nickel*

There are, surprisingly, very few complexes pertinent to this review in which a nickel atom can be described as exercising a structure controlling role in the complex (see Table 12).

To date, only one homonuclear acyclic cluster of nickel has been reported. The complex $[Ni\{(C_{12}H_{17})NiLi\}_2(THF)_4]$, **(173)**, is a minor product of the

TABLE 12

Acyclic cluster complexes of nickel

| Formula | Complex | Fig. | Ref. [a] |
|---|---|---|---|
| $[Ni\{(C_{12}H_{17})NiLi\}_2(THF)_4]$ | **(173)** | 124 | 285* |
| $[Ni(PPh_3)_2\{Co(CO)_3L\}_2]$ (L = CO, $PPh_3$) | **(174)** | - | 286 |
| $[Ni\{Fe(CO)_4(CONR_2)\}_2]$ (R = Me; $R_2 = (CH_2)_4, (CH_2)_5$) | **(175)** | 125 | 287,288* |
| $[Ni\{(\eta^5-C_5H_5)W(CO)_2\}_2(\mu_2-CC_6H_4Me-4)_2]$ | **(176)** | 126 | 39* |
| $[Ni\{(\eta^5-C_5H_5)_2Nb(SMe)_2\}_2]^{2+}$ | **(177)** | 127 | 289*,290,291* |

[a] References marked with an asterisk refer to crystal structure determinations.

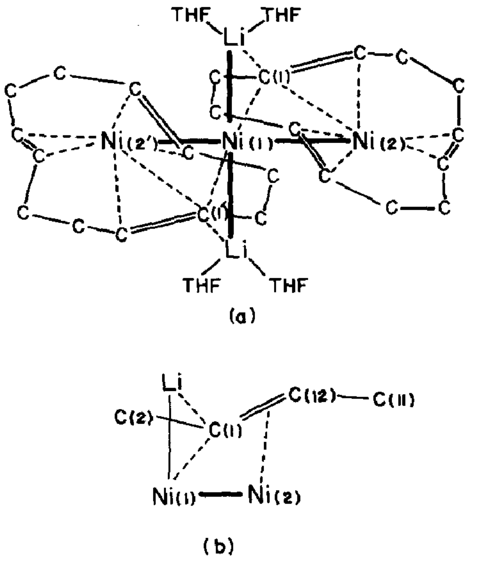

(Hydrogen atoms are omitted for clarity)

Fig. 124.

reaction of $[(C_{12}H_{18})Ni]$ ($C_{12}H_{18}$ = *trans, trans, trans*-1,5,9-cyclododecatriene) with metallic lithium, but it has also been obtained in moderate yield from the reaction of $[(C_{12}H_{18})NiLi_2(tmeda)_2]$ (tmeda = *N,N,N',N'*-tetramethylethylenediamine) with $[(C_{12}H_{18})Ni]$ in tetrahydrofuran. A characteristic of this complex is the linear arrangement of the $Ni_3$ skeleton with an average Ni–Ni bond length of 2.618 Å (see Fig. 124(a)) [285]. A hetero-metal multicentre bond is observed for the five-coordinated carbon atom C(1) of the twelve membered ring which is bonded to Ni(2) through three $\pi$-bonds. This results in an acute Ni(1)–C(1)–Li angle of 78° and is accompanied by a distortion of the $\pi$-bonded interaction Ni(2) to C(1) and C(12) (see Fig. 124(b)) [285].

The hetero-trimetallic complexes $[Ni(PPh_3)_2\{Co(CO)_3L\}_2]$ (**174**; L = CO, $PPh_3$), surprisingly, represent the only nickel examples of the large family of acyclic cluster complexes $[ML_2\{M'L'_n\}_2]$ containing structure controlling nickel, palladium and platinum atoms (see Section B.(vii)(b) and (c)). The synthesis of $[Ni(PPh_3)_2\{Co(CO)_4\}_2]$ has been achieved by the reaction of $[NiCl_2(PPh_3)_2]$ with $Na[Co(CO)_4]$, whereas the substituted derivative $[Ni(PPh_3)_2\{Co(CO)_3(PPh_3)\}_2]$ can be synthesized both by carbonyl substitution on $[Ni(PPh_3)_2\{Co(CO)_4\}_2]$ with $PPh_3$, or by the reaction of $[NiCl_2(PPh_3)_2]$ with $Na[Co(CO)_3(PPh_3)]$ [286]. It is presumed that these complexes contain a linear {Co–Ni–Co} unit, i.e. a *trans* disposition of $\{Co(CO)_3L\}$ groups.

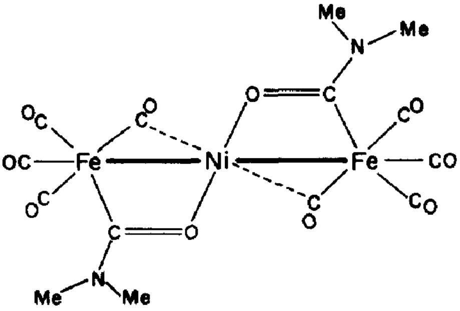

Fig. 125.

The carbamoyl complexes $[Fe(CO)_4(CONR_2)][C(NMe_2)_3]$ ($R = Me$; $R_2 = (CH_2)_4$, $(CH_2)_5$) react with anhydrous nickel bromide to give the complexes $[Ni\{Fe(CO)_4(CONR_2)\}_2]$, (**175**), in good yield [287,288]. The X-ray crystal structure of (**175**; $R = Me$) has been determined [288], showing the molecule to possess a linear Fe–Ni–Fe backbone with an average Fe–Ni bond length of 2.460 Å. Each Fe–Ni bond is bridged by a carbamoyl moiety, and a semi-bridging carbonyl group (Ni–Fe–C (semi-bridging) 62.5°) (Fig. 125). On the basis of spectroscopic properties the other members of this series are assigned a similar structure.

The closely related complex $[Ni\{(\eta^5\text{-}C_5H_5)W(CO)_2\}_2(\mu_2\text{-}CC_6H_4Me\text{-}4)_2]$, (**176**), has been synthesized by the reaction of $[Ni(C_8H_{12})_2]$ ($C_8H_{12}$=cycloocta-1,5-diene) with the alkylidyne complex $[(\eta^5\text{-}C_5H_5)W(CO)_2(\equiv CC_6H_4Me\text{-}4)]$ [39]. The X-ray crystal structure of this complex [39] has shown the molecule to contain an almost linear W–Ni–W core (174.5°) with the Ni–W bonds (2.584 Å mean length) each bridged by an alkylidyne ligand, and a semi-bridging carbonyl group (Ni–W–C (semi-bridging) = 54.05 Å (average

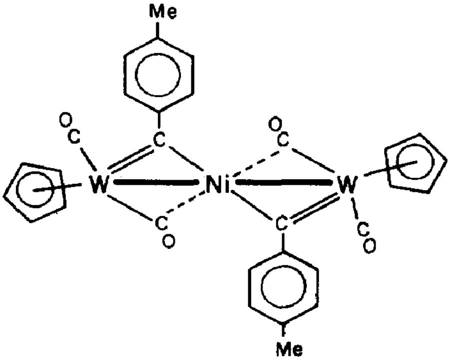

Fig. 126.

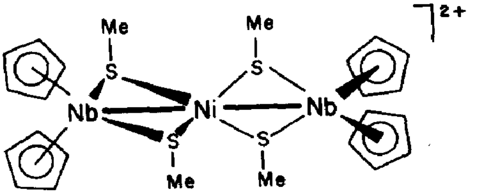

Fig. 127.

value)) (Fig. 126). The metal–metal bonds in this complex are ca. 0.2 Å shorter than that expected for a single bond, and this effect may reflect some multiple bond character associated with delocalization in the dimetallacyclopropene ring system [39]. Platinum and palladium complexes similar to (**176**) have also been synthesized (see Section B.(vii)(b) and (c)).

The $d^1$ niobium complex $[(\eta^5\text{-}C_5H_5)_2Nb(SMe)_2]$ readily adds to $NiCl_2$ giving a complex whose elemental analysis shows it to have the stoichiometry $[Ni\{(\eta^5\text{-}C_5H_5)_2Nb(SMe)_2\}_2]^{2+}$, (**177**), [289,290]. The crystal structure of the tetrafluoroborate salt of this complex has been determined. The molecule contains a linear Nb–Ni–Nb core, the Nb–Ni bonds each bridged by two methylthiolato ligands (see Fig. 127). The relatively short Nb–Ni internuclear distance (2.77 Å) and the geometry of the $\{Nb(\mu_2\text{-}SMe)_2Ni(\mu_2\text{-}SMe)_2Nb\}$ core is consistent with substantial niobium–nickel bonding [291]. Formally, the Ni–Nb bond may be represented as a donor bond from the $d^{10}$ nickel to the 16 electron, $d^0$ niobium atoms [289,290]. Support for this contention comes from the observation that the chemical shift of the cyclopentadienyl hydrogen atoms of the complex is at a lower field (ca. 1.0 ppm) than the corresponding resonance for the cation $[(\eta^5\text{-}C_5H_5)_2Nb(SR)_2]^+$ [290]. A similar argument has been used to invoke metal–metal bonding in the complexes $[(\eta^5\text{-}C_5H_5)_2Ti(SR)_2Mo(CO)_4]$ [292]. Complexes similar to (**177**) have also been synthesized with platinum and palladium as the central metal atom (see Section B.(vii)(b) and (c)).

### *(b) Palladium*

Palladium, in a similar manner to platinum (see Section B.(vii)(c)) forms a range of closely related acyclic cluster species, these being synthesized with relative ease even from mononuclear precursors. The limited number of such complexes known at present, however, suggests that this is still a largely unexplored field (Table 13).

Reaction of the dibenzylideneacetone (dba)–palladium(0) complexes $[Pd_2(dba)_3(CHCl_3)]$ with triarylcyclopropenium bromides $([C_3R^1R^2_2]Br)$ gave the unusual, ring opened trinuclear complexes $[Pd_3(C_3R^1R^2_2)_2Br_2]$ (**178**, $R^1 = R^2 = Ph$, $C_6H_4OMe\text{-}4$; $R^1 = Ph$, $R^2 = C_6H_4OMe\text{-}4$) in good to

TABLE 13

Acyclic cluster complexes of palladium

| Formula | Complex | Fig. | Ref. [a] |
|---|---|---|---|
| $[Pd_3(C_3R^1R^2_2)_2Br_2]$ ($R^1 = R^2 = Ph, C_6H_4OMe\text{-}4$; $R^1 = Ph$; $R^2 = C_6H_4OMe\text{-}4$) | **(178)** | – | 293,294 |
| $[Pd_3(C_3R^1R^2_2)_2(acac)_2]$ ($R^1$, $R^2$ as above) | **(179)** | 128 | 293,294,295* |
| $[Pd_3(CNMe)_8]^{2+}$ | **(180)** | 130 | 296* |
| $[Pd_3(O_2CCH_3)_4(\eta^3\text{-}C_3HR_2)_2]$ ($R = C(O)R'$; $R'$ = alkyl or aryl) | **(181)** | 131 | 298* |
| $[Pd_3Cl_4(\eta^3\text{-}C_3H_2Me\text{-}2)_2]$ | **(182)** | – | 299* |
| $[PdL_2\{ML'_n\}_2]$ ($L$ = py, 3-Mepy, 4-Mepy; $ML'_n = (\eta^5\text{-}C_5H_5)Mo(CO)_3$, $Mn(CO)_5$, $Co(CO)_4$, $Co(CO)_3(PBu^n_3)$) | **(183)** | – | 300–307 |
| $[Pd\{(\eta^5\text{-}C_5H_5)_2Nb\}_2(\mu_2\text{-}SMe)_4]$ | **(184)** | – | 289*,290 |
| $[Pd\{(\eta^5\text{-}C_5H_5)W(CO)_2\}_2(\mu_2\text{-}CC_6H_4Me\text{-}4)]$ | **(185)** | – | 39 |

[a] References marked with an asterisk refer to crystal structure determinations.

excellent yield [293,294]. These products may be derivatized by reaction with Tl(acac) (acac = acetylacetonate) in toluene to give the closely related complexes $[Pd_3(C_3R^1R^2_2)_2(acac)_2]$, **(179)**, [293,294] (see Scheme 22). Analogous platinum complexes have also been synthesized [293,294] (see Section B.(vii)(c)). The X-ray crystal structure of $[Pd_3\{C_3(Ph)(C_6H_4OMe\text{-}4)_2\}_2(acac)_2]$ has been determined [293–295] (see Fig. 128). The molecule has a bent Pd(1)–Pd(2)–Pd(1′) framework (127.2°) with a Pd–Pd bond length of 2.662 Å. The Pd(1)···Pd(1′) internuclear distance (4.769 Å) clearly precludes a bonding interaction between the outer palladium atoms. The bridging $C_3R^1R^2_2$ ligands have C($\alpha$) and C($\gamma$) closer to Pd(1) (2.037 and

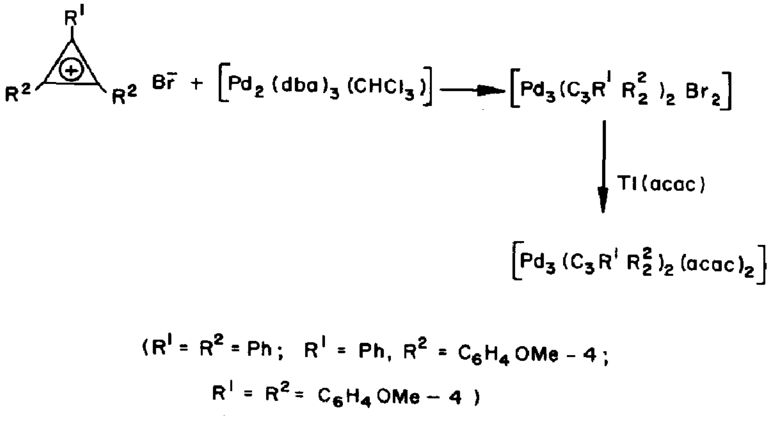

Scheme 22.

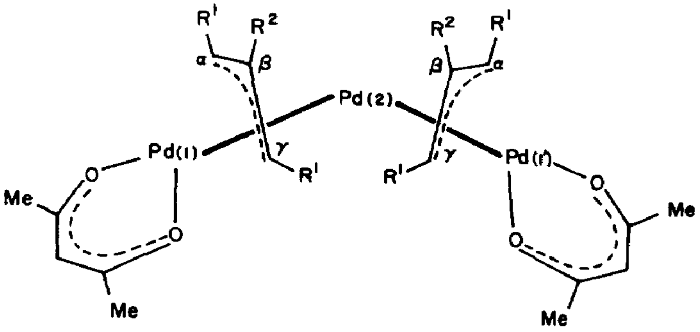

Fig. 128.

1.981 Å) than to Pd(2) (2.164 and 2.106 Å) and C(β) closer to Pd(2) (2.321 Å) than to Pd(1) (2.579 Å).

From a careful examination of the crystallographic data [295], the authors have inferred the existence of isomers in the solid state which arise from a positional variation of the substituents on the $C_3R^1R^2_2$ ligands (Fig. 129(a)–(c)). The distribution 67% (a), 30% (b) and 3% (c) was determined. The existence of other isomers, in solution, has been inferred by $^1H$ NMR spectroscopy [294]. The NMR spectra of the other members of the series $[Pd_3(C_3R^1R^2_2)_2X_2]$ (X = Br, acac) showed that the unusual structure determined for $[Pd_3\{C_3(Ph)(C_6H_4OMe\text{-}4)_2\}_2(acac)_2]$ was present in all the other complexes [294].

The linear tri-palladium cation $[Pd_3(CNMe)_8]^{2+}$, **(180)**, has been isolated as the hexafluorophosphate salt from the reaction of the zerovalent palladium isocyanide complex $[Pd(CNMe)_x]$ with either $[Pd(CNMe)_4]^{2+}$ or $[Pd_2(CNMe)_6]^{2+}$ in acetone solution [296]. $[Pd_3(CNMe)_8](PF_6)_2$ reacts readily with $PPh_3$ to give the disubstituted product $[Pd_3(CNMe)_6(PPh_3)_2](PF_6)_2$. The IR spectra of these products show only terminal ν(NC) vibrations, while the $^1H$ NMR spectra show single, singlet resonances for the methylisocyanide ligands. The X-ray crystal structure of $[Pd_3(CNMe)_6(PPh_3)_2](PF_6)_2$ has been determined [296]. The three palladium atoms form a strictly linear $Pd_3$ unit (Fig. 130) with a short Pd–Pd

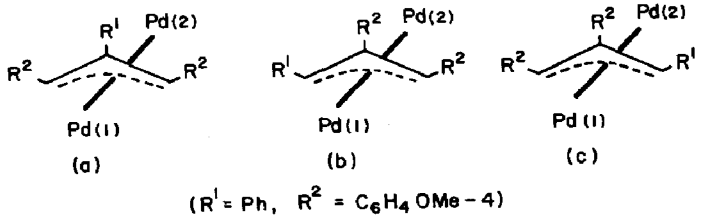

Fig. 129.

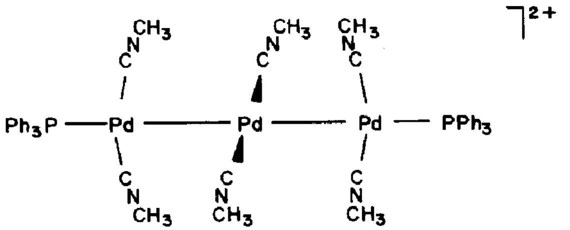

Fig. 130.

bond (2.5921 Å). Each palladium atom, coordinated to two methylisocyanide ligands, exhibits approximate square planar geometry with the square planes twisted away from each other such that the angle between the two five-atom least-squares planes is 74.5°. The equatorial isocyanide ligands are bent towards the centre of the molecule (average Pd–Pd–C = 80.0°), similar to that observed in $[Pd_2(CNCH_3)_6]^{2+}$ (average Pd–Pd–C = 85.0°) [297]. The authors discount steric interactions between the isocyanide ligands and the axial triphenylphosphine group, and suggest that the ligand bending arises from an electronic effect resulting from the interaction between filled *d* orbitals on palladium with empty $\pi^\star$ orbitals on the isocyanide ligands of the adjacent metal [296]. This effect would thus be related to the phenomenon of "semi-bridging" observed for carbonyl ligands.

Two further examples of tri-palladium acyclic clusters are known. The question of the level of metal–metal interaction in these particular complexes has, however, not been fully addressed. The reaction of trimeric palladium acetate $[\{Pd(O_2CCH_3)_2\}_3]$ with 2,6-disubstituted pyrylium salts in boiling acetic acid/water/sodium acetate mixtures gives ring opening and formation of the trinuclear bis(acylallyl)palladium acetates $[Pd_3(O_2CCH_3)_4(\eta^3\text{-}C_3H_3R_2)_2]$ (**181**; R = C(O)Bu$^t$, C(O)Ph, C(O)$C_6H_2Me_3$-2,4,5) [298]. The complex (**181**; R = C(O)Bu$^t$) has been characterized by a single crystal structure determination [298]. The molecule contains a linear arrangement of three palladium atoms with an average Pd · · · Pd distance of 2.864 Å (Fig. 131). While this is longer than would be expected for a palladium–palladium single bond (2.57–2.699 Å) it is shorter than the doubled covalent radius of palladium (2.98 Å), and the authors argue in favour of at least limited metal–metal interaction in these complexes. The acetato ligands in $[Pd_3(O_2CCH_3)_4(\eta^3\text{-}C_3H_3R_2)_2]$ may be replaced by other carboxylate groups; for instance treatment of $[Pd_3(O_2CCH_3)_4\{\eta^3\text{-}C_3H_3(C(O)Bu^t)_2\}_2]$ with benzoic acid gives the corresponding benzoate derivative [298].

A similar linear tripalladium bis(allyl) complex $[Pd_3Cl_4(\eta^3\text{-}C_3H_4Me\text{-}2)_2]$, (**182**), has been synthesized by the reaction of $[PdCl_2(NCC_6H_5)_2]$ with $[\{PdCl(\eta^3\text{-}C_3H_4Me\text{-}2)\}_2]$ [299]. An X-ray crystal structure determination shows the molecule to be centrosymmetric, and to be analogous to the

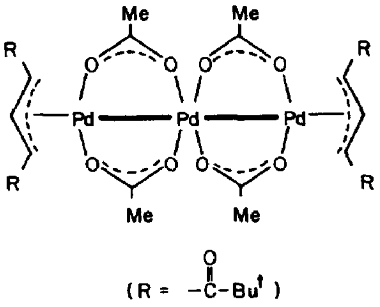

Fig. 131.

carboxylato analogues, but with chloro rather than carboxylato bridges. The palladium–palladium internuclear distance at 3.386 Å is much longer than that observed for the acetate complex $[Pd_3(O_2CCH_3)_4\{C_3H_3(C(O)Bu^t)_2\}_2]$ (2.864 Å), and although the authors do not discuss the possibility of metal–metal bonding, there may be at least a partial bonding interaction.

While, to date, the range of homonuclear palladium acyclic cluster complexes known is limited, a large series of heteronuclear complexes containing palladium in a structure controlling role have been synthesized. In this case though, the range of structural types is much less varied, and with only a few exceptions, all are complexes of the general formulation $[PdL_2\{ML'_n\}_2]$, (**183**) (see Table 13) and are thus expected to contain a linear {M–Pd–M} framework.

Reaction of *trans*-$[PdCl_2(py)_2]$ with $Na[(\eta^5\text{-}C_5H_5)Mo(CO)_3]$ has given $[Pd(py)_2\{(\eta^5\text{-}C_5H_5)Mo(CO)_3\}_2]$ [300–303] in 57% yield. In a similar manner the complexes $[PdL_2\{ML'_n\}_2$ (L = py, 3-Mepy, 4-Mepy; $ML'_n = Mn(CO)_5$ [301,303–305], $Co(CO)_4$ [301–304]; L = py, $ML'_n = Co(CO)_3(PBu^n_3)$ [306]) have also been synthesized by the metathetical reaction between $[PdCl_2L_2]$ and Na $[ML'_n]$. None of these palladium complexes have themselves been the subject of a crystal structure determination, but spectroscopic studies strongly suggest that they have structures similar to the platinum analogues which are both more numerous and better characterized (see Section B.(vii)(c)) and which have been shown to contain a linear trimetal core. A wide range of complexes of the type $[PdL_2\{ML'_n\}_2]$ have been proposed as intermediates in the formation of the clusters $[Pd_2L_2\{ML'_n\}_n]$ [307] although they have not been isolated.

The heteronuclear complex $[Pd\{(\eta^5\text{-}C_5H_5)_2Nb\}_2(\mu_2\text{-}SMe)_4]^{2+}$, (**184**), has been synthesized by the reaction of $[(\eta^5\text{-}C_5H_5)_2Nb(SMe)_2]$ with $[PdCl_2(NCC_6H_5)_2]$ [289,290] and is believed to have a structure related to that of the nickel analogue characterized by X-ray crystallography [289] (see Fig. 127). Similarly, the complex $[Pd\{(\eta^5\text{-}C_5H_5)W(CO)_2\}_2(\mu_2\text{-}CC_6H_4Me\text{-}4)_2]$, (**185**), synthesized by Stone and co-workers [39] from $[Pd(C_7H_{10})_3]$

TABLE 14

Acyclic cluster complexes of platinum

| Formula | Complex | Fig. | Ref. [a] |
|---|---|---|---|
| $[Pt_3(C_3R^1R^2_2)_2Br_2]$ ($R^1 = R^2 = C_6H_4OMe$-4; $R^1 = Ph$; $R^2 = C_6H_4OMe$-4) | **(186)** | – | 294 |
| $[Pt_3(C_3R^1R^2_2)_2(acac)_2]$ ($R^1$, $R^2$ = as above) | **(187)** | – | 294* |
| $[Pt_3\{C_3(C_6H_4OMe\text{-}4)_3\}_2(\eta^5\text{-}C_5H_5)_2]$ | **(188)** | – | 294 |
| $[Pt_3\{C_3(C_6H_4OMe\text{-}4)_3\}_2(S_2CNPr^i)_2]$ | **(189)** | – | 294 |
| $[Pt_3\{C_3(C_6H_4OMe\text{-}4)_3\}_2L_4](PF_6)_2$ ($L = PPh_3$; $L_2$ = COD, bipy, phen) | **(190)** | – | 294 |
| $[Pt_3(PPh_3)_2(\mu_2\text{-}PPh_2)_3(\eta^1\text{-}Ph)]$ | – | 132 | 308* |
| $[Pt_3(COD)_2\{\mu_2\text{-}(CF_3)C{=}C(CF_3)\}_2(\mu_2\text{-}\{(CF_3)C{=}C(CF_3)\}_2)]$ | – | 133 | 309* |
| $[PtL_2\{ML'_n\}_2]$ (L = CO, $Bu^tNC$, $C_6H_{11}NC$, py; $ML'_n = Co(CO)_4$, $Fe(CO)_3NO$, $Mn(CO)_5$, $Re(CO)_5$, $(\eta^5\text{-}C_5H_5)Mo(CO)_3$, $(\eta^5\text{-}C_5H_5)W(CO)_3$) | **(191)** | 134 | 310–312,313*, 314*,315 |
| $[Pt(CO)\{Mn(CO)_4\}_2(\mu_2\text{-}PPh_2)_2]$ | **(192)** | 135 | 315* |
| $[Pt(CNC_6H_{11})\{CN(OEt)C_6H_{11}\}\{(\eta^5\text{-}C_5H_5)Mo(CO)_3\}_2]$ | – | 136 | 316* |
| $[Pt\{(\eta^5\text{-}C_5H_5)_2Nb\}_2(\mu_2\text{-}SMe)_4]$ | **(193)** | – | 289,290 |
| $[Pt\{(\eta^5\text{-}C_5H_5)W(CO)_2\}_2(\mu_2\text{-}CC_6H_4Me\text{-}4)_2]$ | **(194)** | – | 39 |
| $[\{Pt_2(NH_3)_4(C_5H_4ON)_2\}_2](NO_3)_5$ | – | 137 | 325*,326* |
| $[\{Pt_2(NH_3)_4(C_5H_4ON)_2\}_2](NO_3)_4$ | – | – | 327* |
| $[\{Pt_2(NH_3)_4(C_5H_4N_2O_2)_2\}_2](NO_3)_4$ | – | – | 328* |
| $[\{Pt_2(NH_3)_4(C_4H_6ON)_2\}_2](NO_3)_6$ | – | – | 329*,330* |
| $[\{Pt_2(en)_2(C_5H_4NO)_2\}_2](NO_3)_4$ | – | – | 331* |
| $[Pt_4(NH_3)_8(C_4H_6NO)_4](NO_3)_{5.48}$ | – | – | 332* |

[a] References marked with an asterisk refer to crystal structure determinations.

($C_7H_{10}$ = bicyclo[2.2.1]heptene) and $[(\eta^5\text{-}C_5H_5)W(CO)_2(\equiv CC_6H_4Me\text{-}4)]$, has on the basis of its spectroscopic properties, an overall structure related to that of the nickel and platinum analogues [39] (see Fig. 126).

### *(c) Platinum*

Of the metals in the nickel triad, platinum forms the largest group of acyclic cluster complexes (see Table 14).

The tri-platinum complexes $[Pt_3(C_3R^1R^2_2)_2Br_2]$, **(186)**, and $[Pt_3(C_3R^1R^2_2)_2(acac)_2]$ (**187**, $R^1 = R^2 = C_6H_4OMe$-4; $R^1$ = Ph, $R^2 = C_6H_4OMe$-4) have been synthesized by the reaction of the platinum(0) complex $[Pt_2(dba)_3(CHCl_3)]$ (dba = dibenzylideneacetone) with the triarylcyclopropenium bromides, $[C_3R^1R^2_2]Br$ [294]. On the basis of their NMR spectra these complexes are all assigned structures analogous to the crystallographically characterized palladium complex $[Pd_3\{C_3(Ph)(C_6H_4Me\text{-}4)_2\}_2(acac)_2]$ namely a bent trimetallic framework with bridging $C_3R^1R^2_2$ ligands (see Fig.

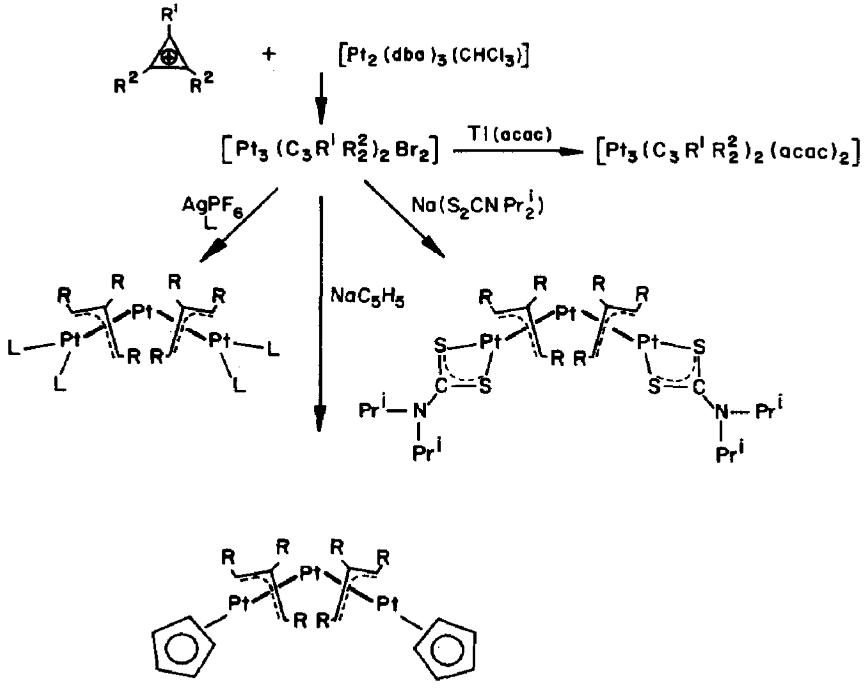

Scheme 23.

128). The platinum complex $[Pt_3\{C_3(C_6H_4OMe\text{-}4)_3\}_2Br_2]$ has also been converted into the complexes $[Pt_3\{C_3(C_6H_4OMe\text{-}4)_3\}_2(\eta^5\text{-}C_5H_5)_2]$, (**188**), and $[Pt_3\{C_3(C_6H_4OMe\text{-}4)_3\}_2(S_2CNPr^i)_2]$, (**189**), by reaction with cyclopentadienylthallium and $Na[S_2CNPr^i]$ respectively [294] (Scheme 23). Similarly the salts $[Pt_3\{C_3(C_6H_4OMe\text{-}4)_3\}_2L_4](PF_6)_2$ (**190**; $L = PPh_3$; $L_2 =$ cycloocta-1,5-diene, 2,2′-bipyridyl, 1,10-phenantholine) [294] have been synthesized by the reaction of $[Pt_3\{C_3(C_6H_4OMe\text{-}4)_3\}_2Br_2]$ with $AgPF_6$ in acetonitrile, followed by treatment with ligand L or $L_2$. None of these complexes have been structurally characterized, although on the basis of NMR spectroscopy, they are assigned a similar overall structure to $[Pd_3\{C_3(Ph)(C_6H_4OMe\text{-}4)_2\}_2(acac)_2]$ [294].

The trinuclear complex $[Pt_3(PPh_3)_2(\mu_2\text{-}PPh_2)_3(Ph)]$ is one of the products obtained by heating $[Pt(PPh_3)_4]$ in benzene for extended periods [308]. The X-ray crystal structure has been determined [308] and the structure is found to be based upon an open $Pt_3$ triangle (Pt–Pt = 2.785 Å (average), Pt–Pt–Pt = 81.34°). Each Pt–Pt bond is bridged by a diphenylphosphido ligand, as is the open edge of the triangle ($Pt \cdots Pt = 3.630$ Å) (Fig. 132).

Reaction of $[Pt(COD)_2]$ (COD = cycloocta-1,5-diene) with hexafluorobut-2-yne affords the complex $[Pt\{C(CF_3)=C(CF_3)\}(COD)]$ which reacts further with hexafluorobut-2-yne to give the tri-platinum complex shown in Fig. 133

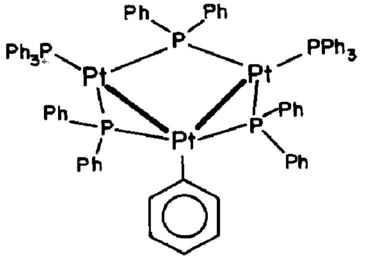

Fig. 132.

[309]. The X-ray crystal structure has been determined showing the three platinum atoms to be in a non-linear arrangement (Pt(1)–Pt(2)–Pt(3) = 160.98°). The Pt(1)–Pt(2) internuclear distance of 2.630 Å is consistent with a direct Pt–Pt bond, whereas the distance between Pt(2) and Pt(3) (2.841 Å) although within the limits for Pt–Pt bonding may not necessarily represent a substantial bonding interaction between these atoms [309].

Similarly to palladium, complexes of the general type $[PtL_2\{ML'_n\}_2]$, (**191**), form the largest, although simplest class of platinum containing heteronuclear acyclic cluster complexes. The synthetic procedures are essentially identical to those detailed above for palladium and nickel complexes, namely reaction of a platinum(II) complex $[PtX_2L_2]$ (X = halide, L = suitable donor ligand) with two molar equivalents of an anionic metal complex $[ML'_n]^-$. In the case of platinum, however, the variety of different ligands, L and L′ is much greater, and also several X-ray structure determinations have been carried out. It is beyond the scope of this review to detail the synthesis of all the complexes $[PtL_2\{ML'_n\}_2]$, and the reader is referred to Table 14 [310–312], where comprehensive literature citations on such complexes are listed. A number of pertinent crystal structure determinations have, however, been reported and these are discussed below.

The X-ray structures of the complexes $[Pt(py)_2\{Co(CO)_4\}_2]$ [313] and $[Pt(py)_2\{Mn(CO)_5\}_2]$ [313] were reported in 1968. In both cases a linear arrangement of metal atoms was observed with average Pt–Co and Pt–Mn bond lengths of 2.613 and 2.743 Å respectively. A notable feature of both

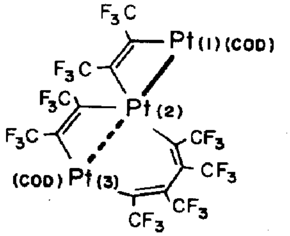

Fig. 133.

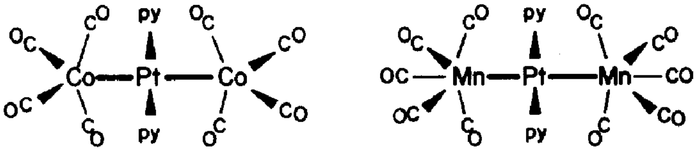

(a) (b)

Fig. 134.

structures is the tendency for four carbonyl groups (two on each outer metal atom) to bend inwards towards the central $\{Pt(py)_2\}$ moiety (e.g. Pt–Co–C = 68.4° (mean), Pt–Mn–C = 69.5° (mean)) (Fig. 134(a) and (b)).

The heterometallic complexes $[Pt(CO)_2\{M(CO)_5\}_2]$ (M = Mn, Re) have been synthesized in high yield from the reaction of $[(COD)PtMe_2]$ with excess $[HM(CO)_5]$ in the presence of carbon monoxide [314]. The dinuclear species $[M_2(CO)_{10}]$ is also formed in this reaction and this is cited as evidence of a radical pathway for this reaction. The X-ray crystal structure of $[Pt(CO)_2\{Re(CO)_5\}_2]$ has been determined [314] and found to consist of the expected linear Re–Pt–Re arrangement (Pt–Re = 2.8309 Å).

Treatment of *cis*-$[PtCl_2(PPh_2Cl)_2]$ with two molar equivalents of $[Mn(CO)_5]^-$ gives two products, $[Pt(CO)_2\{Mn(CO)_5\}_2]$ and $[Pt(CO)\{Mn(CO)_4\}_2(\mu_2\text{-}PPh_2)_2]$, (**192**), [315]. The X-ray crystal structure of (**192**) has shown it to possess a bent Mn–Pt–Mn backbone (Mn(1)–Pt = 2.741 Å, Mn(2)–Pt = 2.747 Å, Mn(1)–Pt–Mn(2) = 159.56°), with the Mn–Pt bonds each bridged by a diphenylphosphido ligand (see Fig. 135). It should be noted that the molecule has no element of symmetry and is thus chiral [315]. In this regard (**192**) is closely related to the cationic heterobimetallic complexes $[Rh\{(\eta^5\text{-}C_5H_4Me)Fe(CO)_2\}_2(\mu_2\text{-}PPh_2)_2]$ discussed in Section B.(vi)(b).

The X-ray structure of $[Pt(CNC_6H_{11})(CN(OEt)C_6H_{11})\{(\eta^5\text{-}C_5H_5)Mo(CO)_3\}_2]$ has been reported [316]. The molecule contains an almost linear Mo–Pt–Mo unit (176.93°) with a Pt–Mo bond length of 2.89 Å. The isocyanide and carbene ligands have a *trans* disposition on the central platinum atom, and there is a marked tendency for two carbonyl ligands on

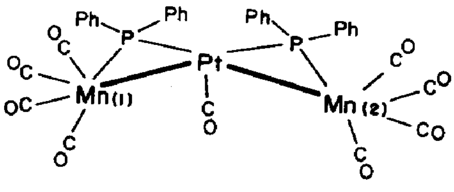

Fig. 135.

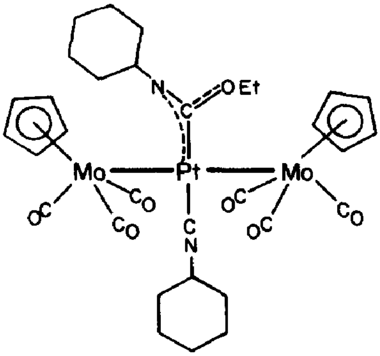

Fig. 136.

each molybdenum atom to bend inwards towards the platinum atom (Pt–Mo–C = 62.7, 65.2, 67.1, 53.4°) and approach the semi-bridging state (Fig. 136).

The mixed metal trinuclear complex $[Pt\{(\eta^5\text{-}C_5H_5)_2Nb\}_2(\mu_2\text{-}SMe)_4]$, (**193**), has been synthesized by the reaction of $[PtCl_2(NCC_6H_5)_2]$ with $[(\eta^5\text{-}C_5H_5)_2Nb(SMe)_2]$ [289,290] and is assigned a structure related to that of the nickel analogue characterized by X-ray crystallography [289] (see Fig. 127). Further, the complex $[Pt\{(\eta^5\text{-}C_5H_5)W(CO)_2\}_2(\mu_2\text{-}CC_6H_4Me\text{-}4)_2]$, (**194**), has been synthesized from $[Pt(C_2H_4)_3]$ and $[(\eta^5\text{-}C_5H_5)W(CO)_2(\equiv CC_6H_4Me\text{-}4)]$ [39] and characterized by X-ray crystallography. The molecule has a bent W–Pt–W core (165.6°) compared to the nearly linear W–Ni–W core (174.5°) found for the analogous nickel complex [39] (see Fig. 126). The average Pt–W bond length is 2.713 Å. A remarkable difference between the platinum and the nickel complexes though, is that whereas in the nickel complex the terminal carbonyl groups on the tungsten atoms each lie *trans* to the tolyl group of the second metallo-cyclopropene ring, in the platinum compound the corresponding carbonyl groups lie one *cis* and one *trans*.

The blue compounds formed from aqueous solutions of platinum(II) and amides have long been known [317–320]. Interest has, however, been revived by the recent discovery that blue complexes are formed from aqueous solutions of the antitumour drug *cis*-$[PtCl_2(NH_3)_2]$ and pyrimidines such as uracil and thymine [321,322] and that these "platinum pyrimidine blues" themselves show high antitumour activity [321–324]. It has been proposed that the "platinum blues" contain complex mixtures of compounds in various stages of oligomerization arrived at via stacking of square planar platinum complexes, and it is probably this tendency to catenation which has prevented the isolation of crystalline products suitable for structural analysis.

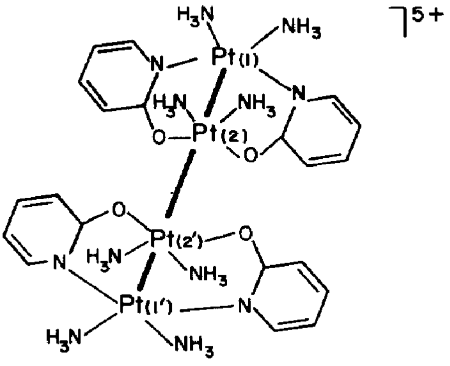

Fig. 137.

Recently, however, Lippard and co-workers have isolated crystalline products of the reaction between *cis*-diammineplatinum(II) compounds and $\alpha$-pyridone which have been instrumental in elucidating the chemistry of the platinum blues. The complex $[\{Pt_2(NH_3)_4(C_5H_4ON)_2\}_2](NO_3)_5$ has been obtained by treatment of a mixture of *cis*-diammineplatinum(II) hydrolysis products with $\alpha$-pyridone and characterized by X-ray crystallography [325,326]. The molecular structure (Fig. 137) shows that the $[\{Pt_2(NH_3)_4(C_5H_4ON)_2\}_2]^{5+}$ cation consists of an oligomeric unit of four platinum atoms linked through amidate bridges, and involving hydrogen bonding and probably, partial metal–metal bonding [326]. Within each dimer, two *cis*-diammineplatinum units are bridged by $\alpha$-pyridonato ligands. The platinum–platinum internuclear distance within the dimer units is 2.7745 Å, while the linkage of these two dinuclear units across the centre of symmetry is achieved by a Pt–Pt bond 2.8770 Å in length. The $Pt_4$ chain is not quite linear (Pt(1)–Pt(2)–Pt(2′) = 164.60°).

Subsequent to this work, a range of closely related complexes have been structurally characterized including $[\{Pt_2(NH_3)_4(C_5H_4ON)_2\}_2](NO_3)_4$ [327], $[\{Pt_2(NH_3)_4(C_4H_5O_2N_2)_2\}_2](NO_3)_4$ [328], $[\{Pt_2(NH_3)_4(C_4H_6ON)_2\}_2](NO_3)_6$ [329,330], $[\{Pt_2(en)_2(C_5H_4ON)_2\}_2](NO_3)_4$ [331], and $[Pt_4(NH_3)_8(C_4H_6ON)_4](NO_3)_{5.48}$ [332]. It is beyond the scope of this review to comprehensively describe this intriguing area of chemistry; suffice it to point out that these complexes fulfill an important role in bridging the understanding of molecular (i.e. discrete) acyclic clusters, and polymers or chains of metal atoms, and are best considered as transition metal oligomers. Recent findings on the nature of metal–metal bonding in $[\{Pt_2(NH_3)_4(C_5H_4ON)_2\}_2](NO_3)_5$ suggest that Pt–Pt bonding is due mainly to $\sigma$-overlap between Pt $d_{z^2}, s$ hybrid orbitals, and significantly, that the net $\sigma$-bonding interaction between the end pairs of platinum atoms in the chain is stronger than between the middle pair, i.e. Pt–Pt · · · Pt–Pt [333].

## (viii) Copper, silver and gold

### (a) Copper

To date, as far as we are aware, no homonuclear copper complexes that fall within the scope of this review have been reported. Heterometallic complexes, structurally controlled by copper include, however, several different structural classes some closely related to classes obtained with silver and gold (Table 15).

The trinuclear anion $[Cu\{Co(CO)_4\}_2]^-$, **(195)**, was obtained as an unexpected product in the attempted synthesis of $[Co_2(CO)_8]$ from $CoI_2$ using metallic copper as a reducing agent [334]. An improved synthesis (yield ca. 75%) from $Na[Co(CO)_4]$ and CuI was also developed and the pure complex was obtained in the form of the tetraethylammonium salt as white crystals from ethanol-hexane solution [334]. A similar method had earlier been used to synthesize the anions $[Cu\{(\eta^5\text{-}C_5H_5)M(CO)_3\}_2]^-$ (**196**; M = Cr, Mo, W) in high yield, i.e. by reaction of $Na[(\eta^5\text{-}C_5H_5)M(CO)_3]$ with CuCl [335,336]. The analogous product $[Cu\{(\eta^5\text{-}C_5H_5)Mo(CO)_3\}\{(\eta^5\text{-}C_5H_5)W(CO)_3\}]^-$ was obtained by the reaction of the polymeric $[\{(\eta^5\text{-}C_5H_5)Mo(CO)_3Cu\}_x]$ with $Na[(\eta^5\text{-}C_5H_5)W(CO)_3]$ [336]. None of these complexes has been structurally characterized but spectroscopic studies and methods of synthesis would suggest linear M–Cu–M structures essentially analogous to the more numerous silver [335] and gold [303,337–340] derivatives. (It should, however, be noted that differences between the IR spectra of the copper and silver derivatives, that could be interpreted in terms of different conformers, could also be indicative of gross structural differences, for instance a bent M–Cu–M framework [336].) Little in terms of chemistry is known of these complex anions. The complex $[Cu\{Co(CO)_4\}_2]^-$ dissociates on dissolving in

TABLE 15

Acyclic cluster complexes of copper

| Formula | Complex | Fig. | Ref. [a] |
|---|---|---|---|
| $[Cu\{Co(CO)_4\}_2]^-$ | **(195)** | – | 334 |
| $[Cu\{(\eta^5\text{-}C_5H_5)M(CO)_3\}_2]^-$ (M = Cr, Mo, W) | **(196)** | – | 335,336 |
| $[Cu\{(\eta^5\text{-}C_5H_5)Mo(CO)_3\}\{(\eta^5\text{-}C_5H_5)W(CO)_3\}]^-$ | – | – | 336 |
| $[Cu\{ReH_5(PMePh_2)_3\}_2]PF_6$ | **(197)** | 138 | 341* |
| $[Cu\{ReH_5(PMe_2Ph)_3\}_2]PF_6$ | – | – | 341 |
| $[Cu\{mer\text{-}IrH_3(PMe_2Ph)_3\}_2]PF_6$ | **(198)** | 139 | 342 |
| $[Cu\{fac\text{-}IrH_3(PMe_2Ph)_3\}_2]PF_6$ | **(199)** | 140 | 342* |
| $[Cu\{Pt(NH_3)_2(\mu_2\text{-1-Me-uracilato})(\mu_2\text{-1-Me-cytosine})\}_2]^{4+}$ | **(200)** | 141 | 343* |

[a] References marked with an asterisk refer to crystal structure determinations.

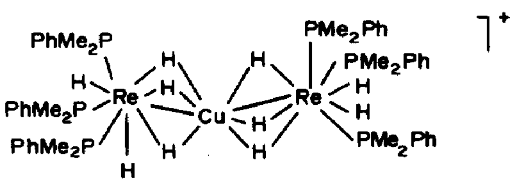

Fig. 138.

acetonitrile to give $[Co(CO)_4]^-$ and $[Cu(NCMe)_x]^+$, a reaction which, remarkably, is reversed on evaporating the solvent [334]. The anions $[Cu\{(\eta^5\text{-}C_5H_5)M(CO)_3\}_2]^-$ (M = Cr, Mo, W) give 1 : 1 adducts when reacted with 1,10-phenanthroline, and when reacted with triphenylphosphine, the products include $[(\eta^5\text{-}C_5H_5)M(CO)_3]^-$ and $[Cu(PPh_3)_4][Cu\{(\eta^5\text{-}C_5H_5)M(CO)_3\}_2]$ [336].

Addition of $[Cu(NCMe)_4]PF_6$ to a THF solution of $[ReH_5(PMePh_2)_3]$ at −70°C, followed by warming to room temperature gives colourless crystals of a complex which, on the basis of the absence of dihydrogen evolution during the reaction, and its $^1$H NMR spectrum, was formulated as $[Cu\{ReH_5(PMePh_2)_3\}_2]PF_6$, (**197**), [341]. An X-ray structure determination [341] has confirmed this, and shown the molecule to consist of an almost linear arrangement of metal atoms (Re–Cu–Re = 169.2°) with a mean Re–Cu internuclear distance of 2.607 Å. There are a number of points of interest which relate to this most remarkable molecule (Fig. 138). The Cu(I) centre is coordinated to six hydrido ligands in an unprecedented octahedral configuration, i.e. each $\{ReH_5(PMePh_2)\}$ unit functions as a tridentate ligand to the copper centre. This is the first isolated molecule in which a Cu(I) centre is ligated exclusively by hydrides although a metal–metal interaction probably occuring via a Re → Cu electron donor mechanism cannot be excluded [341]. A variable temperature $^1$H NMR study on the related complex $[Cu\{ReH_5(PMe_2Ph)_3\}_2]^+$ [341] has shown the presence of a bridge-terminal hydride scrambling process which maintains Re–H bonds; the hydride apparently never migrates past the copper atom (via a terminal Cu–H) to the other rhenium atom.

The closely related complexes $[Cu\{\textit{mer}\text{-}IrH_3(PMe_2Ph)_3\}_2]PF_6$, (**198**), and $[Cu\{\textit{fac}\text{-}IrH_3(PMe_2Ph)_3\}_2]PF_6$, (**199**), have been synthesized from $[Cu(NCMe)_4]PF_6$ and *mer*- and *fac*-$[IrH_3(PMe_2Ph)_3]$ respectively [342]. Complex (**198**) has been characterized by IR and NMR spectroscopy, the data being consistent with a structure containing four bridging hydrides ligating copper (Fig. 139). Complex (**199**) has been characterized by spectroscopic means as well as by X-ray diffraction [342]. On the basis of two types of P–Ir–Cu angles (two small (105° mean) and four large (124° mean)), and the IR data, it is inferred that the copper atom in (**199**) binds to only four of the available six hydrido ligands and that the stereochemistry is not planar

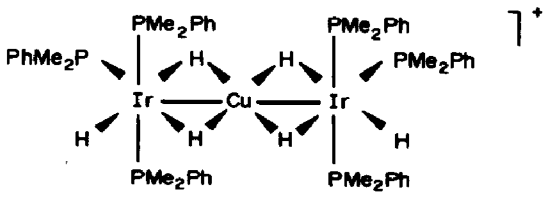

Fig. 139.

but as shown in Fig. 140. This is in direct contrast to the complex $[Cu\{ReH_5(PMePh_2)_3\}_2]PF_6$ which contains an octahedrally coordinated copper atom. The relatively short Ir–Cu internuclear distances of 2.529 and 2.502 Å (Ir–Cu–Ir = 176.0°) suggest a significant bonding interaction.

Recently the complex cation $[Cu\{Pt(NH_3)_2(\mu_2\text{-1-Me-uracilato})(\mu_2\text{-1-methylcytosine})\}_2]^{4+}$, (**200**), has been obtained by the co-crystallization of *cis*-$[Pt(NH_3)_2(\text{1-methyluracilato})(\text{1-methylcytosine})]^+$ and $Cu(NO_3)_2 \cdot 3H_2O$, and structurally characterized (Fig. 141) [343]. Although the Cu–Pt internuclear distances are relatively short (2.681 Å), the authors suggest on the basis of EPR results that this is to be attributed to the geometric requirements of the bridging ligands rather than to significant interaction between the metal atoms [343].

### *(b) Silver*

The complexes $[Ag\{(\eta^5\text{-}C_5H_5)M(CO)_3\}_2]^-$ (**201**; M = Cr, Mo, W) [335,336] and $[Ag\{Co(CO)_4\}_2]^-$, (**202**) [334], are analogues of the corresponding copper complexes, and were prepared by reacting the anions $[(\eta^5\text{-}C_5H_5)M(CO)_3]^-$ and $[Co(CO)_4]^-$ with AgI or $AgNO_3$ respectively. On the basis of their IR spectra these complexes are proposed to contain a linear M–Ag–M framework, isostructural with the neutral M–Hg–M systems [344]. The silver complex anions were generally found to be more inert than the copper analogues discussed above [334,336] (Table 16).

There have also been several reports of cationic heteronuclear complexes containing silver that are formally related to the anionic complexes detailed above. Thus, the complex $[Ag\{(\eta^5\text{-}C_5H_5)Rh(CO)(PPh_3)\}_2]PF_6 \cdot$ toluene, (**203**), was obtained from the reaction of $AgPF_6$ and $[(\eta^5\text{-}C_5H_5)Rh(CO)$

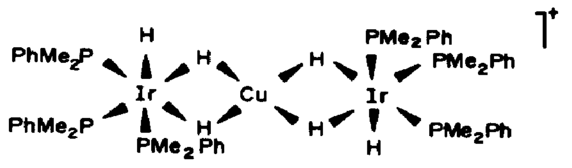

Fig. 140.

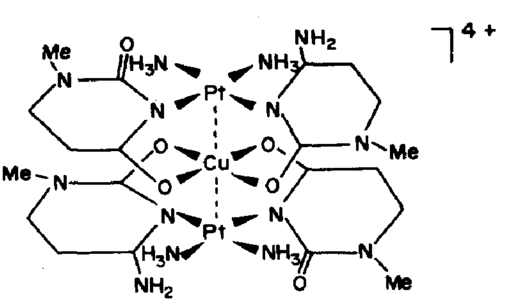

Fig. 141.

$(PPh_3)]$ (ratio 1 : 2) in toluene [345,346]. The stoichiometry was suggested by microanalytical data; the full molecular structure has, however, been established by X-ray crystallography [345,346]. The molecule contains a nearly linear arrangement of metal atoms (Rh–Ag–Rh = 171.0°) with an average Rh–Ag bond length of 2.644 Å (Fig. 142). On the basis of its reactions with radicals, $[Ag\{(\eta^5\text{-}C_5H_5)Rh(CO)(PPh_3)\}_2]^+$ may be regarded in terms of the formal equivalence

$$\left[Ag\left\{\left(\eta^5\text{-}C_5H_5\right)Rh(CO)(PPh_3)\right\}_2\right]^+ \equiv Ag + \left[\left(\eta^5\text{-}C_5H_5\right)Rh(CO)(PPh_3)\right] + \left[\left(\eta^5\text{-}C_5H_5\right)Rh(CO)(PPh_3)\right]^+$$

namely as a silver(0)-stabilized source of the highly reactive radical cation $[(\eta^5\text{-}C_5H_5)Rh(CO)(PPh_3)]^+$. Thus for instance, mixing $CH_2Cl_2$ solutions of $[Ag\{(\eta^5\text{-}C_5H_5)Rh(CO)(PPh_3)\}_2]$ and NO at room temperature instantly yields equimolar quantities of silver metal, $[(\eta^5\text{-}C_5H_5)Rh(CO)(PPh_3)]$ and $[(\eta^5\text{-}C_5H_5)Rh(NO)(PPh_3)]PF_6$ [345,346]. The stable adducts $[Ag\{(\eta^5\text{-}$

TABLE 16

Acyclic cluster complexes of silver

| Formula | Complex | Fig. | Ref. [a] |
|---|---|---|---|
| $[Ag\{(\eta^5\text{-}C_5H_5)M(CO)_3\}_2]^-$ (M = Cr, Mo, W) | **(201)** | – | 335,336 |
| $[Ag\{Co(CO)_4\}_2]^-$ | **(202)** | – | 334 |
| $[Ag\{(\eta^5\text{-}C_5H_5)Rh(CO)(PPh_3)\}_2]PF_6$ | **(203)** | 142 | 345*,346* |
| $[Ag\{(\eta^5\text{-}C_5H_5)Mn(CN)(NO)(PPh_3)\}_2]BF_4$ | **(204)** | – | 345 |
| $[Ag\{M(CO)_4(diphos)\}_2]PF_6$ (M = Mo, W; diphos = dppm, dppe) | **(205)** | – | 345 |
| $[Ag\{ReH_7(PPr^i_2Ph)\}_2]PF_6$ | **(206)** | – | 347* |
| $[AgW_2(\eta^5\text{-}C_5H_5)_2(CO)_4(\mu_2\text{-}CC_6H_4Me\text{-}4)_2]$ | **(207)** | – | 38 |
| $[(NH_3)_4Pt_2(C_5H_4N_2O_2)_2Ag(C_5H_5N_2O_2)_2Pt_2(NH_3)_4]^{5+}$ | **(208)** | 143 | 348* |
| $[Ag\{cis\text{-}Pt(NH_3)_2(C_6H_7N_2O_2)_2\}_2]NO_3$ | – | 144 | 349* |

---

[a] References marked with an asterisk refer to crystal structure determinations.

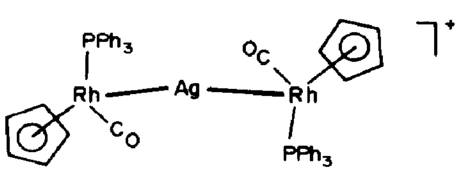

Fig. 142.

$C_5H_5)Mn(CN)(NO)(PPh_3)\}_2]BF_4$, (**204**), and $[Ag\{M(CO)_4(diphos)\}_2]PF_6$ (**205**; M = Mo, W; diphos = dppm, dppe), complexes closely related to $[Ag\{(\eta^5\text{-}C_5H_5)Rh(CO)(PPh_3)\}_2]PF_6$, have also been reported [345].

The salt $AgPF_6$ has also been reacted with $[ReH_7(PPr^i_2Ph)_2]$ giving a complex of stoichiometry $[Ag\{ReH_7(PPr^i_2Ph)_2\}_2]PF_6$, (**206**), [347]. This complex was characterized by extensive $^1H$ and $^{31}P$ NMR spectroscopic studies, and also by X-ray crystallography. In many respects the structure is similar to that of $[Cu\{ReH_5(PMe_2Ph)_3\}_2]PF_6$. The Re–Ag–Re core is nearly linear (Re(1)–Ag–Re(2) = 172.4°, Re(1)–Ag–Re(2′) = 165.7° (disordered sites Re(2) and Re(2′))) with a mean Re–Ag internuclear distance of 2.873 Å [347]. The structure solution was refined to $R = 0.048$ ($R' = 0.047$) but none of the fourteen hydrido ligands could be located [347]. By analogy, however, with $[Cu\{ReH_5(PMePh_2)_3\}_2]PF_6$, several of these hydride ligands might be expected to bridge the Re–Ag bond, with the remainder occupying terminal positions on rhenium. If suitable crystals could be obtained, this molecule would thus be an excellent candidate for a neutron diffraction study.

Only one other trinuclear complex of silver, $[Ag\{(\eta^5\text{-}C_5H_5)W(CO)_2\}_2(\mu_2\text{-}CC_6H_4Me\text{-}4)_2]$, (**207**), is relevant to this review. The nearly linear complex was synthesized from $[Ag(NCMe)_4]^+$ and $[(\eta^5\text{-}C_5H_5)W(CO)_2(\equiv CC_6H_4Me\text{-}4)]$ and isolated in 35% yield [38]. The analogous gold complex was also synthesized and characterized by X-ray crystallography (see Section B.(viii)(c)) and the complex $[Ag\{(\eta^5\text{-}C_5H_5)W(CO)_2\}_2(\mu_2\text{-}CC_6H_4Me\text{-}4)_2]$ is probably iso-structural.

The intriguing chemistry associated with the platinum blues and related systems has been found also to embrace heterometallic complexes (see also Section B.(viii)(a) above). Some examples involving silver are discussed below.

The unusual heteronuclear cation $[(NH_3)_4Pt_2(C_5H_5N_2O_2)_2Ag(C_5H_5N_2O_2)_2Pt_2(NH_3)_4]^{5+}$, (**208**), containing an essentially linear $Pt_2AgPt_2$ chain, was isolated as one of the products of the treatment of an aqueous solution of *cis*-$[Pt_2(NH_3)_4(C_5H_5N_2O_2)_2](NO_3)_2 \cdot H_2O$ with aqueous $AgNO_3$ [348]. The crystal structure determination [348] shows the molecular cation to have crystallographic centrosymmetry with Ag being at the inversion centre. The silver atom has a square planar coordination geometry of four 1-methyl-

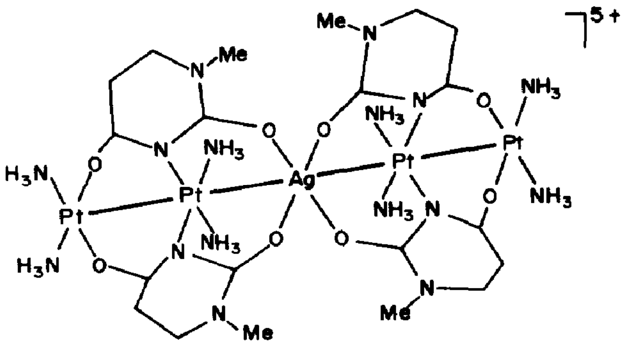

Fig. 143.

uracilato oxygen atoms, two supplied from each platinum dimer. Within each dimer two $\{cis\text{-Pt(NH}_3)_2\}^{2+}$ units are bridged by 1-methyluracilato ligands in a head-to-head arrangement. Adjacent cations are further related by another inversion centre which stacks $Pt_4$ units interrupted by Ag atoms. The molecular geometry is shown in Fig. 143, illustrating the tridentate bonding mode (spanning $Pt_2Ag$) of the methyluracilato ligands. The Pt–Pt–Ag–Pt–Pt core has bond angles of 180.0° (Pt–Ag–Pt) and 177.7° (Pt–Pt–Ag). The Pt–Pt distance within the unit is 2.949 Å (Pt–Ag = 2.787 Å) while the Pt · · · Pt distance between adjacent units is 3.246 Å. It is not at all clear what constitutes metal–metal bonding in such a system, but this complex has been included in order to elaborate upon the diverse chemistry of the platinum blues discussed briefly in Section B.(vii)(c), and also to delineate a highly pertinent, but as yet unresolved, question of bonding.

The closely related complex $[Ag\{cis\text{-Pt(NH}_3)_2(C_6H_7N_2O_2)_2\}_2]NO_3 \cdot 5H_2O$ has been prepared from $cis\text{-[Pt(NH}_3)_2Cl_2]$, $AgNO_3$ and 1-methylthymine [349]. The X-ray crystal structure has been determined [349]; the molecular structure is shown in Fig. 144. The cation is based on two {bis(1-methylthyminato)*cis*-diamminePt(II)} units linked head-to-head via a silver atom (Pt(1)–Ag = 2.849 Å, Pt(2)–Ag = 2.884 Å, Pt(1) · · · Pt(2) = 5.469 Å, Pt(1)–Ag–Pt(2) = 145.11°). Once again, the distances between the platinum and silver atoms are a little long to implicate strong metal–metal bonding, but nevertheless, some metal–metal interaction does appear to be feasible on the basis of the sum of the Pt and Ag covalent radii [349].

### *(c) Gold*

Only one tri-gold complex falls within the scope of this review. The unusual cationic complex $[(C_5Ph_4)Au_3(PPh_3)_3]^+$, **(209)**, was obtained by the reaction of $[(C_5Ph_4H)Au(PPh_3)]$ or $[(C_5Ph_4)Au_2(PPh_3)_2]$ with $[Au(PPh_3)]^+$ [350]. Complex **(209)** has been characterized by X-ray crystallography [350] (Fig. 145(a)). The overall molecular geometry is related to that of the

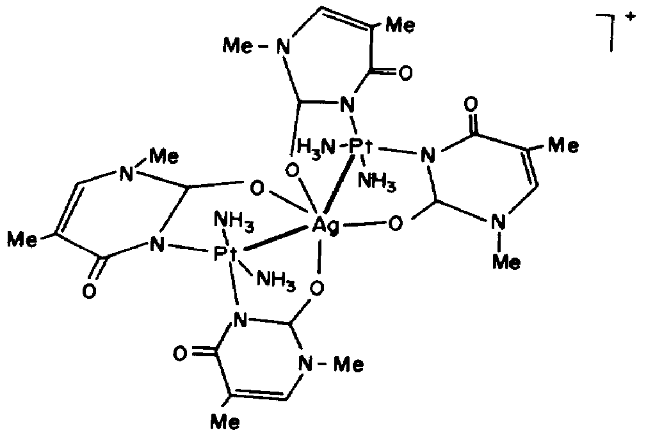

Fig. 144.

heteronuclear cation $[(\eta^5\text{-}C_5H_5)Fe(\eta^5\text{-}C_5H_4)Au_2(PPh_3)_2]^+$, (**210**), [351,352] (Fig. 145(b)). Complex (**209**) has a bent Au–Au–Au core (Au(1)–Au(2) = 3.021 Å, Au(2)–Au(3) = 2.820 Å, Au(1)–Au(2)–Au(3) = 103.93°), whereas (**210**) has an Fe–Au–Au core with metal–metal bond lengths of 2.818 Å (Fe–Au) and 2.768 Å (Au–Au) and a central bond angle of 98.1° (Table 17).

The anionic complexes $[Au\{ML_n\}_2]^-$ (**211**; $ML_n = Co(CO)_4$, $Mn(CO)_5$, $(\eta^5\text{-}C_5H_5)Fe(CO)_2$, $(\eta^5\text{-}C_5H_5)Cr(CO)_3$, $(\eta^5\text{-}C_5H_5)Mo(CO)_3$, $(\eta^5\text{-}C_5H_5)W(CO)_3$) [303,337–340] were synthesized from $[AuCl_2]^-$ or $[Au(C_6F_5)_3(THT)]$ (THT = tetrahydrothiophene) and the anions $[ML_n]^-$. Spectroscopic studies [303] suggest a linear M–Au–M arrangement for all these complexes, a feature confirmed crystallographically for $[N(PPh_3)_2][Au\{Co(CO)_4\}_2]$ [340] (see Fig. 146). The gold atom occupies a crystallographic centre of symmetry, and thus the Co–Au–Co unit is exactly linear with a Co–Au internuclear distance of 2.509 Å. This bond length is not significantly different from that in $[(PPh_3)AuCo(CO)_4]$ (2.50 Å) [353]. The "equatorial" carbonyl

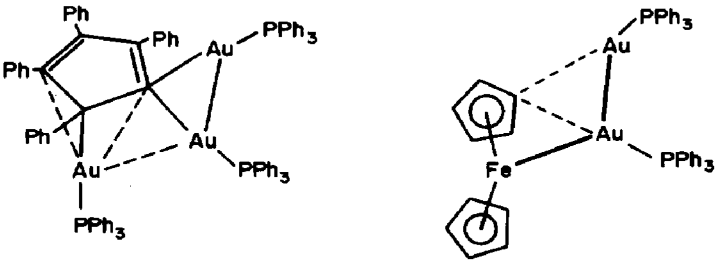

(a) (b)

Fig. 145.

TABLE 17

Acyclic cluster complexes of gold

| Formula | Complex | Fig. | Ref. [a] |
|---|---|---|---|
| $[(C_5Ph_4)Au_3(PPh_3)_3]^+$ | **(209)** | 145 | 350* |
| $[(\eta^5\text{-}C_5H_5)Fe(\eta^5\text{-}C_5H_4)Au_2(PPh_3)_2]^+$ | **(210)** | 145 | 351*,352* |
| $[Au\{ML_n\}_2]^-$ ($ML_n = Co(CO)_4$, $Mn(CO)_5$, $(\eta^5\text{-}C_5H_5)Fe(CO)_2$, $(\eta^5\text{-}C_5H_5)Cr(CO)_3$, $(\eta^5\text{-}C_5H_5)Mo(CO)_3$, $(\eta^5\text{-}C_5H_5)W(CO)_3]$ | **(211)** | 146,147 | 303,337, 338,339*,340* |
| $[AuW_2(\eta^5\text{-}C_5H_5)_2(CO)_4(\mu_2\text{-}CC_6H_4Me\text{-}4)_2]PF_6$ | **(212)** | 148 | 26*,38* |
| $[AuW_2Pt_2(\eta^5\text{-}C_5H_5)_2(CO)_4\text{-}(PMe_3)_4(\mu_3\text{-}CC_6H_4Me\text{-}4)_2]PF_6$ | **(213)** | 149 | 26 |
| $[AuX_2\{Au(py)_2\}_2AuX_2]$ (X = Cl, I) | **(214)** | 150 | 355* |

[a] References marked with an asterisk refer to crystal structure determinations.

groups are staggered (imposed by the centre of symmetry), while the idealized trigonal bipyramidal geometry at cobalt is distorted by the bending of the carbonyl groups towards the gold atom (mean Au–Co–C angle is 78.1°). The same effect has been noted in the isoelectronic complex $[Hg\{Co(CO)_4\}_2]$ [354]. The X-ray crystal structure of $[Bu^nN][Au\{(\eta^5\text{-}C_5H_5)Cr(CO)_3\}_2]$ has also been determined (Fig. 147) [339] and in this case the molecule was found to have a bent trimetal framework (Cr–Au–Cr = 162.2°); the average Au–Cr bond length is 2.638 Å.

Little of the chemical properties of the trinuclear anions $[Au\{ML_n\}_2]^-$ is known. A study has shown that they undergo irreversible reduction (one electron per electroactive molecule) with metallic gold being one of the products. The process

$$[L_nM\text{–}Au\text{–}ML_n]^- + e \rightarrow Au^0 + 2[ML_n]^-$$

has been proposed [337,338], and is in agreement with previously reported reduction mechanisms for related systems.

Treatment of [AuCl(THT)] (THT = tetrahydrothiophene) with $[(\eta^5\text{-}C_5H_5)W(CO)_2(\equiv CC_6H_4Me\text{-}4)]$ in tetrahydrofuran in the presence of $TlPF_6$ affords the salt $[Au\{(\eta^5\text{-}C_5H_5)W(CO)_2\}_2(\mu_2\text{-}CC_6H_4Me\text{-}4)_2]PF_6$, **(212)**,

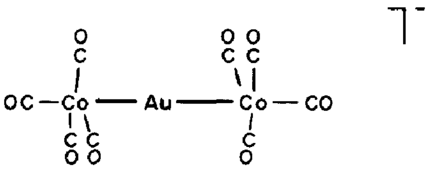

Fig. 146.

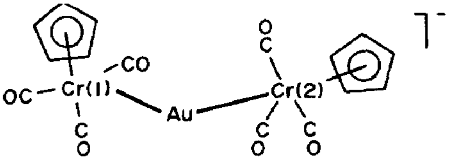

Fig. 147.

[26,38]. This complex and the silver analogue (see Section B.(viii)(b)) were proposed, on the basis of spectroscopic data, to be isostructural. An X-ray diffraction study of the gold complex showed the cation to possess a bent W–Au–W core (W–Au–W = 162.8°) with a mean Au–W bond length of 2.752 Å (Fig. 148).

A complex of stoichiometry $[AuW_2Pt_2(\eta^5\text{-}C_5H_5)_2(CO)_4(PMe_3)_4(\mu_3\text{-}CC_6H_4Me\text{-}4)_2]PF_6$, (**213**), was obtained as green crystals from the reaction of $[AuCl\{S(CH_2)_3CH_2\}]$ and a mixture of $[\{Pt(PMe_3)_2\}\{(\eta^5\text{-}C_5H_5)W(CO)_2\}(\mu_2\text{-}CC_6H_4Me\text{-}4)]$ and $TlPF_6$ [26]. The proposed structure has an open pentanuclear chain of metal atoms (Fig. 149) analogous to the platinum complex $[Pt_3W_2(\eta^5\text{-}C_5H_5)_2(C_8H_{12})_2(CO)_4(\mu_3\text{-}CC_6H_4Me\text{-}4)_2]$ [26].

Two homonuclear tetra-gold complexes of general formula $[AuX_2\{Au(py)_2\}_2AuX_2]$ (**214**; X = Cl, I) were recently reported [355]. These products have been obtained from the reaction of pyridine with $[AuCl\{S(CH_2C_6H_5)_2\}]$ or AuI respectively. Both complexes are light and heat sensitive, but nevertheless both have been structurally characterized [355]. The two molecules consist of $\{AuX_2\}$ and $\{Au(py)_2\}$ units linked by weak Au–Au bonds, but there are surprising geometrical differences. In the centrosymmetrical chloride derivative, a zig-zag $Au_4$ chain is observed (Au(1)–Au(2) = 3.249 Å, Au(2)–Au(2′) = 3.416 Å, Au(1)–Au(2)–Au(2′) = 88.1°), while the iodide complex possesses a linear $Au_4$ structure (Au(1)–Au(2) = 2.990 Å, Au(2)–Au(2′) = 3.291 Å, Au(1)–Au(2)–Au(2′) = 180.0°) (Fig. 150) [355]. These results are also interesting in that they suggest that gold does possess

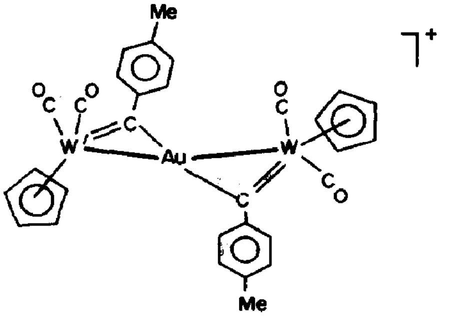

Fig. 148.

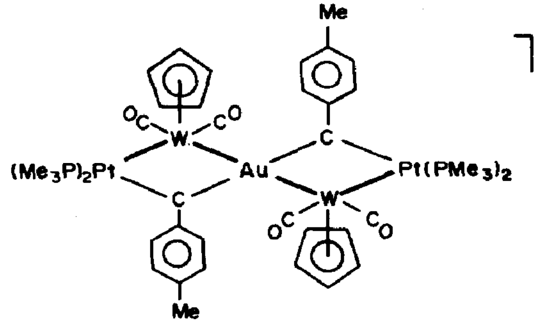

Fig. 149.

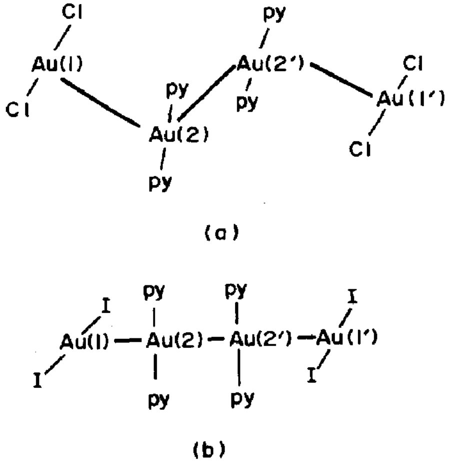

(a)

(b)

Fig. 150.

the ability to readily form oligomeric units such as observed for platinum in the platinum blues, and this could lead to an equally extensive chemistry.

## C. CONCLUSIONS

From the survey presented above several general conclusions may be drawn. These are outlined below.

### *(i) Occurrence of acyclic cluster complexes*

Acyclic cluster complexes have to date been synthesized containing almost every transition element. However, it is striking that more than half of all acyclic clusters contain either iron or osmium, and that more than three quarters contain Group VIII metals. This imbalance may, at least partly, represent the well known tendency of the Group VIII metals to form metal–metal bonds and hence cluster complexes [8], but it probably also reflects the continuing overriding interest in the chemistry of these elements in low oxidation states.

The early transition metal elements are also well known for metal–metal bond formation [356], but to a far lesser extent for cluster formation [8]. However, it is still surprising that almost no acyclic clusters containing metals of Groups IV and V are known, and it is notable that those that have been synthesized, also contain other transition metals. These considerations lead to the expectation that a potentially rich acyclic cluster chemistry of the early transition metals awaits exploitation. In this regard, ligands which might be expected to be prominent in such systems include hydrocarbon moieties, hydrido, alkyl, halo, and oxygen and nitrogen donor ligands, and therefore differ significantly from the ligands (most commonly carbonyl) found in acyclic cluster complexes of the Groups VI to VIII metals. It is, however, also conceivable that a judicious mixture of ligands, including $\pi$-acceptor ligand systems, might be important particularly with regard to heteronuclear complexes involving metals from opposite ends of the transition series.

### *(ii) Synthetic strategies*

From the survey presented above, it is apparent that a wide range of structurally diverse acyclic cluster complexes have been synthesized. It is equally apparent that while several rational synthetic strategies have been applied to the synthesis of acyclic clusters, the vast majority of complexes have been obtained using a multitude of ad hoc synthetic methods.

Vahrenkamp [13], but particularly Roberts and Geoffroy [7], have published analyses of the many reactions prevalent in cluster chemistry and which have as products cluster complexes. Specifically the categories, ligand substitution reactions, addition reactions, condensation reactions and bridge assisted reactions, have been identified by Roberts and Geoffroy [7] for heterometallic clusters, but synthetic reactions leading to acyclic clusters can be classified in a similar manner. It will suffice here then to briefly consider the synthesis of acyclic clusters only in very general terms highlighting the more versatile and successful methods of synthesis.

Briefly, acyclic cluster complexes can be viewed as being obtained by two major synthetic approaches, the first involving a pre-formed cyclic or acyclic cluster, and the second involving the assembly of an acyclic cluster from smaller (e.g. mononuclear, dinuclear) fragments.

Commencing with a pre-formed cyclic or acyclic cluster is generally the simplest approach and is represented, for instance, by ligand substitution/modification reactions, metal exchange reactions and redox processes, and in the case of a cyclic cluster precursor, specifically the scission of one or more metal–metal bonds (usually accompanied by reaction with a ligand system capable of taking up multidentate bridging coordination modes).

The assembly of an acyclic cluster from smaller transition metal fragments provides the greatest hope for the planned synthesis of novel acyclic cluster complexes. Only two general approaches have been utilized to any great extent for the preparation of acyclic clusters. In the first, the use of the isolobal model has been elegantly demonstrated by Stone [46] using primarily metal alkylidene and metal alkylidyne complexes as cluster building blocks. Characteristic of these reactions is the displacement of a labile ligand system and the formation of ligand bridges as the cluster is formed. In the second, the replacement of one or more anionic ligands at a metal centre by anionic metal complexes has proven to be a useful and predictable means of obtaining acyclic cluster complexes. To date, though, this technique has only been applied extensively in nickel, palladium and platinum chemistry, but relatively infrequently elsewhere. Future development of this approach can thus be expected to lead to a far greater variety of structural types when applied more generally in the transition series.

### *(iii) Structures and structure prediction*

Roberts and Geoffroy [7] recently outlined the techniques currently available for establishing the identity of heterometallic cluster complexes and indeed cluster complexes in general, and provided an excellent summary of the uses and limitations of these techniques.

One of the most striking features of the survey presented above is the dominance of X-ray crystallography in the process of product characterization. The various spectroscopies, particularly NMR, have been used to obtain detailed information of the ligand environment of a cluster, but have generally been under-utilized with respect to the characterization of the metal core. Nevertheless, it is clear that given the enormously complex chemistry of cluster complexes, and the increasing availability of X-ray crystallographic facilities, crystallography can be expected to play an increasing role in cluster chemistry in the foreseeable future.

With regard to the structures of acyclic clusters in general, it is apparent from the survey that a number of relatively simple structural types dominate. Of particular note are the ubiquitous $\{M_3(\mu_3\text{-}X)_2\}$ and $\{M_3(\mu_2\text{-}X)_2\}$ structures prevalent in iron, ruthenium and osmium chemistry, and linear trinuclear systems with or without bridging ligands which occur widely in the transition series. Other structural types include bent trinuclear systems without bridging ligands, and higher nuclearity complexes appearing in either linear or bent (zig-zag) forms. The dominance of certain structural types may at least partially be explained in terms of a simple numerical superiority of acyclic cluster complexes of certain elements (specifically iron and osmium), and a preponderance of trinuclear complexes in general. However, the factors which relate to the adoption of a particular structure, an understanding of which would enable some measure of structure prediction, cannot at this stage be discerned. Clearly the steric and electronic properties of the ligands, and the identity of the metal atoms are important considerations, while for instance the possibility of ligand bridging could also be expected to play a decisive role. However, to be able to assign relative contributions to each of these factors in any one example is not a trivial expectation. For the purposes of classification in this survey, heteronuclear acyclic clusters have been categorized in terms of a "structure controlling" atom or groups of atoms. In other words it has been assumed that, broadly speaking, a particular atom or group of atoms can be considered to most influence the structure of the overall cluster when compared to homonuclear analogues and to the coordination chemistry of that metal in general. With only a few exceptions, such a approach does produce significant correlations, and can be used to a certain extent in a predictive capacity with regards the chemistry of the acyclic cluster.

### *(iv) Chemical reactivity*

Without doubt, the main emphasis in acyclic cluster chemistry has, to date, rested on synthesis. The reactivity of acyclic cluster complexes has, in contrast, received little attention, while more fundamental questions regarding the kinetics and thermodynamics of these systems have scarcely been considered. Information relating to these questions would lead to a greater understanding of the occurrence and reactivity of acyclic clusters, and also to an understanding of the relationships between acyclic and cyclic cluster species.

For instance, comparing the substitution chemistry of the cyclic cluster $[Fe_3(CO)_{12}]$ with that of the acyclic cluster complexes $[Fe_3(CO)_9(\mu_3\text{-}X)_2]$ ($X = S$, Se, Te) reveals some intriguing differences, and in essence, three completely different types of behaviour. The cyclic cluster $[Fe_3(CO)_{12}]$ readily undergoes carbonyl ligand substitution with Group V donor ligands to give kinetic substitution products of the type $[Fe_3(CO)_{12-n}L_n]$ which rapidly undergo cluster fragmentation to give thermodynamic mononuclear substitution products $[Fe(CO)_4L]$ and $[Fe(CO)_3L_2]$ [357]. In contrast, the acyclic clusters $[Fe_3(CO)_9(\mu_3\text{-}X)_2]$ ($X = S$, Se) react, via a CO dissociative pathway, with Group V donor ligands to give the thermodynamically stable substitution products $[Fe_3(CO)_{9-n}L_n(\mu_3\text{-}X)_2]$ ($n \leqslant 3$), still containing the intact cluster core [96]. The closely related complex $[Fe_3(CO)_9(\mu_3\text{-}Te)_2]$, however, goes to unusual lengths to achieve ligand substitution [96,97,126]. Initial adduct formation involving metal–metal bond cleavage generates a kinetic product $[Fe_3(CO)_9L(\mu_3\text{-}Te)_2]$. Carbonyl ligand dissociation, and reforming of the metal–metal bond, regenerates the intact $\{Fe_3(\mu_3\text{-}Te)_2\}$ core and produces the thermodynamic substitution product $[Fe_3(CO)_8L(\mu_3\text{-}Te)_2]$, analogous to the products obtained for the S and Se complexes.

Questions which arise concerning these processes thus relate to the relative thermodynamic stabilities of $[Fe_3(CO)_{12}]$ and $[Fe_3(CO)_9(\mu_3\text{-}X)_2]$ and their substitution products, and to the differences in the reaction pathways for these complexes. Such questions, and their answers, are fundamental to solving the problems of rational acyclic cluster synthesis and to the understanding of the chemistry of acyclic clusters, including such aspects as the role of clusters in catalysis. It is difficult to see, however, how much progress can be made in these areas with the paucity of kinetic and thermodynamic data currently available.

### *(v) Future considerations*

This survey has revealed that acyclic cluster complexes form an important and an integral part of cluster and coordination chemistry in general. It has also revealed that there are links between cyclic and acyclic clusters, and between acyclic clusters and oligomeric and chain complexes. It can thus be expected that in the future these links will become more evident, and that, together with an increase in data on the kinetics and thermodynamics of cluster complexes, will lead to realistic expectations and successes in such areas as cluster catalysis.With specific regard to extensions in synthetic endeavours, the early transition metals, heteronuclear clusters, multiple metal–metal bonded systems, higher nuclearity acyclic clusters and complexes containing unusual ligand systems could be expected to provide growth points in the future.

## ACKNOWLEDGEMENTS

We thank Professor J.R. Moss for discussions and we gratefully acknowledge the assistance of Solomon Nkambule and Gillian Harris in gathering and collating material. We also thank Pam Watson for the masterly typing of the manuscript.

## REFERENCES

1 R.D. Johnston, Adv. Inorg. Radiochem., 13 (1970) 471.
2 P. Chini, G. Longoni and V.G. Albano, Adv. Organomet. Chem., 14 (1976) 285.

3 P. Chini and B.T. Heaton, Topics Curr. Chem., 71 (1977) 1.
4 E. Band and E.L. Muetterties, Chem. Rev., 78 (1978) 639.
5 G.L. Geoffroy, Acc. Chem. Res., 13 (1980) 469.
6 W.L. Gladfelter and G.L. Geoffroy, Adv. Organomet. Chem., 18 (1980) 207.
7 D.A. Roberts and G.L. Geoffroy, in G. Wilkinson (Ed.), Comprehensive Organometallic Chemistry, Vol. 6, Pergamon, Oxford, 1982, pp. 763–877.
8 B.F.G. Johnson (Ed.), Transition Metal Clusters, John Wiley, Chichester, 1980.
9 H.F. Schaefer, Acc. Chem. Res., 10 (1977) 287.
10 E.L. Muetterties, T.N. Rhodin, E. Band, C.F. Brucker and W.R. Pretzer, Chem. Rev., 79 (1979) 91.
11 E.L. Muetterties and M.J. Krause, Angew. Chem. Int. Ed. Engl., 22 (1983) 135.
12 R.D. Adams, Acc. Chem. Res., 16 (1983) 67.
13 H. Vahrenkamp, Adv. Organomet. Chem., 22 (1983) 169.
14 H. Vahrenkamp, Angew. Chem. Int. Ed. Engl., 17 (1978) 379.
15 H. Wawersik and F. Basolo, Inorg. Chim. Acta, 3 (1969) 113.
16 L.I.B. Haines, D. Hopgood and A.J. Poë, J. Chem. Soc. A, (1968) 421.
17 D. Sonnenberger and J.D. Atwood, J. Am. Chem. Soc., 102 (1980) 3484.
18 J.D. Atwood, N.J. Wovkulich and D. Sonnenberger, Acc. Chem. Res., 16 (1983) 350.
19 A.M. Stolzenberg and E.L. Muetterties, J. Am. Chem. Soc., 105 (1983) 822.
20 N.J. Coville, A.M. Stolzenberg and E.L. Muetterties, J. Am. Chem. Soc., 105 (1983) 2499.
21 See for example: J.S. Miller and A.J. Epstein, Prog. Inorg. Chem., 20 (1976) 1.
22 See for example: G.J. Leigh and R.L. Richards, in G. Wilkinson (Ed.), Comprehensive Organometallic Chemistry, Vol. 5, Pergamon, Oxford, 1982, pp. 619–620.
23 See for example: T.V. O'Halloran, M.M. Roberts and S.J. Lippard, J. Am. Chem. Soc., 106 (1984) 6427.
24 J.K. Barton and S.J. Lippard, Ann. N.Y. Acad. Sci., 313 (1978) 686.
25 K. Burgess, Polyhedron, 3 (1984) 1175.
26 M.R. Awang, G.A. Carriedo, J.A.K. Howard, K.A. Mead, I. Moore, C.M. Nunn and F.G.A. Stone, J. Chem. Soc., Chem. Commun., (1983) 964.
27 B.F.G. Johnson (Ed.), Transition Metal Clusters, John Wiley, Chichester, 1980, p. 34.
28 M.R. Churchill, B.G. DeBoer and F.J. Rotella, Inorg. Chem., 15 (1976) 1843.
29 R. Bau, R.G. Teller, S.W. Kirtley and T.F. Koetzle, Acc. Chem. Res., 12 (1979) 176.
30 Yu.V. Skipkin, A.A. Pasynskii, V.T. Kalinnikov, M.A. Porai-Koshits, L.Kh. Minacheva, A.S. Antsyshkina and V.N. Ostrikova, J. Organomet. Chem., 231 (1982) 205.
31 F.J. Timmers, W.R. Scheidt, J.A. Labinger and S. Baral, J. Organomet. Chem., 240 (1982) 153.
32 A.A. Pasynskii, I.L. Eremenko, B. Orazsakhatov, Yu.V. Rakitin, V.M. Novotortsev, O.G. Ellert, V.T. Kalinnikov, G.G. Aleksandrov and Yu.T. Struchkov, J. Organomet. Chem., 210 (1981) 385.
33 M. Pfeffer, J. Fischer and A. Mitschler, Organometallics, 3 (1984) 1531.
34 M. Pfeffer, J. Fischer, A. Mitschler and L. Ricard, J. Am. Chem. Soc., 102 (1980) 6338.
35 N.D. Feasey, S.A.R. Knox and A.G. Orpen, J. Chem. Soc., Chem. Commun., (1982) 75.
36 N.D. Feasey and S.A.R. Knox, J. Chem. Soc., Chem. Commun., (1982) 1062.
37 G.A. Carriedo, D. Hodgson, J.A.K. Howard, K. Marsden, F.G.A. Stone, M.J. Went and P. Woodward, J. Chem. Soc., Chem. Commun., (1982) 1006.
38 G.A. Carriedo, J.A.K. Howard, K. Marsden, F.G.A. Stone and P. Woodward, J. Chem. Soc., Dalton Trans., (1984) 1589.
39 T.V. Ashworth, M.J. Chetcuti, J.A.K. Howard, F.G.A. Stone, S.J. Wisbey and P. Woodward, J. Chem. Soc., Dalton Trans., (1981) 763.

40 S. Lu, N. Okura, T. Yoshida, S. Otsuka, K. Hirotsu and T. Higuchi, J. Am. Chem. Soc., 105 (1983) 7470.
41 W.-H. Pan, M.F. Leonowicz and E.I. Stiefel, Inorg. Chem., 22 (1983) 672.
42 A. Müller, H. Bögge and U. Schimanski, Inorg. Chim. Acta, 45 (1980) L249.
43 A. Müller, U. Schimanski and J. Schimanski, Inorg. Chim. Acta, 76 (1983) L245.
44 A. Müller, M. Dartmann, C. Römer, W. Clegg and G.M. Sheldrick, Angew. Chem. Int. Ed. Engl., 20 (1981) 1060.
45 S.F. Gheller, T.W. Hambley, J.R. Rodgers, R.T.C. Brownlee, M.J. O'Connor, M.R. Snow and A.G. Wedd, Inorg. Chem., 23 (1984) 2519.
46 F.G.A. Stone, Angew. Chem. Int. Ed. Engl., 23 (1984) 89.
47 M.J. Chetcuti, K. Marsden, I. Moore, F.G.A. Stone and P. Woodward, J. Chem. Soc., Dalton Trans., (1982) 1749.
48 G.A. Carriedo, J.A.K. Howard and F.G.A. Stone, J. Organomet. Chem., 250 (1983) C28.
49 G.A. Carriedo, J.A.K. Howard and F.G.A. Stone, J. Chem. Soc., Dalton Trans., (1984) 1555.
50 A. Winter, O. Scheidsteger and G. Huttner, Z. Naturforsch., Teil B, 38 (1983) 1525.
51 L.R. Krauth-Siegel, W. Schulze and M.L. Ziegler, Angew. Chem. Int. Ed. Engl., 19 (1980) 397.
52 M. Hohmann, L. Krauth-Siegel, K. Weidenhammer, W. Schulze and M.L. Ziegler, Z. Anorg. Allg. Chem., 481 (1981) 95.
53 E. Königer-Ahlborn and A. Müller, Angew. Chem. Int. Ed. Engl., 14 (1975) 573.
54 A. Müller, W. Rittner, A. Neumann, E. Königer-Ahlborn and R.G. Bhattacharyya, Z. Anorg. Allg. Chem., 461 (1980) 91.
55 W. Rittner, A. Müller, A. Neumann, W. Bäther and R.C. Sharma, Angew. Chem., 91 (1979) 565.
56 K. Hanewald, G. Kiel and G. Gattow, Z. Anorg. Allg. Chem., 478 (1981) 215.
57 K. Hanewald and G. Gattow, Z. Anorg. Allg. Chem., 476 (1981) 159.
58 A. Müller, R.G. Bhattacharyya, E. Königer-Ahlborn, R.C. Sharma, W. Rittner, A. Neumann, G. Henkel and B. Krebs, Inorg. Chim. Acta, 37 (1979) L493.
59 J.C. Huffman, R.S. Roth and A.R. Siedle, J. Am. Chem. Soc., 98 (1976) 4340.
60 A. Müller, H. Bögge and E. Königer-Ahlborn, Z. Naturforsch., Teil B, 34 (1979) 1698.
61 D. Coucouvanis, N.C. Baenziger, E.D. Simhon, P. Stremple, D. Swenson, A. Simopoulos, A. Kostikas, V. Petrouleas, V. Papaefthymiou, J. Am. Chem. Soc., 102 (1980) 1732.
62 D. Coucouvanis, E.D. Simhon, P. Stremple, M. Ryan, D. Swenson, N.C. Baenziger, A. Simopoulos, V. Papaefthymiou, A. Kostikas and V. Petrouleas, Inorg. Chem., 23 (1984) 741.
63 A. Müller and H.-H. Heinsen, Chem. Ber., 105 (1972) 1730.
64 A. Müller, N. Mohan and H. Bögge, Z. Naturforsch., Teil B, 33 (1978) 978.
65 M.D. Curtis, Inorg. Chem., 11 (1972) 802.
66 R. Bau, S.W. Kirtley, T.N. Sorrell and S. Winarko, J. Am. Chem. Soc., 96 (1974) 988.
67 P. Lemoine, A. Giraudeau and M. Gross, Electrochim. Acta, 21 (1976) 1.
68 W.A. Herrmann, M.L. Ziegler and K. Weidenhammer, Angew. Chem. Int. Ed. Engl., 15 (1976) 368.
69 K. Weidenhammer and M.L. Ziegler, Z. Anorg. Allg. Chem., 457 (1979) 174.
70 F. Mathey, J. Organomet. Chem., 93 (1975) 377.
71 J.M. Rosalky, B. Metz, F. Mathey and R. Weiss, Inorg. Chem., 16 (1977) 3307.
72 W. Fellmann and H.D. Kaesz, Inorg. Nucl. Chem. Lett., 2 (1966) 63.
73 J.M. Smith, K. Mehner and H.D. Kaesz, J. Am. Chem. Soc., 89 (1967) 1759.
74 H.D. Kaesz, R. Bau and M.R. Churchill, J. Am. Chem. Soc., 89 (1967) 2775.
75 M.D. Curtis, Inorg. Nucl. Chem. Lett., 6 (1970) 859.

76 R.W. Harrill and H.D. Kaesz, Inorg. Nucl. Chem. Lett., 2 (1966) 69.
77 M.R. Churchill and R. Bau, Inorg. Chem., 6 (1967) 2086.
78 L.B. Handy, J.K. Ruff and L.F. Dahl, J. Am. Chem. Soc., 92 (1970) 7312.
79 M.R. Churchill, K.N. Amoh and H.J. Wasserman, Inorg. Chem., 20 (1981) 1609.
80 P. Rustemeyer, E.O. Fischer, K. Ackermann and U. Schubert, Z. Naturforsch., Teil B, 37 (1982) 1279.
81 P.J. Vergamini, H. Vahrenkamp and L.F. Dahl, J. Am. Chem. Soc., 93 (1971) 6326.
82 W. Hieber and J. Gruber, Z. Anorg. Allg. Chem., 296 (1958) 91.
83 R. Harlin and G.R. Knox, J. Organomet. Chem., 4 (1965) 247.
84 R.B. King, Inorg. Chem., 2 (1963) 326.
85 C.H. Wei and L.F. Dahl, Inorg. Chem., 4 (1965) 493.
86 L.F. Dahl and P.W. Sutton, Inorg. Chem., 2 (1963) 1067.
87 H. Schumann, M. Magerstädt and J. Pickardt, J. Organomet. Chem., 240 (1982) 407.
88 J.A. de Beer and R.J. Haines, Chem. Commun., (1970) 288.
89 J.A. de Beer and R.J. Haines, J. Organomet. Chem., 24 (1970) 757.
90 D. Seyferth and H.P. Withers, Jr., Organometallics, 1 (1982) 1294.
91 H. Alper and A.S.K. Chan, J. Am. Chem. Soc., 95 (1973) 4905.
92 R. Meij, J. van der Helm, D.J. Stufkens and K. Vrieze, J. Chem. Soc., Chem. Commun., (1978) 506.
93 R. Meij, D.J. Stufkens, K. Vrieze, A.M.F. Brouwers, J.D. Schagen, J.J. Zwinselman, A.R. Overbeek and C.H. Stam, J. Organomet. Chem., 170 (1979) 337.
94 M.K. Chaudhuri, A. Haas and N. Welcman, J. Organomet. Chem., 85 (1975) 85.
95 D.A. Lesch and T.B. Rauchfuss, Inorg. Chem., 20 (1981) 3583.
96 G. Cetini, P.L. Stanghellini, R. Rossetti and O. Gambino, Inorg. Chim. Acta, 2 (1968) 433.
97 S. Aime, L. Milone, R. Rossetti and P.L. Stanghellini, J. Chem. Soc., Dalton Trans., (1980) 46.
98 G. Cetini, P.L. Stanghellini, R. Rossetti and O. Gambino, J. Organomet. Chem., 15 (1968) 373.
99 R. Rossetti, P.L. Stanghellini, O. Gambino and G. Cetini, Inorg. Chim. Acta, 6 (1972) 205.
100 P.M. Treichel, W.K. Deans and W.M. Douglas, Inorg. Chem., 11 (1972) 1609.
101 S.L. Cook, J. Evans, L.R. Gray and M. Webster, J. Organomet. Chem., 236 (1982) 367.
102 H. Vahrenkamp and D. Wolters, J. Organomet. Chem., 224 (1982) C17.
103 H. Vahrenkamp, E.J. Wucherer and D. Wolters, Chem. Ber., 116 (1983) 1219.
104 J.K. Kouba, E.L. Muetterties, M.R. Thompson and V.W Day, Organometallics, 2 (1983) 1065.
105 G. Huttner, G. Mohr, A. Frank and U. Schubert, J. Organomet. Chem., 118 (1976) C73.
106 M. Jacob and E. Weiss, J. Organomet. Chem., 131 (1977) 263.
107 P.E. Baikie and O.S. Mills, Chem. Commun., (1967) 1228.
108 M.M. Bagga, P.E. Baikie, O.S. Mills and P.L. Pauson, Chem. Commun., (1967) 1106.
109 M. Dekker and G.R. Knox, Chem. Commun., (1967) 1243.
110 R.J. Doedens, Inorg. Chem., 8 (1969) 570.
111 H. Alper, Inorg. Chem., 11 (1972) 976.
112 L. Markó, B. Markó-Monostory, T. Madach and H. Vahrenkamp, Angew. Chem. Int. Ed. Engl., 19 (1980) 226.
113 B.K. Teo, M.B. Hall, R.F. Fenske and L.F. Dahl, Inorg. Chem., 14 (1975) 3103.
114 A. Winter, L. Zsolnai and G. Huttner, J. Organomet. Chem., 234 (1982) 337.
115 I.-P. Lorenz and J. Messelhäuser, Z. Naturforsch., Teil B, 39 (1984) 403.

116 E. Lindner and G.A. Weiss, J. Organomet. Chem., 244 (1983) C9.
117 E. Lindner, G.A. Weiss, W. Hiller and R. Fawzi, J. Organomet. Chem., 255 (1983) 245.
118 A. Winter, I. Jibril and G. Huttner, J. Organomet. Chem., 247 (1983) 259.
119 D. Seyferth, R.S. Henderson, J.P. Fackler, Jr. and A.M. Mazany, J. Organomet. Chem., 213 (1981) C21.
120 G.J. Kruger, L. Linford, H.G. Raubenheimer and A.A. Chalmers, J. Organomet. Chem., 262 (1984) 69.
121 W.-K. Wong, G. Wilkinson, A.M.R. Galas, M.A. Thornton-Pett and M.B. Hursthouse, Polyhedron, 1 (1982) 842.
122 W.-K. Wong, K.W. Chiu, G. Wilkinson, A.M.R. Galas, M. Thornton-Pett and M.B. Hursthouse, J. Chem. Soc., Dalton Trans., (1983) 1557.
123 A. Winter, L. Zsolnai and G. Huttner, J. Organomet. Chem., 232 (1982) 47.
124 A. Winter, L. Zsolnai and G. Huttner, J. Organomet. Chem., 250 (1983) 409.
125 M.K. Chaudhuri, A. Haas and N. Welcman, J. Organomet. Chem., 91 (1975) 81.
126 D.A. Lesch and T.B. Rauchfuss, Organometallics, 1 (1982) 499.
127 G. Dettlaf, P. Hübener, J. Klimes and E. Weiss, J. Organomet. Chem., 229 (1982) 63.
128 A. Benoit, J.-Y. Le Marouille, C. Mahé and H. Patin, J. Organomet. Chem., 233 (1982) C51.
129 W.R. Cullen, D.A. Harbourne, B.V. Liengme and J.R. Sams, Inorg. Chem., 9 (1970) 702.
130 F.W.B. Einstein and A.-M. Svensson, J. Am. Chem. Soc., 91 (1969) 3663.
131 F.W.B. Einstein, A.-M. Pillotti and R. Restivo, Inorg. Chem., 10 (1971) 1947.
132 F.W.B. Einstein and R.D.G. Jones, J. Chem. Soc., Dalton Trans., (1972) 2563.
133 R.P. Dodge and V. Schomaker, J. Organomet. Chem., 3 (1965) 274.
134 R.C. Job and M.D. Curtis, Inorg. Chem., 12 (1973) 2514.
135 A.J. Carty, G. Ferguson, H.N. Paik and R. Restivo, J. Organomet. Chem., 74 (1974) C14.
136 R.J. Restivo and G. Ferguson, J. Chem. Soc., Dalton Trans., (1976) 893.
137 A. Winter, L. Zsolnai and G. Huttner, Z. Naturforsch., Teil B, 37 (1982) 1430.
138 N.S. Nametkin, V.D. Tyurin, A.I. Nekhaev, Yu.P. Sobolev, M.G. Kondrat'eva, A.S. Batsanov and Yu.T. Struchkov, J. Organomet. Chem., 243 (1983) 323.
139 N.S. Nametkin, V.D. Tyurin, V.V. Trusov and A.M. Krapivin, J. Organomet. Chem., 254 (1983) 243.
140 P.A.W. Dean, D.G. Ibbott and G.M. Bancroft, J. Chem. Soc., Chem. Commun., (1976) 901.
141 F.W.B. Einstein, T. Jones, R.K. Pomeroy and P. Rushman, J. Am. Chem. Soc., 106 (1984) 2707.
142 C.E. Coffey, J. Lewis and R.S. Nyholm, J. Chem. Soc., (1964) 1741.
143 A.S. Kasenally, R.S. Nyholm and M.H.B. Stiddard, J. Chem. Soc. A, (1965) 5343.
144 B. Chiswell and L.M. Venanzi, J. Chem. Soc. A, (1966) 901.
145 B. Munchenbach and J. Dehand, Naturwissenschaften, 59 (1972) 647.
146 E.H. Schubert and R.K. Sheline, Z. Naturforsch., Teil B, 20 (1965) 1306.
147 G.O. Evans, J.P. Hargaden and R.K. Sheline, Chem. Commun., (1967) 186.
148 G.O. Evans and R.K. Sheline, J. Inorg. Nucl. Chem., 30 (1968) 2862.
149 D.J. Robinson, M.Sc. Thesis, University of the Witwatersrand, Johannesburg, 1984.
150 P.A. Agron, R.D. Ellison and H.A. Levy, Acta Crystallogr., 23 (1967) 1079.
151 H.A. Levy, personal communication.
152 G.O. Evans, W.T. Wozniak and R.K. Sheline, Inorg. Chem., 9 (1970) 979.
153 D.R. Tyler, R.A. Levenson and H.B. Gray, J. Am. Chem. Soc., 100 (1978) 7888.
154 G. Nagarajan and M.W. Lindauer, Phys. Rev. A, 5 (1972) 557.
155 D.A. Lesch and T.B. Rauchfuss, Inorg. Chem., 22 (1983) 1854.

156 L.E. Bogan, Jr., D.A. Lesch and T.B. Rauchfuss, J. Organomet. Chem., 250 (1983) 429.

157 G. Huttner, G. Mohr and A. Frank, Angew. Chem. Int. Ed. Engl., 15 (1976) 682.

158 G. Huttner, J. Schneider, H.-D. Müller, G. Mohr, J. von Seyerl and L. Wohlfahrt, Angew. Chem. Int. Ed. Engl., 18 (1979) 76.

159 H. Schäfer-Stahl, J. Schneider and G. Huttner, Z. Naturforsch., Teil B, 37 (1982) 610.

160 J. Schneider, L. Zsolnai and G. Huttner, Cryst. Struct. Commun., 11 (1982) 943.

161 J. Schneider and G. Huttner, Chem. Ber., 116 (1983) 917.

162 J. Schneider, L. Zsolnai and G. Huttner, Cryst. Struct. Commun., 11 (1982) 1227.

163 D.F. Jones, U. Oehmichen, P.H. Dixneuf, T.G. Southern, J.-Y. Le Marouille and D. Grandjean, J. Organomet. Chem., 204 (1981) C1.

164 D.F. Jones, P.H. Dixneuf, T.G. Southern, J.-Y. Le Marouille, D. Grandjean and P. Guenot, Inorg. Chem., 20 (1981) 3247.

165 D.F. Jones, P.H. Dixneuf, A. Benoit and J.-Y. Le Marouille, Inorg. Chem., 22 (1983) 29.

166 A.W. Coleman, D.F. Jones, P.H. Dixneuf, C. Brisson, J.-J. Bonnet and G. Lavigne, Inorg. Chem., 23 (1984) 952.

167 E. Keller and H. Vahrenkamp, Angew. Chem. Int. Ed. Engl., 16 (1977) 542.

168 E. Keller and H. Vahrenkamp, Chem. Ber., 112 (1979) 2347.

169 B.F.G. Johnson, J. Lewis, P.G. Lodge, P.R. Raithby, K. Kendrick and M. McPartlin, J. Chem. Soc., Chem. Commun., (1979) 719.

170 C.E. Kampe, N.M. Boag, C.B. Knobler and H.D. Kaesz, Inorg. Chem., 23 (1984) 1390.

171 J. Norton, D. Valentine, Jr. and J.P. Collman, J. Am. Chem. Soc., 91 (1969) 7537.

172 J.R. Norton, J.P. Collman, G. Dolcetti and W.T. Robinson, Inorg. Chem., 11 (1972) 382.

173 P. Mastropasqua, A. Riemer, H. Kisch and C. Krüger, J. Organomet. Chem., 148 (1978) C40.

174 C.E. Kampe, N.M. Boag and H.D. Kaesz, J. Am. Chem. Soc., 105 (1983) 2896.

175 S. Aime, D. Osella, A.J. Deeming, A.M. Manotti Lanfredi and A. Tiripicchio, J. Organomet. Chem., 244 (1983) C47.

176 R. Fahmy, K. King, E. Rosenberg, A. Tiripicchio and M. Tiripicchio Camellini, J. Am. Chem. Soc., 102 (1980) 3626.

177 P. Braunstein, G. Predieri, A. Tiripicchio and E. Sappa, Inorg. Chim. Acta, 63 (1982) 113.

178 M. Catti, G. Gervasio and S.A. Mason, J. Chem. Soc., Dalton Trans., (1977) 2260.

179 S.A. MacLaughlin, N.J. Taylor and A.J. Carty, Organometallics, 3 (1984) 392.

180 M.R. Churchill, Adv. Chem. Ser., 167 (1978) 36.

181 H.D. Kaesz and P. Humphries, Prog. Inorg. Chem., 25 (1981) 145.

182 E. Sappa, A.M. Manotti Lanfredi and A. Tiripicchio, Inorg. Chim. Acta, 36 (1979) 197.

183 E. Sappa, A.M. Manotti Lanfredi and A. Tiripicchio, Inorg. Chim. Acta, 42 (1980) 255.

184 V. Busetti, G. Granozzi, S. Aime, R. Gobetto and D. Osella, Organometallics, 3 (1984) 1510.

185 R.D. Adams and D.A. Katahira, Organometallics, 1 (1982) 53.

186 G. Lavigne and J.-J. Bonnet, Inorg. Chem., 20 (1981) 2713.

187 J.A. van Doorn and P.W.N.M. van Leeuwen, J. Organomet. Chem., 222 (1981) 299.

188 R.A. Jones, G. Wilkinson, A.M.R. Galas, M.B. Hursthouse and K.M.A. Malik, J. Chem. Soc., Dalton Trans., (1980) 1771.

189 N. Cook, L.E. Smart, P. Woodward and J.D. Cotton, J. Chem. Soc., Dalton Trans., (1979) 1032.

190 E.W. Abel, R.A.N. McLean and S. Moorhouse, Inorg. Nucl. Chem. Lett., 7 (1971) 587.

191 N.D. Feasey, N.J. Forrow, G. Hogarth, S.A.R. Knox, K.A. MacPherson, M.J. Morris and A.G. Orpen, J. Organomet. Chem., 267 (1984) C41.

192 J.S. Field, R.J. Haines, D.N. Smit, K. Natarajan, O. Scheidsteger and G. Huttner, J. Organomet. Chem., 240 (1982) C23.
193 R.D. Adams, I.T. Horvâth, B.E. Segmüller and L.-W. Yang, Organometallics, 2 (1983) 144.
194 B.F.G. Johnson, J. Lewis, P.G. Lodge and P.R. Raithby, Acta Crystallogr., Sect. B, 37 (1981) 1731.
195 R.D. Adams, I.T. Horvâth and B.E. Segmüller, J. Organomet. Chem., 262 (1984) 243.
196 P.V. Broadhurst, B.F.G. Johnson, J. Lewis and P.R. Raithby, J. Organomet. Chem., 194 (1980) C35.
197 R.D. Adams, I.T. Horvâth and H.-S. Kim, Organometallics, 3 (1984) 548.
198 B.F.G. Johnson, R.D. Johnston, J. Lewis, I.G. Williams and P.A. Kilty, Chem. Commun., (1968) 861.
199 B.F.G. Johnson, J. Lewis and P.A. Kilty, J. Chem. Soc. A, (1968) 2859.
200 B.F.G. Johnson, R.D. Johnston, P.L. Josty, J. Lewis and I.G. Williams, Nature (London), (1967) 901.
201 D. Hartley, P.A. Kilty and M.J. Ware, Chem. Commun., (1968) 493.
202 N. Cook, L. Smart and P. Woodward, J. Chem. Soc., Dalton Trans., (1977) 1744.
203 J.P. Candlin and J. Cooper, J. Organomet. Chem., 15 (1968) 230.
204 A.J. Deeming, B.F.G. Johnson and J. Lewis, J. Chem. Soc. A, (1970) 897.
205 C.W. Bradford and R.S. Nyholm, Chem. Commun., (1968) 867.
206 J.R. Moss and W.A.G. Graham, J. Organomet. Chem., 18 (1969) P24.
207 A.C. Willis, G.N. van Buuren, R.K. Pomeroy and F.W.B. Einstein, Inorg. Chem., 22 (1983) 1162.
208 J.R. Moss and W.A.G. Graham, Inorg. Chem., 16 (1977) 75.
209 M. Gochin and J.R. Moss, J. Organomet. Chem., 192 (1980) 409.
210 J.R. Moss and W.A.G. Graham, J. Chem. Soc., Dalton Trans., (1977) 89.
211 J. Evans, S.J. Okrasinski, A.J. Pribula and J.R. Norton, J. Am. Chem. Soc., 98 (1976) 4000.
212 W.J. Carter, J.W. Kelland, S.J. Okrasinski, K.E. Warner and J.R. Norton, Inorg. Chem., 21 (1982) 3955.
213 M.R. Churchill, reference 20 in [212].
214 J.W. Kelland and J.R. Norton, J. Organomet. Chem., 149 (1978) 185.
215 B.F.G. Johnson, J. Lewis and P.A. Kilty, Chem. Commun., (1968) 180.
216 V.F. Allen, R. Mason and P.B. Hitchcock, J. Organomet. Chem., 140 (1977) 297.
217 A.J. Deeming, B.F.G. Johnson and J. Lewis, J. Organomet. Chem., 17 (1969) P40.
218 S. Bhaduri, B.F.G. Johnson, J. Lewis, D.J. Watson and C. Zuccaro, J. Chem. Soc., Chem. Commun., (1977) 477.
219 S. Bhaduri, B.F.G. Johnson, J. Lewis, D.J. Watson and C. Zuccaro, J. Chem. Soc., Dalton Trans., (1979) 557.
220 B.F.G. Johnson, J. Lewis, P.R. Raithby and C. Zuccaro, J. Chem. Soc., Chem. Commun., (1979) 916.
221 S. Bellard and P.R. Raithby, Acta Crystallogr., Sect. B, 36 (1980) 705.
222 P.V. Broadhurst, B.F.G. Johnson and J. Lewis, J. Chem. Soc., Dalton Trans., (1982) 1881.
223 C.M. Jensen, Y.J. Chen and H.D. Kaesz, J. Am. Chem. Soc., 106 (1984) 4046.
224 C.M. Jensen, C.B. Knobler and H.D. Kaesz, J. Am. Chem. Soc., 106 (1984) 5926.
225 F.W.B. Einstein, S. Nussbaum, D. Sutton and A.C. Willis, Organometallics, 2 (1983) 1259.
226 F.W.B. Einstein, S. Nussbaum, D. Sutton and A.C. Willis, Organometallics, 3 (1984) 568.

227 K. Burgess, B.F.G. Johnson, J. Lewis and P.R. Raithby, J. Organomet. Chem., 224 (1982) C40.
228 K. Burgess, B.F.G. Johnson, J. Lewis and P.R. Raithby, J. Chem. Soc., Dalton Trans., (1982) 2119.
229 S.A. MacLaughlin, J.P. Johnson, N.J. Taylor, A.J. Carty and E. Sappa, Organometallics, 2 (1983) 352.
230 G. Süss-Fink, U. Thewalt and H.-P. Klein, J. Organomet. Chem., 224 (1982) 59.
231 S.C. Brown, J. Evans and L.E. Smart, J. Chem. Soc., Chem. Commun., (1980) 1021.
232 A.J. Deeming, I.P. Rothwell, M.B. Hursthouse and J.D.J. Backer-Dirks, J. Chem. Soc., Dalton Trans., (1981) 1879.
233 R.D. Adams, D.A. Katahira and L.-W. Yang, Organometallics, 1 (1982) 235.
234 R.D. Adams, N.M. Golembeski and J.P. Selegue, J. Am. Chem. Soc., 101 (1979) 5862.
235 R.D. Adams and N.M. Golembeski, J. Am. Chem. Soc., 101 (1979) 1306.
236 R.D. Adams, N.M. Golembeski and J.P. Selegue, J. Am. Chem. Soc., 103 (1981) 546.
237 R.D. Adams, N.M. Golembeski and J.P. Selegue, Organometallics, 1 (1982) 240.
238 R.D. Adams, N.M. Golembeski and J.P. Selegue, J. Organomet. Chem., 193 (1980) C7.
239 R.D. Adams and D.A. Katahira, Organometallics, 1 (1982) 460.
240 R.D. Adams and Z. Dawoodi, J. Am. Chem. Soc., 103 (1981) 6510.
241 R.D. Adams, Z. Dawoodi, D.F. Foust and B.E. Segmüller, Organometallics, 2 (1983) 315.
242 A.M. Brodie, H.D. Holden, J. Lewis and M.J. Taylor, J. Organomet. Chem., 253 (1983) C1.
243 R.D. Adams and I.T. Horvâth, J. Am. Chem. Soc., 106 (1984) 1869.
244 P.V. Broadhurst, B.F.G. Johnson, J. Lewis, A.G. Orpen, P.R. Raithby and J.R. Thornback, J. Organomet. Chem., 187 (1980) 141.
245 S. Aime, A.J. Deeming, M.B. Hursthouse and J.D.J. Backer-Dirks, J. Chem. Soc., Dalton Trans., (1982) 1625.
246 B.F.G. Johnson, J. Lewis, P.R. Raithby and S.W. Sankey, J. Organomet. Chem., 231 (1982) C65.
247 Z. Dawoodi, M.J. Mays and P.R. Raithby, J. Chem. Soc., Chem. Commun., (1979) 721.
248 Z. Dawoodi and M.J. Mays, J. Chem. Soc., Dalton Trans., (1984) 1931.
249 R.D. Adams and L.-W. Yang, J. Am. Chem. Soc., 104 (1982) 4115.
250 R.D. Adams and L.-W. Yang, J. Am. Chem. Soc., 105 (1983) 235.
251 R.D. Adams, I.T. Horvâth and P. Mathur, J. Am. Chem. Soc., 105 (1983) 7202.
252 R.D. Adams, I.T. Horvâth and P. Mathur, J. Am. Chem. Soc., 106 (1984) 6296.
253 R.D. Adams, I.T. Horvâth and L.-W. Yang, Organometallics, 2 (1983) 1257.
254 R.D. Adams, Z. Dawoodi and D.F. Foust, Organometallics, 1 (1982) 411.
255 R.D. Adams, D.F. Foust and B.E. Segmüller, Organometallics, 2 (1983) 308.
256 R.D. Adams, Z. Dawoodi, D.F. Foust and B.E. Segmüller, J. Am. Chem. Soc., 105 (1983) 831.
257 R.D. George, S.A.R. Knox and F.G.A. Stone, J. Chem. Soc., Dalton Trans., (1973) 972.
258 L.J. Farrugia, J.A.K. Howard, P. Mitrprachachon, F.G.A. Stone and P. Woodward, J. Chem. Soc., Dalton Trans., (1981) 162.
259 J.M. Boncella and R.A. Anderson, J. Chem. Soc., Chem. Commun., (1984) 809.
260 K.P.C. Vollhardt and E.C. Walborsky, J. Am. Chem. Soc., 105 (1983) 5507.
261 E. Singleton and H.E. Oosthuizen, Adv. Organomet. Chem., 22 (1983) 209.
262 K.R. Mann, J.G. Gordon II and H.B. Gray, J. Am. Chem. Soc., 97 (1975) 3553.
263 K.R. Mann, N.S. Lewis, R.M. Williams, H.B. Gray and J.G. Gordon II, Inorg. Chem., 17 (1978) 828.

264 N.S. Lewis, K.R. Mann, J.G. Gordon II and H.B. Gray, J. Am. Chem. Soc., 98 (1976) 7461.

265 I.S. Sigal and H.B. Gray, J. Am. Chem. Soc., 103 (1981) 2220.

266 V.M. Miskowski, I.S. Sigal, K.R. Mann, H.B. Gray, S.J. Milder, G.S. Hammond and P.R. Ryason, J. Am. Chem. Soc., 101 (1979) 4383.

267 I.S. Sigal, K.R. Mann and H.B. Gray, J. Am. Chem. Soc., 102 (1980) 7252.

268 K.R. Mann, M.J. Di Pierro and T.P. Gill, J. Am. Chem. Soc., 102 (1980) 3965.

269 A.L. Balch and M.M. Olmstead, J. Am. Chem. Soc., 101 (1979) 3128.

270 R.R. Guimerans, M.M. Olmstead and A.L. Balch, J. Am. Chem. Soc., 105 (1983) 1677.

271 M.M. Olmstead, R.R. Guimerans and A.L. Balch, Inorg. Chem., 22 (1983) 2473.

272 A.L. Balch, R.R. Guimerans and M.M. Olmstead, J. Organomet. Chem., 268 (1984) C38.

273 F.E. Wood, M.M. Olmstead and A.L. Balch, J. Am. Chem. Soc., 105 (1983) 6332.

274 D.A. Bohling, T.P. Gill and K.R. Mann, Inorg. Chem., 20 (1981) 194.

275 K.R. Mann and H.B. Gray, Adv. Chem. Ser., 173 (1979) 225.

276 K.R. Mann, J.A. Thich, R.A. Bell, C.L. Coyle and H.B. Gray, Inorg. Chem., 19 (1980) 2462.

277 R.J. Haines, N.D.C.T. Steen and R.B. English, J. Chem. Soc., Chem. Commun., (1981) 587.

278 R.J. Haines, N.D.C.T. Steen and R.B. English, J. Chem. Soc., Dalton Trans., (1983) 1607.

279 R.J. Haines, R. Mason, J.A. Zubieta and C.R. Nolte, J. Chem. Soc., Chem. Commun., (1972) 990.

280 R. Mason and J.A. Zubieta, J. Organomet. Chem., 66 (1974) 279.

281 R.J. Haines, J.C. Burckett-St. Laurent and C.R. Nolte, J. Organomet. Chem., 104 (1976) C27.

282 J.C.T.R. Burckett-St. Laurent, R.J. Haines, C.R. Nolte and N.D.C.T. Steen, Inorg. Chem., 19 (1980) 577.

283 A. Agapiou, R.F. Jordan, L.A. Zyzyck and J.R. Norton, J. Organomet. Chem., 141 (1977) C35.

284 A. Agapiou, S.E. Pedersen, L.A. Zyzyck and J.R. Norton, J. Chem. Soc., Chem. Commun., (1977) 393.

285 K. Jonas, C. Krüger and J.C. Sekutowski, Angew. Chem. Int. Ed. Engl., 18 (1979) 487.

286 F. Faraone, S. Sergi and R. Pietropaolo, Inorg. Nucl. Chem. Lett., 5 (1969) 679.

287 W. Petz, J. Organomet. Chem., 133 (1977) C25.

288 W. Petz, C. Krüger and R. Goddard, Chem. Ber., 112 (1979) 3413.

289 W.E. Douglas, M.L.H. Green, C.K. Prout and G.V. Rees, Chem. Commun., (1971) 896.

290 W.E. Douglas and M.L.H. Green, J. Chem. Soc., Dalton Trans., (1972) 1796.

291 L.F. Dahl, E.D. de Gil and R.D. Feltham, J. Am. Chem. Soc., 91 (1969) 1653.

292 T.S. Cameron, C.K. Prout, G.V. Rees, M.L.H. Green, K.K. Joshi, G.R. Davies, B.T. Kilbourn, P.S. Braterman and V.A. Wilson, Chem. Commun., (1971) 14.

293 A. Keasey, P.M. Bailey and P.M. Maitlis, J. Chem. Soc., Chem. Commun., (1977) 178.

294 A. Keasey and P.M. Maitlis, J. Chem. Soc., Dalton Trans., (1978) 1830.

295 P.M. Bailey, A. Keasey and P.M. Maitlis, J. Chem. Soc., Dalton Trans., (1978) 1825.

296 A.L. Balch, J.R. Boehm, H. Hope and M.M. Olmstead, J. Am. Chem. Soc., 98 (1976) 7431.

297 S.Z. Goldberg and R. Eisenberg, Inorg. Chem., 15 (1976) 535.

298 L.Yu. Ukhin, N.A. Dolgopolova, L.G. Kuz'mina and Yu.T. Struchkov, J. Organomet. Chem., 210 (1981) 263.

299 P.M. Bailey, E.A. Kelley and P.M. Maitlis, J. Organomet. Chem., 144 (1978) C52.

300 P. Braunstein and J. Dehand, J. Organomet. Chem., 24 (1970) 497.

301 P. Braunstein and J. Dehand, J. Chem. Soc., Chem. Commun., (1972) 164.
302 P. Braunstein and J. Dehand, Bull. Soc. Chim. Fr., (1975) 1997.
303 P. Braunstein and J. Dehand, J. Organomet. Chem., 88 (1975) C24.
304 P. Braunstein and J. Dehand, C.R. Acad. Sci., Ser. C, 274 (1972) 175.
305 P. Braunstein and J. Dehand, J. Organomet. Chem., 81 (1974) 123.
306 S. Cenini, B. Ratcliff and R. Ugo, Gazz. Chim. Ital., 104 (1974) 1161.
307 R. Bender, P. Braunstein, J.-M. Jud and Y. Dusausoy, Inorg. Chem., 22 (1983) 3394.
308 N.J. Taylor, P.C. Chieh and A.J. Carty, J. Chem. Soc., Chem. Commun., (1975) 448.
309 L.E. Smart, J. Browning, M. Green, A. Laguno, J.L. Spencer and F.G.A. Stone, J. Chem. Soc., Dalton Trans., (1977) 1777.
310 J.-P. Barbier and P. Braunstein, J. Chem. Res. M, (1978) 5028.
311 R.G. Pearson and J. Dehand, J. Organomet. Chem., 16 (1969) 485.
312 P. Braunstein, D. Matt, O. Bars, M. Louër, D. Grandjean, J. Fischer and A. Mitschler, J. Organomet. Chem., 213 (1981) 79.
313 D. Moras, J. Dehand and R. Weiss, C.R. Acad. Sci., 267 (1968) 1471.
314 M.A. Urbancic, S.R. Wilson and J.R. Shapley, Inorg. Chem., 23 (1984) 2954.
315 P. Braunstein, D. Matt, O. Bars and D. Grandjean, Angew. Chem. Int. Ed. Engl., 18 (1979) 797.
316 P. Braunstein, E. Keller and H. Vahrenkamp, J. Organomet. Chem., 165 (1979) 233.
317 K.A. Hofmann and G. Bugge, Ber., 41 (1908) 312.
318 R.D. Gillard and G. Wilkinson, J. Chem. Soc., (1964) 2835.
319 D.B. Brown, R.D. Burbank and M.B. Robin, J. Am. Chem. Soc., 90 (1968) 5621.
320 D.B. Brown, R.D. Burbank and M.B. Robin, J. Am. Chem. Soc., 91 (1969) 2895.
321 J.P. Davidson, P.J. Faber, R.G. Fischer, Jr., S. Mansy, H.J. Peresie, B. Rosenberg and L. van Camp, Cancer Chemother. Rep., 59 (1975) 287.
322 B. Rosenberg, Cancer Chemother. Rep., 59 (1975) 589.
323 R.J. Speer, H. Ridgway, L.M. Hall, D.P. Stewart, K.E. Howe, D.Z. Lieberman, A.D. Newman and J.M. Hill, Cancer Chemother. Rep., 59 (1975) 629.
324 J.M. Hill, E. Loeb, A. MacLellan, N.O. Hill, A. Khan and J.J. King, Cancer Chemother. Rep., 59 (1975) 647.
325 J.K. Barton, H.N. Rabinowitz, D.J. Szalda and S.J. Lippard, J. Am. Chem. Soc., 99 (1977) 2827.
326 J.K. Barton, D.J. Szalda, H.N. Rabinowitz, J.V. Waszczak and S.J. Lippard, J. Am. Chem. Soc., 101 (1979) 1434.
327 L.S. Hollis and S.J. Lippard, J. Am. Chem. Soc., 103 (1981) 1230.
328 J.-P. Laurent, P. Lepage and F. Dahan, J. Am. Chem. Soc., 104 (1982) 7335.
329 K. Matsumoto and K. Fuwa, J. Am. Chem. Soc., 104 (1982) 897.
330 K. Matsumoto, H. Takahashi and K. Fuwa, Inorg. Chem., 22 (1983) 4086.
331 L.S. Hollis and S.J. Lippard, Inorg. Chem., 22 (1983) 2600.
332 K. Matsumoto, H. Takahashi and K. Fuwa, J. Am. Chem. Soc., 106 (1984) 2049.
333 A.P. Ginsberg, T.V. O'Halloran, P.E. Fanwick, L.S. Hollis and S.J. Lippard, J. Am. Chem. Soc., 106 (1984) 5430.
334 P. Chini, S. Martinengo and G. Longoni, Gazz. Chim. Ital., 105 (1975) 203.
335 P. Hackett and A.R. Manning, J. Chem. Soc., Chem. Commun., (1973) 71.
336 P. Hackett and A.R. Manning, J. Chem. Soc., Dalton Trans., (1975) 1606.
337 P. Lemoine, A. Giraudeau, M. Gross and P. Braunstein, J. Chem. Soc., Chem. Commun., (1980) 77.
338 A. Giraudeau, P. Lemoine, M. Gross and P. Braunstein, J. Organomet. Chem., 202 (1980) 455.

339 P. Braunstein, U. Schubert and M. Burgard, Inorg. Chem., 23 (1984) 4057.
340 R. Usón, A. Laguna, M. Laguna, P.G. Jones and G.M. Sheldrick, J. Chem. Soc., Dalton Trans., (1981) 366.
341 L.F. Rhodes, J.C. Huffman and K.G. Caulton, J. Am. Chem. Soc., 105 (1983) 5137.
342 L.F. Rhodes, J.C. Huffman and K.G. Caulton, J. Am. Chem. Soc., 106 (1984) 6874.
343 B. Lippert, U. Thewalt, H. Schöllhorn, D.M.L. Goodgame and R.W. Rollins, Inorg. Chem., 23 (1984) 2807.
344 R.D. Fischer and K. Noack, J. Organomet. Chem., 16 (1969) 125.
345 N.G. Connelly, A.R. Lucy and A.M.R. Galas, J. Chem. Soc., Chem. Commun., (1981) 43.
346 N.G. Connelly, A.R. Lucy, J.D. Payne, A.M.R. Galas and W.E. Geiger, J. Chem. Soc., Dalton Trans., (1983) 1879.
347 N.G. Connelly, J.A.K. Howard, J.L. Spencer and P.K. Woodley, J. Chem. Soc., Dalton Trans., (1984) 2003.
348 B. Lippert and D. Neugebauer, Inorg. Chem., 21 (1982) 451.
349 B. Lippert and D. Neugebauer, Inorg. Chim. Acta, 46 (1980) 171.
350 T.V. Baukova, Yu.L. Slovokhotov and Yu.T. Struchkov, J. Organomet. Chem., 221 (1981) 375.
351 V.G. Andrianov, Yu.T. Struchkov and E.R. Rossinskaja, J. Chem. Soc., Chem. Commun., (1973) 338.
352 A.N. Nesmeyanov, E.G. Perevolova, K.I. Grandberg, D.A. Lemenovskii, T.V. Baukova and O.B. Afanassova, J. Organomet. Chem., 65 (1974) 131.
353 T.L. Blundell and H.M. Powell, J. Chem. Soc. A, (1971) 1685.
354 G.M. Sheldrick and R.N.F. Simpson, J. Chem. Soc. A, (1968) 1005.
355 H.N. Adams, W. Hiller and J. Strähle, Z. Anorg. Allg. Chem., 485 (1982) 81.
356 F.A. Cotton and R.A. Walton, Multiple Bonds Between Metal Atoms, John Wiley, New York, 1982.
357 A.F. Clifford and A.K. Mukherjee, Inorg. Chem., 2 (1963) 151; A.F. Clifford and A.K. Mukherjee, Inorg. Synth., 8 (1966) 185.